ZooKeys 1158: 1–26 (2023)
doi: 10.3897/zookeys.1158.100518
https://zookeys.pensoft.net

RESEARCH ARTICLE

A peer-reviewed open-access journal
ZooKeys
Launched to accelerate biodiversity research

Revision of the genus *Atholus* Thomson, 1859 (Coleoptera, Histeridae, Histerinae) from the Philippines with additional records

Ian Niel dela Cruz[1,2,3], Masahiro Ôhara[3]

1 *Entomological Laboratory, Graduate School of Agriculture, Hokkaido University, N9, W9, Sapporo, 060-8589, Japan* **2** *Department of Biology, College of Mathematics and Natural Sciences, Caraga State University, Butuan City, 8600, Philippines* **3** *The Hokkaido University Museum, Hokkaido University, N10, W8, Sapporo, 060-0810, Japan*

Corresponding author: Ian Niel dela Cruz (histermushi@gmail.com)

Academic editor: Michael Caterino | Received 13 January 2023 | Accepted 12 March 2023 | Published 12 April 2023

https://zoobank.org/047C3E08-B3F2-44F4-8405-0AD39F23E9E8

Citation: dela Cruz IN, Ôhara M (2023) Revision of the genus *Atholus* Thomson, 1859 (Coleoptera, Histeridae, Histerinae) from the Philippines with additional records. ZooKeys 1158: 1–26. https://doi.org/10.3897/zookeys.1158.100518

Abstract

The Philippine species of the genus *Atholus* Thomson, 1859 are revised and re-examined based on museum as well as freshly collected specimens. *Atholus torquatus* (Marseul, 1854) is re-described, and SEM micrographs and illustrations of both male and female genitalia are provided. *Atholus bakeri* (Bickhardt, 1914) and *Atholus nitidissimus* Desbordes, 1925 are also re-described based on images of syntypes. *Atholus pirithous* (Marseul, 1873) and *A. torquatus* (Marseul, 1854) are new to the Philippine archipelago. *Atholus coelestis* (Marseul, 1857) and *A. philippinensis* (Marseul, 1854) are provided with diagnostic descriptions and images. A key to the Philippine species is provided.

Keywords

Coleoptera, genitalia, Histerini, new record, SEM, taxonomy

Introduction

Atholus Thomson, 1859 is a cosmopolitan genus of Histerinae: Histerini (Coleoptera: Histeridae) spread across the world, with the exception of the Continental Australia and Antarctica. The genus contains 77 described species hitherto; almost half of them occur in the Oriental Region (Mazur 2011).

Philippine *Atholus* have received only limited attention, and in the recent worldwide catalogue of Histeridae (Mazur 2011), only two species – *A. nitidissimus* Desbordes, 1925 and *A. bakeri* (Bickhardt, 1914) from the archipelago were reported as Philippine endemics. Few species were indicated generally in the catalogue to occur in the Oriental region, such as *Atholus coelestis* (Marseul, 1857); Mazur et al. (2015), however, reported this species from Luzon Island.

Thirteen species of *Atholus* are also currently recorded in Indonesia: *A. tenuistriatus* (Lewis, 1889) from Borneo; *A. crenatifrons* (Lewis, 1899); *A. famulus* (Lewis, 1892); *A. gestroi* (Schmidt, 1897); *A. singalanus* (Marseul, 1880); *A. tetricus* (Lewis, 1902) from Sumatra; and *A. bifrons* (Marseul, 1854); and *A. pinnulae* (Lewis, 1900) reported from both Borneo and Sumatra islands. Moreover, *A. myrmidon* (Marseul, 1862) from Sulawesi and *A. terraemotus* (Lewis, 1900) from Java were also in the checklist, with *A. coelestis* (Marseul, 1857), *A. philippinensis* (1854), and *A. torquatus* (Marseul, 1854), which are also found on these islands. *Atholus bifrons* (Marseul, 1854) was recently reported from Borneo, as well as north towards the Ryukyus islands of Japan (dela Cruz and Ôhara 2022), suggesting that this species might also occur in the Philippines. In addition, *A. bifrons* (Marseul, 1854) was also recorded in Taiwan (Mazur 2008, 2009).

While Ôhara (1992, 1993, 1999b) re-described several Oriental *Atholus* taxa, other species did not receive much attention. This paper provides the first re-description of *A. torquatus* (Marseul, 1854) with illustrations of both male and female genitalia. Additional records, diagnoses, re-descriptions, and figures of all Philippine *Atholus* are provided herein.

Materials and methods

Fresh specimens were collected by the senior author under ruminant dung and decaying banana stumps. All museum specimens were loaned from the following institutes: the Hokkaido University Museum, Sapporo (**SEHU**; M. Ôhara), except the syntypes from Muséum National d'Histoire Naturelle, Paris, France (**MNHN**; A. Mantilleri) and Naturhistorisches Museum Berlin, Germany (**MNHUB**; B. Jäger). General observations and dissections were carried out under stereomicroscopes Nikon SMZ745T and Nikon SMZ800. Detailed observations of several structures were performed using SEM (JEOL JSM-6510). Genitalia were dissected and treated according to methods of Ôhara (1994). In this paper, we treat the number of denticles of both apical and outer lateral margins of protibia combined as the 'outer margin', and denticles along the outer lateral margin as the denticles on 'outer sublateral margin', and compare it with the result of Ôhara (1992, 1993). Body measurements are as follows: **PEL** (length between anterior angles of pronotum and apices of elytra), **APW** (width between anterior angles of pronotum), **PPW** (width between posterior angles of pronotum), **EL** (length of elytron along sutural line), and **EW** (maximal width between outer margins of elytra). General morphological terminology follows Ôhara (1994) and Lackner (2010). Regarding syntypes of *A. nitidissimus* Desbordes, 1925 and *A. bakeri* (Bickhardt, 1914), only images of syntypes were available.

Systematics

Genus *Atholus* Thomson, 1859

Atholus Thomson, 1859: 76 [type species: *Hister bimaculatus* Linnaeus, 1758: 358, originally designated]; Schmidt 1885: 288; Ganglbauer 1889: 369; Lewis 1906: 402; Bickhardt 1917: 159, 162; 1919: 13, 137, 139; Auzat 1916: 93; Arnett 1962: 378, 381; Halstead 1963: 7, 8; Witzgall 1971: 179, 183; Kryzhanovskij and Reichardt 1976: 382; Mazur 1984: 210, 1997: 128, 2011: 103.

Peranus Lewis, 1906: 401 [type species: *Hister scutellaris* Erichson, 1834: 151], synonymized by Kryzhanovskij and Reichardt 1976: 384.

Atholister Reitter, 1909: 286 [type species: *Hister scutellaris* Erichson], synonymized by Heyden, 1910: 317.

Euatholus Kryzhanovskij in Kryzhanovskij & Reichardt, 1976: 387 [type species: *Hister duodecimstriatus* Schrank, 1781: 39], synonymized by Mazur 1984: 210.

Key to the Philippine species of the genus *Atholus* Thomson, 1859

1 Sutural elytral stria absent ..... ***A. nitidissimus* Desbordes, 1925**
– Sutural elytral stria present **2**
2 Dorsal elytral striae 1–3 complete. Dorsal elytral stria 4 present on apical half ..... ***A. philippinensis* (Marseul, 1854)**
– Dorsal elytral 1–4 striae complete **3**
3 Apical end of dorsal elytral 3 stria strongly bent inwards. Anterior margin of mesoventrite slightly emarginated ..... ***A. coelestis* (Marseul, 1857)**
– Apical end of dorsal elytral 3 stria straight, not bent. Anterior margin of mesoventrite outwardly arcuate and no emargination **4**
4 Lateral pronotal stria not interrupted, connected to anterior marginal stria behind head ..... ***A. pirithous* (Marseul, 1873)**
– Lateral pronotal stria broadly interrupted in anterolateral angles **5**
5 Propygidium punctate, punctures becoming finer on pygidium; protibial teeth conspicuous, growing in size apically ..... ***A. torquatus* (Marseul, 1854)**
– Both propygidium and pygidium strongly punctate ..... ***A. bakeri* (Bickhardt, 1914)**

Atholus philippinensis (Marseul, 1854)

Figs 1, 7, 8, 35–37

Hister philippinensis Marseul, 1854: 547 [Malaisie (îles Philippines)].

Hister philippensis (sic): Gemminger and Harold 1868: 771.

Hister (*Atholus*) *philippinensis*: Bickhardt 1910: 54 [catalogued]; 1913: 173 [Hoozan, Taihorin]; 1917: 194 [catalogued]; Miwa 1931: 57 [Hoozan, Taihorin]; Kamiya and Takagi 1938: 31.

Hister sectator Lewis, 1901: 375, synonymized by Bickhardt, 1917: 194.
Atholus sectator: Lewis 1906: 402.
Atholus philippinensis: Lewis 1906: 402; 1915: 55; Mazur 1984: 215; 1997: 132; 2011: 106 [catalogued]; Ôhara 1999b: 32–36 [Taiwan].

Specimens examined. 3 ♂♂, 3 ♀♀. **Mindanao Island**, Agusan del Norte, Butuan, Taligaman, 3 ♂♂, 3 ♀♀ [IC-21-18], 08.56894°N, 125.38534°E 60 m a.s.l., 2021-VI-02 [AN-21-IDC-002], I.N. DELA CRUZ leg.

Diagnosis. *Atholus philippinensis* (Marseul, 1854) (Fig. 1) is easily distinguished from other Philippine congeners by entire dorsal elytral striae 1–3 (fourth stria is incomplete), and dense punctation of propygidium and pygidium. Among Philippine species, it is the largest one in size, with its markedly wider elytra and posterior angles of pronotum. The number of denticles of the outer sublateral margin of protibia is four.

Additional description. ***Female genitalia*:** anterior portion of valvifers (Figs 35, 36) paddle-shaped; gonocoxite (Fig. 37) slightly elongate, almost twice as long as broad, shovel-like; inner and outer surfaces differentiated; inner face moderately separated from outer face by elevated lateral ridge; sclerotized setae on apical half of outer face short and somewhat dense; inner face with short and sparse setae; apex of gonocoxite with two teeth; gonostyli present, freely articulated; spermathecae multiple, consisting of four sacs; sacs gradually enlarged and elongate, not sclerotized.

Distribution. Philippines; Malaysia; Indonesia (Sumatra, Borneo, Java); Myanmar, Vietnam; India (Meghalaya); China (Hainan); Taiwan (Mazur 2011).

Biology. This species occurs in decaying banana stumps and are often found along with some species of *Platylister* (Platysomatini, Histerinae, Histeridae).

Remarks. The protibial teeth of *A. philippinensis* (Marseul, 1854) are not as prominent as they are in other species. Moreover, in comparison to the description of Ôhara (1999b), the number of denticles may vary, ranging from 9–11 on the outer margin, one on the inner apical angle, and four or five on the outer sublateral margin. This species was already re-described based on specimens of Taiwan and western Kalimantan, Indonesia (Ôhara, 1999b), including the illustrations of male genitalia and spermatheca of female. Ôhara (1999b) also provided a figure of the spermatheca; we add illustrations of the female gonocoxite and valvifers here (Figs 35–37).

Atholus coelestis (Marseul, 1857)

Figs 2, 9–14, 38–40

Hister coelestis Marseul, 1857: 416, tome, 10, fig. 59 [China].
Hister (*Atholus*) *coelestis*: Bickhardt 1910: 53 [catalogued]; 1917: 193 [catalogued]; Desbordes 1919: 399 [Tonkin, Annam, Cochinchine]; 1921: 10 [India]; Kamiya and Takagi 1938: 31 [listed].

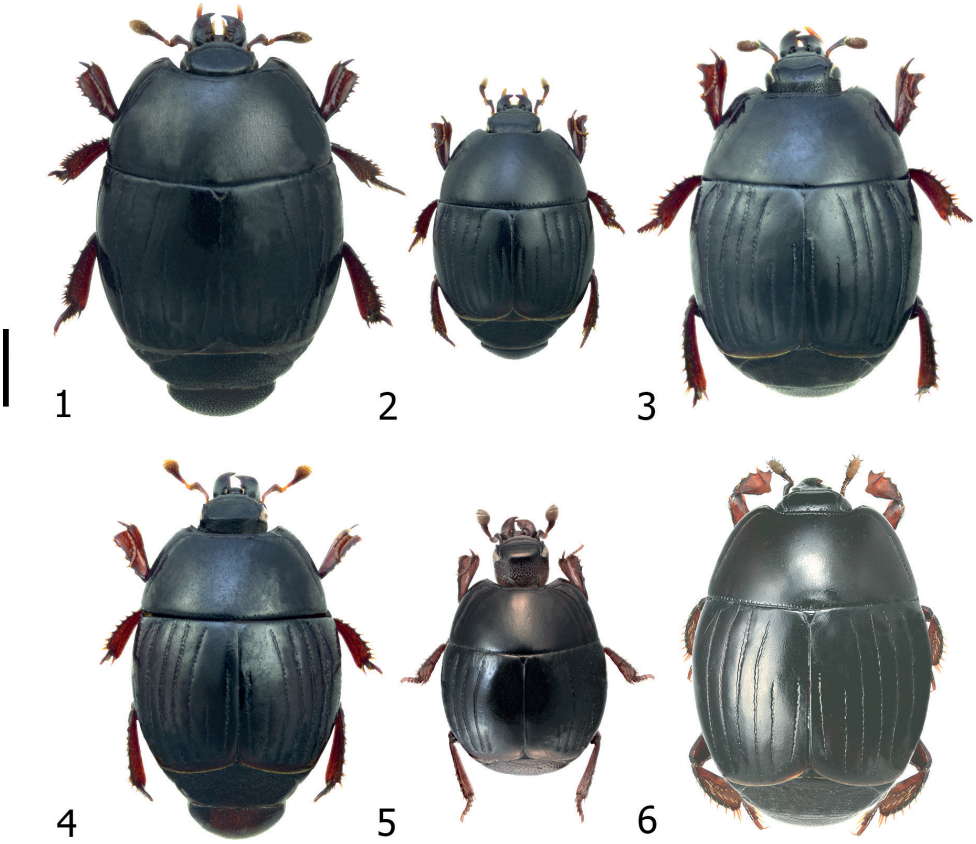

Figures 1–6. Philippine *Atholus*, dorsal habitus **1** *A. philippinensis* (Marseul, 1854) [IC-21-18] **2** *A. coelestis* (Marseul, 1857) [IC-21-20] **3** *A. torquatus* (Marseul, 1854) [IC-21-49] **4** *A. pirithous* (Marseul, 1873) [IC-21-47] **5** *A. nitidissimus* Desbordes, 1925 [syntype image] **6** *A. bakeri* (Bickhardt, 1914) [syntype image, No. 1639]. Scale bar: 1.00 mm.

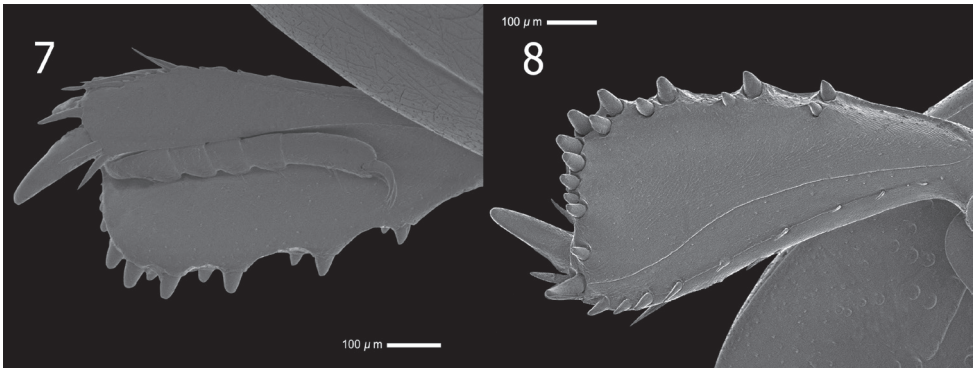

Figures 7, 8. *Atholus philippinesis* (Marseul, 1854) [IC-21-18] **7** protibia, dorsal view **8** ditto, ventral view.

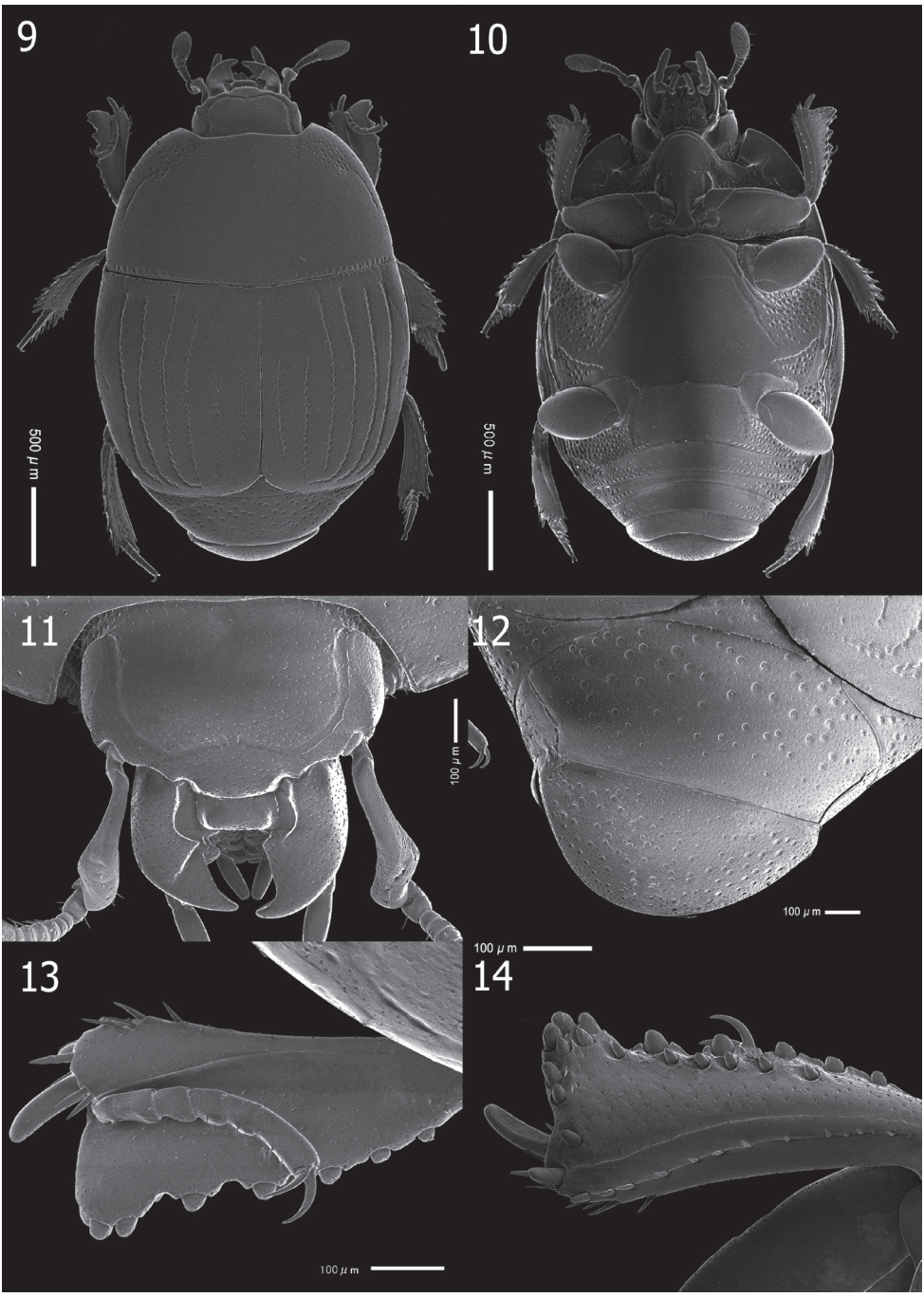

Figures 9–14. *Atholus coelestis* (Marseul, 1857) [IC-21-20] **9** habitus, dorsal view **10** ditto, ventral view **11** head, dorsal view **12** propygidium and pygidium **13** protibia, dorsal view **14** ditto, ventral view.

Atholus coelestis: Lewis 1906: 402; 1915: 55 [Formosa=Taiwan]; Mazur 1984: 212; 1997: 129; 2011: 104 [catalogued]; Mazur et al. 2015: 1454 [Philippines]; Ôhara, 1992: 173–176; 1994: 137; 1999: 110 [Nansei Islands]; 1999b: 31–32 [Taiwan].
Atholus (*Euatholus*) *coelestis*: Hisamatsu and Kusui 1984: 17 [noted, key].
Atholus (*Euatholus*) *coelestes* [sic]: Hisamatsu 1985: 228, pl. 41, f. 61 [noted, key, image].
Hister femoralis Motschulsky, 1863: 449, synonymized by Lewis 1885: 465.

Specimens examined. 13 ♂♂, 2 ♀♀ and 4 specimens of undetermined sex. **Luzon Island,** Isabela, Angadanan, Pissay, 1 ♂, 16.44207°N, 121.46277°E 60 m a.s.l., 2019-VII-20 [IS-19-IDC-001], I.N. DELA CRUZ leg.; Pangasinan, Asingan, Bantog, 1 ♂, 15.59384°N, 120.41151°E 50 m a.s.l., 2019-VII-22 [PG-19-IDC-001], I.N. DELA CRUZ leg.; Batangas, Calatagan, Balitoc, 1 ♀, 13.51417°N, 120.38138°E 10 m a.s.l., 2019-VI-26 [BG-19-IDC-001], I.N. DELA CRUZ leg. **Mindoro Island,** Oriental Mindoro, Mt. Halcon, 1 ex., 2005-IV. **Panay Island**, Capiz, Dumarao, Bugsuan, 3 ♂♂, 11.14422°N, 122.44405°E 76 m a.s.l., 2019-VIII-03 [CP-19-IDC-001], I.N. DELA CRUZ leg.; Antique, Patnongon, Igbobon, 1 ♂, 1 ex. [IC-21-20], 10.55434°N, 121.59592°E -10 m a.s.l., 2019-VIII-02 [AQ-19-IDC-001], I.N. DELA CRUZ leg.; Iloilo, Calinog, Simsiman, 1 ♂, 11.07008°N, 122.32289°E 70 m a.s.l., 2019-VIII-01 [II-19-IDC-001], I.N. DELA CRUZ leg. **Guimaras Island,** Guimaras, Jordan, Alaguisoc, 1 ♂, 10.37576°N, 122.36379°E 153 m a.s.l., 2019-VII-30 [GU-19-IDC-001], I.N. DELA CRUZ leg. **Negros Island,** Negros Occidental, La Carlota, La Granja, 1 ♂, 10.23566°N, 122.59334°E 90 m a.s.l., 2019-VII-29 [NC-19-IDC-002], I.N. DELA CRUZ leg.; Negros Occidental, Mt. Canlaon, 1 ex., 1988-IV-11-30, D. MOHGAN leg.; Negros Oriental, Tanjay, Azagra, 1 ex., 09.29363°N, 122.08473°E 0 m a.s.l., 2019-VII-31 [NR-19-IDC-001], I.N. DELA CRUZ leg. **Cebu Island,** Cebu, Tuburan, Poblacion, 1 ♂, 10.43204°N, 123.49155°E 15 m a.s.l., 2019-VII-27 [CE-19-IDC-001], I.N. DELA CRUZ leg. **Mactan Island,** Buyong Maribago, Lapulapu City, 1 ex., 1996-IV-3, S. SHIMANO leg. **Mindanao Island,** Agusan del Norte, Butuan, Tiniwisan, 1 ♂, 1 ♀ [IC-21-11], 08.57694°N, 125.35521°E 20 m a.s.l., 2021-V-01 [AN-21-IDC-001], I.N. DELA CRUZ leg.; Taligaman, 2 ♂♂, 08.56894°N, 125.38534°E 60 m a.s.l., 2021-VI-14 [AN-21-IDC-003], I.N. DELA CRUZ leg.

Diagnosis. *Atholus coelestis* (Marseul, 1857) is best characterized by its third dorsal elytral stria extending inwardly towards the apical end of the fourth and fifth striae. The slight emargination on the anterior margin of the mesoventrite is also a distinct character of this species. The number of denticles of the protibia (Figs 13, 14), is 11 on the outer margin, one one the inner apical angle, and eight on the outer sublateral margin. The protibial teeth are slightly prominent only on the outer apical angle, topped with three denticles. The number of denticles on the outer margin may range from 11–13 denticles. The shape of the gonocoxite of *A. coelestis* (Marseul, 1857) is slenderer, becoming narrower towards the apex compared to *A. philippinensis* (Marseul, 1854). Moreover, the presence of a single occipital fovea on the posterior portion

of the head of *A. coelestis* (Marseul, 1857) (Fig. 11) is rather a remarkable character differentiating it from other species that has not been previously described.

Additional description. ***Female genitalia*:** anterior portion of valvifers (Figs 38, 39) paddle-shaped; gonocoxite (Fig. 40) elongate, almost 4× as long as broad, not shovel-like, more narrowed on apical end; inner and outer surfaces differentiated; inner face weakly separated from outer face by elevated lateral ridge; sclerotized setae on apical half of outer face short and sparse; inner face with short setae and moderate setae; apex of gonocoxite with two teeth; gonostyli present, freely articulated; spermathecae multiple, consisting of four sacs; sacs gradually enlarged and elongate, not sclerotized.

Distribution. Widely distributed in the Oriental Region including China, Taiwan, Ryukyu Islands (Japan). Also present in the Palearctic Region: Tajikistan and in the Afrotropical Region: Comoros Islands (Mazur 2011).

Biology. All individuals of *A. coelestis* (Marseul, 1857) were collected from dungs of cows and water buffaloes of lowland farms and pastures across all islands of the archipelago. This species may also seem to be moisture-specific, as they were observed to dwell only on more desiccated dungs during field collection.

Remarks. *Atholus coelestis* (Marseul, 1857) (Fig. 2) is a widespread species across the Philippine archipelago showing a consistent morphology in all individuals examined. *Atholus coelestis* (Marseul, 1857) was re-described by Ôhara (1992) based on specimens collected from Ryukyu Islands (Japan). Here, SEM micrographs (Figs 9–14) and illustrations of female gonocoxite and valvifers (Figs 38–40) complement Ôhara's description (1992).

Atholus torquatus (Marseul, 1854)

Figs 3, 15–28, 29–34, 41–43

Hister torquatus Marseul, 1854: 587 [India].
Hister (*Atholus*) *torquatus*: Bickhardt 1910: 55 [catalogued]; 1917: 194 [catalogued].
Atholus torquatus: Lewis 1906: 402; Mazur 1984: 218; 1997: 134; 2011: 106 [catalogued]; 2015: 1454.
Hister genuae Lewis, 1888: 639; synonymized by Bickhardt 1913b: 698.
Atholus genuae: Lewis 1906: 402.
Hister mundulus Lewis, 1902: 238; synonymized by Desbordes 1919: 399.

Specimens examined. 8 ♂♂, 14 ♀♀ and 7 exs. **Luzon Island,** Bataan, Abucay, Gabon, 8 ♂♂ [IC-21-23], 12 ♀♀ [IC-21-53], 5 exs., 14.42329°N, 120.26222°E 570 m a.s.l., 2019-VII-21 [BA-19-IDC-001], I.N. DELA CRUZ leg.; Laguna, Northern Lucena, Kinabuhayan, 2 ♀♀ [IC-21-49], 1989-II, N. Monreal leg. **Mindoro Island,** Oriental Mindoro, Mt. Halcon, 1 ex., 2005-IV. **Palawan Island,** Puerto Princesa, Barrio Talabigan, 1 ex., 1979-III-24, K. Wada leg.

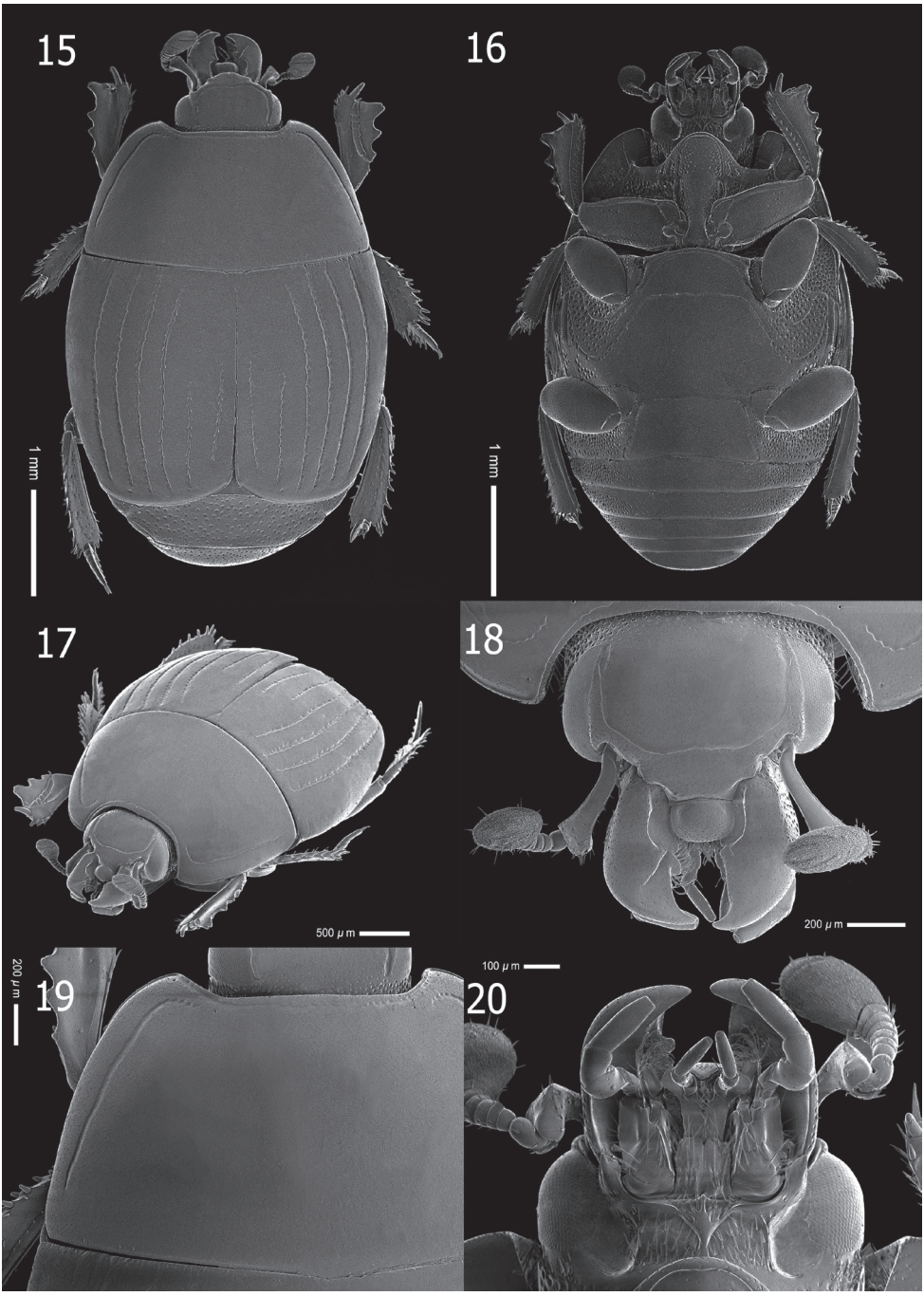

Figures 15–20. *Atholus torquatus* (Marseul, 1854) [IC-21-23] **15** habitus, dorsal view **16** ditto, ventral view **17** ditto, oblique view **18** head, dorsal view **19** pronotum **20** mouthparts, ventral view.

Diagnosis. *Atholus torquatus* (Marseul, 1854) is recognized with a combination of its interrupted lateral pronotal stria in the anterolateral angle, and fine punctations on the apical portion of its pygidium. This species also possesses remarkable teeth of protibia, increasing in size apically. The structure of the female genitalia of this species is described here for the first time, showing its similarity to the shape of the gonocoxite of *A. philippinensis* (Marseul, 1854), which is broad and shovel-like.

Re-description. Male and female. ***Body length*****:** PEL: 3.13–4.32 mm; APW: 1.11–1.47 mm; PPW: 2.35–2.90 mm; EL: 1.89–2.74 mm; EW: 2.66–3.56 mm. Body (Figs 3, 15–17) oval, moderately convex and black; tibiae, antennae, mouthparts and apical elytral margin rufous.

Head**:** apical margin of clypeus (Fig. 18) short, entire and slightly forward, but anterolateral margin widely crenate; frontal stria rounded, complete and deeply impressed; disk sparsely clothed with fine punctures, separated by 2–3× their diameter; interspaces with alutaceous microsculpture; occipital fovea absent; labrum dorsally finely punctate, raised and transversely long; short labral fringe (Lackner, 2010) present antero-laterally; mandibles covered with fine and even punctures, outer margin rounded, curved inwardly; sub-apical tooth on left mandible large; mandibular apex acutely pointed; eyes large and convex, clearly visible dorsally.

Pronotum**:** marginal pronotal stria laterally complete, continuous onto apical angle and behind head; lateral pronotal stria (Fig. 19) deeply impressed, slightly crenate and complete; lateral stria rather distant from margin, its basal end abbreviated to basal fourth of pronotal length; apical end bent inwardly behind apical angle; anterior pronotal stria absent; disk with sparse microscopic punctures, wholly covered with alutaceous microsculpture; area behind apical angles bare; posterior margin without row of coarse punctures; ante-scutellar region with a single short longitudinal puncture.

Elytra**:** basal margin with a row of short, longitudinal striae; elytral epipleuron sparsely clothed with fine punctures, with few, coarse punctures on apical half; marginal epipleural stria present on apical half; marginal elytral stria complete, moderately impressed; external subhumeral stria (Fig. 22) generally absent, occasionally noticeable on basal half, abbreviated on basal eighth; internal subhumeral stria absent; oblique humeral elytral stria slightly impressed on basal third; dorsal elytral striae 1–4 (Fig. 21) complete; elytral stria 5 present on apical half; sutural elytral stria abbreviated on basal third; elytral disk covered with sparse, fine punctures, separated by 3–4× their diameter; medio-basal area with alutaceous ground sculpture.

Propygidium and pygidium**:** propygidium (Fig. 26) densely covered with coarse, round and shallow punctures, about 25 μm in diameter, separated by 1–4× their diameter; interspaces with irregular, sparse and fine punctations, separated by 2–3× their diameter; surface with alutaceous sculpture; pygidial punctation (Fig. 25) similar to that of propygidium, coarse punctures of pygidium becoming sparser and finer apically; interspaces with fine punctations.

Prosternum**:** prosternal lobe with anterior margin (Fig. 23) round; medio-apical end of prosternal lobe ascending; marginal prosternal stria deeply impressed, carinate and shortly interrupted medially; short striae present on both baso-lateral corners; lobe with few setiferous coarse punctures inside and outside of marginal stria on both sides,

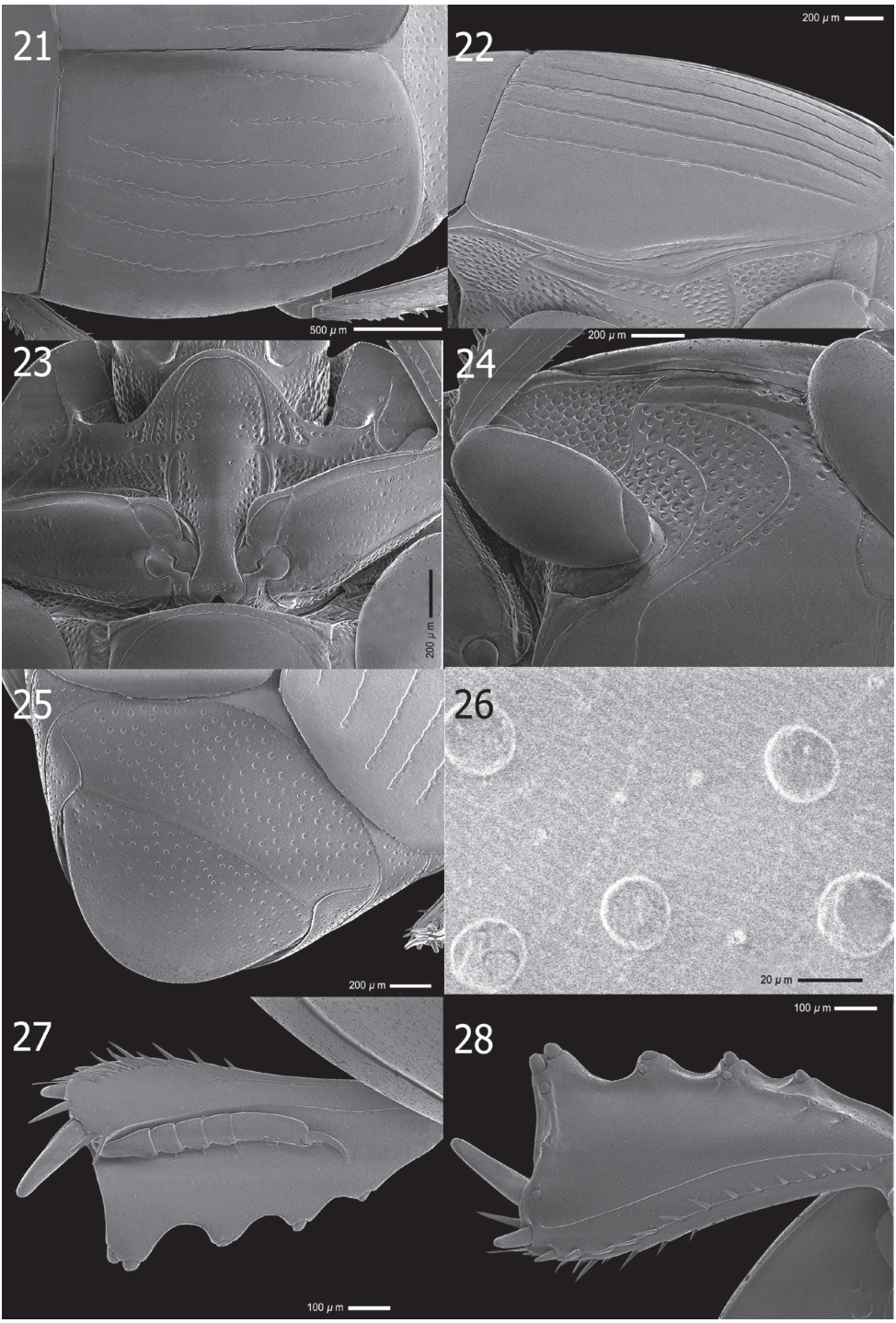

Figures 21–28. *Atholus torquatus* (Marseul, 1854) [IC-21-23] **21** elytra, dorsal view **22** ditto, oblique view **23** prosternal process **24** meso-and metaventrite **25** propygidium and pygidium **26** propygidium (punctation) **27** protibia, dorsal view **28** ditto, ventral view.

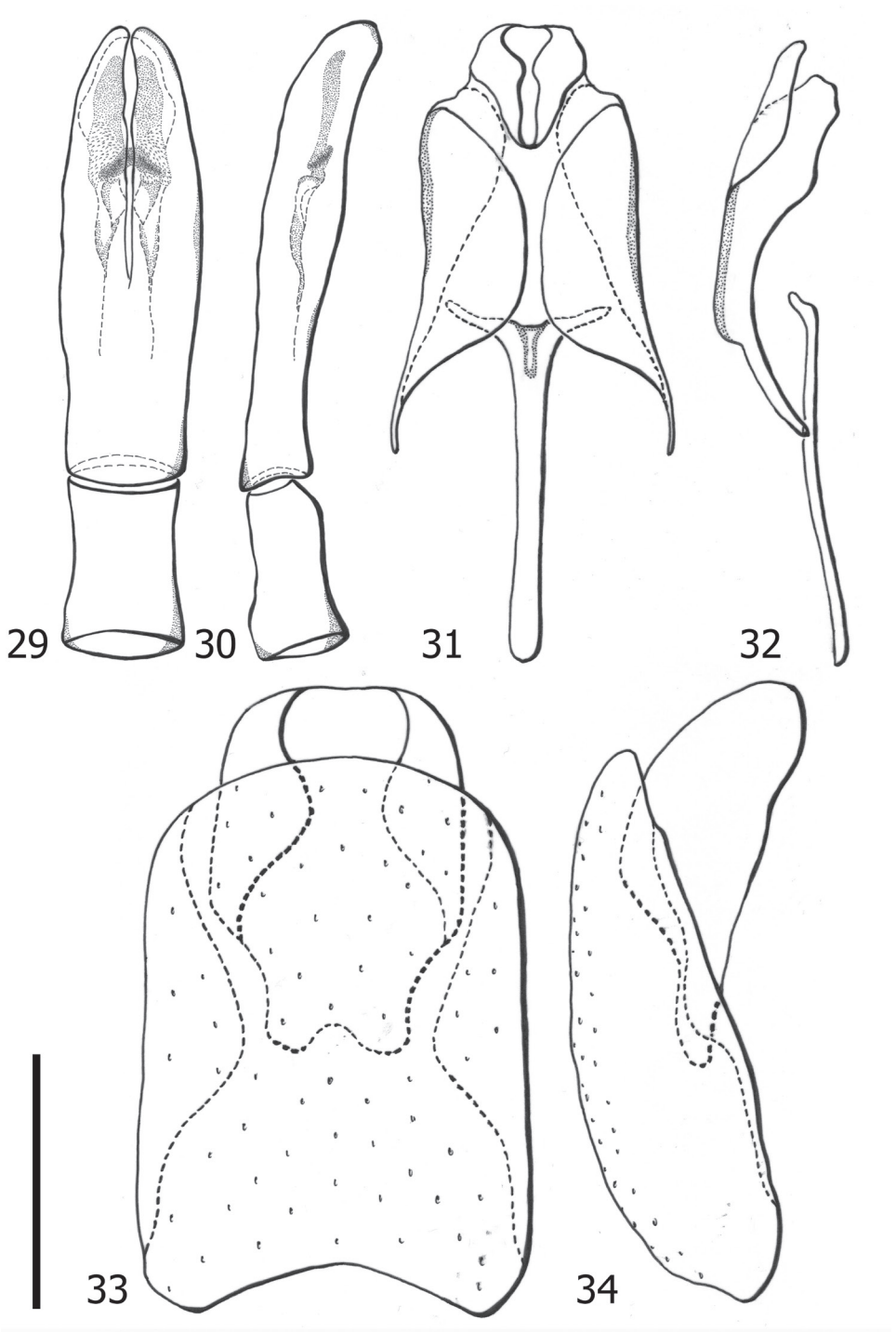

Figures 29–34. *Atholus torquatus* (Marseul, 1854), male genitalia [IC-21-23] **29** aedeagus, dorsal view **30** ditto, lateral view **31** ninth and tenth tergites, dorsal view **32** ditto, lateral view **33** eighth tergite and sternite, dorsal view **34** ditto, lateral view. Scale bar: 0.50 mm.

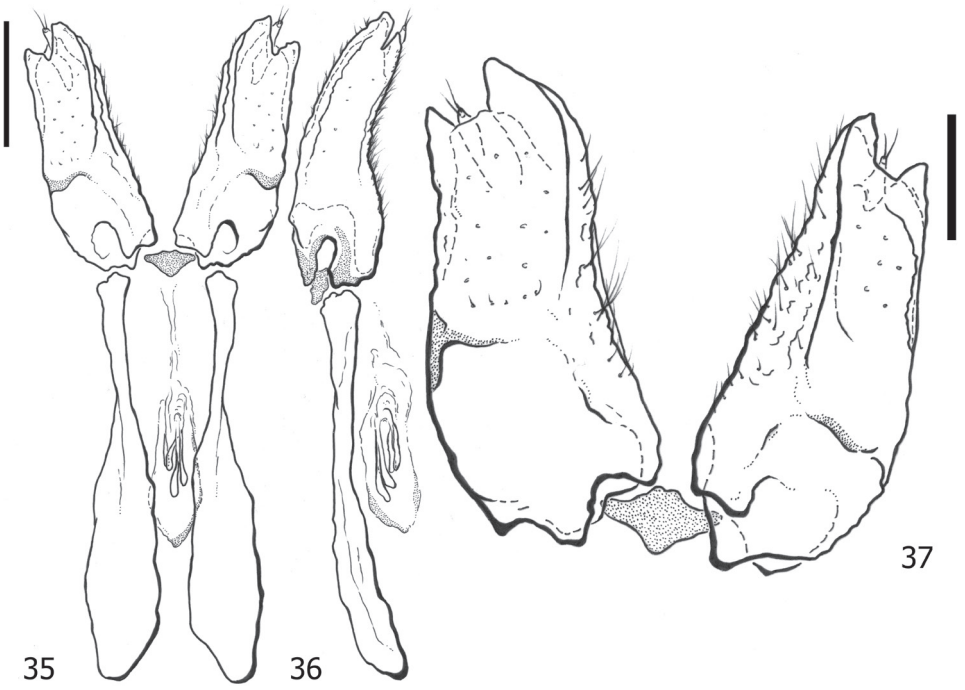

Figures 35–37. *Atholus philippinensis* (Marseul, 1854), female genitalia [IC-21-18] **35** dorsal view **36** lateral view **37** dorsolateral view of gonocoxite. Scale bars: 0.20 mm.

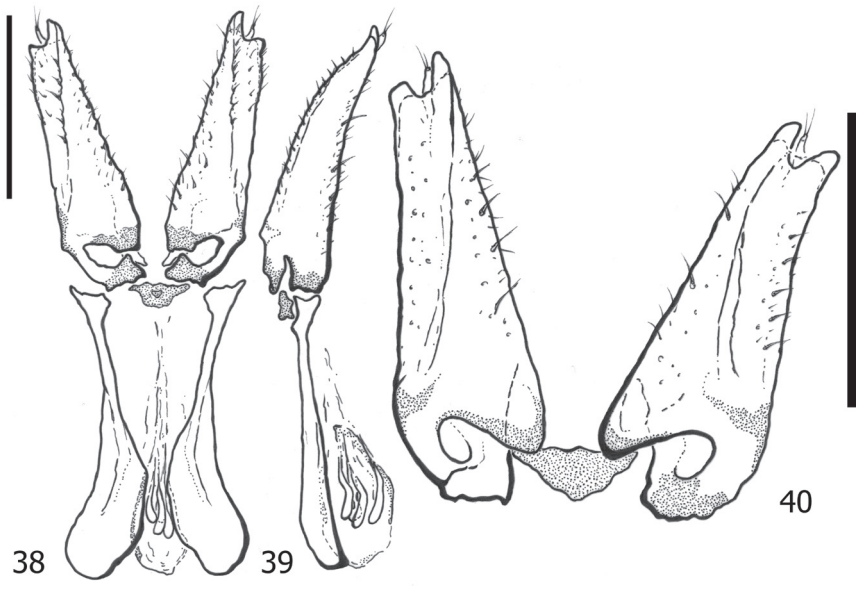

Figures 38–40. *Atholus coelestis* (Marseul, 1857), female genitalia [IC-21-11] **38** dorsal view **39** lateral view **40** dorsolateral view of gonocoxite. Scale bars: 0.20 mm.

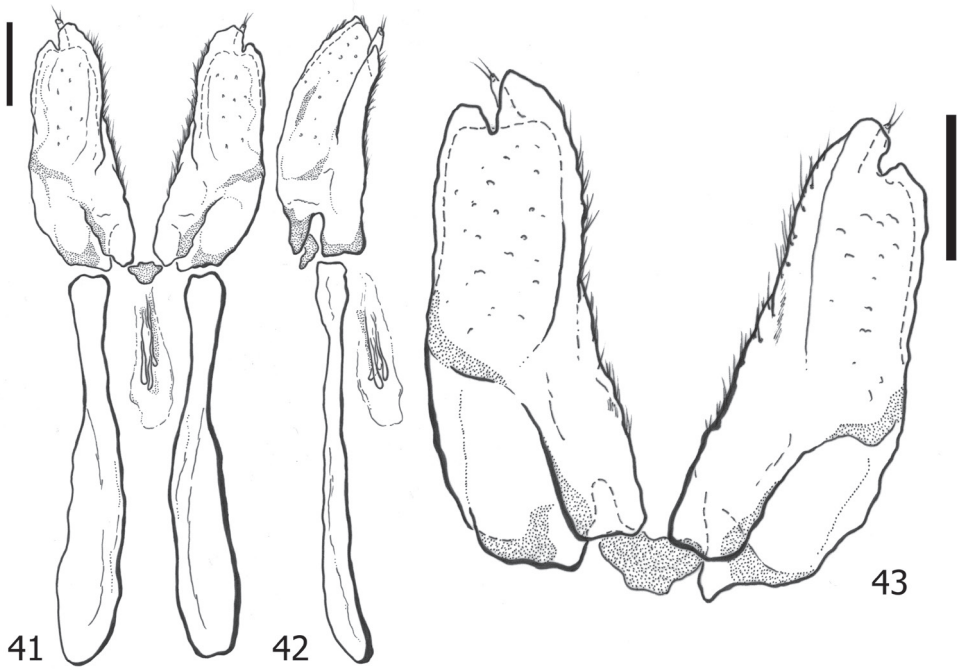

Figures 41–43. *Atholus torquatus* (Marseul, 1854), female genitalia [IC-21-53] **41** dorsal view **42** lateral view **43** dorsolateral view of gonocoxite. Scale bars: 0.20 mm.

separated by their 1–2× their diameter; disk covered with sparse, finer punctures on apical half; prosternal suture lightly impressed; prosternal process covered with few, setiferous fine punctures; lateral sides descending; lateral prosternal striae deeply impressed and complete; lateral disk with several coarse setiferous punctures; basal half narrow; posterior margin of basal lobe strongly emarginated.

***Meso- and metaventrite*:** anterior margin of mesoventrite outwardly arcuate (Fig. 24); marginal mesoventral stria complete, carinate, sparsely crenate; stria behind anterolateral angle present; mesoventral disk sparsely clothed with fine punctures separated by 4–5× their diameter; meso-metaventral suture clearly impressed, complete and medially angulate; lateral metaventral stria deeply impressed, carinate, extending obliquely and posteriorly, united with oblique stria which inwardly extends from basal third of metaventro-metepisternal suture; post-mesocoxal stria extending posteriorly and strongly curved along posterior mesocoxal margin, almost attaining metaventro-mesepimeral suture; punctures of metaventral disk similar to those of mesoventrite; a row of coarse punctures present along inside lateral metaventral stria; longitudinal suture of metaventrite lightly impressed; lateral disk of metaventrite moderately covered with setiferous large round and shallow punctures; interspaces with sparse, coarse to fine punctations; mesepimeron, metepimeron and lateral disk of first abdominal ventrite with dense setiferous, large

punctures; interspaces with few coarse to fine punctations; metepisternum with sparse punctures on apical half; punctation of intercoxal disk of first abdominal ventrite similar to that of metaventrite; lateral stria deeply impressed, slightly carinate and complete.

***Legs*:** anterior face of protibia (Fig. 27) flattened, dilated and clothed with few, fine ocelloid punctures; basal to median area with weak strigate sculpture; outer lateral margin with four teeth, becoming stronger apically; topped by minute denticles; protarsal groove shallow, with few coarse punctures; anterior protibial stria lightly impressed; inner marginal stria present on basal half, along stria a slightly depressed with row of coarse punctures present; near tarsal insertion with two spine-like tarsal denticles; another one, more distant and longer, located at inner anterior angle; protibial spur moderately long, wider on basal margin, approximately half the length of protarsus; posterior face of protibia (Fig. 28) with sparse, fine punctures and strigate ground sculpture from basal to median surface; number of denticles on outer margin eight, one on inner apical angle, outer sublateral margin three or four; median posterior stria moderately impressed and abbreviated on apical end; inner posterior stria moderately impressed with row of sclerotized setae, terminating in three inner posterior denticles; inner margin of setae present on apical half, with a row of short setae on basal half; inner margin with strigate ground sculpture; profemur sparsely clothed with fine, ocelloid punctations; surface with lightly strigate ground sculpture; marginal stria complete; anterior stria present on apical half; femoral stria almost complete, shortened on basal end; posterior margin with large punctations; a row of setae present on both basal and apical ends.

***Genitalia*:** aedeagus (Figs 29, 30) moderately slender, apically slightly curved ventrad; parameres relatively longer, about as almost as thrice the length of phallobase, slightly fused on basal half; median lobe sclerotized; eighth tergite (Figs 33, 34) entire, with longitudinal fold on both lateral sides; ninth tergite (Figs 31, 32) with lateral folds; tenth tergite dorsally longitudinally divided; spiculum gastrale almost as same length as ninth tergite.

Anterior portion of valvifers (Figs 41, 42) paddle-shaped; gonocoxite (Fig 43) slightly elongate, almost as twice as long as broad, shovel-like; inner and outer surfaces differentiated; inner face moderately separated from outer face by elevated lateral ridge; sclerotized setae on apical half of outer face short and slightly dense; inner face with short and sparse setae; apex of gonocoxite with two teeth; gonostyli present, freely articulated; spermathecae multiple, consisting of four sacs; sacs gradually enlarged and elongate, not sclerotized.

Distribution. Widespread in the Oriental Region including Indonesia, Myanmar, Laos, Thailand, Vietnam, India, Nepal, and China (Sichuan) (Mazur 2011); Philippines (new record).

Biology. *Atholus torquatus* (Marseul, 1854) were collected within the dung of cows located in a higher elevation and semi-forested area. The substrate also differs from *A. coelestis* (Marseul, 1857), as *A. torquatus* (Marseul, 1854) was typically observed in soggy, moist dung.

Remarks. *Atholus torquatus* (Marseul, 1854) is a quite variable species regarding the external subhumeral stria on its elytra, either clearly marked or totally absent. This character is also mentioned by Desbordes (1917) who mentions the stria can be aberrant. Although the type specimen of *A. torquatus* (Marseul, 1854) according to the original description possesses no external subhumeral stria, we have examined one specimen with the subhumeral stria present. This corresponds to Desbordes' (1917) observation. Our observations confirm the variability of this character among specimens ranging across Continental as well as Insular Southeast Asia. On the other hand, male and female genitalia exhibit little variation. We therefore propose to drop the external subhumeral stria as the primary key character for delimiting this species from others.

Atholus pirithous (Marseul, 1873)

Figs 4, 44–49

Hister pirithous Marseul, 1873: 224 [Japan: Hiogo and Nangasaki].
Hister (*Atholus*) *pirithous*: Bickhardt 1910: 54 [catalogued]; 1913: 173; 1917: 194 [catalogued]; Desbordes 1919: 400 [Tonkin]; 1921: 10; Kamiya and Takagi 1938: 31 [listed]; Ôsawa and Nakane 1951: 7.
Atholus pirithous: Lewis 1906, 402; 1915, 55 [Formosa = Taiwan]; Nakane 1981: 10; Mazur 1984: 215; 1997: 132; 2009: 115; 2011: 106 [catalogued]; Mazur et al. 2014: 1269.
Atholus (*Euatholus*) *pirithous*: Kryzhanovskij and Reichardt 1976: 390; Hisamatsu and Kusui 1984: 23; Hisamatsu 1985: 223, pl. 41, fig. 19 [key; noted; image]; Ôhara 1993: 141–147; 1994: 138; 1999: 110 [Japan]; 1999b: 36 [Taiwan].
Hister reitteri Bickhardt, 1918: 231 [Japan]; synonymized by Reichardt 1930: 48; Kamiya and Takagi 1938: 31 [listed].
Hister pirithous ab. *reitteri*: Reichardt 1930: 48.

Specimens examined. Seven specimens of undetermined sex. **Luzon Island,** Laguna, northern Lucena, Kinabuhayan, 7 exs. [IC-21-47], 1994-V-VI, N. Monreal leg.

Diagnosis. *Atholus pirithous* (Marseul, 1873) is generally recognized for its light excavation in the area behind the anterolateral angle of the pronotum.

Distribution. Japan, Russia: Far East, China (Guandong, Shanghai), Korea, Taiwan, Vietnam, Nepal, Oman (Mazur 2011); Philippines (new record).

Biology. Unknown.

Remarks. All seven examined individuals of *Atholus pirithous* (Marseul, 1873) (Fig. 4) lack internal subhumeral stria, but traces of dots and short lines can be observed in the apical end. The outer apical protibial tooth of this species is moderately prominent, topped by three denticles. The total number of protibial denticles on the outer margin

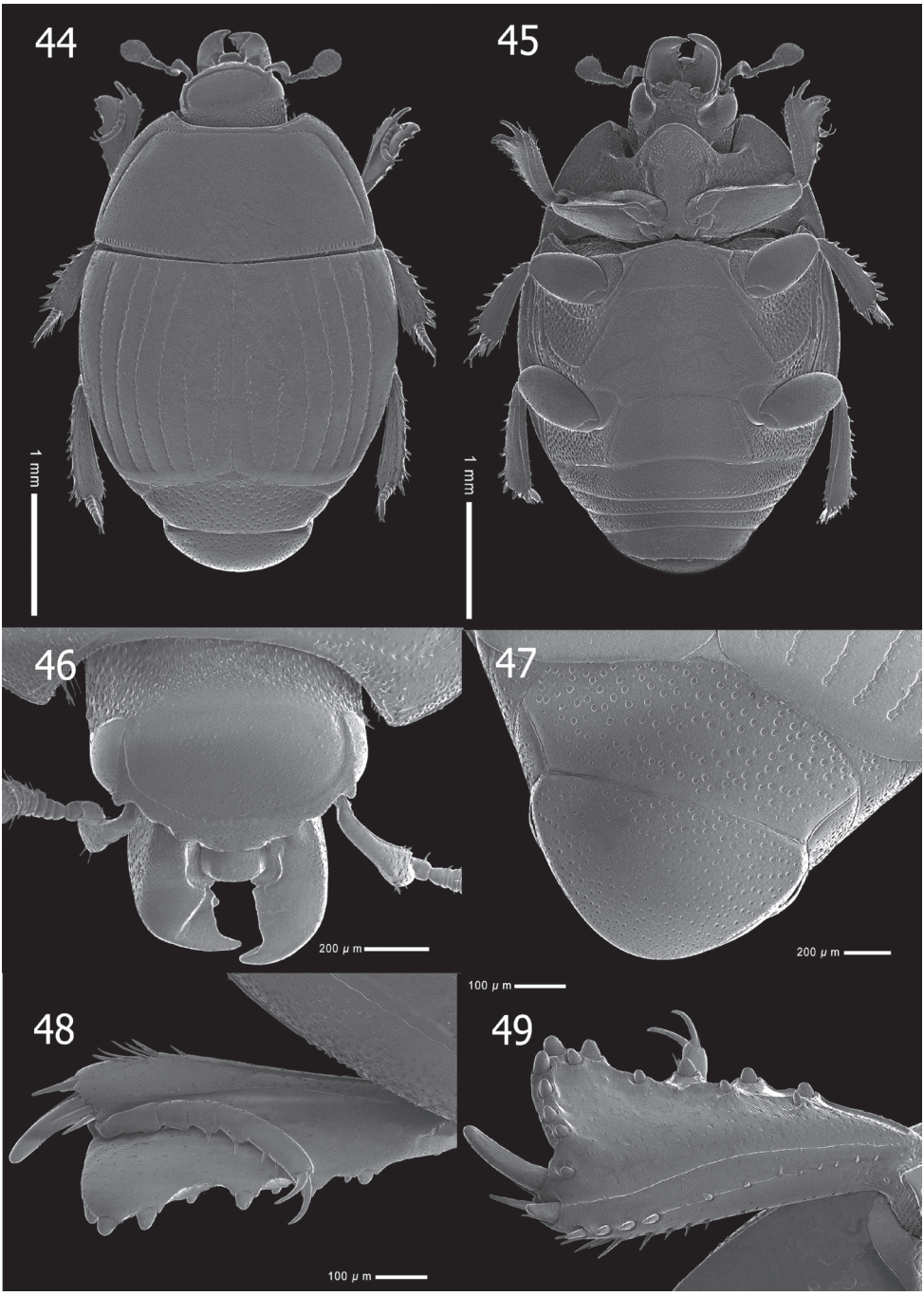

Figures 44–49. *Atholus pirithous* (Marseul, 1873) [IC-21-47] **44** habitus, dorsal view **45** ditto, ventral view **46** head, dorsal view **47** propygidium and pygidium **48** protibia, dorsal view **49** ditto, ventral view.

is ten, one on the inner apical angle (Figs 48, 49), compared with the Japanese specimens described that bore only nine denticles (Ôhara, 1993), but the outer sublateral margin of the Philippine species has only four denticles; when compared to Ôhara (1993) who observed five to six denticles. Moreover, all examined specimens lost their genitalia prior to examination.

Atholus nitidissimus Desbordes, 1925

Figs 5, 50–53

Atholus nitidissimus Desbordes, 1925: 87 [**Leyte Island**]; Mazur 1984: 215; 1997: 131; 2011: 105 [catalogued].

Specimens examined. Two syntypes of undetermined sex housed in MNHN have been examined by N. Dégallier. The following re-description is based on images provided by him.

Diagnosis. This species is easily distinguished by its almost circular body and absence of sutural elytral striae. Judging by the images of two examined syntypes, this species is clearly distinct in its pattern of dorsal elytral striation, differing from other species by the absence of the fifth or sutural elytral striae. *Atholus nitidissimus* Desbordes, 1925 (Fig. 5) is similar to *A. coelestis* (Fig. 2), albeit it is comparatively smaller in size than other species examined.

Re-description. ***Body*** **(Fig. 5)** ***length*****:** PEL: 2.15 mm; APW: 0.85 mm; PPW: 1.75 mm; EL: 1.15 mm; EW: 1.95 mm. Body almost circular, convex, and black; tibiae and antennae rufous.

Head**:** clypeus (Fig. 50) slightly crenate on anterolateral margin, apical margin projecting; frontal stria round, complete, and moderately impressed; eyes clearly visible dorsally; mandibles with rounded outer margin curved inwardly; mandibular apex acutely pointed.

Pronotum**:** marginal pronotal stria (Fig. 50) laterally complete, continuous onto the apical angle and behind head; lateral pronotal stria moderately impressed; apical end shortened and bent inwardly; lateral portion rather distant from margin; its basal end obsolete on basal sixth of pronotal length.

Elytra**:** external and internal subhumeral striae absent (Fig. 5); oblique humeral elytral stria lightly impressed on basal third; dorsal elytral striae 1–3 complete; elytral stria 4 present on apical half or shorter; elytral stria 5 either absent or very short; sutural elytral stria absent.

Propygidium and pygidium**:** propygidium (Fig. 51) moderately covered with coarse, round, and shallow punctures; interspaces with fine punctations; pygidial punctures similar to those of propygidium, albeit slightly denser.

Prosternum**:** anterior margin of prosternal lobe (Fig. 52) round; medio-apical end ascending; marginal prosternal stria impressed, shortly interrupted medially; short striae

Figures 50–53. *Atholus nitidissimus* Desbordes, 1925 **50** anterior view **51** ditto, caudal view **52** prosternal process **53** habitus, ventral view.

present on both baso-lateral ends; prosternal lobe with several punctures alongside marginal prosternal stria on both sides; entire disk covered with finer punctures; prosternal suture moderately impressed; prosternal process with few fine punctures; lateral sides descending; lateral prosternal striae deeply impressed; basal half of prosternal process narrow.

***Meso- and metaventrite*:** anterior margin of mesoventrite (Fig. 53) truncate; marginal mesoventral stria complete; meso-metaventral suture clearly impressed, complete and carinate; lateral metaventral stria moderately impressed, carinate, extending obliquely and posteriorly, united with oblique humeral stria that inwardly extends from metaventro-metepisternal suture; post-mesocoxal stria extending posteriorly, strongly curved along the posterior mesocoxal margin, almost attaining the metaventro-mesepimeral suture; punctation of intercoxal disk of metaventrite similar to that of mesoventrite; longitudinal suture of metaventrite lightly impressed; lateral disk of metaventrite moderately covered with large, round, shallow punctures.

***Legs*:** posterior surface of protibia (Figs 52, 53) flattened and dilated; outer lateral margin with four teeth, topped with minute denticles.

Distribution. Endemic to the Philippines (Mazur 2011).

Biology. Unknown.

***Atholus bakeri* (Bickhardt, 1914)**
Figs 6, 54–57

Hister bakeri Bickhardt, 1914: 428 [Luzon Island].
Hister (*Atholus*) *bakeri*: Bickhardt 1917: 193 [catalogued].
Atholus bakeri: Bickhardt 1914: 428; Mazur 1984: 211; 1997: 129; 2011: 103 [catalogued].

Specimens examined. 1 syntype [**Luzon Island**] based on images, "*Atholus bakeri* n. sp. Bickh. / Los Banos, / P.I., Baker. / 1639" [sex undetermined, measurements not available] (MNHUB).

Diagnosis. This species has lateral pronotal striae interrupted in the anterolateral angle, and strong punctations on its entire pygidium. According to the original description of Bickhardt (1914), *Atholus bakeri* (Bickhardt, 1914) is most similar to *A. torquatus* (Marseul, 1854) except that the propygidium and pygidium of *A. bakeri* (Bickhardt, 1914) are strongly punctate. However, based on the syntype observed, the punctation is not as prominent as described and, in fact quite similar to that of *A. torquatus* (Marseul, 1854). The punctures are finer towards the apical end of the pygidium. Another distinguishable feature of *A. bakeri* (Bickhardt, 1914) is the medially straight frontal stria, while in *A. torquatus* (Marseul, 1854) it is weakly bent inwardly. However, several studied individuals of *A. torquatus* (Marseul, 1854) likewise seem to have their frontal stria medially straight.

Re-description. ***Body*** (Fig. 6) oval, moderately convex and black; tibia and antenna rufous.

Head**:** clypeus (Figs 54, 55) slightly crenate on anterolateral margin, apical margin slightly extended; frontal stria medially straight, complete, moderately impressed; eyes large, convex, clearly visible dorsally; mandibles with rounded outer margin curved inwardly; sub-apical tooth on left mandible large; mandibular apex acutely pointed.

Pronotum**:** marginal pronotal stria (Figs 54, 55) laterally complete, continuous onto apical angle and crenate behind head; lateral pronotal stria moderately impressed, slightly crenate; apical end shortened and bent inwardly in a curved hook; lateral portion rather distant from margin; its basal end abbreviated from basal fifth of pronotal length.

Elytra**:** elytral epipleuron (Fig. 57) with few coarse punctures on apical half; marginal epipleural stria present on apical half; marginal elytral stria (Fig. 6) complete, slightly impressed; external and internal subhumeral striae absent; oblique humeral stria lightly impressed on basal third; dorsal elytral striae 1–4 complete; dorsal elytral stria 5 and sutural elytral stria present on apical half; disk with fine punctures.

Abdomen**:** propygidium (Fig. 56) moderately covered with coarse, round, and shallow punctures; interspaces with fine punctations; pygidial punctations similar to those of propygidium, becoming sparser apically.

Meso- and metaventrite**:** anterior margin of mesoventrite (Fig. 57) outwardly arcuate; marginal mesoventral stria crenate and complete; meso-metaventral suture

Figures 54–57. *Atholus bakeri* (Bickhardt, 1914) **54** head and pronotum, dorsal view **55** head, frontal view **56** propygidium and pygidium **57** habitus, ventral view.

clearly impressed, complete, medially angulate; punctations of intercoxal disk of metaventrite similar to those of mesoventrite; longitudinal suture of metaventrite lightly impressed; lateral disk of metaventrite moderately covered with large, round, shallow punctures.

***Legs*:** posterior surface of protibia (Fig. 57) flattened and strongly dilated; outer lateral margin with four weak, almost inconspicuous teeth, topped by minute denticles.

Distribution. Endemic to the Philippines (Mazur 2011).

Biology. Unknown.

Remarks. The examined syntype of *A. bakeri* (Bickhardt, 1914) exhibits characters similar to a typical *A. torquatus* (Marseul, 1854). According to Desbordes (1917), *A. torquatus* (Marseul, 1854) and *A. bakeri* (Bickhardt, 1914) are very similar, being set apart by the pygidial punctation (strong in *A. bakeri* and apically finer in *A. torquatus*). Although the only examined specimen of *A. bakeri* (Bickhardt, 1914) possesses similar pygidial punctations to *A. torquatus* (Bickhardt, 1914), this character remains the primary distinction until further examinations of other types is established. The authors would also encourage a comprehensive observation of both male and female genitalia for future works.

Discussion

Structures of the protibia in almost all Oriental species of *Atholus* were not described in detail in the original descriptions, particularly regarding the number and localization of denticles of protibia. In the previous works of Ôhara (1992, 1993, 1999b), the occurrence of denticles on designated margins such as lateral outer margin, anterior margin, and apical angle were described. However, since the protibial teeth of some *Atholus* species are not as strong as in others, it seems that the denticles on the apical angle may be ambiguously considered as denticles of either the apical margin, or of the outer lateral margin.

The gonocoxites of *A. philippinensis* (Marseul, 1854) and *A. torquatus* (Marseul, 1854) are relatively similar in their forms, appearing to be shovel-like in shape. We have observed this similarity with the gonocoxite of *Atholus bifrons* (Marseul, 1854) (dela Cruz and Ôhara 2022) from Ryukyus (Japan) and Borneo (Indonesia). On the other hand, the shape of the gonocoxite of *A. coelestis* (Marseul, 1857) is narrow and cone-like and becoming slenderer apically. Nevertheless, the number of spermathecal sacs (four) of *A. philippinensis* (Marseul, 1854), *A. coelestis* (Marseul, 1857), *A. torquatus* (Marseul, 1854), and even *A. bifrons* (Marseul, 1854) (dela Cruz and Ôhara 2022) is consistent among these species. Although we have not included this structure in the taxonomic key, since the female genitalia of other species examined were not available, the gonocoxite of *Atholus* might also become a useful tool for morphological diagnosis in the future.

Atholus species are generally widespread throughout the Oriental Region. A few species appear to be endemic to some regions such as *A. nitidissimus* Desbordes, 1925, only recorded so far from the island of Leyte in the Philippines, and *A. bakeri* (Bickhardt, 1914), reported only from Luzon Island hitherto. In this study, *A. coelestis* (Marseul, 1857) is revealed to be a ubiquitous species, spread across the islands of the Philippine archipelago. *Atholus pirithous* (Marseul, 1873) and *A. torquatus* (Marseul, 1854) are new records for Philippines. We examined six species of Philippine *Atholus* in this work; yet, we expect the number to rise in the future since the archipelago is situated in the vicinity of the Greater Sunda Islands in the Indonesian archipelago. It is therefore plausible that other species occurring there might also occur in the Philippines.

Acknowledgements

We would like to give thanks to Tomáš Lackner (Munich, Germany) as well as Nicolas Dégallier (Paris, France), for obtaining the images of *A. bakeri* (Bickhardt, 1914) from MNHUB, and helping with images of the syntype of *A. nitidissimus* Desbordes, 1925 housed in MNHN. Antoine Mantilleri (MNHN) and Bernard Jäger (MNHUB) are acknowledged for their assistance with type specimens. We are also grateful to the following farmlands in the Philippines for allowing us to collect specimens in the field: Philippine Carabao Centers (PCC) [(PCC-Don Mariano Marcos Memorial State University, PCC-La Carlota Stock Farm, PCC-West Visayas State University)], Cagayan

State University-Piat Campus, Rancho Martin Integrated Farm Corp., Hacienda Bigaa, Inc., Department of Agriculture-Antique Research Outreach Station, Guimaras Wonders Farm, Department of Agriculture-Negros Occidental Research Outreach Station, and Foundation University Dairy Focus Farm, as well as to the following people – Jan Marty Guanzon (Bataan), Kim Turaja (Pangasinan), Gilbert Arsenio (Iloilo), and Niño Catalbas (Negros Oriental) who wholeheartedly assisted us during the field collection in various provinces across the country. We would also like to extend our thanks to Maki Murakami and Alyssa Lee Suzumura of Hokkaido University Museum, Sapporo for laboratory assistance, and Dr. Satoshi Shimano of Hosei University, Tokyo for the additional specimens. Lastly, the reviewers, as well as the editor of the Histeroidea at ZooKeys are thanked for their meticulous work, useful comments and edits, thorough grammar check – all of which resulted in high quality of this contribution.

References

Arnett RH (1962) The Beetles of the United States. Washington, 1112 pp.

Auzat V (1916) Histeridae Gallo-Rhénans, Miscellanea Entomologica 24 (1–4): [iii–iv +] 5–66.

Bickhardt H (1910) Histeridae. In: Junk W, Schenkling S (Eds) Coleopterorum Catalogus, pars 24. W. Junk, Berlin, 137 pp.

Bickhardt H (1913) H. Sauter's Formosa-Ausbeute. Histeridae II. (Col.) (16. Beitrag zur Kenntnis der Histeriden). Entomologische Mitteilungen 2: 166–177.

Bickhardt H (1913b) 19. Beitrag zur Kenntnis der Histeriden. Histeridenstudien. Deutsche Entomologische Zeitschrift 1913: 696–701.

Bickhardt H (1914) Philippinische Histeriden: I. Philippine Journal of Science 9(D): 423–429.

Bickhardt H (1917) Histeridae. In: Wytsman P (Ed.) Genera Insectorum, fascicules 166b: 113–302. [La Haye.]

Bickhardt H (1918) Neue paläarktische Histeriden und Bemerkungen zu bekannten Arten (35. Beitrag zur Kenntnis der Histeriden). Entomologische Blätter 14: 226–232.

Bickhardt H (1919) Die Histerini der aethiopischen Faunengebiets (Coleoptera, Histeridae) (41. Beitrag zur Kenntnis der Histeriden), Abhandlungen und Berichte des Verein Naturkunde. Cassel 81–83(1916–1919): 1–158.

dela Cruz IN, Ôhara M (2022) New records and redescription of *Atholus bifrons* (Marseul, 1854) (Coleoptera, Histeridae) from the Ryukyus, Japan and Borneo island, Indonesia. Elytra, Tokyo. New Series 12(2): 237–245.

Desbordes H (1917) Contribution à la connaissance des Histérides. 2e mémoire. Synopsis de divers groupes d'Histeridae. Annales de la Société Entomologique de France, Paris 85: 297–326.

Desbordes H (1919) Contribution à la connaissance des Histérides. 4e mémoire. Étude des Histeridae de l'Indochine (Tonkin, Laos, Siam, Annam, Cambodge, Cochinchine). Annales de la Société Entomologique de France 87(1918–1919): 341–424.

Desbordes H (1921) Insectes Coléoptères Histeridae. Mission Guy Babault dans les provinces centrales de l'Inde et dans la région occidentale de l'Himalaya. 1914. Résultats scientifiques. Ed. Blondel La Rougery, Paris, 14 pp.

Desbordes H (1925) Description de trois Histerides nouveaux des îles Philippines (Coleoptera). Bulletin de la Société Entomologique de France 1925(5): 85–88. https://doi.org/10.3406/bsef.1925.27460

Erichson WF (1834) Uebersicht der Histeroides der Sammlung. Jahrbuch der Insekten-Kunde 1: 83–208.

Ganglbauer L (1889) Die Käfer von Mitteleuropa. Die Käfer der österreichisch-ungarischen Monarchie, Deutschlands, der Schweiz, sowie des französischen und italienischen Alpengebietes. III, 1. Familienreihe Staphylinoidea. 2. Theil; Scydmenidae, Silphidae, Clambidae, Leptinidae, Platypsyllidae, Corylophidae Sphaeriidae, Trichopterygidae, Hydroscaphidae, Scaphidiidae, Histeridae. Carl Gerold's Sohn, Wien, 408 pp.

Gemminger M, Harold E (1868) Catalogus Coleopterorum Hucusque Descriptorum Synonymicus et Systematicus. Monachii, sumptu E.H. Gummi, 1868–1876. [753–978 + [5] pp.] https://doi.org/10.5962/bhl.title.9089

Halstead DGH (1963) Histeridae. Handbook for Identification of British Insects 4(10): 1–16. [London]

Heyden L (1910) Corrigenda zum II. Band. In: Reitter E (Ed.) Fauna Germanica. Die Käfer des Deutschen Reiches. V. Band. Schriften Deutsche Lehrerver Naturkunde 33: 317.

Hisamatsu S (1985) Histeridae. In Uéno S-I, et al. (Eds) The Coleoptera of Japan in Color, 2: 220–230. Hoikusha, Osaka. [In Japanese]

Hisamatsu S, Kusui Y (1984) Notes on Histeridae from Shin-etsu district. Transactions of Essa Entomological Society, Niigata (57): 15–18. [In Japanese]

Kamiya K, Takagi S (1938) A list of Japanese Histeridae. Scientia Agrícola 19(1): 21–32.

Kryzhanovskij OL, Reichardt AN (1976) Zhuki Nadsemeystva Histeroidea (semeystva Sphaeritidae, Histeridae, Synteliidae). [Beetles of the superfamily Histeroidea (families Sphaeritidae, Histeridae, Syntelidae)]. Fauna USSR, Zhestokrylye, Vyp. 4 Nauka, Leningrad, 434 pp. [In Russian]

Lackner T (2010) Review of the Palearctic genera of the Saprininae (Coleoptera: Histeridae). Acta Entomologica Musei Nationalis Pragae, 50 (suppl): e254.

Lewis G (1885) New species of Histeridae, with synonymical notes. Annals and Magazine of Natural History 15(5): 456–473. https://doi.org/10.1080/00222938509459368

Lewis G (1886) On the nomenclature of sundry Histeridae, including a note on a fourth species of European *Dendrophilus*. Wiener entomologische Zeitung 5: e280. https://doi.org/10.5962/bhl.part.20599

Lewis G (1888) Viaggio di Leonardo FEA in Birmania e regioni vicine. XII. Histeridae, Annali del Museo Civico Storia Naturale di Genova (2) 6(26): 630–645.

Lewis G (1901) On new species of Histeridae. Annals & Magazine of Natural History 8(7): 366–383. https://doi.org/10.1080/03745480109443334

Lewis G (1902) On new species of Histeridae and notices of others. Annals & Magazine of Natural History 10(7): 223–239. https://doi.org/10.1080/00222930208678661

Lewis G (1906) On new species of Histeridae and notices of others. Annals & Magazine of Natural History 18(7): 397–403. https://doi.org/10.1080/00222930608562636

Lewis G (1915) On new species of Histeridae and notices of others. Annals & Magazine of Natural History 16(8): 54–56. https://doi.org/10.1080/00222931508693684

Linnaeus C (1758) Systema Naturae per Regna Tria Naturae, Secundum Classes, Ordines, Genera, Species, cum Characteribus, Differentiis, Synonymis, locis. Editio decima, reformata. Tomus I, Holmiae, [4] + 823 pp. https://doi.org/10.5962/bhl.title.542

Marseul SA (1854) Essai monographique sur la famille des Histérides (suite). Annales de la Société Entomologique de France 2(3): 161–311. [525–592, 671–707.]

Marseul SA (1857) Essai monographique sur la famille des Histérides (suite). Annales de la Société Entomologique de France 5(3): 109–167. [397–516.]

Marseul SA (1873) Coléoptères du Japon recueillis par M. Georges Lewis. Énumération des Histérides et des Hétéromères avec la description des espèces nouvelles. Annales de la Société Entomologique de France 3(5): 219–230.

Mazur S (1984) A world catalogue of Histeridae. Polskie Pismo Entomologiczne 54(3–4): 1–376.

Mazur S (1997) A world catalogue of Histeridae (Coleoptera: Histeroidea). Genus International Journal of Invertebrate Taxonomy (Supplement), Polskie Towarzystwo Taksonomiczne 1–373.

Mazur S (2008) New records of histerid beetles (Coleoptera: Histeridae) from Taiwan, with description of a new species. Baltic Journal of Coleopterology 8(1): 89–95.

Mazur S (2009) Notes on some species of the genus *Atholus* Thomson, 1859 (Coleoptera: Histeridae) in Taiwan. Formosan Entomologist 29: 113–118.

Mazur S (2011) A Concise Catalogue of the Histeridae (Insecta: Coleoptera). Warsaw University of Life Sciences SGGW Press, Warsaw, 332 pp.

Mazur S (2013) On new and little-known histerids (Coleoptera: Histeridae) from Laos with additional notes on species composition and zoogeography. Entomologica Basiliensia et Collectionis Frey 34: 179–206.

Mazur S, Shavrin AV, Anichtchenko AV (2014) Contribution to the knowledge of the histerid beetles (Coleoptera, Histeridae) of North India. Linzer Biologische Beitrage 46(2): 1267–1275.

Mazur S, Shavrin AV, Anichtchenko AV, Barševskis A (2015) The histerid beetles (Coleoptera, Histeridae) of the Oriental region deposited in the Beetle Collection of Daugavpils University (DUBC). Linzer Biologische Beitrage 47(2): 1451–1466.

Miwa Y (1931) Histeridae and Niponiidae. In: A systematic catalogue of Formosan Coleoptera. Department of Agriculture Government Research Institute, Formosa, Japan, Report 55: 49–58.

Motschulsky V (1860) Coléoptères rapportés de la Sibérie orientale et notamment des pays situés sur les bords du fleuve Amour par MM. Schrenck, Maack, Ditmar, Voznessenski etc. In Schrenck, L., Reisen und Forschungen im Amur-Lande in den Jahren 1854–1856 im Auftrage der Keiserl. Akademie der Wissenschaften zu St. Petersburg ausgefürt und in Verbindung mit mehreren Gelehrten herausgegeben. Band II. Zweite Lieferung. Coleopteren, 258 pp. [St. Petersburg]

Motschulsky V (1863) Essai d'un catalogue des insectes de l'ile Ceylan (suite), Bulletin de la Société impériale des naturalists de Moscou 36, 1: 421–532.

Nakane T (1981) Histeroid beetles hitherto recorded from Kyushu, Japan. Transactions of the Biological Society, Nagasaki (21): 7–10. [In Japanese]

Ôhara M (1992) A revision of the Japanese species of the genus *Atholus* (Coleoptera, Histeridae), Part 1. Elytra 20(2): 167–182.

Ôhara M (1993) A revision of the Japanese species of the genus *Atholus* (Coleoptera, Histeridae), Part 2. Elytra 21(1): 135–150.

Ôhara M (1994) A revision of the superfamily Histeroidea of Japan (Coleoptera). Insecta Matsumurana, New series 51: 1–283.

Ôhara M (1999) A revision of the superfamily Histeroidea of Japan (Coleoptera), Supplementum 1. Insecta Matsumurana, New series 55: 75–132.

Ôhara M (1999b) A revision of the tribe Histerini (Coleoptera, Histeridae) in Taiwan. Insecta Matsumurana, New Series 56: 3–50.

Ôsawa S, Nakane T (1951) Studies on Japanese Histeridae (1) – Histeridae of Noziri – (N. Shinano, Japan). Bulletin Takarazuka Insectarium (79): 1–10. [In Japanese]

Reichardt AN (1930) Zametki o palearkticheskich Histeridae (Coleoptera), II. Revue Russe d'Entomologiya 24: 45–46.

Reitter E (1909) Fauna Germanica. Die Käfer des Deutschen Reiches. II Band. Schriften Deutsche Lehrerver Naturkunde 24: 1–392.

Schmidt J (1885) Bestimmungs-Tabellen der europäischen Coleopteren. XIV. Histeridae. Berliner Entomologische Zeitung 29: 279–330. https://doi.org/10.1002/mmnd.18850290213

Schrank FP (1781) Enumeratio Insectorum Austriae Indigenorum. Cum figuris. [24]+548 pp. Viena.

Thomson CG (1859) Skandinaviens Coleoptera, synoptiskt bearbetade. I, Lund 290 pp. https://doi.org/10.5962/bhl.title.138677

Witzgall K (1971) Histeridae. In: Freude H, Harde KW, Lohse GA (Eds) Die Käfer Mitteleuropas 3: 156–189. [Goecke & Evers, Krefeld]

ZooKeys 1158: 27–48 (2023)
doi: 10.3897/zookeys.1158.99077
https://zookeys.pensoft.net

RESEARCH ARTICLE

A peer-reviewed open-access journal
ZooKeys
Launched to accelerate biodiversity research

A new *Bolitoglossa* (Amphibia, Caudata, Plethodontidae) from the Cordillera Oriental of Colombia

Yeny Rocio López-Perilla[1,2], Juan David Fernández-Roldán[3], Fabio Leonardo Meza-Joya[4,5], Guido Fabian Medina-Rangel[2,6]

1 *Fundación Natura, Bogotá D.C., Colombia* **2** *Grupo de Morfología y Ecología Evolutiva, Instituto de Ciencias Naturales, Universidad Nacional de Colombia, Bogotá D.C., Colombia* **3** *Laboratorio de Anfibios, Instituto de Ciencias Naturales, Universidad Nacional de Colombia, Bogotá D.C., Colombia* **4** *Grupo de Investigación en Biotecnología Industrial y Biología Molecular, Escuela de Biología, Universidad Industrial de Santander, Piedecuesta, Santander, Colombia* **5** *Wildlife & Ecology, School of Natural Sciences, Massey University, Private Bag 11-222, Palmerston North, New Zealand* **6** *Grupo Biodiversidad y Conservación, Instituto de Ciencias Naturales, Universidad Nacional de Colombia, Bogotá D.C., Colombia*

Corresponding author: Yeny Rocio López-Perilla (yrlopezp@unal.edu.co)

Academic editor: U. García-Vázquez | Received 21 December 2022 | Accepted 12 March 2023 | Published 19 April 2023

https://zoobank.org/57A79842-A71A-4A25-917F-57A33D3334F5

Citation: López-Perilla YR, Fernández-Roldán JD, Meza-Joya FL, Medina-Rangel GF (2023) A new *Bolitoglossa* (Amphibia, Caudata, Plethodontidae) from the Cordillera Oriental of Colombia. ZooKeys 1158: 27–48. https://doi.org/10.3897/zookeys.1158.99077

Abstract

A new salamander species of the genus *Bolitoglossa* is here described from the cloud forests of the western slopes of the Cordillera Oriental of Colombia, in the Cundinamarca department. The most salient characters of this new species are its numerous maxillary and vomerine teeth, its moderate webbing on hands and feet, its short and robust tail, and its chromatic variation. Based on molecular analyses this new species is assigned to the *adspersa* species group and its status established as the sister species of *B. adspersa*, with which it was previously confused. Lastly, the distribution, natural history, and conservation status of the new species are discussed.

Resumen

Describimos una nueva especie de salamandra del género *Bolitoglossa* proveniente de los bosques nublados de la vertiente occidental de la Cordillera Oriental de Colombia, en el departamento de Cundinamarca. Los caracteres más sobresalientes de esta nueva especie son sus numerosos dientes maxilares y vomerinos, su palmeadura moderada en pies y manos, su cola corta pero robusta, y su variación cromática. Basados en

análisis moleculares asignamos esta nueva especie al grupo de especies *adspersa* y establecemos su estatus como especie hermana de *B. adspersa*, con la cual era previamente confundida. Finalmente, discutimos algunos aspectos de su distribución, historia natural y su estado de conservación.

Keywords
Biodiversity, coloration, phylogenetic systematics, salamanders, taxonomy

Palabras clave
Biodiversidad, coloración, salamandras, sistemática filogenética, taxonomía

Introduction

Bolitoglossa Duméril, Bibron & Duméril, 1854 is currently the largest and most diverse genus of salamanders (Amphibia: Caudata) with a total of 138 species recorded from northeastern Mexico to central Bolivia (Frost 2023). However, the actual diversity of *Bolitoglossa* in South America may be underestimated given the existence of cryptic forms (Jaramillo et al. 2020). Colombia currently has 24 species (Frost 2023), of which only seven have been described in this century, while the remainder are descriptions prior to 1973 (Frost 2023). As for the phylogenetic relationships for the species of the country, little is known; there are some works that include species distributed in the Colombian Amazon (Cusi et al. 2020; Jaramillo et al. 2020), as well as phylogenies presented in the most recent descriptions of species in the country (Acevedo et al. 2013; Meza-Joya et al. 2017).

The genus *Bolitoglossa* has its highest diversity in the Cordillera Oriental (Meza-Joya et al. 2017), where a total of 11 species have been described: *B. adspersa* (Peters, 1863), *B. altamazonica* (Cope, 1874), *B. capitana* Brame & Wake, 1963, *B. guaneae* Acosta-Galvis & Gutierrez, 2012, *B. leandrae* Acevedo, Wake, Márquez, Silva, Franco & Amézquita, 2013, *B. lozanoi* Acosta-Galvis & Restrepo, 2001, *B. nicefori* Brame & Wake, 1963, *B. palmata* (Werner, 1897), *B. pandi* Brame & Wake, 1963, *B. tamaense* Acevedo, Wake, Márquez, Silva, Franco & Amézquita, 2013, and *B. yariguiensis* Meza-Joya, Hernández-Jaimes & Ramos-Pallares, 2017.

These 'mushroom-tongued' or 'tropical lungless' salamanders, as they are commonly known, are characterized by lacking a sublingual fold; having a very long and rapidly projected tongue; a tendency towards tarsal reductions; extensive webbing associated with climbing behavior; and fully terrestrial to arboreal habits (Wake and Lynch 1976; Köhler 2011; Angarita-Sierra et al. 2020; Ponssa et al. 2022). These salamanders inhabit a variety of ecosystems, from lowland rainforests to highland areas, where they are particularly diverse in montane cloud forests and less so in paramo ecosystems (Köhler 2011).

In this paper, we describe a new species of *Bolitoglossa* using morphological and molecular data, associated with the existing remnants of Andean montane forests on the western flank of the Cordillera Oriental, and we compared it with other known species of the genus in Cundinamarca, Colombia.

Materials and methods

Specimen collection and fieldwork

The holotype and most of the paratypes were collected within vereda Roble Hueco, Bojacá municipality, Cundinamarca department, Colombia (4.6963, -74.3624, 2630 m a.s.l.; Fig. 1). Specimens were captured by hand using free searches over two 10-day field trips, kept in plastic bags until weighed and photographed, and then euthanized by applying 2% lidocaine gel. Tissue samples were obtained from the tail or liver of individuals and preserved in absolute ethanol. Specimens were then fixed in 10% formaldehyde and then stored in 70% ethanol. All specimens were deposited at Colección de Anfibios, Instituto de Recursos Biológicos Alexander von Humboldt, Villa de Leyva, Boyacá, Colombia (**IAvH**).

Morphology and taxonomy

Measurements and counts of morphological characters were taken using a Neiko digital caliper rounded to the nearest 0.1 mm under a Leica Stemi 2000 stereoscope, using the diagrams in Bingham et al. (2018) as a model. The following morphological traits were analyzed for all specimens: snout-vent length (**SVL**); head length (**HL**); head width (**HW**); tail length (**TL**); maxillary teeth (**MT**); vomerine teeth (**VT**); and additional measurements only for the description of the holotype: interorbital distance (**IOD**); eye diameter (**EYD**); snout length (**SNL**). Color descriptions are based on field notes and photographs of preserved specimens using the color catalogue of Köhler (2012). Format of diagnosis and description follows Meza-Joya et al. (2017). Species comparisons were made following Brame and Wake (1963) or their original descriptions for those species described after 1963, as well as by examining *Bolitoglossa* specimens housed at Colección de Anfibios, Instituto de Recursos Biológicos Alexander von Humboldt, Villa de Leyva, Boyacá, Colombia (**IAvH**), Laboratorio de Anfibios, Instituto de Ciencias Naturales, Universidad Nacional de Colombia, Bogotá D.C., Colombia (**ICN**), Colección de Anfibios, Museo La Salle, Universidad de La Salle, Bogotá D.C., Colombia (**MLS**) and Colección Herpetológica of Universidad Industrial de Santander, Bucaramanga, Colombia (**UIS**).

Molecular and phylogenetic analyses

We extracted whole genomic DNA from liver or muscle tissue of specimens of *Bolitoglossa* preliminary identified as *B. adspersa*, using the DNeasy Blood & Tissue Kit (Qiagen, #69506). Extracted DNA samples were amplified by PCR for the partial non-coding 16S rRNA (16S ≈ 517 bp) and the protein-coding cytochrome b (cyt b ≈ 742 bp) mitochondrial genes, using the primers 16Sar-L and 16Sbr-H (Palumbi et al. 1991) and MVZ15 and MVZ16 (Moritz et al. 1992), respectively. Amplification protocols (reaction mix and thermocycler programs) are as described in Meza-Joya et al. (2017). The amplicons were cleaned and then sequenced at Macrogen Inc. (Seoul,

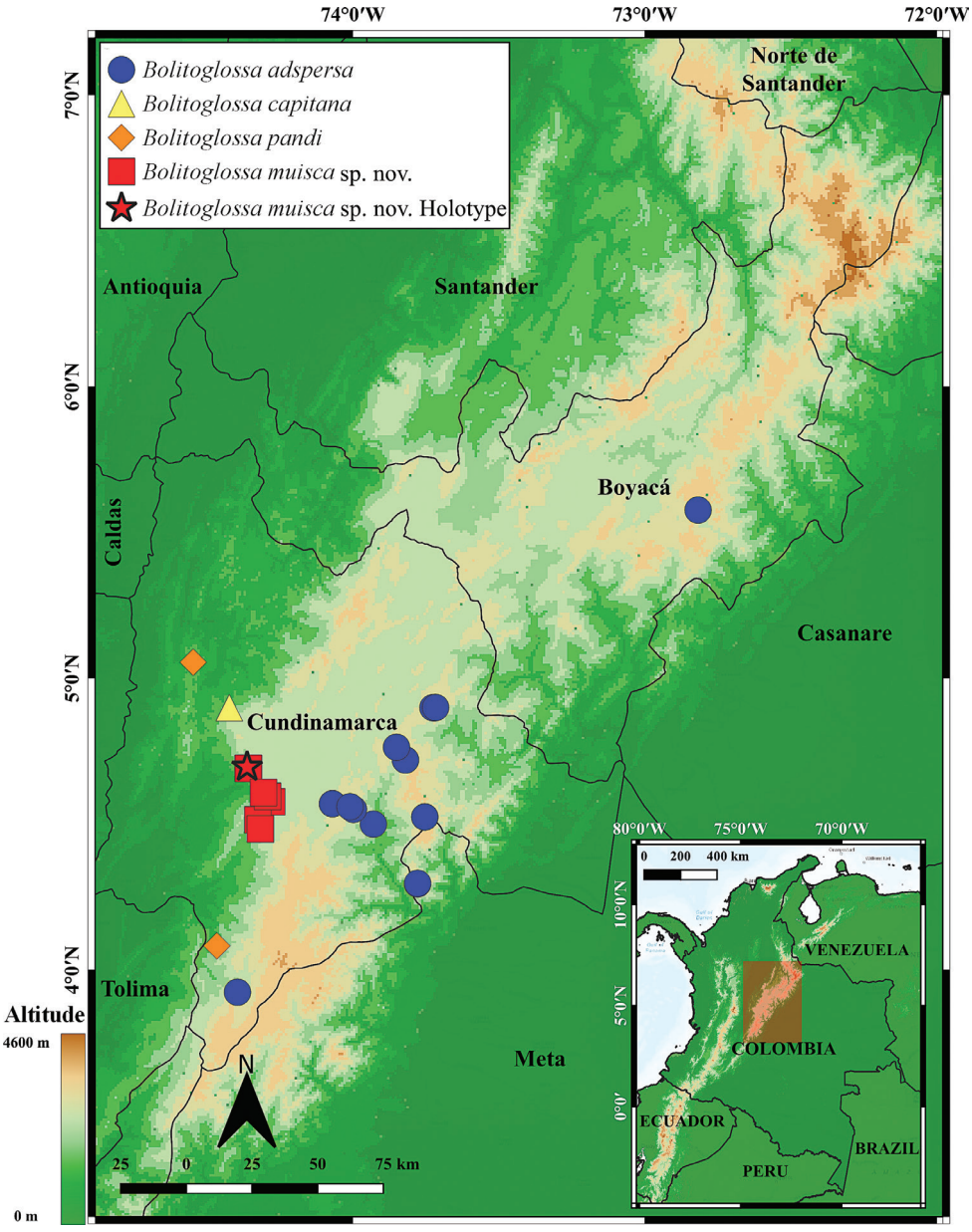

Figure 1. Map of Colombia showing the distribution records of *Bolitoglossa muisca* and other sympatric *Bolitoglossa* species in the Cordillera Oriental.

Korea) by capillary electrophoresis using an ABI3730 genetic analyzer. The partial sequences obtained were visualized, cleaned, and assembled with Geneious v. 9.1.6 (Kearse et al. 2012); we only used sequences with a quality score higher than 90%. DNA sequences were deposited in GenBank (Appendix 1).

Homologous sequences from other *Bolitoglossa* in the *adspersa* group were downloaded from GenBank and compared with our molecular data. Representatives from other species groups within *Eladinea* (*epimela*, *schizodactyla*, and *subpalmata*) were used as outgroups (Appendix I). We also included partial sequences of the nuclear protein-coding recombination activating gene 1 (RAG1 ≈ 792 bp), a relatively well-sampled gene fragment, for other species of *Bolitoglossa*. We performed multiple alignments in MAFFT v. 7.304 (Katoh and Standley 2013) using the G-INS-i algorithm. Phylogenetic analyses were performed on the concatenated dataset. We inferred the best-fit partition scheme and the best-fit evolution models with PartitionFinder v. 2.1.1 (Lanfear et al. 2017) under the Bayesian Information Criterion (BIC). For this, we performed an exhaustive search of all possible partitioning schemes on our dataset, placing the 16S gene in a separate partition whereas protein-coding genes were further partitioned by codon position. We performed a maximum likelihood (ML) phylogenetic analysis on IQ-TREE 2.0 (Nguyen et al. 2015), running 10,000 ultrafast bootstrap pseudoreplicates for internal node support (Hoang et al. 2018). We also conducted a Bayesian Inference (BI) analysis with the software MrBayes 3.2.6 (Ronquist et al. 2012), using four chains on two runs for 10 million generations and a sampling frequency of 10,000 generations with a burn-in of 0.10. Stationarity was determined with the software Tracer 1.6 (Rambaut et al. 2018).

For species delimitation, we first calculated uncorrected pairwise genetic p-distances for the 16S and cyt b genes between the two distinct evolutionary lineages identified within *B. adspersa*, with 1,000 bootstrap replicates using MEGA X (Kumar et al. 2018). Then, we split genetic lineages into candidate species using the Automatic Barcode Gap Discovery (ABGD) method (Puillandre et al. 2012). This analysis was based on the 16S gene matrix, the best-represented gene in our dataset, using K2P distances, prior for maximum value of intraspecific divergence between 0.001 and 0.1, ten recursive steps, and a gap width of 1.5. We also used the tree-based method as implemented in the Species Delimitation plugin in Geneious (Masters et al. 2011), using the ML phylogeny as a guide tree to calculate the mean probability of the ratio of intra- to interspecific genetic distances for the initial two-species hypothesis within *B. adspersa* (Brame and Wake 1963).

Results

Molecular and phylogenetic analyses

The concatenated data matrix contains 2,070 bp for 67 terminals (excluding outgroups) from 26 described species of the *Bolitoglossa adspersa* group, as well as nine candidate species and the new species described herein: 64 samples for 16S (516 bp), 45 for cyt b (759 bp), and 26 for RAG1 (795 bp). The best partition scheme (LnL = -14128.62, BIC = 29,677.40) for our concatenated dataset includes five subsets, each with an evolution model: (16S, cyt b pos1: GTR+I+G) (cyt b pos2: HKY+I+G) (cyt b pos3: GTR+G)

(RAG1 pos1, RAG1 pos2: K81+I) (RAG1 pos3: HKY+G). The resulting topologies from the ML and BI were congruent; thus, here we present only the ML tree (Fig. 2).

The inferred phylogenetic relationships were largely consistent with those from recent studies (Meza-Joya et al. 2017; Cusi et al. 2020; Jaramillo et al. 2020), with incongruences likely resulting from differences in taxon sampling. The *Bolitoglossa adspersa* species group was rendered as monophyletic with significant support (UFB = 99, PP = 1.0). All species included in our analyses were monophyletic with strong support, yet their relationships remained largely unresolved. As expected, samples from the new species were within the *adspersa* group, forming a well-supported clade (UFB = 100, PP = 1.0) sister to samples of *B. adspersa* from its type-locality, Bogotá, Cundinamarca department, Colombia, and surroundings, with significant support (UFB = 98, PP = 0.99). This clade was recovered as a sister to a clade grouping species from northeastern Colombia and Venezuela, but this relationship was poorly supported. GenBank sequences of a specimen from El Soche, Cundinamarca, Colombia, identified as *Bolitoglossa* sp. 1 (MVZ 167947, corrected here as MVZ 167997 based on the actual number on the MVZ catalog) by Parra-Olea et al. 2004, correspond with the new species described here. This specimen has long been recognized as different from *adspersa* (Hanken and Wake 1982; Parra-Olea et al. 2004).

With respect to species delimitation, all methods supported the two-species hypothesis within *B. adspersa* (Brame & Wake, 1963). Uncorrected pairwise p-distances between these two sister lineages were 2.1% (± 0.003%) for 16S and 7.0% for cyt b. The ABGD analysis resulted in five partitions separating the data into five ($P \leq 0.0028$) or two putative species ($P \geq 0.0046$), yet the new species described here was recovered as a candidate taxon in all partitions. Taxonomic distinctiveness for the new species was also supported under either relaxed or strict tree-based criteria (P ID Liberal = 1.00, CI = 0.86–1.00; P ID Strict = 0.79, CI = 0.62–0.97) with significant support: Rosenberg's P_{AB} statistics = 0.01 and P_{RD} (randomly distinct) > 0.05. Furthermore, as it is shown below, morphological comparisons consistently support the recognition of this lineage as a new species.

Bolitoglossa muisca **sp. nov.**

https://zoobank.org/63BA9285-C4FE-45B0-B828-BDB37F4E06BF

Figs 2–7, Tables 1, 2

Common English name: Muisca salamander

Common Spanish name: Salamandra Muisca

Type material. ***Holotype.*** IAvH-Am-17413, an adult female from Finca La Esmeralda, vereda Roble Hueco, Bojacá municipality, Cundinamarca department, Colombia (4.6963, -74.3624, 2630 m a.s.l.), collected by Y.R. López-Perilla on 4 February 2021 (Fig. 1).

Paratypes **(*n* = 8: 3 females, 5 males).** IAvH-Am-17417 (adult male), IAvH-Am-17419 (adult female), IAvH-Am-17421 (adult male) and IAvH-Am-17422 (adult male) from Finca La Esmeralda, vereda Roble Hueco, Bojacá municipality, Cundinamarca department, Colombia (4.6963, -74.3624, 2630 m a.s.l.), collected by Y.R. López-Perilla

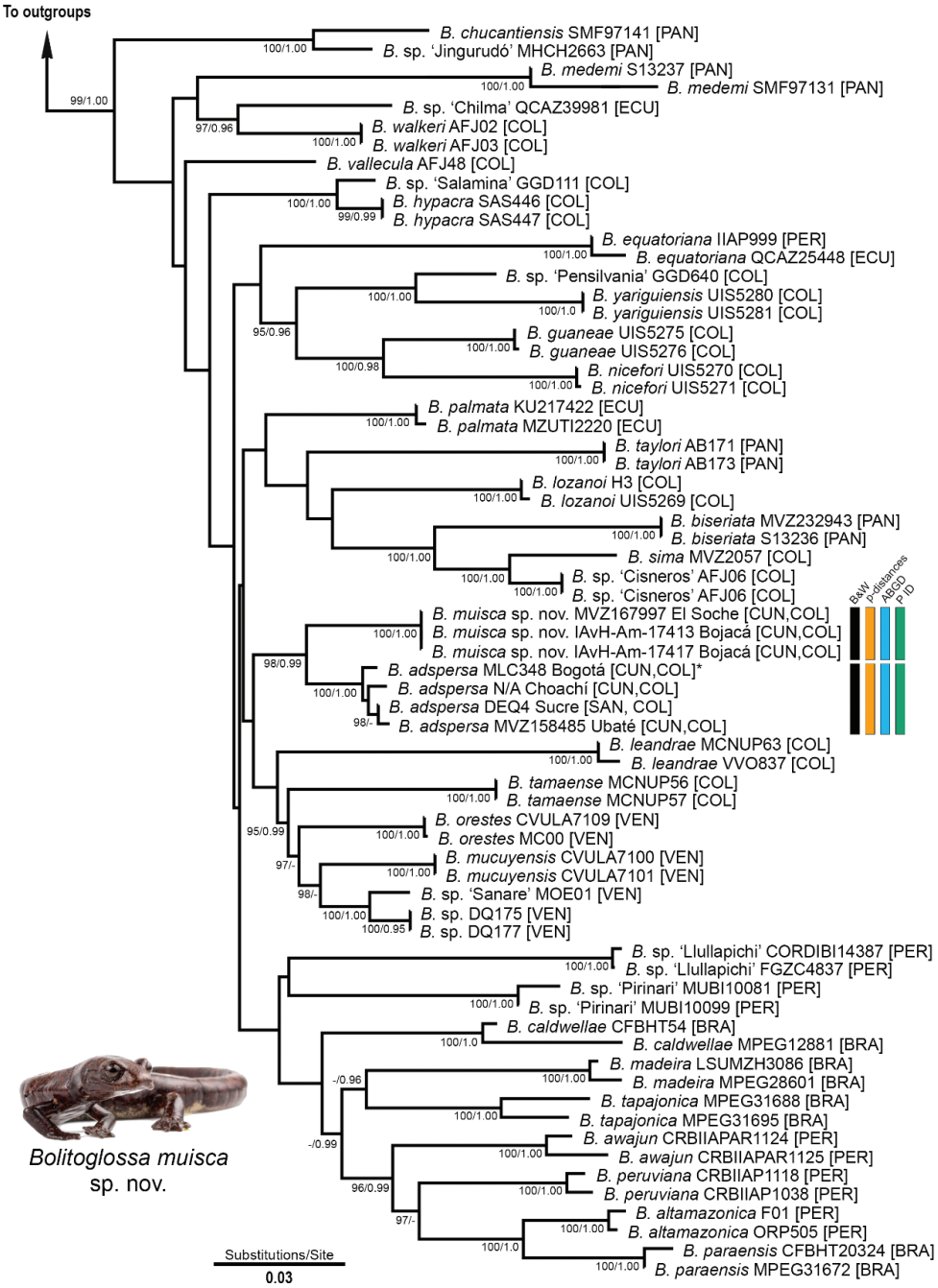

Figure 2. Maximum-likelihood tree of *Bolitoglossa* (*Eladinea*) *adspersa* group showing the phylogenetic position of *Bolitoglossa muisca*. Vertical bars indicate the two-species hypothesis within *Bolitoglossa adspersa* with the supported species partitions inferred using genetic data (p-distances, ABGD, and P ID). Support values for well-supported nodes correspond to ML ultrafast bootstrap (> 95) and Bayesian posterior probabilities (> 0.95), respectively. Photograph by JDF.

in February 2021 (Fig. 5). IAvH-Am-17423 (adult male), IAvH-Am-17425 (adult male) and IAvH-Am-17428 (adult female) from Finca Peñas Blancas, vereda Roble Hueco, Bojacá municipality, Cundinamarca department, Colombia (4.6916, -74.3581, 2390 m a.s.l.), collected by Y.R. López-Perilla in February 2021. IAvH-Am-17429 (adult female) from vereda Cascajal, Soacha municipality, Cundinamarca department, Colombia (4.5954, -74.2922, 2700 m a.s.l.), collected by G.F. Medina-Rangel in September 2022.

Referred specimens (*n* = 36: 7 females, 29 juveniles and subadults). ICN 3544–48, five adult females from Hacienda 'El Soche', Granada municipality, Cundinamarca department, Colombia (4.5153, -74.3240, 2600 m a.s.l.) obtained by Rurithza Velandia in December 1977; specimen ICN 3545 is cleared and stained; MVZ 167997, a juvenile obtained by Pere Alberch on 17 December 1978. ICN 58245–58268, a batch of 23 juvenile and subadult specimens from Hacienda 'La Tribuna', vereda Noruega Alta, Silvania municipality, Cundinamarca department, Colombia (4.4836, -74.3203, 2700 m a.s.l.) obtained by Cesar Monguí in September 2008. ICN 60319–20, two juveniles from vereda Roquemonte, San Antonio del Tequendama municipality, Cundinamarca department, Colombia (4.6056, -74.3008, 2600 m a.s.l.) obtained by J.D. Fernández in August 2013. ICN 60321–22, a juvenile and an adult female (respectively) also from vereda Roquemonte, San Antonio del Tequendama municipality, Cundinamarca department, Colombia (4.6056, -74.3008, 2600 m a.s.l.) obtained by J.D. Fernández in March 2017. ICN 60323–25, two juveniles and an adult female (respectively) from vereda Roquemonte, San Antonio del Tequendama municipality, Cundinamarca department, Colombia (4.6056, -74.3008, 2600 m a.s.l.), also obtained by J.D. Fernández in January 2018.

Diagnosis. *Bolitoglossa muisca* is a member the subgenus *Eladinea* and of the *adspersa* species group. The new species is characterized by the following morphological characters: a large-size body; a broad head; a rounded snout in dorsal and ventral views; a very thick postocular fold; a moderate subgular fold; smooth skin texture; moderately long limbs; moderate webbing on third finger and toe; and a short, robust tail.

Even though *Bolitoglossa adspersa* and *B. muisca* share their moderate webbing on hands and feet, we regard the former as having less webbing than the latter. Moreover, the tips of the fingers and toes are separated from the distal margin of the webbing, exposing their subcircular-shaped digits; unlike those of *B. muisca* (Fig. 4). The new species is slightly larger on average than *B. adspersa* (mean SVL 52.8±3.4 mm; range 33.0–72.1 mm; *n* = 22 vs. 45.0±3.4 mm; range 30.7–66.3 mm; *n* = 26), additionally, the tail of *B. adspersa* is thin and long in relation to the trunk but thick and short in relation to the trunk in *B. muisca* (Table 1). *Bolitoglossa muisca* differs from *B. capitana* by having moderately webbed hands and feet (vs. almost fully webbed hands and feet in *B. capitana*), by being overall smaller in size (mean SVL 52.8±3.4 mm; range 33.0–72.1 mm; *n* = 22 vs. 75.2±10.9 mm; range 59.2–85.5 mm; *n* = 5), by having fewer maxillary teeth (mean MT 24.4±3.0; range 14–36; *n* = 17 vs. 30.4±5.1; range 22–37; *n* = 5) by having fewer vomerine teeth (mean VT 35.1±4.0; range 24–53; *n* = 17 vs. 66.4±14.8; range 46–87; *n* = 5), and because the new species bears a faint, very small gular fold that is large, thick and notable in *B. capitana* (Cruz-Rodríguez et al. 2021: figs 13, 14). *Bolitoglossa muisca* differs from *B. pandi* because the tips of the third digit

Figure 3. Holotype of *Bolitoglossa muisca* (IAvH-Am-17413) in **A** dorsal **B** ventral and **C** lateral views. Photographs by JDF. Scale bar: 10 mm.

and toe of the latter are triangular and pointed in outline (vs. third digits and toes oval and webbed to a higher degree in *B. muisca*), by being a slightly larger species (mean SVL 52.8±3.4 mm; range 33.0–72.1 mm; *n* = 22 vs. 44.0±2.9 mm; range 35.9–52 mm; *n* = 12), and by having mostly smooth skin (vs. coarse skin in *B. pandi*); moreover, the tail of *B. pandi* tapers gradually and symmetrically from broad to slender anteroposteriorly, unlike that of the new species, which is slightly rectangular in outline, becoming abruptly wider than the base, and ending in a rounded tip (Table 1).

Description of the holotype. An adult female (SVL = 61.3 mm) with a broad head (HW/SVL = 0.16); head longer than wide (HW/HL = 0.90); neck with a small, faint gular fold; snout short and truncated in profile, and dorsal view, but less so in ventral view (SNL = 3.1 mm); large eyes that do not extend beyond the outline of the head in dorsal view and smaller than interorbital distance (EYD = 3.18 mm, IOD = 3.37 mm); with a thick post ocular fold that extends past the posterior commissure of the eye onto the anterior margin of the gular fold; canthus rostralis subtle, small, rounded in outline; 33 maxillary teeth, 16 to the right and 17 to the left; vomerine teeth 25, these are not arranged in a single row but grouped towards the margins of the parasphenoid bone; with three premaxillary teeth that pierce the upper lip in males; nasolabial grooves well developed; moderate interdigital webbing on hands but third finger extends slightly further than the other fingers; toes with less interdigital webbing than fingers, toes II–V with less membrane than toe I; with subterminal pads on digits, digits in order of increasing length I<II<IV>III; toes I<II<III<IV>V; longest digits of hand and feet are subcircular (L3T and L3F), limbs relatively long (FL/SVL = 0.23, HLL/SVL = 0.23); tail not exceeding standard length (TL/SVL 0.93), narrower than the body at the base (posterior to the vent), slightly rectangular in outline, becoming abruptly wider than the base and ending in a rounded tip, but this condition is artefactual because the tip of the tail is missing; a long trunk (52.5 mm); with 13 costal grooves (Fig. 3). See Table 2 for meristic data of all type specimens.

Table 1. Meristic data and morphological comparisons of *Bolitoglossa adspersa*, *B. capitana*, *B. muisca*, and *B. pandi*. For abbreviations see methods section.

Characters/ Species	*B. adspersa*	*B. capitana*	*B. muisca*	*B. pandi*
VT	26.1±2.5 (18–38) [*n* = 17]	66.4±14.8 (46–87) [*n* = 5]	35.1±4 (24–53) [*n* = 17]	31.8±4 (21–42) [*n* = 12]
MT	17.6±1.5 (13–29) [*n* = 18]	30.4±5.1 (22–37) [*n* = 5]	24.4±3 (14–36) [*n* = 17]	18.3±2.2 (13–26) [*n* = 12]
SVL	45±3.4 (30.7–66.3) [*n* = 26]	75.2±10.9 (59.2–85.5) [*n* = 5]	52.8±3.4 (33–72.1) [*n* = 22]	44±2.9 (35.9–52) [*n* = 12]
TL	35±3.7 (21.2–54.2) [*n* = 26]	61.0±7.4 (53.2–70.8) [*n* = 4]	38.9±4.3 (11.6–55.5) [*n* = 22]	29.1±5.2 (15.4–42.8) [*n* = 11]
HW	6.6±0.4 (4.9–9.5) [*n* = 27]	10.9±1.5 (8.8–12.5) [*n* = 5]	7.9±0.4 (5.4–10.3) [*n* = 22]	6.6±0.5 (5.3–8.2) [*n* = 12]
HL	8.2±0.5 (5.8–10.2) [*n* = 27]	12.2 [*n* = 1]	9.1±0.7 (5.6–14.5) [*n* = 22]	7.47±0.6 (6.3–10.2) [*n* = 12]
TL/SVL	0.8±0.1 (0.6–1.1) [*n* = 11]	0.8±0.1 (0.7–1.1) [*n* = 4]	0.72±0.1 (0.2–0.9) [*n* = 22]	0.6±0.1 (0.34–1.1) [*n* = 11]
Webbing on third finger	Moderate	Extensive	Moderate	Moderate
Webbing on third toe	Moderate	Extensive	Moderate	Moderate
Postocular fold	Thick	Absent	Very thick	Absent
Subgular fold	Very thick	Thick	Moderate	Faint
Snout in dorsal and ventral view	Truncated	Truncated	Rounded	Truncated
Tail shape	Tapered	Tapered	Stout	Tapered

Figure 4. Ventral views of the hands and feet of **A** *Bolitoglossa muisca* (IAvH-Am-17413) **B** *Bolitoglossa adspersa* (ICN 4885). Photographs by JDF. Scale bar: 10 mm.

Table 2. Meristic data and measurements of the type series of *Bolitoglossa muisca*.

Characters/ Type series	IAvH-Am-17413 *	IAvH-Am-17417	IAvH-Am-17419	IAvH-Am-17421	IAvH-Am-17422	IAvH-Am-17423	IAvH-Am-17425	IAvH-Am-17428	IAvH-Am-17429
Sex	Female	Male	Female	Male	Male	Female	Male	Female	Female
SVL (mm)	61.3	50.6	60.3	58.1	57.4	72.1	54	51.5	65.9
TL (mm)	53.2	40.8	46.6	49.8	51.6	14.4+	45.8	36.5	42.6
HW (mm)	9.6	7.7	9.2	7.7	8.7	9.8	8.5	8.2	10.3
HL (mm)	10.6	8.9	10.7	9.4	9.7	11.6	9	9.1	14.5
HW/SVL	0.1	0.1	0.1	0.1	0.1	0.1	0.1	0.1	0.1
TL/SVL	0.8	0.8	0.7	0.8	0.9	--	0.8	0.7	0.6
VT	25	23	26	18	23	36	22	32	36
MT	33	24	28	36	44	44	36	41	44

* Denotes de holotype. + regenerated tail. -- No data. For abbreviations see Materials and methods section.

Coloration of the holotype in life. The color pattern of the holotype is described based on a photograph taken the day after capture. The dorsal surfaces of the head, the body and the tail are Raw Umber (280), strongly speckled with Dark Salmon (59); white stipples on the lateral surface of the head; the flanks, dorsum, legs, and tail have an irregular thin white stripe; the iris is Light Sky Blue (191) with Pratt's Rufous (72) reticulations. The throat and ventral surfaces are white with Raw Umber (280) speckles and reticulations; the ventral surfaces of the limbs and tails with some Light Orange Yellow (7) vermiculated; underside of hands and feet are Olive-Brown (278).

Coloration of the holotype in preservative. The color pattern of the holotype was recorded after approximately five months stored in 70% ethanol. The dorsal surfaces of the head, the body and the tail are Raw Umber (280), strongly speckled with Dark Salmon (59); the flanks, dorsum, legs, and tail have an irregular Smoke Gray (266) stripe; the iris is Amber (51) with Orange Rufous (56) reticulations. The throat and ventral surface are Smoke Gray (266) with Raw Umber (280) speckles and reticulations; hands and feet soles are Grayish Horn (268) ventrally (Fig. 3).

Color variation. The specimens IAvH-Am-17414–16 have the dorsal surfaces of the head, flanks, dorsum, front legs and vertebral band Orange-Rufous (56), strongly speckled with Raw Umber (280); paravertebral area, tail, and hind legs back Light-Yellow Ocher (13) with Raw Umber (280) dashes, and bordered with a wide Raw Umber (280) band; white stipples on the lateral surface of the head and back of the legs. The specimen IAvH-Am-17425 has the dorsal surfaces of the head, body, legs, and tail Dark Salmon (59), strongly speckled with Raw Umber (280), with greater concentration at the nape of the neck. Ventral markings or blotches on the ventral surfaces of the body and tail vary in shape and size; often with irregular margins but are consistently white or cream-colored independent of sex and age (Figs 5–7).

Etymology. Named after the native human inhabitants of the Altiplano Cundiboyacense and Sabana de Bogotá. The Muiscas regarded amphibians as sacred creatures associated with sex, fertility, and the arrival of the rainy season. The specific epithet is used as a noun in apposition.

Distribution. At present, *Bolitoglossa muisca* is known only from small cloud forest remnants on the western slopes of the Cordillera Oriental of Colombia in Bojacá, Granada, San Antonio del Tequendama, Silvania, and Soacha municipalities, Cundinamarca department. All specimens collected between 2390–2700 m a.s.l. (Fig. 2).

Natural history. Individuals from Bojacá municipality were regularly found at night on the base (on the *mantillo*) and leaves of Cyatheaceae ferns, which are dominant in the cloud forests of the Tequendama region of Cundinamarca department (Fig. 8). Most individuals from San Antonio del Tequendama municipality were found active at night perching on small branches of shrubs (Araceae and Melastomataceae), usually far away from rivers or streams. During the day, a few individuals were found inactive inside bromeliads below two meters height. When handled, these salamanders produced a sticky whiteish mucoserous substance; we consider this to be a defense mechanism against potential predators (Arrivillaga and Brown 2018). Two frog species (*Pristimantis* sp. and *P. uisae*) and a lizard (*Anolis heterodermus*) were found in sympatry with *Bolitoglossa muisca*; no other salamander species were found within our fieldwork area.

Other material examined. Countries are indicated in bold capitals, departments in regular capitals, municipalities, and localities in plain text. * Denotes specimens examined via photographs.

Bolitoglossa adspersa (*n* = 29). **Colombia**: Boyacá: Duitama, Páramo de la Rusia: ICN 4301, 4310; Toquilla, Páramo de Toquilla: ICN 9487. Cundinamarca: Bogotá, D.C., Páramo de Cruz Verde: IAvH-Am-8917, San Cristobal, Tánques de Vitelma,

Figure 5. Paratype of *Bolitoglossa muisca* (IAvH-Am-17419) in life. Photographs by JDF.

finca La Marranera: IAvH-Am-696, 2947, 2954, 2957-58, 2964, 2967, 2972, Usme, represa El Hato: ICN 37555; Cabrera: vereda de Hoyerías: IAvH-Am-13253 Fómeque, Laguna de Chingaza: ICN 4884, 4891; Guasca, Páramo de Guasca: ICN 4521, 4525, 4546; Fómeque, laguna Chingaza: ICN 4885; Fusagasugá, km 50 carretera Fusagasugá-La Florida: ICN 39096; Guatavita, vereda Montenquiva: IAvH-Am-13174–75, ICN 55420; Guayabetal: Páramo Atravezado: IAvH-Am-14808; Páramo de Palacio, P.N.N. Chingaza: IAvH-Am-3101, 3096, Quétame, km 22 carretera central Villavicencio-Alto del Tigre: ICN 7123; Ubaque, reserva ecológica Matarredonda: IAvH-Am-13254.

Bolitoglossa capitana (*n* = 4). **Colombia:** Cundinamarca: Albán, Granjas del Padre Luna: ICN 9221 & MLS 182–184*.

Bolitoglossa guaneae (*n* = 27). **Colombia:** Santander: Charalá, Virolín, Cañaverales, sector El Reloj: ICN 5197, 8555, 8557, 12770–72, 34230, Cuchilla del Fara: ICN 47980, Hacienda La Sierra: ICN 34229–30, km 56: ICN 19558, UIS-A 1369, UIS-A 2078, UIS-A 2082, UIS-A 2179, UIS-A 2317, UIS-A 2325–6, UIS-A 2891, UIS-A 2893, UIS-A 2895, UIS-A 2898–9, paratypes UIS-A 2203, UIS-A 2320, UIS-A 2324, UIS-A 2897.

Figure 6. Chromatic variation of *Bolitoglossa muisca* in life. Notice some individuals bear white blotches on the ventral surfaces of the body and the tail. Photographs by YLP.

Bolitoglossa muisca (*n* = 54). **Colombia:** Cundinamarca: Bojacá, vereda Roble Hueco, predio La Esmeralda: IAvH-Am-17413–22, Predio Peñas Blancas: IAvH-Am-17423–28; Granada, hacienda El Soche: ICN 3544–48, MVZ 167997*;

Figure 7. A non-captured individual of *Bolitoglossa muisca* from the surroundings of Reserva Chicaque, San Antonio del Tequendama, Cundinamarca, Colombia, photographed by JDF in October 2015. Notice the striking contrasting dark brown background coloration with ochre markings primarily on the dorsal surfaces of the body.

San Antonio del Tequendama, vereda Roquemonte, cerca de entrada Parque Chicaque: ICN 60319–25; Silvania, vereda Noruega Alta, Hacienda La Tribuna: ICN 58245–58268; Soacha, vereda Cascajal: IAvH-Am-17429.

Bolitoglossa nicefori (*n* = 13). **Colombia:** Santander: Floridablanca, El Mortiño, quebrada Torrentosa: ICN 50000, 58227, 58231; Zapatoca, finca Los Puentes, quebrada Uchuvala: ICN 58223–24, 58226; Piedecuesta, vereda Los Monos: UIS-A 2987, UIS-A 2991; Los Santos, vereda El Carrizal, finca Utopía: UIS-A 5273–4; Guapotá, vereda Las Flores, finca La Chocolatera: UIS-A 5264; San Gil, vereda San José, finca La Esperanza: UIS-A 5270–1.

Bolitoglossa pandi (*n* = 20). **Colombia:** Cundinamarca: Pandi, vereda Buenos Aires Alta: ICN 45500, Supatá, vereda Las Lajas, reserva Cuzcungos: ICN 58492–05, Villeta, La Esmeralda: IAvH-Am-10303–08.

Discussion

Taxonomic background

Brame and Wake (1963: 44) examined a single specimen of *Bolitoglossa* from the Tequendama region of Cundinamarca (ICNB Tequendama), which was regarded as an

Figure 8. The Andean cloud forests of Bojacá, Cundinamarca, and the habitat of *Bolitoglossa muisca*. Photographs by YLP.

undescribed species morphologically similar to *B. adspersa*. Despite finding diagnostic morphological differences between this specimen and those from *B. adspersa*, the limited sample size precluded any attempt by these authors to describe it as a new species.

Our morphological and molecular results support Brame and Wake's (1963) hypothesis. Through our conversations with Giovanni Chaves-Portilla we came across an unpublished manuscript written by the late David B. Wake and Arden H. Brame, dated sometime between the late 1980s and early 1990s (John D. Lynch pers. comm.), in which they proposed descriptions of three new *Bolitoglossa* from Colombia. One of these new species corresponds to *Bolitoglossa muisca* and is known from a site called Hacienda 'El Soche', Granada municipality, Cundinamarca department, Colombia, 2600 m a.s.l., i.e., from the same locality of MVZ 167997 (Fig. 1). Wake and Brame had planned to designate four types for this new species housed at Colección de Anfibios, Instituto de Ciencias Naturales, Universidad Nacional de Colombia, Bogotá D.C., namely ICN 3544–46 and ICN 3550. We managed to examine these specimens and confirm them to be conspecific with *Bolitoglossa muisca*, but unfortunately these are not in the best condition and are therefore designated as referred material.

Phylogenetic status

Our taxonomic sampling indicates that *Bolitoglossa muisca* is sister to *B. adspersa* and both are reciprocally monophyletic (Fig. 1). These two species are close geographically and their genetic uncorrected p-distance for the 16S and cyt b (7.0%) fragments were relatively low (2.1 and 7%, respectively). Yet, lower distances between morphologically well-defined sister species of *Bolitoglossa* have been previously reported (Batista et al. 2014; Meza-Joya et al. 2017), with the smallest divergence reaching 0.5% for 16S (Parra-Olea et al. 2004). In addition, species delimitation analyses provided support to the distinctiveness of *B. muisca* as a new species.

Threats and conservation status

Deforestation, logging, and forest clearing are the main threats faced by the habitat of the new species in the remnant cloud forests of the Tequendama region in Cundinamarca department, Colombia. Nonetheless, the type locality of *Bolitoglossa muisca* is located within the regional protected area 'Distrito de Manejo Integrado Cerro Manjui – Salto del Tequendama', a conservation project led by Empresas Públicas de Medellín (EPM) and Fundación Natura that focuses on improving connectivity among cloud forests remnants of the Tequendama region. The calculated Extent of Occurrence (EOO) using the localities where the species is distributed is 102 km^2 (estimate made with GeoCAT; Bachman et al. 2011). *Bolitoglossa muisca* is only known from an area of 102 km^2 and only the type locality has a certain degree of protection. However, based on our results and field observation we consider that this species should be considered as Endangered (EN) using the IUCN criteria B1b(iii) of the IUCN, given its small known range (< 5000 km), and the current threats to its native habitat. The consequent loss of native vegetation may be causing the new species described here to be most likely threatened by habitat loss, and a monitoring program is warranted to better assess the current status of its few known populations (Liu et al. 2022).

Acknowledgements

For access to specimens and making available museum working space during our visits we thank Sandra Galeano (IAvH), John D. Lynch and Mauricio Rivera-Correa (ICN), and Fernando Sarmiento (MLS). Giovanni Chaves-Portilla provided clarification regarding the distribution patterns of various *Bolitoglossa* obtained during his fieldwork in western Cundinamarca and shared unpublished data with us. We thank Carlos Hernández for his invaluable laboratory assistance and Nelsy Pinto Sánchez, Martha Lucía Calderón, and Juan Carvajal Cogollo for kindly sharing their tissues and sequences with us. Sequencing was possible thanks to the funding provided by the Conservation Leadership Programme to FLMJ. We also thank Jorge Hernández, who kindly allowed us to use the equipment and space at his lab CINBIN. This project was funded by Empresas Públicas de Medellín (EPM) and Fundación Natura, Bogotá D.C., Colombia, via Acuerdo no. 894 of 2020; collection and research permits were granted by Autoridad Nacional de Licencias Ambientales de Colombia (ANLA), Resolución 0047-2015. The manuscript was greatly improved by comments and suggestions from Sean M. Rovito, Larry David Wilson, and Carlos Vásquez-Almazán.

References

Acevedo AA, Wake DB, Márquez R, Silva K, Franco R, Amézquita A (2013) Two new species of salamanders, genus *Bolitoglossa* (Amphibia: Plethodontidae), from the eastern Colombian Andes. Zootaxa 3609(1): 69–84. https://doi.org/10.11646/zootaxa.3609.1.5

Angarita-Sierra T, Bonilla-Gómez MA, Sánchez DA, Acosta-Galvis AR, Medina-Ovalle H, Solano-Moreno A, Ulloa-Rengifo S, Guevara-Guevara D, Torres-Ramírez JJ, Curaca-Fierro S, Cabrera-Amaya DM, Infante-Betancour JA, Londoño-Montaño LF, Albarán-Montoya DX, Peña-Baez LR (2020) Distribution, habitat suitability, conservation state and natural history of endangered salamander *Bolitoglossa pandi*. PeerJ 8: e9901. https://doi.org/10.7717/peerj.9901

Arrivillaga C, Brown T (2018) Primary descriptions of defense mechanisms employed by neotropical salamanders (*Bolitoglossa*, *Oedipina*, *Nototriton*, and *Cryptotriton* sp.: Plethodontidae) in Cusuco National Park, Honduras. I RCF Reptiles & Amphibians 25(2): 99–103. https://doi.org/10.17161/randa.v25i2.14253

Bachman S, Moat J, Hill AW, de la Torre J, Scott B (2011) Supporting Red List threat assessments with GeoCAT: geospatial conservation assessment tool. In: Smith V, Penev L (Eds) e-Infrastructures for data publishing in biodiversity science. ZooKeys 150: 117–126. https://doi.org/10.3897/zookeys.150.2109

Batista A, Köhler G, Mebert K, Vesely M (2014) A new species of *Bolitoglossa* (Amphibia: Plethodontidae) from eastern Panama, with comments on other species of the *adspersa* species group from eastern Panama. Mesoamerican Herpetology 1: 97–121.

Bingham RE, Papenfuss TJ, Lindstrand L III, Wake D (2018) Phylogeography and species boundaries in the *Hydromantes shastae* complex, with description of two new species

(Amphibia; Caudata; Plethodontidae). Bulletin of the Museum of Comparative Zoology 161(10): 403–427. https://doi.org/10.3099/MCZ42.1

Brame Jr AH, Wake DB (1963) The salamanders of South America. Contributions in Science 69: 1–73. https://doi.org/10.5962/p.241017

Cruz-Rodríguez C, Lynch JD, Cárdenas JS, Caicedo-Portilla JR (2021) Type specimens housed in the herpetological collections at Museo La Salle Bogotá and their historical importance for the consolidation of herpetology in Colombia. Zootaxa 4965(2): 261–292. https://doi.org/10.11646/zootaxa.4965.2.3

Cusi JC, Gagliardi-Urrutia G, Brcko IC, Wake DB, Von May R (2020) Taxonomic status of the Neotropical salamanders *Bolitoglossa altamazonica* and *Bolitoglossa peruviana* (Amphibia: Caudata: Plethodontidae), with the description of a new species from Northern Peru. Zootaxa 4834(3): 365–406. https://doi.org/10.11646/zootaxa.4834.3.3

Frost DR (2023) Amphibian species of the world: An online reference. Version 6.1. Electronic Database. https://doi.org/10.5531/db.vz.0001 [Accessed 17 February 2023]

Hanken J, Wake DB (1982) Genetic differentiation among plethodontid salamanders (genus *Bolitoglossa*) in Central and South America: Implications for the South American invasion. Herpetologica 38: 272–288. http://www.jstor.org/stable/3892329

Hoang DT, Chernomor O, von Haeseler A, Minh BQ, Vinh LS (2018) UFBoot2: Improving the ultrafast bootstrap approximation. Molecular Biology and Evolution 35(2): 518–522. https://doi.org/10.1093/molbev/msx281

Jaramillo AF, De La Riva I, Guayasamin JM, Chaparro JC, Gagliardi-Urrutia G, Gutiérrez RC, Brckok I, Vilàl C, Castroviejo-Fisher S (2020) Vastly underestimated species richness of Amazonian salamanders (Plethodontidae: *Bolitoglossa*) and implications about plethodontid diversification. Molecular Phylogenetics and Evolution 149: 1–23. [106841] https://doi.org/10.1016/j.ympev.2020.106841

Katoh K, Standley DM (2013) MAFFT multiple sequence alignment software version 7: Improvements in performance and usability. Molecular Biology and Evolution 30(4): 772–780. https://doi.org/10.1093/molbev/mst010

Kearse M, Moir R, Wilson A, Stones-Havas S, Cheung M, Sturrock S, Buxton S, Cooper A, Markowitz S, Duran C, Thierer T, Ashton B, Mentjies P, Drummond A (2012) Geneious Basic: An integrated and extendable desktop software platform for the organization and analysis of sequence data. Bioinformatics 28(12): 1647–1649. https://doi.org/10.1093/bioinformatics/bts199

Köhler G (2011) Amphibians of Central America. Herpeton, Verlag Elke Köhler, Offenbach, Germany, 374 pp.

Köhler G (2012) Color Catalogue for Field Biologists. Herpeton, Offenbach, Germany, 49 pp.

Kumar S, Stecher G, Li M, Knyaz C, Tamura K (2018) MEGA X: Molecular evolutionary genetics analysis across computing platforms. Molecular Biology and Evolution 35(6): 1547–1549. https://doi.org/10.1093/molbev/msy096

Lanfear R, Frandsen PB, Wright AM, Senfeld T, Calcott B (2017) PartitionFinder 2: New methods for selecting partitioned models of evolution for molecular and morphological phylogenetic analyses. Molecular Biology and Evolution 34(3): 772–773. https://doi.org/10.1093/molbev/msw260

Liu J, Slick F, Zheng S, Lindenmayer DB (2022) Undescribed species have higher extinction risk than known species. Conservation Letters 15(3): e12876. https://doi.org/10.1111/conl.12876

Masters BC, Fan V, Ross HA (2011) Species Delimitation – a Geneious plugin for the exploration of species boundaries. Molecular Ecology Resources 11(1): 154–157. https://doi.org/10.1111/j.1755-0998.2010.02896.x

Meza-Joya FL, Hernández-Jaimes C, Ramos-Pallares E (2017) A new species of salamander (Caudata, Plethodontidae, *Bolitoglossa*) from Serranía de los Yariguíes, Colombia. Zootaxa 4294(1): 93–111. https://doi.org/10.11646/zootaxa.4294.1.4

Moritz C, Schneider CJ, Wake DB (1992) Evolutionary relationships within the *Ensatina eschscholtzii* complex confirm the ring species interpretation. Systematic Biology 41(3): 273–291. https://doi.org/10.1093/sysbio/41.3.273

Nguyen LT, Schmidt HA, von Haeseler A, Minh BQ (2015) IQ-TREE: A fast and effective stochastic algorithm for estimating maximum likelihood phylogenies. Molecular Biology and Evolution 32(1): 268–274. https://doi.org/10.1093/molbev/msu300

Palumbi S, Martin A, Romano S, McMillan WO, Stice L, Grabowski G (1991) The Simple Fool's Guide to PCR. University of Hawaii, Honolulu, 47 pp.

Parra-Olea G, García-París M, Wake DB (2004) Molecular diversification of salamanders of the tropical American genus *Bolitoglossa* (Caudata: Plethodontidae) and its evolutionary and biogeographical implications. Biological Journal of the Linnean Society. Linnean Society of London 81(3): 325–346. https://doi.org/10.1111/j.1095-8312.2003.00303.x

Ponssa ML, Fratani J, Barrionuevo JS (2022) Phalanx morphology in salamanders: A reflection of microhabitat use, life cycle or evolutionary constraints? Zoology (Jena, Germany) 154: 126040. https://doi.org/10.1016/j.zool.2022.126040

Puillandre N, Lambert A, Brouillet S, Achaz G (2012) ABGD, automatic barcode gap discovery for primary species delimitation. Molecular Ecology 21(8): 1864–1877. https://doi.org/10.1111/j.1365-294X.2011.05239.x

Rambaut A, Drummond AJ, Xie D, Baele G, Suchard MA (2018) Posterior summarization in Bayesian phylogenetics using Tracer 1.7. Systematic Biology 67(5): 901–904. https://doi.org/10.1093/sysbio/syy032

Ronquist F, Teslenko M, van der Mark P, Ayres DL, Darling A, Höhna S, Larget B, Liu L, Suchard MA, Huelsenbeck JP (2012) MrBayes 3.2: Efficient Bayesian phylogenetic inference and model choice across a large model space. Systematic Biology 61(3): 539–542. https://doi.org/10.1093/sysbio/sys029

Wake DB, Lynch JF (1976) The distribution, ecology, and evolutionary history of plethodontid salamanders in tropical America. Science bulletin – Natural History Museum. Los Angeles County 25: 1–65.

Appendix 1

Table A1. GenBank accession numbers of the *Bolitoglossa* and outgroup (*) sequences used in the phylogenetic analysis. Accession numbers in bold correspond to the new sequences presented in this paper. Subspecies and species group sensu Parra-Olea et al. (2004).

Species	Subspecies	Group	16S	cyt *b*	Rag–1	Voucher	Locality
B. adspersa	*Eladinea*	*adspersa*	OQ681031	OQ685920	–	MLC348	Colombia: Cundinamarca, La Calera
B. adspersa	*Eladinea*	*adspersa*	AF218492	AF212984	–	MVZ 158485	Colombia: Cundinamarca, Ubaté
B. adspersa	*Eladinea*	*adspersa*	OQ681032	–	–	N/A	Colombia: Cundinamarca, Choachí
B. adspersa	*Eladinea*	*adspersa*	OQ681033	–	–	DEQ4	Colombia: Santander, Sucre
B. altamazonica	*Eladinea*	*adspersa*	MT301583	MT301731	MT301938	ORP 505	Peru: Loreto, near Nauta
B. altamazonica	*Eladinea*	*adspersa*	MT301579	MT301799	MT301913	F 01	Peru: Loreto, near Nauta
B. awajun	*Eladinea*	*adspersa*	MG944411	MG944420	MG944441	CRBIIAPAR1124	Peru: San Martín, San Martín, San Antonio, Cordillera Escalera
B. awajun	*Eladinea*	*adspersa*	MG944412	MG944422	MG944442	CRBIIAPAR1125	Peru: San Martín, San Martín, San Antonio, Cordillera Escalera
B. biseriata	*Eladinea*	*adspersa*	AY526118	AY526161	–	S13236	Panamá: Kuna Yala, Nusagandi
B. biseriata	*Eladinea*	*adspersa*	–	AY526161	KC614436	MVZ 232943	Panamá: Kuna Yala, Nusagandi
B. caldwellae	*Eladinea*	*adspersa*	AY526129	AY526168	–	MPEG 12881	Brazil: Acre, Porto Walter
B. caldwellae	*Eladinea*	*adspersa*	MT301584	–	–	CFBHT 54	Brazil: Acre, Serra do Divisor
B. chucantiensis	*Eladinea*	*adspersa*	KM527324	–	–	SMF 97141	Panamá: Darién, Chepigana, Cerro Chucantí
B. equatoriana	*Eladinea*	*adspersa*	MT301585	MT301789	–	IIAP999	Peru: Loreto, Maynas, Curaray river
B. equatoriana	*Eladinea*	*adspersa*	–	DQ353842	KC614451	QCAZ 25448	Ecuador: Napo, Estación Biológica Jatun Sacha
B. guaneae	*Eladinea*	*adspersa*	KU985264	KX458162	–	UIS-A 5275	Colombia: Santander, Charalá, Virolín
B. guaneae	*Eladinea*	*adspersa*	KU985265	KX458163	–	UIS-A 5276	Colombia: Santander, Charalá, Virolín
B. hypacra	*Eladinea*	*adspersa*	MT301588	–	–	SAS 446	Colombia: Antioquia, Paramo Frontino
B. hypacra	*Eladinea*	*adspersa*	MT301589	–	–	SAS 447	Colombia: Antioquia, Paramo Frontino
B. leandrae	*Eladinea*	*adspersa*	KC257102	–	–	MCNUP 63	Colombia: Norte de Santander, San Antonio
B. leandrae	*Eladinea*	*adspersa*	MT301592	MT301732	MT301921	VVO 837	Colombia: Meta, Villavicencio
B. lozanoi	*Eladinea*	*adspersa*	KU985266	KX458164	–	H 3	Colombia: Santander, Floridablanca
B. lozanoi	*Eladinea*	*adspersa*	KU985267	KX458165	–	UIS-A 5269	Colombia: Santander, Girón
B. madeira	*Eladinea*	*adspersa*	AY526128	AY526167	–	LSUMZ-H 3086	Brazil: Amazonas, Ituxi river, Madeireira Scheffer
B. madeira	*Eladinea*	*adspersa*	MT301594	MT301733	MT301895	MPEG 28601	Brazil: Acre: Fazenda Experimental Catuaba, Branco river
B. medemi	*Eladinea*	*adspersa*	AY526123	AY526163	KC614437	S13237	Panamá: Kuna Yala, Nusagandi
B. medemi	*Eladinea*	*adspersa*	KM527327	–	–	SMF 97131	Panamá: Darién, Serranía de San Blas
B. mucuyensis	*Eladinea*	*adspersa*	JN635335	JQ665282	–	CVULA 7100	Venezuela: Mérida, La Mucuy
B. mucuyensis	*Eladinea*	*adspersa*	JN635336	–	–	CVULA 7101	Venezuela: Mérida, La Mucuy
B. nicefori	*Eladinea*	*adspersa*	KX458176	KX458166	–	UIS-A 5270	Colombia: Santander, San Gil
B. nicefori	*Eladinea*	*adspersa*	KX458177	KX458167	–	UIS-A 5271	Colombia: Santander, San Gil
B. orestes	*Eladinea*	*adspersa*	JN635340	JQ665280	–	CVULA 7109	Venezuela: Mérida, Sierra La Culata
B. orestes	*Eladinea*	*adspersa*	JN635351	JQ665281	–	MC00	Venezuela: Mérida, Sierra La Culata
B. palmata	*Eladinea*	*adspersa*	AY526125	AY526164	–	KU 217422	Ecuador: Napo, Cordillera de Guacamayos
B. palmata	*Eladinea*	*adspersa*	MT301595	–	MT301941	MZUTI 2220	Ecuador: Napo, Cordillera de los Guacamayos, La Virgen
B. paraensis	*Eladinea*	*adspersa*	MT301596	–	–	CFBHT 20324	Brazil: Para, Moju, Moju river
B. paraensis	*Eladinea*	*adspersa*	MT301597	MT301734	MT301892	MPEG 31672	Brazil: Para, Santa Izabel, Semente Etérea, Vila do Carapuru

Species	Subspecies	Group	16S	cyt *b*	Rag–1	Voucher	Locality
B. peruviana	*Eladinea*	*adspersa*	MG944408	MG944417	MG944436	CRBIIAP AR1118	Peru: Loreto, Alto Amazonas, Cordillera Escalera
B. peruviana	*Eladinea*	*adspersa*	MT301600	MT301791	MT301900	CRBIIAP AR1038	Peru: Loreto, Alto Amazonas, Balsa Puerto, Shawi
B. muisca	*Eladinea*	*adspersa*	AY526135	AY526173	–	MVZ 167997	Colombia: Cundinamarca, El Soche
B. muisca	*Eladinea*	*adspersa*	OQ681034	–	–	IAvH-Am-17414	Colombia: Cundinamarca, Bojacá
B. muisca	*Eladinea*	*adspersa*	OQ681035	–	–	IAvH-Am-17417	Colombia: Cundinamarca, Bojacá
B. sima	*Eladinea*	*adspersa*	AY526134	AY526172	–	MVZ 2057	Colombia: Valle del Cauca
B. sp. 'Chilma'	*Eladinea*	*adspersa*	–	KC614431	KC614456	QCAZ 39981	Ecuador: Carchi, Chilma Bajo
B. sp. 'Cisneros'	*Eladinea*	*adspersa*	MT301603	MT301735	MT301876	AFJ 006	Colombia: Valle del Cauca, Buenaventura, Cisneros, Los Turbos
B. sp. 'Cisneros'	*Eladinea*	*adspersa*	MT301602	–	–	AFJ 010	Colombia: Valle del Cauca, Buenaventura, Cisneros, Los Turbos
B. sp. 'Jingurudó'	*Eladinea*	*adspersa*	KM527329	–	–	MHCH 2663	Panamá: Darién, Chepigana, Serranía de Jingurudó
B. sp. 'Llullapichi'	*Eladinea*	*adspersa*	MT301618	MT301741	MT301898	FGZC 4837	Peru, Huánuco, Panguana station, lower Llullapichis river
B. sp. 'Llullapichi'	*Eladinea*	*adspersa*	MT301614	MT301739	MT301905	CORBIDI 14387	Peru: Huanuco, Puerto Inca, Llullapichis: Cordillera del Sira
B. sp. 'Pensilvania'	*Eladinea*	*adspersa*	MT301607	MT301793	MT301917	GGD 640	Colombia: Caldas, Pensilvania, road to Arboleda
B. sp. 'Pirinari'	*Eladinea*	*adspersa*	MT301700	–	–	MUBI 10081	Peru: Loreto, Parinari, Hamburgo, Samiria river
B. sp. 'Pirinari'	*Eladinea*	*adspersa*	MT301701	MT301778	MT301885	MUBI 10099	Peru: Loreto, Parinari, Pithecia, Samiria river
B. sp. 'Salamina'	*Eladinea*	*adspersa*	MT301606	MT301736	MT301875	GGD 111	Colombia: Caldas, Salamina, Tribunas farm
B. sp. 'Sanare'	*Eladinea*	*adspersa*	MT301608	MT301737	MT301926	MOE 01	Venezuela: Lara, Sanare, El Blanquito, Yacambu National Park
B. sp.	*Eladinea*	*adspersa*	MT301604	MT301792	–	DQ 175	Venezuela
B. sp.	*Eladinea*	*adspersa*	MT301605	–	MT301871	DQ 177	Venezuela
B. tamaense	*Eladinea*	*adspersa*	KC257098	–	–	MCNUP 56	Colombia: Norte de Santander, Los Remansos
B. tamaense	*Eladinea*	*adspersa*	KC257099	–	–	MCNUP 57	Colombia: Norte de Santander, Los Remansos
B. tapajonica	*Eladinea*	*adspersa*	MT301711	MT301802	MT301933	MPEG 31688	Brazil: Para, Juruti
B. tapajonica	*Eladinea*	*adspersa*	MT301712	MT301786	MT301934	MPEG 31695	Brazil: Para, Lorena
B. taylori	*Eladinea*	*adspersa*	KM527337	–	–	AB 171	Panamá: Darién, Pinogana, Serranía de Pirre
B. taylori	*Eladinea*	*adspersa*	KM527335	–	–	AB 173	Panamá: Darién, Pinogana, Serranía de Pirre
B. vallecula	*Eladinea*	*adspersa*	MT301713	MT301787	MT301874	AFJ 48	Colombia: Valle del Cauca, El Cairo, Cerro del Inglés
B. walkeri	*Eladinea*	*adspersa*	MT301714	MT301788	MT301873	AFJ 02	Colombia: Valle del Cauca, Cali, San Antonio
B. walkeri	*Eladinea*	*adspersa*	MT301715	–	–	AFJ 03	Colombia: Valle del Cauca, Cali, San Antonio
B. yariguiensis	*Eladinea*	*adspersa*	KU985275	KX458173	–	UIS-A 5280	Colombia: Santander, San Vicente de Chucurí
B. yariguiensis	*Eladinea*	*adspersa*	KU985276	KX458174	–	UIS-A 5281	Colombia: Santander, San Vicente de Chucurí
*B. cerroensis**	*Eladinea*	*epimela*	AF199233	AF199195	KC614459		
*B. epimela**	*Eladinea*	*epimela*	AY526120	AF212097	–		
*B. minutula**	*Eladinea*	*epimela*	AY526124	AF212098	KC614434		
*B. nigrescens**	*Eladinea*	*schizodactyla*	JQ899164	JQ899194	–		
*B. robusta**	*Eladinea*	*schizodactyla*	EU448109	EU448110	–		
*B. schizodactyla**	*Eladinea*	*schizodactyla*	AY526133	AY526171	–		
*B. splendida**	*Eladinea*	*subpalmata*	JQ899150	JQ899181	–		
*B. subpalmata**	*Eladinea*	*subpalmata*	AF416697	AF212094	–		
*B. tica**	*Eladinea*	*subpalmata*	JQ899162	JQ899192	–		

ZooKeys 1158: 49–67 (2023)
doi: 10.3897/zookeys.1158.99411
https://zookeys.pensoft.net

RESEARCH ARTICLE

A peer-reviewed open-access journal
ZooKeys
Launched to accelerate biodiversity research

Five new species of *Bradina* Lederer (Lepidoptera, Crambidae) from China, with remarks on the morphology of the genus

Jia-Ming Guo[1], Xi-Cui Du[1]

1 *College of Plant Protection, Southwest University, Chongqing, China*

Corresponding author: Xi-Cui Du (duxicui@hotmail.com; duxicui@swu.edu.cn)

Academic editor: R. Mally | Received 30 December 2022 | Accepted 30 March 2023 | Published 19 April 2023

https://zoobank.org/A3AD0A1D-9178-4B91-BC2C-0C1A1AC65312

Citation: Guo J-M, Du X-C (2023) Five new species of *Bradina* Lederer (Lepidoptera, Crambidae) from China, with remarks on the morphology of the genus. ZooKeys 1158: 49–67. https://doi.org/10.3897/zookeys.1158.99411

Abstract

Bradina is a species-rich genus that differs from most other Spilomelinae genera because of its distinctive wing venation. Most species of this genus are very similar in appearance. In this study, we have studied morphological characteristics of the genus and eight closely related species from China. Among them, *B. falciculata* Guo & Du, **sp. nov.**, *B. fusoidea* Guo & Du, **sp. nov.**, *B. spirella* Guo & Du, **sp. nov.**, *B. ternifolia* Guo & Du, **sp. nov.** and *B. torsiva* Guo & Du, **sp. nov.** are described as new to science. *Bradina megesalis* (Walker, 1859), *B. translinealis* Hampson, 1896 and *B. subpurpurescens* (Warren, 1896) are redescribed based on their holotypes and additional material, and the latter two are newly recorded from China and their genitalia are described for the first time. The images of the habitus and genitalia of these eight species are provided, with a key to their identification.

Keywords

Genitalia, identification key, morphology, Pyraloidea, Spilomelinae, taxonomy

Introduction

Bradina Lederer, 1863 is the most species-rich genus in the Spilomelinae tribe Steniini Guenée, 1854, redefined by Mally et al. (2019). So far, there are 89 species recorded in this genus worldwide (Nuss et al. 2003–2023) and they are mainly distributed in the Oriental and Australian regions. Numerous endemic species are present in the Australian and Pacific islands.

In Spilomelinae, *Bradina* can be differentiated from most other genera by the forewings with Rs_1 anastomosed with Rs_2+s_3 at the base, which is common in Acentropinae. Therefore, this genus was placed in Hydrocampinae (= Acentropinae Stephens, 1835) for a long time (Hampson 1896; Hampson 1897; Rothschild 1915; Schaus 1924; Caradja 1925). Inoue (1955) transferred the genus to Pyraustinae (s. l.). Systematics research on *Bradina* is inadequate globally besides some early studies (Hampson 1896; Hampson 1897; Yamanaka 1984; Du 2008). Seizmair (2021) recorded *Bradina* from the Arabian Peninsula and divided the genus into seven groups according to wing pattern.

Species identification of *Bradina* is difficult because of their very similar appearance, so the genitalia characteristics are necessary in the identification of most species. The large spinose crescent-shaped signum of the female genitalia is a diagnostic characteristic of the genus, but shows little difference among species. In male genitalia, the valvae and uncus are very diverse in morphology, which is very valuable for interspecific identification. Before this study, 13 species were recorded in China (Lu and Guan 1953; Wang and Speidel 2000; Du 2008). In the present study, eight *Bradina* species with externally similar adults and male genitalia morphology are recorded, including five new species and two newly recorded species from China.

Materials and methods

Specimens examined, including the types of new species, are deposited in the College of Plant Protection, Southwest University, Chongqing, China (**SWU**) except for two holotypes and 38 paratypes which are deposited in the Insect Collection of the College of Life Science, Nankai University, Tianjin, China (**NKU**). The corresponding author examined many specimens of *Bradina* deposited in Natural History Museum, London, United Kingdom (**NHMUK**), including some types.

The photographs of the adults were taken with a digital camera (Canon EOS 5D), and those of the genitalia were obtained with a digital camera (Leica DFC 450) attached to a stereomicroscope (Leica M205 A).

The preparation of genitalia mainly follows Li and Zheng (1996). Morphological terminology mainly refers to Maes (1995) as well as Mally and Nuss (2011).

Taxonomic account

Bradina Lederer, 1863

Bradina Lederer, 1863: 424. Type species: *Bradina impressalis* Lederer, 1863; subsequent designation by Hampson 1896.

Erilita Lederer, 1863: 426. Type species: *Erilita modestalis* Lederer, 1863, by monotypy.

Pleonectusa Lederer, 1863: 426. Type species: *Botys admixtalis* Walker, 1859; subsequent designation by Moore 1884.

Trematarcha Meyrick, 1886: 233. Type species: *Marasmia erilitalis* Felder, Felder & Rogenhofer, 1875; subsequent designation by Klima 1937.

Diagnosis. ***Head*** (Fig. 1A). Frons rounded. Antenna annulated, male with short cilia ventrally. Labial palpus obliquely upturned, second segment with broad scales ventrally, third joint minute and forward, apex blunt. Maxillary palpus filiform. ***Thorax.*** Forewing long and narrow usually; length of cell c. half of wing; discocellulars incurved; R from cell at c. four fifths above; Rs_1 anastomosed with Rs_2+s_3 at base and with a long stalk c. two fifths of Rs_3; Rs_2 and Rs_3 stalked c. three fifths of Rs_3; basal half of Rs_4 straight and clearly separated from $Rs_1+s_2+s_3$; M_2, M_3 and CuA_1 uniformly from posterior angle of cell at base (except for *B. diagonalis* Hampson, 1896); CuA_2 from cell at three quarters below. Hindwing with length of cell c. one third of wing; discocellulars incurved; Sc+R and Rs stalked c. one third of Rs; Rs and M_1 from anterior angle of cell; M_2, M_3 and CuA_1 uniformly from posterior angle of cell; CuA_2 from cell at four fifths below (Fig. 1B). Legs long and slender; middle tibia with outer distal spur c. half-length of inner spur. ***Abdomen.*** Male abdomen long and slender (except for *B. melanoperas* Hampson, 1896).

Male genitalia. Uncus diverse, apex with setae dorsally. Valva narrow or broad, some with well-developed setal cluster. Saccus developed. Phallus long and cylindrical.

Female genitalia. Papillae anales densely setose. Apophyses anteriores c. twice length of apophyses posteriores. Ostium bursae well developed. Corpus bursae rounded or oval, inside usually densely studded with tiny spines; signum crescent and densely spinose, spines on concave side developed.

Remarks. The generic characteristics were summarized by Khan (2000), but the description about wing venation was incomplete. In addition, the lengths of the maxillary palpus and labial palpus were identical in Khan's description, while we found that both have their ends at the same height but they are of different lengths. Therefore, the generic characteristics are revised in the present study.

The bodies of *Bradina* species are usually brown, yellowish brown, or pale brown, except for a few species with white bodies, and have nearly identical wing markings. The male genitalia, on the other hand, are very diverse among species of this genus. We found that the male genitalia can be divided into three types according to the morphological characteristics of the valvae. The first type, represented by *B. admixtalis*, have long and narrow valvae; the second type, represented by *B. melanoperas*, have short and broad valvae; the third type, represented by *B. megesalis*, have broad valvae in which the costa is arched near the base or middle. Species in the present study have the third valva type, accompanied by the following common characteristics: body brown of various shades. Uncus broad, distal part bilobed, with dense short setae dorsally. Valva broad; costa arched near base or middle and accompanied by a cluster of long setae, usually followed by a depression. Saccus nearly trapezoidal, slightly concaved terminally. Juxta nearly rounded, split posteriorly. Phallus distinctly inflated at anterior end. Apophyses anteriores expanded at c. one third from base.

Key to *Bradina* species in the present study based on genitalia

1 Sacculus with a cluster of long setae near middle **2**
– Sacculus without long setal cluster **5**
2 Phallus with one fusiform cornutus composed of short and blunt spines, and one subcircular sclerotized cornutus ..... ***B. fusoidea* sp. nov.**
– Phallus with various cornuti, but not as above **3**
3 Phallus with three long leaf-like cornuti tapered apically ..... ***B. ternifolia* sp. nov.**
– Cornuti not as above **4**
4 Posterior phallus with two developed spear-like cornuti ..... ***B. megesalis***
– Phallus with one short and spiral band-like cornutus tapered at posterior end, along with two lamellar cornuti in posterior half ..... ***B. spirella* sp. nov.**
5 Valva nearly rectangular, broad distally ..... ***B. subpurpurescens***
– Valva nearly elliptical or narrowed distally **6**
6 Phallus with one broad and spiral band-like cornutus ..... ***B. torsiva* sp. nov.**
– Phallus with cornutus not as above **7**
7 Phallus with one fusiform cornutus medially, and with two lamellar cornuti posteriorly. Ductus bursae slender, membranous ..... ***B. translinealis***
– Phallus with one small fusiform cornutus anteriorly, and with two sickle-shaped cornuti posteriorly. Ductus bursae relatively thick, slightly sclerotized medially ..... ***B. falciculata* sp. nov.**

***Bradina megesalis* (Walker, 1859)**
Figs 1A, 2A, 3A–E

Botys megesalis Walker, 1859: 663. Type locality: North China. Type depository: NHMUK.
Bradina megesalis: Hampson, 1897: 200.

Material examined. *Holotype*, ♂ North China, from Mr Fortune's collection (Walker, 1859), genitalia slide no. 8735 (NHMUK).

Additional material. China, Chongqing Municipality, 2 ♂♂, 6 ♀♀, Bashan Town, Chengkou County, alt. 900 m, 10 July 2017, Ji-Ping Wan leg.; 2 ♂♂, 4 ♀♀, Jinfo Mountain, alt. 918 m, 27 August 2019, You Zeng leg.; 1 ♂, Simian Mountain, alt. 1280 m, 12 July 2012, Gui-Qing He leg.; **Guangdong Prov.**, 2 ♂♂, 2 ♀♀, Dadong Mountain, Lian County, 5–8 July 2008, Feng-Xia He leg., genitalia slide no.: GJM21078 ♂; 1 ♂, 2 ♀♀, Qianjin Conservation Station, Shimentai Nature Reserve, Qingyuan City, alt. 523 m, 26 May 2021, Xing-Hai Zuo leg., genitalia slide no.: GJM21073 ♂; **Guangxi Zhuang Autonomous Region**, 1 ♂, Yinshan Park, Dayao Mountain, alt. 1564 m, 8 July 2013, Xiao-Hua Chen leg.; **Guizhou Prov.**, 2 ♂♂, 4 ♀♀, Leigong Mountain, Leishan County, alt. 1198 m, 14–15 July 2013, Xiao-Hua Chen leg., genitalia slide no.: GJM21076 ♂; **Hubei Prov.**, 18 ♂♂, 33 ♀♀, Dabie

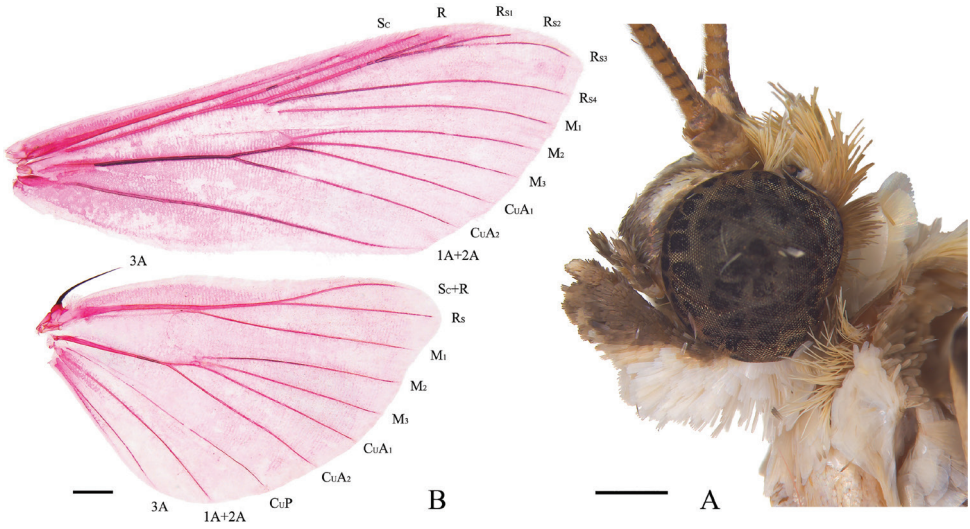

Figure 1. *Bradina megesalis*, male **A** head **B** wing venation, wing slide no. GJM21001. Scale bars: 0.5 mm (**A**); 1.0 mm (**B**).

Mountain, alt. 590 m, 24–25 June 2014, Li-Jun Xu leg.; **Hainan Prov.**, 1 ♂, 1 ♀, Bawangling National Forest Park, 8–10 June 2010, Li Kang leg.; **Hunan Prov.**, 5 ♀♀, Wuyunjie Nature Reserve, alt. 178 m, 19 June 2019, Ying Yang leg.; **Sichuan Prov.**, 2 ♂♂, 1 ♀, Longcanggou Forest Park, Xingjing County, alt. 1388 m, 17 June 2021, Shuai Yu leg., genitalia slide no.: GJM21074 ♂, GJM21080 ♀; **Shaanxi Prov.**, 1 ♂, Zuoshui County, Shangluo City, alt. 810 m, 29 June 2021, Jin-Hang Han leg.; 1 ♂, 5 ♀♀, Hanyin County, Ankang City, alt. 410 m, 26 June 2021, Jin-Hang Han leg.; **Yunnan Prov.**, 9 ♂♂, 6 ♀♀, Baihualing Village, Baoshan City, alt. 1487 m, 20–23 June 2020, Ying Yang & Hong Zhao leg.; 2 ♂♂, 1 ♀, Cuanlong Village, Mangba Town, Tengchong City, Baoshan City, alt. 1329 m, 8 August 2015, Jing-Xia Zhao & Hao Wei leg.; **Zhejiang Prov.**, 6 ♂♂, 7 ♀♀, Jiulongshan Forest Park, 4–6 August 2011, Xiao-Bing Fu leg.; 6 ♂♂, 34 ♀♀, Tianmu Mountain, alt. 800 m, 29 July 2011, Xi-Cui Du & Xiao-Bing Fu leg.

Redescription. ***Adult*** (Figs 1A, 2A). Wingspan 31.0–39.0 mm, forewing length 15.0–19.0 mm. Body and wings pale brown. Frons brown, with lateral sides white above. Vertex yellowish white. Antenna brownish yellow, with black ring dorsally; ventral cilia c. one quarter length of diameter of male flagellomeres. Labial palpus with basal two thirds white, black-brown distally. Maxillary palpus yellowish brown, white at base. Patagium pale brown, yellowish. Thorax white ventrally. Forewing pale brown, darker along basal two thirds costa, stigmata and lines brown; discoidal stigma crescent; postmedial line at c. two thirds of wing, straight and nearly parallel to terminal margin. Hindwing with postmedial line and discoidal stigma pale brown, inconspicuous usually; discoidal stigma crescent. Cilia pale brown, yellowish white on inner margin of hindwing. Legs pale yellow, coxae and femora with white gloss. Middle tibia brown;

hind tibia with outer middle spurs c. two thirds length of inner spurs. Abdomen pale brown dorsally, with each segment pale terminally; yellowish white ventrally.

Male genitalia (Fig. 3A, B). Valva distally gradually narrowed and bearing dense long setae; costa sharply arched near middle and accompanied by a cluster of long curved setae; sacculus gradually narrowed to apex, with a cluster of long setae near middle. Posterior phallus with two developed spear-like cornuti.

Female genitalia (Fig. 3C–E). Antrum broad. Ductus bursae posteriorly sharply inflated into a thorny irregular protrusion, adjoined posteriorly by crescent colliculum laterally, anterior half gradually widened to corpus bursae. Corpus bursae nearly rounded, with dense tiny spines inside, transverse signum crescent and densely spinose.

Distribution. China (Chongqing, Fujian, Gansu, Guangdong, Guangxi, Guizhou, Hubei, Hainan, Hunan, Sichuan, Shaanxi, Yunnan, Zhejiang), Japan (Shibuya 1929).

Remarks. We found that the coremata of some male individuals of this species were protruded out of the body, forming a cluster of white hairs at the end of the abdomen.

Bradina fusoidea **Guo & Du, sp. nov.**

https://zoobank.org/CEACA386-3CD0-4FFF-85F5-1140F4B86FEF

Figs 2B, 3F–K

Type material. ***Holotype*****,** ♂ **China: Sichuan Prov.**, Qingcheng Mountain, Dujiangyan city, alt. 860 m, 30°92'N, 103°50'E, 22 July 2021, Shuai Yu, Xiao-Ju Zhu, Di Zhang leg. (NKU), genitalia slide no. GJM21117. ***Paratypes*****. China: Sichuan Prov.**, 6 ♂♂, 1 ♀, other same data as holotype (NKU), genitalia slide no.: GJM21112 ♂, GJM21118 ♀; 1 ♂, Emei Mountain, Leshan City, alt. 847 m, 22 July 2021, Shuai Yu, Xiao-Ju Zhu, Di Zhang leg. (NKU), genitalia slide no.: GJM21113; **Guangdong Prov.,** 2 ♂♂, 1 ♀, Heishiding Nature Reserve, Fengkai County, Zhaoqing City, 14–16 June 2009, Feng-Xia He leg., genitalia slide no.: GJM21114 ♂, GJM21180 ♀.

Diagnosis. This species is similar to *B. megesalis*. The difference in appearance is that the distance between discoidal stigma and postmedial line on forewing of this species is longer than that of *B. megesalis*; the postmedial line and terminal margin of forewing is obviously unparallel in this species, while is nearly parallel in the latter. It also can be distinguished by the setal cluster near middle of sacculus being shorter than that of the latter, phallus with one fusiform cornutus and one subcircular cornutus (two spear-like cornuti in *B. megesalis*), posterior ductus bursae inflated but not forming irregular protrusion as in *B. megesalis*, plus subposterior section of ductus bursae widened along half of ductus length, a feature that is absent in *B. megesalis*.

Description. ***Adult*** (Fig. 2B). Wingspan 31.0–33.0 mm, forewing length 15.0–16.0 mm. Frons white, except brown on frontal base and middle near vertex. Vertex white. Antenna yellow, with pale brown ring dorsally; ventral cilia c. half-length of flagellomere diameter of male. Labial palpus with basal two thirds white, black-brown distally. Maxillary palpus black-brown. Patagium yellowish white. Tegula pale brown. Thorax pale brown dorsally, white ventrally. Wings pale brown, gradually darkened to terminal; stigmata and lines dark brown. Forewing black-brown along basal half of

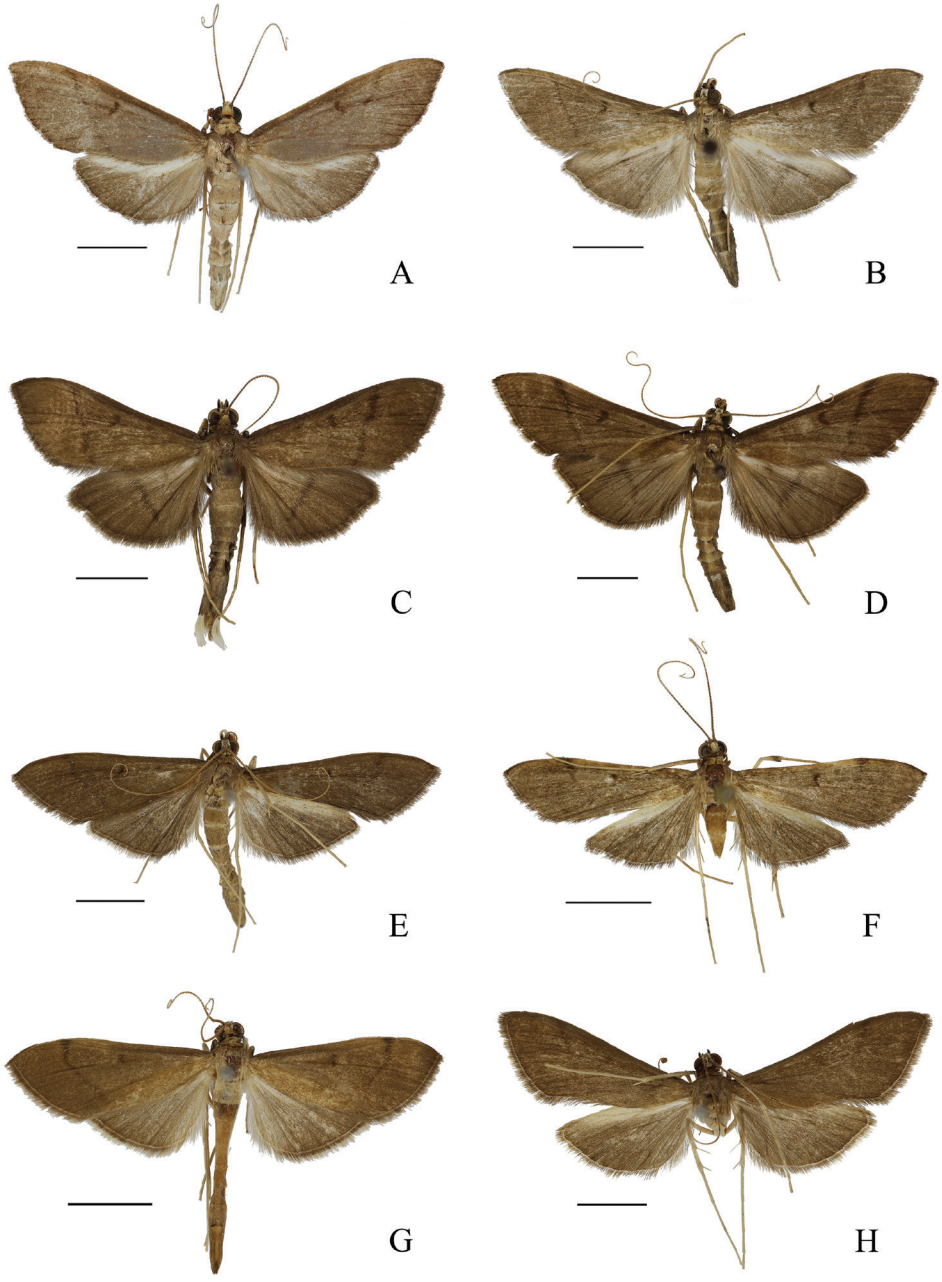

Figure 2. Habitus of *Bradina* species, male **A** *B. megesalis* **B** *B. fusoidea* sp. nov., holotype **C** *B. spirella* sp. nov., holotype **D** *B. torsiva* sp. nov., holotype **E** *B. subpurpurescens* **F** *B. falciculata* sp. nov., holotype **G** *B. translinealis* **H** *B. ternifolia* sp. nov., holotype. Scale bars: 0.5 cm.

costa; orbicular stigma very small; discoidal stigma crescent; postmedial line at c. two thirds of wing, straight and unparallel to terminal margin. Hindwing with postmedial line straight, towards to tornus, only middle part obvious. Cilia pale brown, with a

white line at base, except yellowish white on inner margin of the hindwing. Legs pale yellow. Front and middle tibiae brown; hind tibia with outer middle spurs c. two thirds length of inner spurs. Abdomen with basal half pale brown and distal half dark brown dorsally, each segment pale terminally; yellowish white ventrally.

Male genitalia (Fig. 3F–H). Valva distally gradually narrowed and bearing dense long setae; costa arched near middle and accompanied by a cluster of long curved setae; sacculus gradually narrowed to apex, with a cluster of long setae near middle. Phallus with one fusiform cornutus medially, composed of short and blunt spines, c. one third length of phallus, and one subcircular sclerotized cornutus posteriorly.

Female genitalia (Fig. 3I–K). Antrum broad. Posterior ductus bursae inflated and thorny, adjoined posteriorly by colliculum, posterior half inflated, weakly sclerotized, narrowed medially, then gradually widened to corpus bursae. Corpus bursae nearly rounded, with dense tiny spines inside, transverse signum crescent and densely spinose.

Etymology. The specific name is derived from the Latin *fusoideus* (meaning 'fusiform'), in reference to a fusiform cornutus.

Distribution. China (Guangdong, Sichuan).

Bradina spirella Guo & Du, sp. nov.

https://zoobank.org/2AF3F855-1103-42AA-94DD-D6634879BB67
Figs 2C, 3L–P

Type material. ***Holotype*****,** ♂ **China: Hunan Prov.**, Xianchijie, Wuyunjie National Nature Reserve, alt. 720 m, 28°90'N, 111°48'E, 24 June 2019, Ying Yang leg., genitalia slide no. GJM21161. ***Paratypes*****. China: Hunan Prov.**, 9 ♂♂, 4 ♀♀, Bamian Mountain Nature Reserve, Guidong County, alt. 973 m, 16 June 2015, Kai Chen leg., genitalia slide no.: GJM21160 ♂; 5 ♂♂, 2 ♀♀, Zhushan Village, Wuyunjie National Nature Reserve, alt. 100 m, 15 June 2019, Ying Yang leg.; 34 ♂♂, 14 ♀♀, Jindongjie, Wuyunjie National Nature Reserve, alt. 178 m, 16–19 June 2019, Ying Yang leg.; 66 ♂♂, 22 ♂♂, 18–24 June 2019, other same data as holotype, genitalia slide no.: GJM21048 ♂, GJM21049 ♂, GJM21162 ♂, GJM21163 ♂, GJM21164 ♀; **Jiangxi Prov.**, 4 ♂♂, 2 ♀♀, Jinggang Mountain, 30 June 2011, Jin-Wei Li leg., genitalia slide no.: GJM21159 ♂, GJM21183 ♀.

Diagnosis. This species is similar to *B. megesalis*. The difference in appearance is that wings of this species are darker in color and hindwings are slightly broader; the postmedial line and terminal margin of forewing are obviously unparallel in this species, while nearly parallel in the latter. It also can be distinguished by phallus with one short, spiral band-like cornutus and two lamellar cornuti, and some tiny spines on the vesica medially; the posterior ductus bursae is inflated into a thick finger-like protrusion. In *B. megesalis*, the phallus has two spear-like cornuti and is without spines on the vesica; the posterior ductus bursae is inflated into an irregular protrusion.

Description. ***Adult*** (Fig. 2C). Wingspan 29.0–32.0 mm, forewing length 14.0–15.5 mm. Frons brown, with lateral sides yellowish white above. Vertex pale yellow. Antenna brownish yellow, with black-brown ring dorsally, basal segments of flagellum

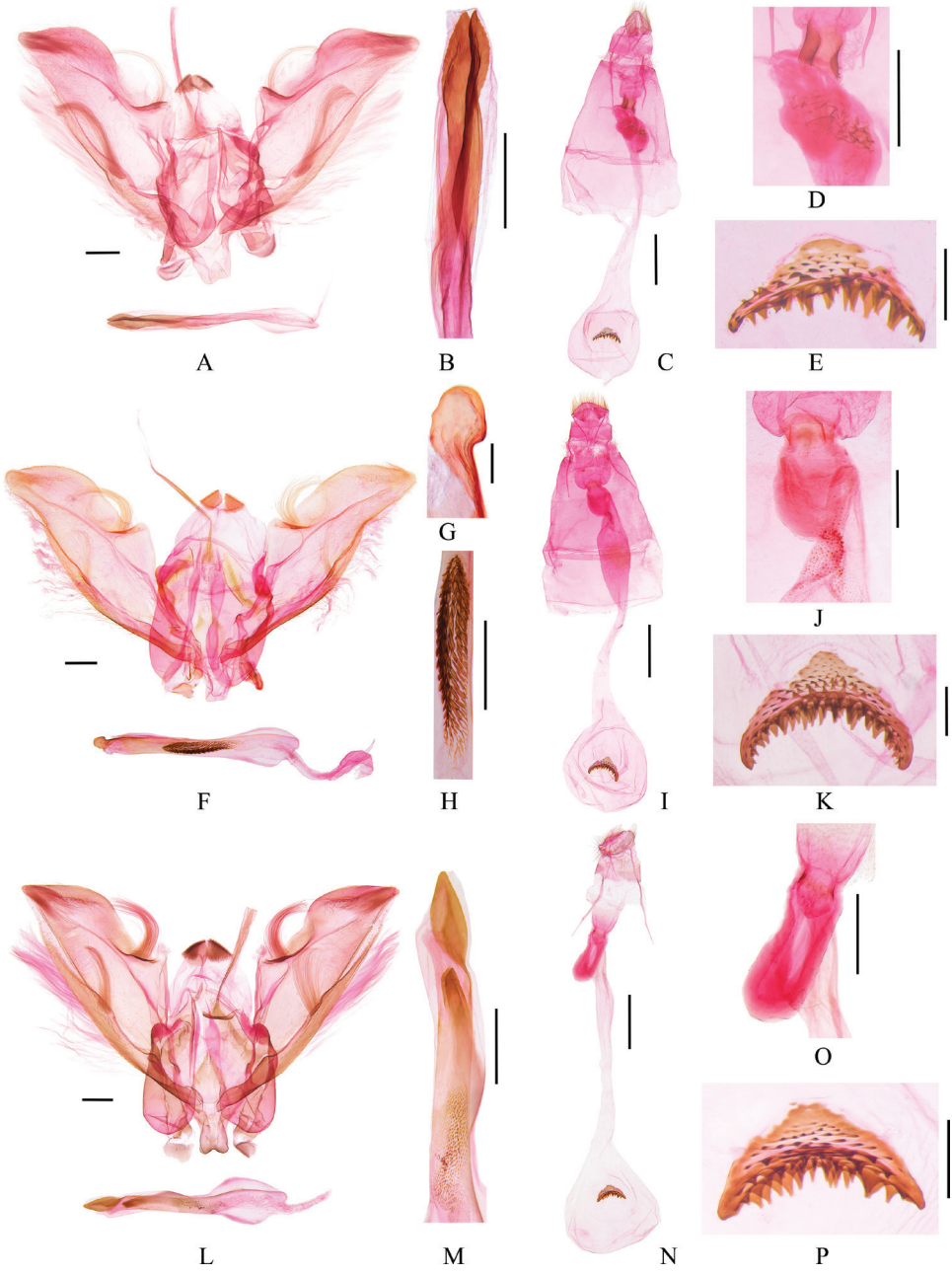

Figure 3. Genitalia of *Bradina* species **A–E** *B. megesalis* **A, B** male, slide no. GJM21074 **C–E** female, slide no. GJM21080 **F–K** *B. fusoidea* sp. nov. **F–H** male holotype, slide no. GJM21117 **I–K** female, paratype, slide no. GJM21118 **L–P** *B. spirella* sp. nov. **L, M** male, holotype, slide no. GJM21161 **N–P** female, paratype, slide no. GJM21164 **B, G, H, M** partial enlargement of phallus **D, J, O** partial enlargement of ductus bursae **E, K, P** signum. Scale bars: 0.2 mm (**E, G, K, P**); 0.5 mm (**A, B, D, F, H, J, L, M, O**); 1.0 mm (**C, I, N**).

black-brown dorsally; ventral cilia c. one third length of flagellomere diameter of male. Labial palpus with basal two thirds white, black-brown distally. Maxillary palpus black-brown. Patagium and tegula dark brown. Thorax dark brown dorsally, white ventrally. Wings dark brown, stigmata and lines black-brown. Forewing black-brown along costa, slightly paler distally; orbicular stigma very small; discoidal stigma crescent; postmedial line at c. two thirds of wing, inconspicuously waved and unparallel to terminal margin. Hindwing pale at base; postmedial line straight, only middle part obvious. Cilia greyish brown. Legs pale yellow. Front and middle tibiae dark brown; hind tibia with outer middle spurs c. same length as inner spurs. Abdomen brown dorsally, with each segment pale terminally; yellowish white ventrally.

Male genitalia (Fig. 3L, M). Valva with the distal part gradually narrowed and bearing dense long setae; costa arched near middle and accompanied by a cluster of long curved setae; sacculus gradually narrowed to apex, with a cluster of long setae near middle. Juxta narrowed distally. Phallus with one short and spiral band-like cornutus tapered at posterior end, along with two lamellar cornuti in posterior half; some tiny spines on vesica medially.

Female genitalia (Fig. 3N–P). Antrum broad. Ductus bursae slender, posteriorly inflated into a thick finger-like protrusion, adjoined posteriorly by colliculum. Corpus bursae nearly oval, without spines inside, transverse signum crescent and densely spinose.

Etymology. The specific name is derived from the Latin *spirellus* (meaning 'small spiral-like'), in reference to a short and spiral band-like cornutus.

Distribution. China (Hunan, Jiangxi).

Remark. Coremata of some male individuals of this species were protruded out of the body, forming a cluster of white hairs at the end of the abdomen.

Bradina torsiva **Guo & Du, sp. nov.**
https://zoobank.org/3DF230C3-6BA8-4D7F-AB54-61C46C1CE689
Figs 2D, 4A–E

Type material. ***Holotype*****,** ♂ **China: Hunan Prov.**, Chenzhou Nature Reserve, alt. 1233 m, 25°78'N, 113°01'E, 3 June 2019, Xiao-Qiang Lu & Ying Yang leg., genitalia slide no. GJM21102. ***Paratypes*****. China: Hunan Prov.**, 4 ♂♂, other same data as holotype, genitalia slide no.: GJM21103 ♂; 1♂, Zhushan Village, Taoyuan County, Changde City, alt. 100 m, 15 June 2019, Xiao-Qiang Lu & Ying Yang leg., genitalia slide no.: GJM21101; 2 ♂♂, Maozhu River, Shimen County, Changde City, alt. 350 m, 6 June 2017, Jian-Yue Qiu & Hao Xu leg.; **Guangdong Prov.**, 2 ♂♂, 1 ♀, Dadong Mountain, Lianzhou City, alt. 650 m, 21 June 2004, Dan-Dan Zhang leg., genitalia slide no.: GJM21100 ♂; 1 ♀, Qingyuan City, alt. 270 m, 7 June 2019, Xiao-Qiang Lu & Ying Yang leg.; 1 ♂, 2 ♀♀, Babaoshan Conservation Station, Nanling National Nature Reserve, alt. 980 m, 19 May 2021, Xing-Hai Zuo leg. (NKU), genitalia slide no.: GJM21099 ♂; 5 ♂♂, 2 ♀♀, Yangmeikeng Village, Shimentai National Nature Reserve, alt. 870 m, 27 May 2021, Xing-Hai Zuo leg. (NKU), genitalia slide no.: GJM21104 ♀.

Diagnosis. This species is similar to *B. megesalis*. The difference in appearance is that wings of this species are darker in color, and hindwings are slightly broader; the postme-

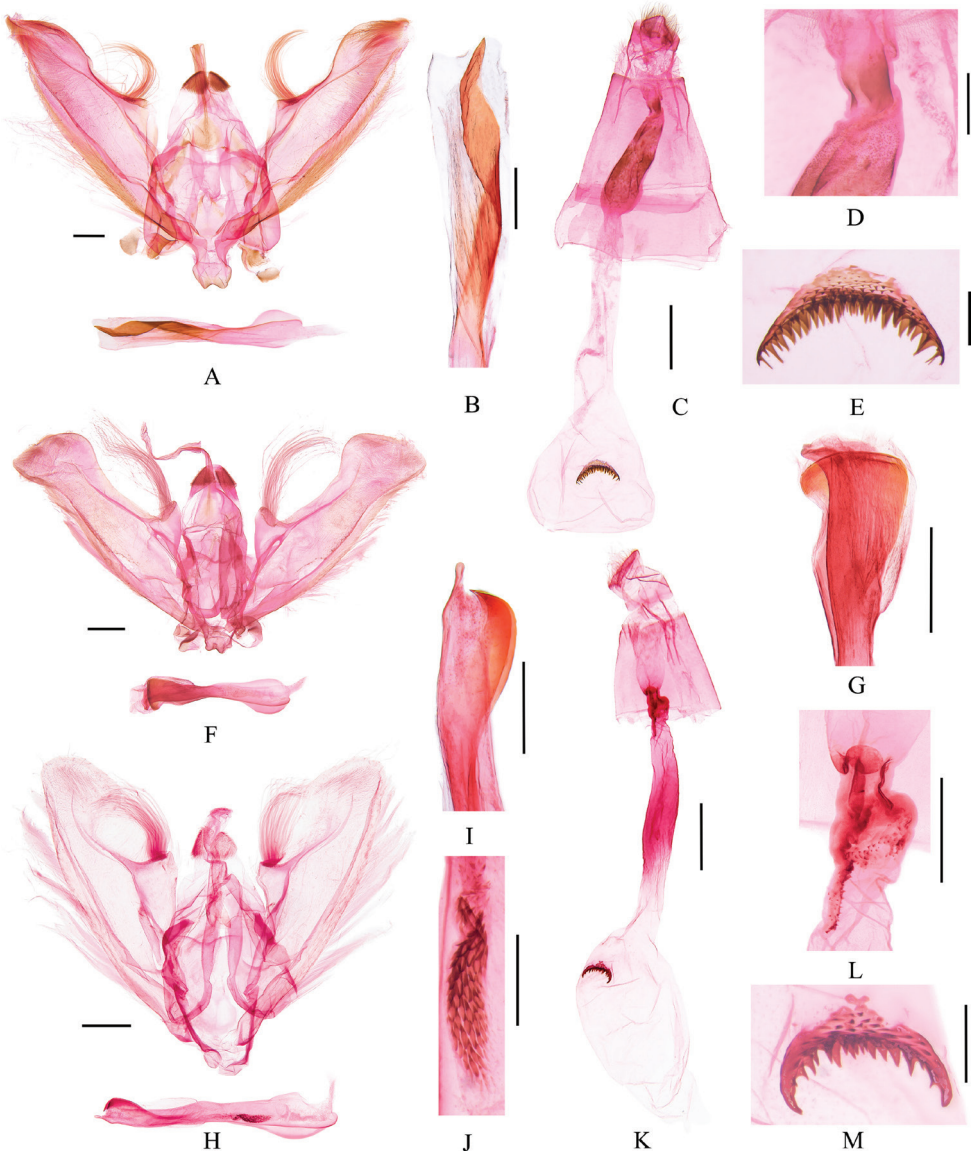

Figures 4. Genitalia of *Bradina* species **A–E** *B. torsiva* sp. nov. **A, B** male, holotype, slide no. GJM21102 **C–E** female, paratype, slide no. GJM21104 **F, G** *B. subpurpurescens* male, slide no. GJM21018 **H–M** *B. falciculata* sp. nov. **H–J** male, holotype, slide no. GJM21084 **K–M** female, paratype, slide no. GJM21085 **B, G, I, J** partial enlargement of phallus **D, L** partial enlargement of ductus bursae **E, M** signum. Scale bars: 0.2 mm (**D, E, J, M**); 0.5 mm (**A, B, F–I, L**); 1.0 mm (**C, K**).

dial line and terminal margin of forewing is obviously unparallel in this species, while it is nearly parallel in the latter. It also can be distinguished by the sacculus without long setal cluster, the phallus with one broad, spiral, band-like cornutus; the posterior third of ductus bursae with slightly sclerotized elongate inflation, but not forming irregular protru-

sion. In *B. megesalis*, the sacculus has long setal cluster near middle, and the phallus has two spear-like cornuti; the posterior ductus bursae is inflated into an irregular protrusion.

Description. ***Adult*** (Fig. 2D). Wingspan 36.0–37.0 mm, forewing length 17.5–18.0 mm. Frons brown, with lateral sides yellowish white above. Vertex yellowish white. Antenna brownish yellow, with black-brown ring dorsally, ventral cilia c. half-length of flagellomere diameter of male. Labial palpus with basal two thirds white, black-brown distally. Maxillary palpus black-brown or brown. Patagium yellowish white. Tegula dark brown. Thorax dark brown dorsally, white ventrally. Wings dark brown, stigmata and lines black-brown. Forewing black-brown along costa, slightly paler distally; orbicular stigma very small; discoidal stigma crescent; postmedial line at c. two thirds of wing, unparallel to terminal margin. Hindwing slightly pale at base; postmedial line inconspicuously waved, only middle part obvious. Cilia pale yellow, with a black-brown line at base, except black-brown on inner margin. Legs yellow. Front and middle tibiae dark brown; hind tibia with outer middle spurs c. three fifths length of inner spurs. Abdomen brown dorsally, each segment pale terminally; paler ventrally.

Male genitalia (Fig. 4A, B). Valva with the distal part gradually narrowing and with dense long setae; costa arched near middle and accompanied by a cluster of long curved setae; sacculus narrowed distally, without long setal cluster. Juxta narrowed distally. Phallus slightly inflated, with one broad and spiral band-like cornutus posteriorly.

Female genitalia (Fig. 4C–E). Ductus bursae broad, with posterior third inflated, sclerotized, and thorny, adjoined posteriorly by colliculum, gradually widened to corpus bursae. Corpus bursae nearly oval, truncated terminally, with dense tiny spines inside, transverse signum crescent and densely spinose.

Etymology. The specific name is derived from the Latin *torsivus* (meaning 'spiral'), in reference to a spiral band-like cornutus.

Distribution. China (Guangdong, Hunan).

Remark. Coremata of some male individuals of this species were protruded out of the body, forming a cluster of white hairs at the end of the abdomen.

Bradina subpurpurescens (Warren, 1896)

Figs 2E, 4F, G

Pleonectusa subpurpurescens Warren, 1896: 147. Type locality: India. Type depository: NHMUK.

Bradina subpurpurescens: Hampson, 1896: 227.

Material examined. ***Holotype*****,** ♂ **India:** Khasis, X. 1894, Nat. Coll (NHMUK).

Additional material. China: Yunnan Prov., 1 ♂, Meizihu Park, Simao District, Pu'er City, alt. 1400 m, 11 May 2018, Xi-Cui Du & Xiao-Qiang Lu leg., genitalia slide no.: GJM21019; 1 ♂, Yunpan Mountain, Pu'er City, alt. 1400 m, 9 July 2013, Zhen-Guo Zhang leg., genitalia slide no.: GJM21018; 1 ♂, Taiyanghe National Forest Park, Puer City, alt. 1659 m, 29 June 2021, Yao Shen & Ci Tang leg., genitalia slide no.: GJM21020.

Redescription. ***Adult*** (Fig. 2E). Wingspan 26.0–33.0 mm, forewing length 14.5–16.0 mm. Frons brown, with lateral sides white above. Vertex brownish yellow. Antenna brownish yellow, with pale brown ring dorsally; length of ventral cilia c. one quarter of the flagellomere diameter of male. Labial palpus with basal two thirds white, black-brown distally. Maxillary palpus black-brown, pale brown at base. Patagium and tegula brown. Thorax pale brown distally, white ventrally. Wings dark brown, stigmata and lines black-brown. Forewing black-brown along basal costa; orbicular stigma very small; discoidal stigma crescent; postmedial line at c. three quarters of wing, nearly parallel to terminal margin, slightly excurved near costa. Hindwing with postmedial line slightly beyond basal half of wing, only middle part obvious. Cilia pale brown on forewing, yellowish white on hindwing; a brown line at base. Legs pale yellow. Front and middle tibiae yellowish brown; hind tibia with outer middle spurs c. half-length of inner spurs. Abdomen pale yellowish brown dorsally, each segment pale terminally.

Male genitalia (Fig. 4F, G). Valva nearly rectangular, broad distally; costa sharply arched near base and accompanied by a cluster of long curved setae, then slightly concave towards apex; sacculus gradually narrowed distally, without long setal cluster. Phallus narrow medially, significantly inflated anteriorly and posteriorly, posterior half sclerotized; cornutus absent.

Distribution. China (Yunnan), India.

Remarks. This species is recorded in China for the first time, and its male genitalia are also described for the first time. It can be distinguished from the other species (except *B. falciculata*) in the present study by the forewing relatively narrower; cilia pale brown on forewing, yellowish white on hindwing. The female of this species is unknown.

Bradina falciculata **Guo & Du, sp. nov.**

https://zoobank.org/9F1E4111-1E29-42C2-AD1D-300EAC54E761

Figs 2F, 4H–M

Type material. ***Holotype*****,** ♂ **China: Tibet Autonomous Region**, Medog County, alt. 1100 m, 29°32'N, 95°33'E, 14 August 2003, Xin-Pu Wang & Huai-Jun Xue leg. (NKU), genitalia slide no. GJM21084. ***Paratypes*****. China: Tibet Autonomous Region**, 5 ♂♂, 3 ♀♀, other same data as holotype, genitalia slide no.: GJM21082 ♂; 5 ♂♂, 8 ♀♀, Bomi-Medog Highway, Medog County, alt. 880 m, 14 August 2003, Xin-Pu Wang & Huai-Jun Xue leg. (NKU), genitalia slide no.: GJM21083 ♂, GJM21085 ♀, GJM21086 ♀.

Diagnosis. This species is similar to *B. subpurpurescens*. The difference in appearance is that wings are paler in color and the postmedial line of the forewing is placed at two thirds from the wing base in this new species, but at three quarters in the latter. It also can be distinguished by an elliptical valva and the phallus inconspicuously inflated distally. In *B. subpurpurescens*, the valva is nearly rectangular and the phallus is significantly inflated distally.

Description. ***Adult*** (Fig. 2F). Wingspan 25.0–27.0 mm, forewing length 12.0–13.0 mm. Frons brown, with lateral sides yellowish white above. Vertex yellowish white. An-

tenna yellow, with pale brown ring dorsally; ventral cilia c. half-length of flagellomere diameter of male. Labial palpus with basal two thirds white, dark brown distally. Maxillary palpus dark brown. Patagium and tegula pale brown. Thorax pale brown dorsally, white ventrally. Wings yellowish brown, stigmata and lines brown. Forewing with discoidal stigma crescent; postmedial line at basal two thirds of wing, slightly excurved and nearly parallel to terminal margin. Hindwing with postmedial line straight, usually not obvious. Cilia pale brown, with a darker line at base, except greyish white on inner margin of the hindwing. Legs pale yellow. Front and middle tibiae black-brown on distal half; hind tibia with outer middle spurs c. half-length of inner spurs. Abdomen pale brown dorsally, yellowish white ventrally.

Male genitalia (Fig. 4H–J). Valva elliptical; costa arched near middle and accompanied by a cluster of long curved setae; sacculus gradually narrowed to apex, without long setal cluster. Juxta narrowed distally. Phallus with one small fusiform cornutus anteriorly, composed of short and blunt spines, c. one sixth length of phallus, and with two sickle-shaped cornuti posteriorly.

Female genitalia (Fig. 4K–M). Antrum broad. Ductus bursae with one oval sclerotized piece close to crescent-shaped colliculum, then inflated and thorny, slightly sclerotized medially. Corpus bursae nearly oval, with dense tiny spines inside, transverse signum crescent and densely spinose.

Etymology. The specific name is derived from the Latin *falciculatus* (meaning 'falcate'), in reference to two sickle cornuti of posterior phallus.

Distribution. China (Tibet).

Bradina translinealis Hampson, 1896

Figs 2G, 5A–F

Bradina translinealis Hampson, 1896: 228. Type locality: N. W. Himalayas. Type depository: NHMUK.

Material examined. ***Holotype***, ♂. Moore Coll. 94–106, genitalia slide no. 8734. (NHMUK).

Additional material. China, Yunnan Prov., 5 ♂♂, 2 ♀♀, Baihualing Village, Baoshan City, alt. 1520 m, 11–13 August 2007, Dan-Dan Zhang leg., genitalia slide no.: GJM21165 ♂, GJM21166 ♂, GJM21167 ♀, GJM21182 ♀.

Redescription. ***Adult*** (Fig. 2G). Wingspan 25.0–30.0 mm, forewing length 12.0–13.0 mm. Frons brown, with lateral sides yellowish white above. Vertex yellowish white. Antenna brownish yellow, with brown ring dorsally; ventral cilia c. quarter length of flagellomere diameter of male. Labial palpus with basal two thirds white, black-brown distally. Maxillary palpus black-brown, yellowish white at base. Patagium and tegula pale brown. Thorax pale brown dorsally, white ventrally. Forewing yellowish brown, dark brown along basal half of costa; stigmata and lines black-brown; discoidal stigma reniform; postmedial line at c. two thirds of wing, slightly excurved near costa. Hindwing pale yellowish brown dorsally, yellowish white to pale brown ventrally; paler

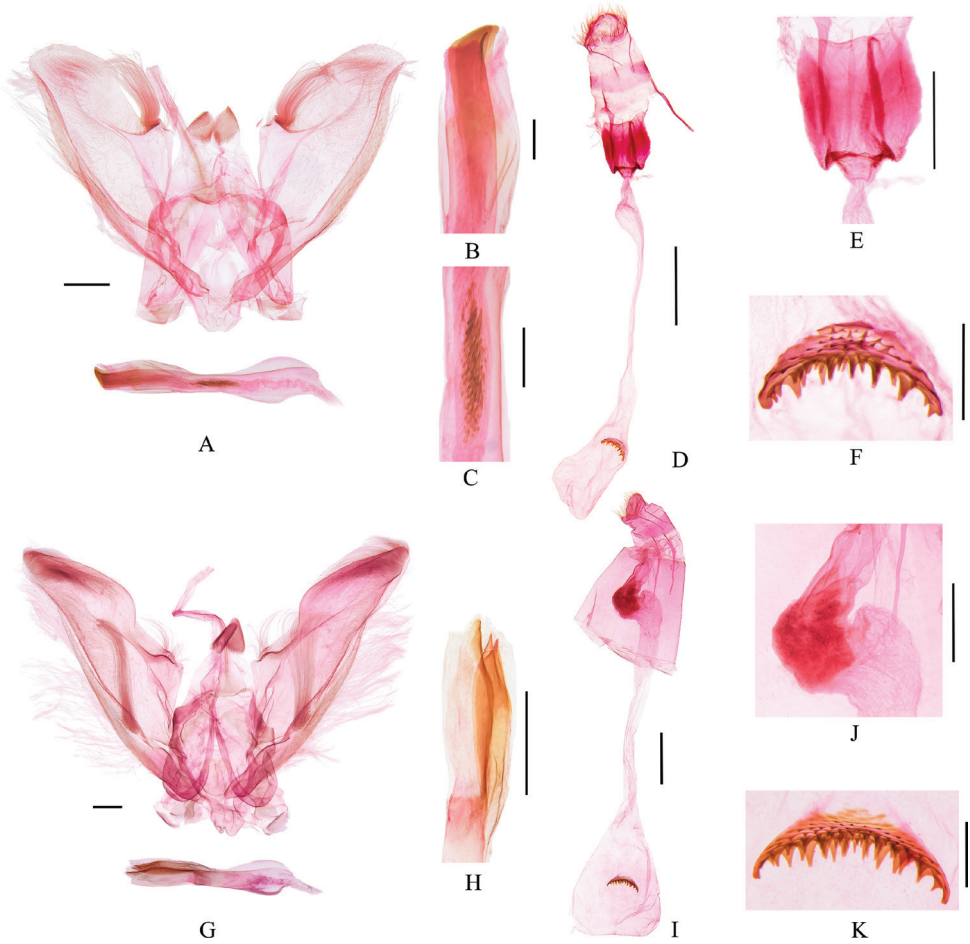

Figure 5. Genitalia of *Bradina* species **A–F** *B. translinealis* **A–C** male, slide no. GJM21165 **D–F** female, slide no. GJM21167 **G–K** *B. ternifolia* sp. nov. **G, H** male, holotype, slide no. GJM21173 **I–K** female, paratype, slide no. GJM21178 **B, C, H** partial enlargement of phallus **E, J** partial enlargement of ductus bursae **F, K** signum. Scale bars: 0.2 mm (**B, C, F, K**); 0.5 mm (**A, E, G, H, J**); 1.0 mm (**D, I**).

at base; postmedial line pale brown, inconspicuous, extending beyond basal half of wing. Cilia pale brown on forewing, yellowish white on hindwing, a brown line at base. Legs yellowish white. Front and middle tibiae brown; hind tibia with outer middle spurs c. half-length of inner spurs. Abdomen pale yellowish brown dorsally, yellowish white ventrally.

Male genitalia (Fig. 5A–C). Valva nearly elliptical, bearing dense long setae distally; costa arched near middle and accompanied by a cluster of long setae; sacculus gradually narrowed distally, without long setal cluster. Phallus with one fusiform cornutus medially, composed of short and blunt spines, c. one fifth length of phallus; posterior half slightly inflated, and with two weakly sclerotized lamellar cornuti posteriorly.

Female genitalia (Fig. 5D–F). Antrum broad and sclerotized, strongly sclerotized laterally, anteriorly adjoined by colliculum. Posterior ductus bursae slender, inflated, widened close to corpus bursae. Corpus bursae nearly oval, truncated terminally; with dense tiny spines inside, transverse signum crescent and densely spinose.

Distribution. China (Yunnan), N. W. Himalayas.

Remarks. This species is first recorded in China and its genitalia are described for the first time. It can be distinguished by the valva being nearly elliptical, the phallus with one fusiform cornutus medially and two weakly sclerotized lamellar cornuti posteriorly.

Bradina ternifolia **Guo & Du, sp. nov.**
https://zoobank.org/F49AC3BF-5605-4538-A1AF-145EA7B517FF
Figs 2H, 5G–K

Type material. ***Holotype*****,** ♂ **China: Yunnan Prov.**, Dahaoping Village, Tengchong City, 25°02'N, 98°49'E, 6 August 2007, Dan-Dan Zhang leg., genitalia slide no. GJM21173. ***Paratypes*****. China: Yunnan Prov.**, 2 ♂♂, 7 ♀♀, other same data as holotype, genitalia slide no.: GJM21174 ♂, GJM21175 ♂, GJM21176 ♀, GJM21177 ♀, GJM21178 ♀, GJM21181 ♀; 2 ♀♀, 5 August 2007, other same data as holotype.

Diagnosis. This species is similar to *B. translinealis*. It can be distinguished by postmedial line of forewing straight; valva elongated and narrowed comparatively, sacculus with long setal cluster near middle, posterior phallus with three long leaf-like cornuti; antrum membranous. In *B. translinealis*, postmedial line of forewing slightly excurved near costa; sacculus has no setal cluster, phallus has one fusiform cornutus medially and two lamellar cornuti posteriorly; antrum broader and sclerotized.

Description. ***Adult*** (Fig. 2H). Wingspan 31.0–33.0 mm, forewing length 15.0–16.0 mm. Frons brown, except black-brown above. Vertex yellowish white mixed with brownish yellow. Antenna pale yellow, with pale brown ring dorsally; ventral cilia c. half-length of flagellomeres diameter of male. Labial palpus with basal half yellowish white, brown or black-brown distally. Maxillary palpus brown or black-brown. Patagium and tegula dark brown. Thorax dark brown dorsally, white ventrally. Wings brown, stigmata and lines black-brown. Forewing black-brown along costa; discoidal stigma reniform; postmedial line at c. two thirds of wing, straight and nearly parallel to terminal margin. Hindwing with discoidal stigma crescent; postmedial line beyond basal half of wing, usually inconspicuous. Cilia pale brown on forewing, greyish white on hindwing, a darker line at base. Legs pale yellow. Front and middle tibiae brown; hind tibia with outer middle spurs c. three fifths length of inner spurs. Abdomen dark brown dorsally, each segment pale terminally; slightly pale ventrally.

Male genitalia (Fig. 5G, H). Valva gradually narrowed and bearing dense long setae distally; costa arched near base and accompanied by a cluster of short and curved setae; sacculus gradually narrowed to apex, with a cluster of long setae near middle. Posterior phallus inflated slightly, with three long leaf-like cornuti tapered apically.

Female genitalia (Fig. 5I–K). Antrum membranous. Ductus bursae slender, adjoined posteriorly by crescent colliculum laterally, then inflated and bent. Corpus bursae nearly oval, with dense tiny spines inside, transverse signum crescent and densely spinose.

Etymology. The specific name is derived from the Latin *ternifolius* (meaning 'trifoliate'), in reference to three long leaf-like cornuti.

Distribution. China (Yunnan).

Remark. Coremata of some male individuals of this species were protruded out of the body, forming a cluster of white hairs at the end of the abdomen.

Discussion

The species in the present study, represented by *B. megesalis*, have a broad valva, whose costa is arched near the base or middle and accompanied by a cluster of long curved setae. The cornuti of the phallus of these species are diverse and therefore useful for interspecific identification. Seizmair (2021) divided *Bradina* into seven groups according to wing pattern characteristics, such as forewing and hindwing of the same color or of different colors, and whether the postmedial line is absent or present, and in the latter case whether it is straight or curved. In our opinion, however, it is difficult to divide the genus based only on wing pattern and color, and it would be more convincing to divide it by combining the appearance and morphology of the genitalia. In addition, most species of the *B. diagonalis* group in Seizmair's study are similar to the species in the present study both in appearance and genitalia. However, we found that *B. diagonalis*, as representative species of the *B. diagonalis* group, is different from most other species of this group in wing venation and genitalia. Therefore, further study on more species globally and in more detail is needed to clarify this confusion. In addition, the transverse crescent signum of *Bradina* is a distinctive feature. Like *Bradina*, the Steniini genera *Diathrausta* and *Perisyntrocha* also have an arched, transverse signum in the female genitalia's corpus bursae (Mally et al. 2019). This could indicate an evolutionary relatedness of these three genera, which is expected to be addressed in the future research.

Acknowledgements

We sincerely thank the other members of our laboratory as well as to Jian-Yue Qiu and Hao Xu for their efforts in collecting specimens, to Dr Dan-Dan Zhang (Sun Yat-Sen University, China) for sending specimens, and to Prof. Hou-Hun Li (Nankai University, China) for lending us specimens. Cordial thanks are given to the Natural History Museum, London, United Kingdom) for providing access to the corresponding author for examining type specimens of *Bradina*. Our special thanks are given to Dr Richard Mally (Czech University of Life Sciences, Czech Republic) and to the other anonymous reviewer for their academic suggestion and detailed revision of our manuscript. The research was funded by the National Natural Sciences Foundation of China (No. 31772500) and the Natural Sciences Foundation Project of Chongqing (No. CSTB2022NSCQ-MSX1164).

References

Caradja AV (1925) Ueber Chinas Pyraliden, Tortriciden, Tineiden nebst kurze Betrachtungen, zu denen das Studium dieser Fauna Veranlassung gibt (Eine biogeographische Skizze). Memoriile Sectiunii Stiintifice, Academia Romana seria 3 3(7): 257–383. [pls 1–2]

Du XC (2008) Taxonomic Study on Spilomelinae from China (Lepidoptera: Pyraloidea: Crambidae). PhD Thesis, Nankai University, Tianjing, China.

Felder C, Felder R, Rogenhofer AF (1875) Heterocera. In: Felder C, Felder R, Rogenhofer AF, Reise der österreichischen Fregatte Novara um die Erde in den Jahren 1857, 1858, 1859 unter den Befehlen des Commodore B. von Wüllerstorf-Urbair. Zoologischer Theil. Band 2. Abtheilung 2. Lepidoptera. Heft 5 (Schluss). Aus der Kaiserlich-Königliche Hof- und Staatsdruckerei, Wien, 1–20. [pls 121–140]

Guenée MA (1854) Deltoïdes et Pyralites. In: de Boisduval JBAD, Guenée MA (Eds) Histoire Naturelle des Insectes. Species Général des Lépidoptères, 8. Roret, Paris, 448 pp.

Hampson GF (1896) Moths. The Fauna of British India, including Ceylon and Burma, London, Vol. 4, 594 pp.

Hampson GF (1897) On the classification of two subfamilies of moths of the family Pyralidae: The Hydrocampinae and Scoparianae. The Transactions of the Entomological Society of London 45(2): 127–240. https://doi.org/10.1111/j.1365-2311.1897.tb01679.x

Inoue H (1955) Pyralidae. Check List of the Lepidoptera of Japan, Vol. 2. Rikusuisha, Tokyo, 120–196.

Khan ZH (2000) Biosystematic Studies on Pyralid Pests of Rice Crop in India (Pyralidae: Lepidoptera). PhD Thesis, Aligarh Muslim University, Aligarh, India. http://hdl.handle.net/10603/52039

Klima A (1937) Pyralidae: Subfam.: Scopariinae et Nymphulinae. In: Bryk F (Ed.) Lepidopterorum Catalogus 84. Dr. W. Junk, 's-Gravenhage, 226 pp. https://doi.org/10.5962/bhl.title.124187

Lederer J (1863) Beitrag zur Kenntniss der Pyralidinen. Wiener Entomologische Monatschrift 7(8, 10–12): 243–280, 331–504. [pls 2–18]

Li HH, Zheng ZM (1996) Methods and techniques of specimens of Microlepidoptera. Journal of Shaanxi Normal University 24(3): 63–70. [natural science edn.]

Lu JR, Guan ZH (1953) List of Chinese pyralid insects, addendum of Hu "List of Chinese Insects", part 2, Nymphulinae, Scopariinae, Anerastiinae. Acta Entomologica Sinica 3(2): 203–244.

Maes KVN (1995) A comparative morphological study of the adult Crambidae (Lepidoptera, Pyraloidea). Bulletin et Annales de la Société Royale Belge d'Entomologie 131: 383–434.

Mally R, Nuss M (2011) Molecular and morphological phylogeny of European *Udea* moths (Insecta: Lepidoptera: Pyraloidea). Arthropod Systematics & Phylogeny 69(1): 55–71.

Mally R, Hayden JE, Neinhuis C, Jordal BH, Nuss M (2019) The phylogenetic systematics of Spilomelinae and Pyraustinae (Lepidoptera: Pyraloidea: Crambidae) inferred from DNA and morphology. Arthropod Systematics & Phylogeny 77(1): 141–204. https://doi.org/10.26049/ASP77-1-2019-07

Meyrick E (1886) Descriptions of Lepidoptera from the South Pacific. The Transactions of the Entomological Society of London 34(3): 189–296. https://doi.org/10.1111/j.1365-2311.1886.tb01626.x

Moore F (1884) The Lepidoptera of Ceylon, Vol. 3. Reeve L and Co., London, 578 pp. [pls 144–215]

Nuss M, Landry B, Mally R, Vegliante F, Tränkner A, Bauer F, Hayden J, Segerer A, Schouten R, Li H, Trofimova T, Solis MA Prins, De J, Speidel W (2003–2023) Global Information System on Pyraloidea. http://www.pyraloidea.org [Accessed 2023-03-29]

Rothschild LW (1915) On the Lepidoptera from the islands of Ceram (Seram), Buru, Bali, and Misol. Novitates Zoologicae 22: 209–227. https://doi.org/10.5962/bhl.part.1914

Schaus W (1924) New species of Pyralidae of the subfamily Nymphulinae from tropical America (Lepid.). Proceedings of the Entomological Society of Washington 26(5): 93–130.

Seizmair M (2021) First records of the genus *Bradina* lederer, 1863 (Lepidoptera, Crambidae, Spilomelinae) from the Arabian Peninsula with remarks on the taxonomy of the genus and description of a new species. International Journal of Entomological Research 6(6): 307–312.

Shibuya J (1929) On the Japanese Hydrocampinae. Insecta Matsumurana 3(2–3): 120–136.

Stephens JF (1835) Illustrations of British Entomology; or, a synopsis of indigenous insects: containing their generic and specific distinctions; with an account of their metamorphoses, times of appearance, localities, food, and economy, as far as practicable. Baldwin and Cradock, London, 3–240. [pls 28–34]

Walker F (1859) Pyralides. List of the Specimens of Lepidopterous Insects in the Collection of the British Museum, London 18: 509–798.

Wang HY, Speidel W (2000) Pyraloidea (Pyralidae, Crambidae). Guide book to insects in Taiwan (19). Shu Shin Books, Taipei, 295 pp.

Warren W (1896) New genera and species of Pyralidae, Thyrididae, and Epiplemidae. Annals & Magazine of Natural History 17(98): 131–150. https://doi.org/10.1080/00222939608680339

Yamanaka H (1984) Revisional study of some species of *Bradina* Lederer from Japan, China and Taiwan (Lepidoptera: Pyralidae, Pyraustinae). Tinea 11(19): 161–176.

ZooKeys 1158: 69–89 (2023)
doi: 10.3897/zookeys.1158.98868
https://zookeys.pensoft.net

RESEARCH ARTICLE

A peer-reviewed open-access journal
ZooKeys
Launched to accelerate biodiversity research

A multivariate approach to morphological study of shell form in cowries (Gastropoda, Cypraeidae): a case study with *Umbilia armeniaca* (Verco, 1912)

Paul C. Southgate[1], Thane A. Militz[1]

1 *School of Science, Technology and Engineering, and Australian Centre for Pacific Islands Research, University of the Sunshine Coast, Maroochydore, Queensland 4556, Australia*

Corresponding author: Paul C. Southgate (psouthgate@usc.edu.au)

Academic editor: Frank Köhler | Received 15 December 2022 | Accepted 29 March 2023 | Published 19 April 2023

https://zoobank.org/7D4A9771-3551-4137-868A-CB8D1AA45C1E

Citation: Southgate PC, Militz TA (2023) A multivariate approach to morphological study of shell form in cowries (Gastropoda, Cypraeidae): a case study with *Umbilia armeniaca* (Verco, 1912). ZooKeys 1158: 69–89. https://doi.org/10.3897/zookeys.1158.98868

Abstract

Multivariate approaches to morphological study of shell form have rarely been applied to cowries (Gastropoda: Cypraeidae) with preference, instead, for comparing formulaic notations of shell form that report averages (i.e., means) for key morphometrics such as shell dimensions, their ratios, and counts of apertural teeth. Although widely applied, the "shell formula" does not account for variation among individuals or support statistical comparison between taxa. This study applied a multivariate approach to analyse shell form within the four accepted subspecies of the cowrie, *Umbilia armeniaca* (Verco, 1912) and included a previously unstudied, and most northerly, population of *U. armeniaca* from Lancelin, Western Australia. Multivariate analyses readily separated the recognised subspecies of *U. armeniaca* (*U. a. armeniaca*, *U. a. diprotodon*, *U. a. clarksoni* and *U. a. andreyi*), but did not separate the Lancelin population from *U. a. andreyi*, indicating that the former represents a northward extension of *U. a. andreyi* that is not morphometrically distinguishable. These results provide improved understanding of infraspecific differences in shell form of *U. armeniaca* across its broad distribution, and demonstrate the utility of multivariate morphometric methods for statistical comparison of shell form between taxa. This approach is complimentary to existing research practices and has broad potential application in future morphometric studies of both extant and fossil taxa within the family Cypraeidae.

Keywords

Cowry, gastropod, marine, morphometrics, shell form, taxonomy, *Umbilia*

Introduction

The family Cypraeidae Rafinesque, 1815 (cowries) comprises a large group of marine gastropods characterised by colourful, generally glossy, shells with a narrow, elongate aperture bordered by teeth. Cowries demonstrate variable inter- and infraspecific shell morphology (Lorenz 2017a) reflecting evolution, sexual dimorphism, and ecophenotypic plasticity (Schilder and Schilder 1968; Burgess 1970; Tissot 1988; Wilson and Clarkson 2004; Irie 2006; Lorenz and Beals 2013). Where geographically or bathymetrically discrete populations of a species are considered conchologically distinct, reference to a particular population can be aided by assigning subspecies designation. In the most recent review of the family, for example, Lorenz (2017a) recognised 262 living species, of which 42% have at least one subspecies and nearly 20% have more than two subspecies.

Despite broad application of molecular approaches in modern gastropod taxonomy (e.g., Meyer 2003, 2004; Meyer and Paulay 2005), morphological study of shell form remains the primary means of differentiation (Cruz et al. 2012; Lorenz 2017a), and has particular relevance in the study of fossils and of taxa known only from shell remains, for which genetic testing is not possible. Based on precedent established by Vayssière (1910), morphological study of shell form in modern cowrie systematics utilises a formulaic notation, or "shell formula", to describe various shell traits (i.e., morphometrics) for given populations or taxa. Various arrangements of this notation, reflecting changes to the morphometrics considered, have been employed as a basis for characterising and comparing cowries for more than 100 years (Schilder and Schilder 1938–1939, 1952; Lorenz and Hubert 2000; Lorenz 2001, 2002; Bridges and Lorenz 2013; Lorenz 2017a). While formulaic notations can assist in comparing central tendencies (e.g., mean or median) for a given morphometric between or among *a priori* assigned groups, such as populations or taxa (Bridges and Lorenz 2013), this approach does not account for variation among individuals within groups (Tissot 1984, 1988; Irie 2006) and, according to Landau and Groves (2011), should not be used in isolation to distinguish between taxa. By considering central tendencies in isolation, without accounting for variability, the possibility that putative differences may have arisen by random chance cannot be dismissed, potentially leading to incorrect conclusions. Statistical tests offer a solution to these issues, whereby estimating the probability that differences between central tendencies may have arisen by random chance (i.e., the null hypothesis), a statement of significance can be assigned.

Application of statistical tests to compliment comparisons of shell form between and among groups of cowries can, in its simplest form, assess differences for each morphometric separately (e.g., univariate analysis). When considering a morphometric in this manner (e.g., Lorenz and Beals 2013), only one aspect of morphological variation is represented as independent of other, potentially covariate, morphometrics. It is, therefore, more beneficial to use a multivariate approach to summarise morphological variation. Multivariate approaches, which summarise variation in shell form, are based

on multidimensional space where each dimension represents an aspect of morphological variation (a morphometric) and each biological observation (i.e., specimen) can be placed within this space based on their morphometric values. In this manner, morphological configurations of shell form relate mathematically within multidimensional space, based on a measure of resemblance (often distance) between specimens (Mitteroecker and Huttegger 2009). To help comprehend patterns in multidimensional space, ordination techniques can be used to visualise specimens in a new space of reduced dimensions, while maintaining the requirement that similar specimens are closer together than dissimilar ones. Statistical tests can complement visualisation by assessing how a particular morphometric differs among specimens or estimating the probability that *a priori* assigned groups share the same central tendency (i.e., centroid) or variation (i.e., dispersion) within multidimensional space (Guillerme et al. 2020). While prior applications of a multivariate approach for morphological study of cowries have been few (Tissot 1984, 1988), improved availability of open-access software to support multivariate analyses has greatly increased opportunities for their integration into cowrie systematics (e.g., Southgate et al. 2021).

To demonstrate how a multivariate approach to morphological study of shell form might benefit research into cowrie systematics, this study validates existing infraspecific taxonomy for the Australian endemic *Umbilia armeniaca* (Verco, 1912). Specific conchological attributes are attributable to location (Wilson and Clarkson 2004) and infraspecific taxonomy has been established by comparing shell formulae and univariate analysis (Lorenz and Beals 2013). Since secondary data for *U. armeniaca* exist in prior studies of shell form (Bridges and Lorenz 2013; Lorenz and Beals 2013), this species provides novel opportunity to demonstrate how primary data from unstudied specimens can supplement secondary data derived from prior studies for both validating existing geographical subspecies and characterising a previously unstudied population of this species.

Materials and methods

Study populations

The cowrie genus *Umbilia* Jousseaume, 1884 is represented by five living species endemic to Australia. They have limited larval dispersal because of intracapsular development (Wilson 1985) and are characterised by conchologically distinct geographic and bathymetric populations (Wilson and Clarkson 2004). Within the genus, *Umbilia armeniaca* has the most extensive geographic range, extending from Kangaroo Island in South Australia to at least Lancelin, north of Perth, in Western Australia, a distance of ~ 3,000 km (Fig. 1). In addition to considerable morphological variation within this range, variation is also apparent within known populations (Bridges and Lorenz 2013; Lorenz and Beals 2013).

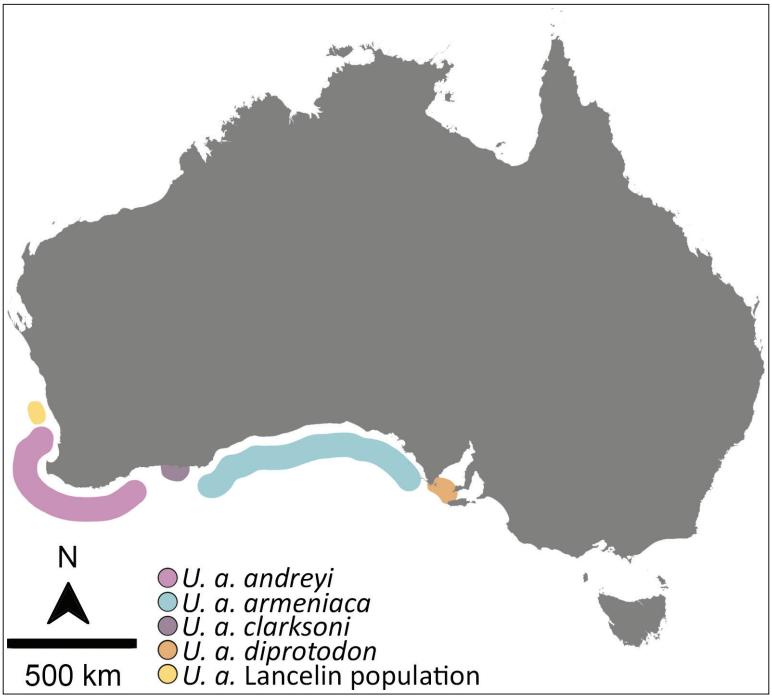

Figure 1. Approximate distributions of the four recognised subspecies of *Umbilia armeniaca* and the newly discovered Lancelin population of the species.

Four subspecies of *Umbilia armeniaca* are currently recognised (Lorenz and Beals 2013): the nominate *U. a. armeniaca* which ranges across the Great Australian Blight from around the Eyre Peninsula, South Australia, to east of Esperance, Western Australia at depths of ~ 100–200 m (Fig. 2A); *U. a. diprotodon* (Lorenz & Beals, 2013), which ranges from Thorny Passage to western Kangaroo Island and in areas of the Spencer Gulf, South Australia, at depths of 20–60 m (Fig. 2B); *U. a. clarksoni* (Lorenz & Beals, 2013), which is restricted to shallow waters (40–45 m) between Woody Island and Cape Le Grand near Esperance, Western Australia (Fig. 2C); and *U. a. andreyi* (Lorenz & Beals, 2013), which ranges along the south-west coast from Rottnest Island to Windy Harbour, Western Australia, at depths of 100–220 m (Fig. 2D). The four subspecies are considered conchologically distinct, based on comparisons of shell formulae and univariate analysis of selected morphometrics, as well as qualitative differences in colour pattern (Bridges and Lorenz 2013; Lorenz and Beals 2013). In addition to these subspecies, recent exploration using remotely operated vehicles (ROV) discovered a novel population of *U. armeniaca* living at a depth of ~ 200 m off Lancelin, more than 100 km north of what was previously considered the northernmost extent of this species distribution (i.e., Rottnest Island). Only three live specimens have so far been recovered and molecular analysis of this population has not been possible. However, sufficient specimens of complete, empty shells (i.e., collected without tissue) are available to support morphological study of shell form for this northern population (Fig. 2E).

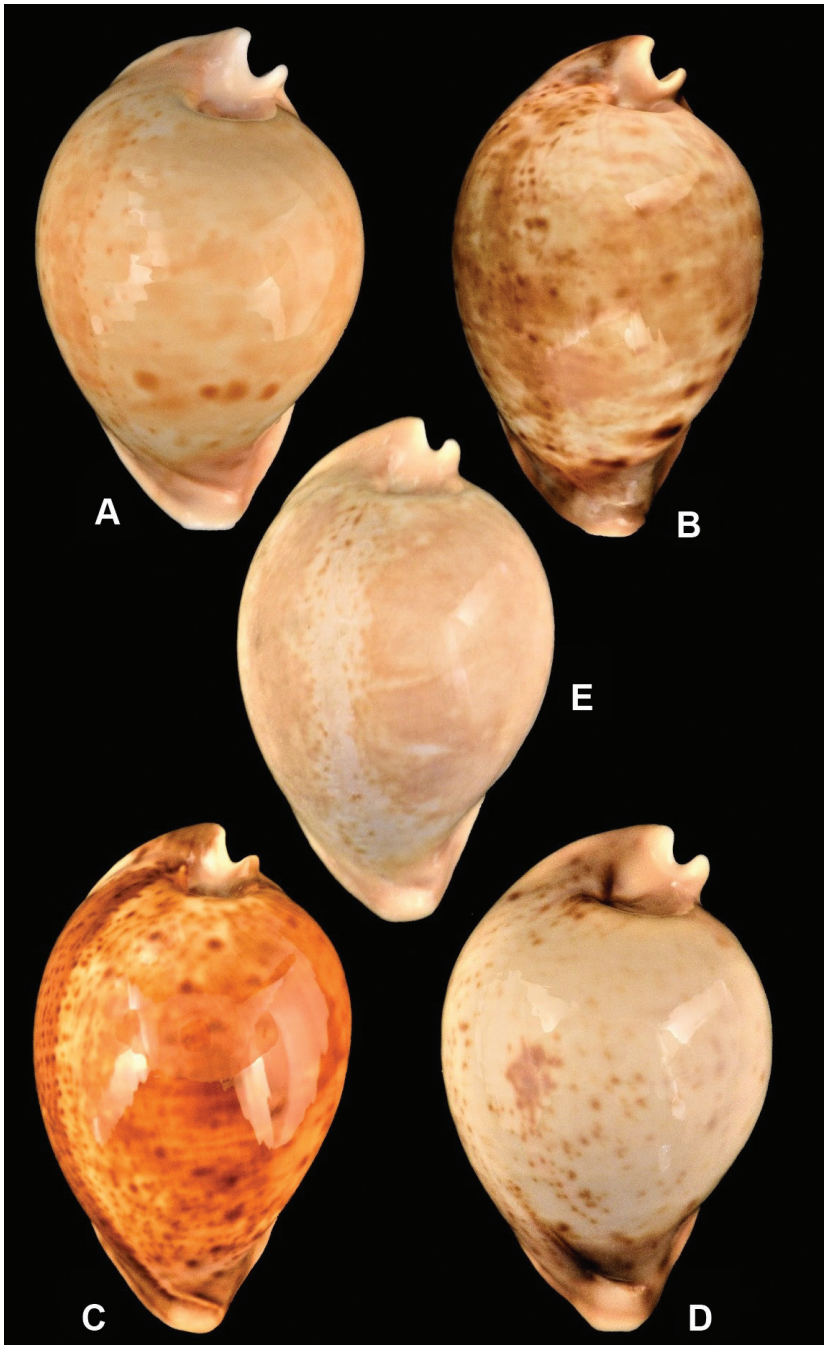

Figure 2. Specimens of the four recognised subspecies of *Umbilia armeniaca* **A** *U. armeniaca armeniaca*, trawled off Ceduna, Great Australian Bight, 90–120 m, 105 mm **B** *U. armeniaca diprotodon*, taken by diver, Thorny Passage, Port Lincoln, South Australia, 35 m, 102 mm **C** *U. armeniaca clarksoni*, taken by diver off Cape Le Grande, Esperance, Western Australia, 30–35 m, 94.1 mm **D** *U. armeniaca andreyi*, collected using ROV, off Augusta, Western Australia, 150 m, 84.2 mm and **E** *U. armeniaca* from the Lancelin population, collected using ROV, off Lancelin, Western Australia, 200 m, 68.9 mm.

Data sources

Primary data for shell length (L), shell width (W), and shell height (H), columellar (CT) and labral (LT) tooth counts, and shell mass (M) were collected from previously unstudied specimens of *U. a. armeniaca* (n = 21), *U. a. diprotodon* (n = 1), *U. a. clarksoni* (n = 2) and *U. a. andreyi* (n = 4), following the methodology of Lorenz (2017a) (Fig. 3A). Data for the same morphometrics were also collected from previously unstudied specimens of *U. armeniaca* (n = 17) originating from the newly discovered population off Lancelin (hereafter "Lancelin population"). Secondary data for L, W, H, CT, LT, and M were sourced from the original descriptions of the *U. armeniaca* subspecies (Lorenz and Beals 2013) and a concurrently published study (Bridges and Lorenz 2013) (Fig. 3A). Only specimens of *U. a. armeniaca* (n = 30), *U. a. diprotodon* (n = 29), *U. a. clarksoni* (n = 15) and *U. a. andreyi* (n = 15) with data available for all the above mentioned morphometrics were considered in this study.

Data analyses

All data analyses were performed using R (version: 4.2.1), an open-access software environment for statistical testing and graphics, with the *stats* (R Core Team 2022), *vegan* (Oksanen et al. 2022), and *emmeans* (Length 2022) packages. For statistical testing, significance was accepted at a value of $P < 0.01$ to conservatively establish infraspecific differences in shell form. Data summaries are presented in-text as mean ($\bar{x}$) ± standard deviation (SD).

Multivariate methods

The morphometrics considered in this study were those proposed by Bridges and Lorenz (2013) and now commonly adopted for description of Cypraeidae (Lorenz 2017a): shell length (L), height:length ratio (H/L), width:length ratio (W/L), height:width ratio (H/W), normalised columellar tooth count (nCT), normalised labral tooth count (nLT), and relative mass (mR) (Fig. 3B). For each specimen, nCT and nLT were calculated as described by Schilder (1937) and H/L, W/L, H/W and mR were calculated as described by Lorenz (2017a).

Because both dimensionless (e.g., ratios) and differently scaled (e.g., length vs. tooth counts) morphometrics were considered, values were transformed to Z-scores prior to ordination and statistical testing (R function: *scale*) (Fig. 3C). Transformation ensured each morphometric was centred, with a mean of zero, and uniformly scaled, with values expressed in terms of deviation from the mean. Morphometric Z-scores were then scanned for potential outliers, indicative of atypical specimens. One specimen of *U. a. andreyi* (paratype 13: $Z_{H/L} = 3.27$, $Z_{H/W} = 6.71$), one specimen of *U. a. clarksoni* (paratype 5: $Z_{nLT} = 3.80$), and two specimens of *U. a. diprotodon* (paratype 22: $Z_{W/L} = 4.23$; paratype 33: $Z_{H/W} = 3.82$) were atypical, with at least one morphometric exceeding three standard deviations of the mean (i.e., $|Z\text{-score}| > 3$). All were censored from statistical testing since their morphometric values were derived from secondary data that could not be validated (Fig. 3C).

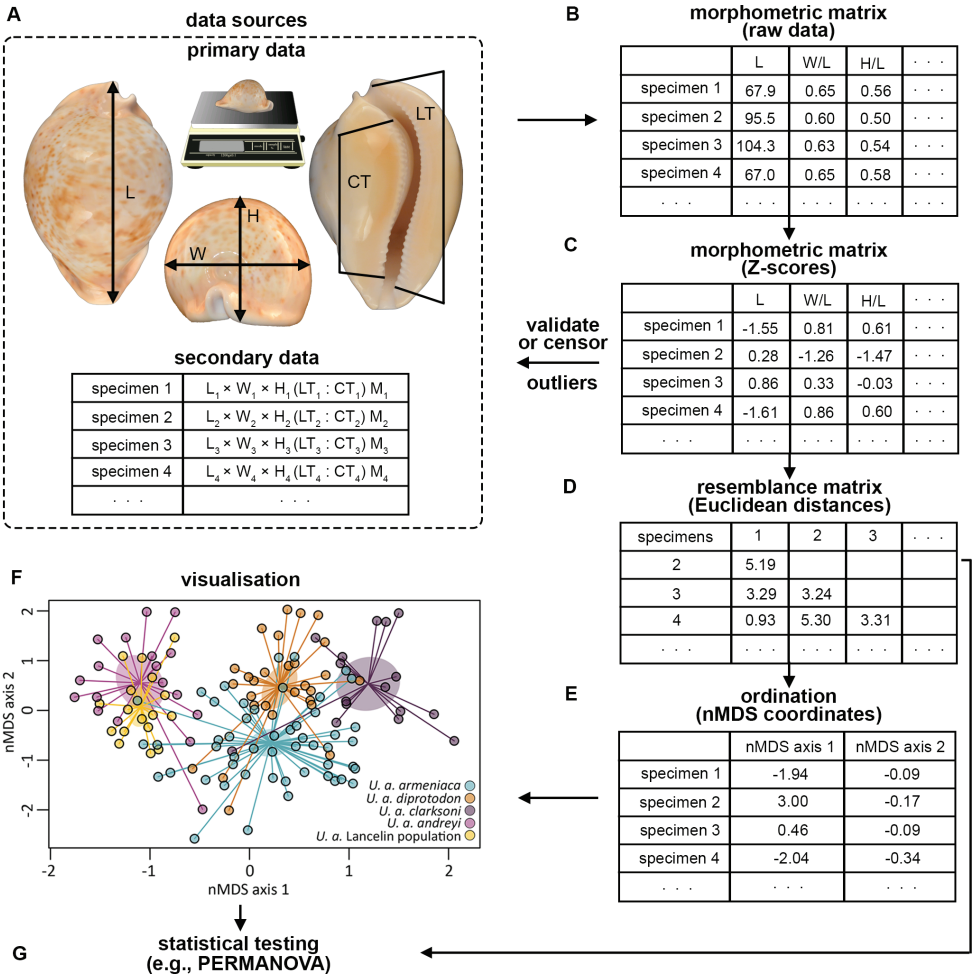

	L	W/L	H/L	· · ·
specimen 1	67.9	0.65	0.56	· · ·
specimen 2	95.5	0.60	0.50	· · ·
specimen 3	104.3	0.63	0.54	· · ·
specimen 4	67.0	0.65	0.58	· · ·
· · ·	· · ·	· · ·	· · ·	· · ·

	L	W/L	H/L	· · ·
specimen 1	-1.55	0.81	0.61	· · ·
specimen 2	0.28	-1.26	-1.47	· · ·
specimen 3	0.86	0.33	-0.03	· · ·
specimen 4	-1.61	0.86	0.60	· · ·
· · ·	· · ·	· · ·	· · ·	· · ·

specimens	1	2	3	· · ·
2	5.19			
3	3.29	3.24		
4	0.93	5.30	3.31	
· · ·	· · ·	· · ·	· · ·	· · ·

	nMDS axis 1	nMDS axis 2
specimen 1	-1.94	-0.09
specimen 2	3.00	-0.17
specimen 3	0.46	-0.09
specimen 4	-2.04	-0.34
· · ·	· · ·	· · ·

Figure 3. Diagrammatic representation of how a multivariate approach to morphological study of shell form for cowries was applied in this study, using *Umbilia armeniaca* as an example (see Suppl. material 1 for an outline of code used) **A** data were sourced by examining unstudied specimens (primary data) or sourced from prior studies (secondary data) **B** data for morphometrics deemed representative of shell form were **C** transformed to *Z*-scores and atypical specimens either validated (primary data) or censored (secondary data) before **D** computing a resemblance matrix based on Euclidean distance between specimens **E** non-metric multidimensional scaling (nMDS) was then used for dimensionality reduction to **F** permit visualisation in a new space of two dimensions and **G** statistical testing was employed to validate visual observations by estimating the probability that a priori assigned groups (taxa or populations) shared the same centroid and dispersion within multidimensional space.

Using the morphometric *Z*-scores for uncensored specimens of *U. a. armeniaca* (n = 51), *U. a. diprotodon* (n = 28), *U. a. clarksoni* (n = 16), *U. a. andreyi* (n = 18), and the Lancelin population (n = 17), a resemblance matrix was computed based on Euclidean distances between specimens (R function: *vegedist*) (Fig. 3D).

Non-metric multidimensional scaling (nMDS) was then used for dimensionality reduction to permit visualisation of the resemblance matrix in a new space of two dimensions (R function: *metaMDS*) (Fig. 3E, F). This ordination technique finds a monotonic relationship between ranks of distances in the resemblance matrix and ranks of distances in a new space of reduced dimensions such that the relative similarity (or dissimilarity) between specimens is represented as closely as possible within the new space. Whilst there are other techniques (e.g., principal component analysis) for ordinating resemblance matrices, nMDS is demonstrably preferred for resolving group differences when studying shell form among Cypraeidae (Tissot 1984).

The influence of each morphometric on the patterns visualised with nMDS (Fig. 3F) was evaluated by testing strength and significance of correlation between each morphometric and the plot configuration (R function: *envfit*). Significant correlations were visualised by fitting a two-dimensional thin-plate generalised additive model spline for the corresponding morphometric as a function of the plot configuration, with results overlayed on the existing nMDS ordination as lines reflecting morphometric clines (R function: *ordisurf*).

Despite numerous advantages of ordination, visual interpretations of multidimensional data after reducing dimensionality can be subjective (Guillerme et al. 2020). Multivariate statistical tests which do not require resemblance matrices to be ordinated are, therefore, useful for objectively validating differences in shell form among groups (Fig. 3G). To test the hypothesis that there were no differences in central tendency of shell form among the five *U. armeniaca* groups examined (i.e., *U. a. armeniaca*, *U. a. diprotodon*, *U. a. clarksoni*. *U. a. andreyi*, and the Lancelin population) a one-factor permutational analysis of variance (PERMANOVA) was used to fit a linear model to the resemblance matrix (R function: *adonis2*). Pairwise comparisons proceeded detection of a significant group effect, using PERMANOVA for each comparison and controlling for the family-wise error rate with the Holm (1979) procedure. Additionally, to test hypotheses that there were no differences in variation of shell form between any of the *U. armeniaca* groups, permutation-based tests for homogeneity of multivariate dispersions were used to compare the distance of specimens from their group centroid (R function: *permutest.betadisper*), controlling for the family-wise error rate with the Holm (1979) procedure.

Univariate methods

To contextualise how the multivariate approach compared with a univariate approach, an analysis of variance (ANOVA), constructed as a linear model, was used to test whether the means of each morphometric differed among the five *U. armeniaca* groups examined (R function: *lm*). Pairwise comparisons between groups were made using linear hypothesis tests of the estimated marginal means (R function: *emmeans*), controlling for the family-wise error rate with the Holm (1979) procedure. Boxplots were used to visualise differences in central tendencies (e.g., mean and median) and variation (e.g., range and quantiles) of morphometrics among groups.

Results

Multivariate approach

Among the studied specimens of *Umbilia armeniaca*, the *a priori* assigned groups (i.e., *U. a. armeniaca*, *U. a. diprotodon*, *U. a. clarksoni*, *U. a. andreyi*, and the Lancelin population) were able to explain a significant amount (R^2 = 0.48, F = 29.32, P < 0.001) of the variation in shell form (Fig. 4A). Between the *U. armeniaca* subspecies, differences in central tendencies (i.e., centroids) of shell form were highly significant (Table 1), with *U. a. andreyi* and *U. a. clarksoni* the most dissimilar (D = 4.66, R^2 = 0.64, P = 0.001) and *U. a. armeniaca* and *U. a. diprotodon* the most similar (D = 1.61, R^2 = 0.47, P = 0.001). Central tendency of shell form for the Lancelin population was distinct from *U. a. armeniaca* (D = 2.89, R^2 = 0.31, P = 0.001), *U. a. clarksoni* (D = 4.60, R^2 = 0.71, P = 0.001), and *U. a. diprotodon* (D = 3.41, R^2 = 0.56, P = 0.001), but was comparable to that of *U. a. andreyi* with the distinction between the two only explaining 9% of the variation in shell form among the corresponding specimens (D = 1.00, R^2 = 0.09, P = 0.012; Fig. 4A, Table 1).

Results also indicated that a similar degree of variation (i.e., dispersion) in shell form existed for the *U. armeniaca* subspecies (Fig. 4A, Table 2). For the Lancelin population, variation in shell form was similar to that of *U. a. andreyi* (t = 2.96, P = 0.041), *U. a. clarksoni* (t = 1.66, P = 0.568), and *U. a. diprotodon* (t = 1.90, P = 0.376), but significantly less than that of *U. a. armeniaca* (t = 4.80, P = 0.001; Fig. 4A, Table 2).

Table 1. Results of pairwise comparisons testing the hypotheses that there were no differences in central tendency (i.e., centroid) of shell form among the studied *Umbilia armeniaca* groups (subspecies or population). The Euclidean distance (D) between centroids, coefficient of determination (R^2), and Holm-adjusted probability that the distance between centroids arose by random chance (P) are presented.

***U. armeniaca* group**	*andreyi*			*armeniaca*			*clarksoni*			*diprotodon*		
	D	***R²***	***P***	***D***	***R²***	***P***	***D***	***R²***	***P***	***D***	***R²***	***P***
armeniaca	2.86	0.29	0.001	–	–	–	–	–	–	–	–	–
clarksoni	4.66	0.64	0.001	2.48	0.23	0.001	–	–	–	–	–	–
diprotodon	3.20	0.47	0.001	1.61	0.14	0.001	2.70	0.40	0.001	–	–	–
Lancelin population	1.00	0.09	0.012	2.89	0.31	0.001	4.60	0.71	0.001	3.41	0.56	0.001

Table 2. Results of pairwise comparisons testing the hypotheses that there were no differences in variation (i.e., dispersion) in shell form among the studied *Umbilia armeniaca* groups (subspecies or population). The mean ($\bar{x}$) ± standard deviation (SD) and range in Euclidean distance that specimens were from their group centroid are presented. Shared alphabetic superscripts identify group means that are not significantly (Holm-adjusted $P \geq 0.01$) different.

***U. armeniaca* group**	**distance from centroid***	
	($\bar{x}$ ± SD)	**range**
andreyi	1.72 ± 0.53^{ab}	0.88 – 3.29
armeniaca	1.94 ± 0.56^{a}	0.87 – 3.24
clarksoni	1.53 ± 0.61^{ab}	0.73 – 2.91
diprotodon	1.50 ± 0.49^{ab}	0.63 – 2.59
Lancelin population	1.22 ± 0.46^{b}	0.48 – 2.20

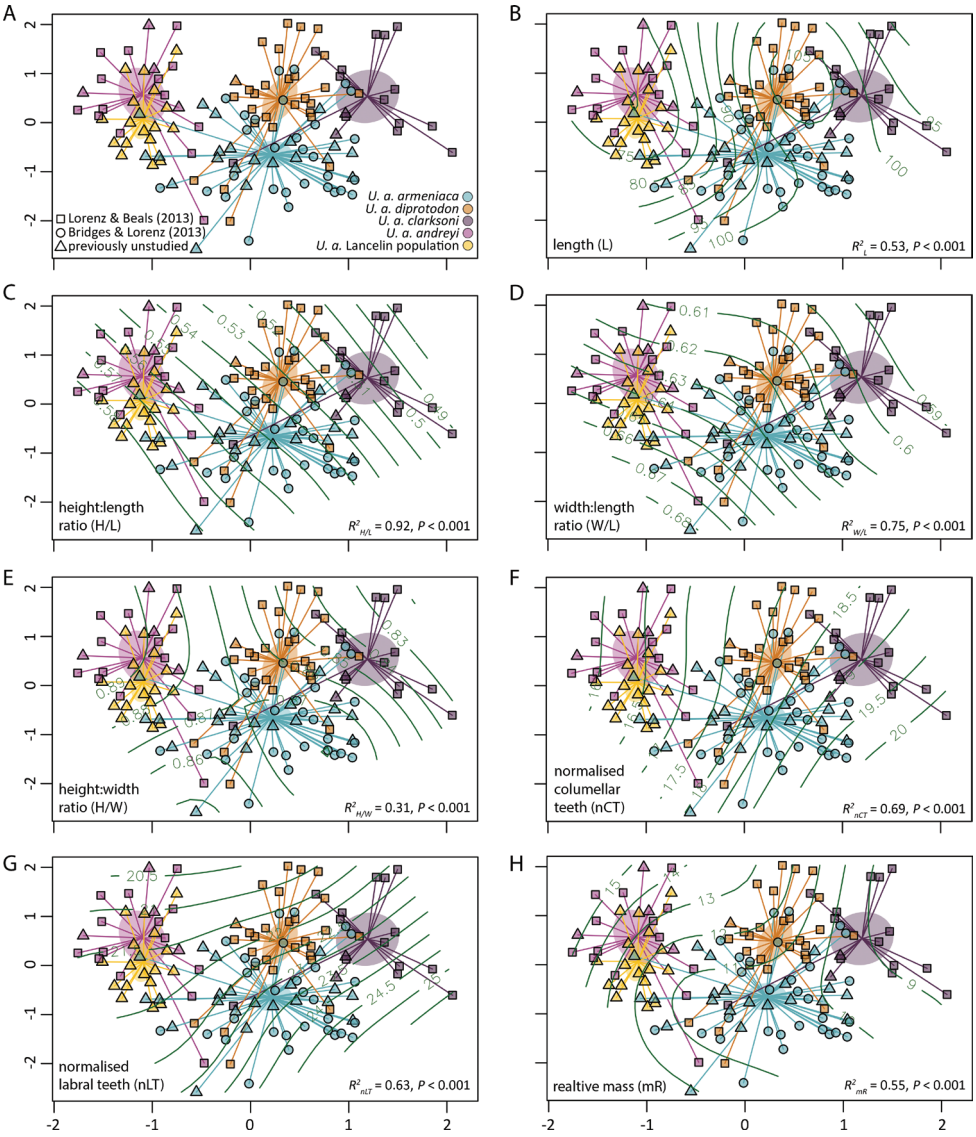

Figure 4. A nMDS ordination (stress = 0.16) of the resemblance matrix for *Umbilia armeniaca*, where shaded ellipses indicate the 95% confidence interval of group (subspecies or population) centroids and plot characters indicate data source **B–H** Associations between ordination structure and morphometrics influencing this structure, where the green lines illustrate **B** length **C** height:length ratio **D** width:length ratio **E** height:width ratio **F** normalised columellar tooth count **G** normalised labral tooth count, and **H** relative mass contour lines.

All morphometrics considered representative of shell form (i.e., L, H/L, W/L, H/W, nCT, nLT, mR) significantly influenced the ordination structure of the *U. armeniaca* groups visualised in Fig. 4. The most important morphometric (based on R^2) was H/L (R^2 = 0.92, P < 0.001), followed by W/L (R^2 = 0.75, P < 0.001), nCT (R^2 = 0.69,

$P < 0.001$), nLT ($R^2 = 0.63$, $P < 0.001$), mR ($R^2 = 0.55$, $P < 0.001$), L ($R^2 = 0.53$, $P < 0.001$), and H/W ($R^2 = 0.31$, $P < 0.001$). Based on the associations between each morphometric and nMDS plot configuration (Fig. 4B–H), relative differences in shell form could be inferred. For example, shell form of *U. a. andreyi* and the Lancelin population was typified by lesser L and nCT, and greater mR, when compared to the other subspecies. In contrast, shell form of *U. a. clarksoni* was typified by lesser H/L, W/L, H/W and mR, while *U. a. diprotodon* was typified by greater L. *Umbilia a. armeniaca* was not typified by any extreme in the morphometrics assessed, with a central tendency in shell form intermediate to that of the other subspecies and the Lancelin population.

Univariate approach

By examining each morphometric independently, relative differences in morphometric values among groups inferred from the nMDS ordination (Fig. 4) could be quantified and validated. For example, the typical shell length of *U. a. diprotodon* was significantly greater than that of any of the other groups considered (Fig. 5A). Likewise, shell form of *U. a. clarksoni* was typified by a significantly lesser H/L, W/L and H/W (Fig. 5B–D). Only three morphometrics (H/L, H/W and mR) differentiated the four subspecies of *U. armeniaca*; shell length was unable to differentiate between *U. a. armeniaca* and *U. a. clarksoni*, W/L was unable to differentiate between *U. a. andreyi*, *U. a. armeniaca*, and *U. a. diprotodon*, nCT was unable to differentiate between *U. a. clarksonii*, *U. a. armeniaca*, and *U. a. diprotodon*, and nLT was unable to differentiate between *U. a. clarksoni* and *U. a. armeniaca* or *U. a. diprotodon* and *U. a. andreyi* (Fig. 5). Measures of central tendency (e.g., mean and median) and variation (e.g., standard deviation and range) for all morphometrics studied are presented separately for each group in Appendix 1.

Considering that not all morphometrics were consistently similar or dissimilar between groups, it was not possible to conclude whether groups differed in overall shell form from univariate comparisons alone. This conundrum is best illustrated by a comparison of *U. a. andreyi* and the Lancelin population, where specimens from these groups differed in central tendencies of relative mass (Fig. 5G). A statistical difference in this morphometric alone, however, did not result in a statistical difference in overall shell form, as determined from the multivariate approach (Fig. 4, Table 1).

Discussion

Our results confirm that variation in shell form is prominent within and between populations of *Umbilia armeniaca.* Such variability may represent ecophenotypic responses in shell form to environmental factors, random genetic variations independent of adaptive value, or natural selection. Results of this study cannot directly distinguish between these, or other possible causal mechanisms promoting variation in the shell form of cowries, within or between populations, which have seen much discussion elsewhere (see Griffiths 1959; Orr 1959; Kay 1961; Renaud 1976; Tissot 1984, 1988; Irie and Iwasa 2005; Irie 2006). Rather, the following discussion will focus on the implications of such variation, from a

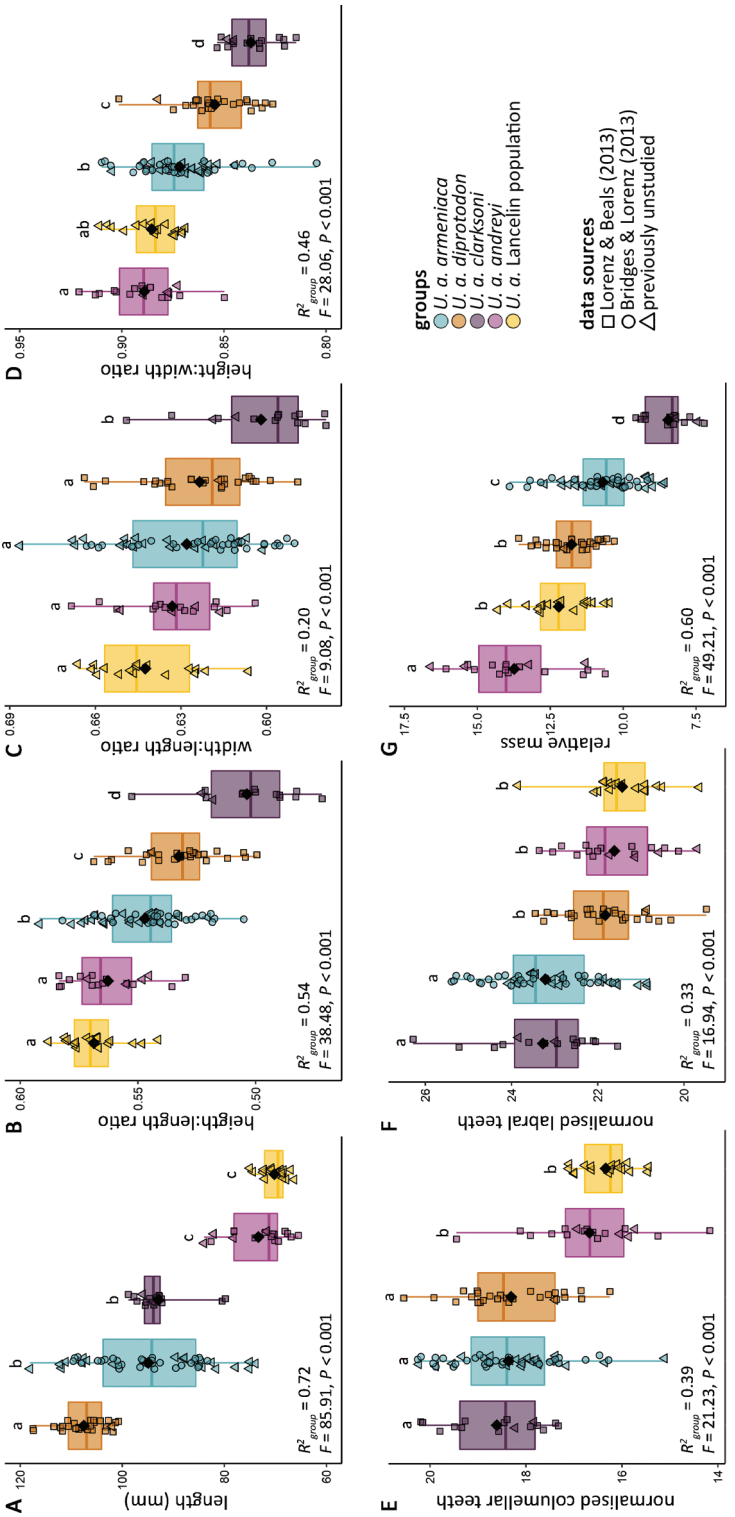

Figure 5. Box plots showing univariate comparisons of **A** shell length **B** height:length ratio **C** width:length ratio **D** height:width ratio **E** normalised columellar tooth count **F** normalised labral tooth count, and **G** relative mass among the studied *Umbilia armeniaca* groups (subspecies or population). Black diamonds represent group means, boxes illustrate first and third quartile as box edges and median as central line. Shared alphabetic superscripts identify group means that are not statistically different (Holm-adjusted $P \geq 0.01$) for a morphometric.

systematic perspective, by first discussing the infraspecific taxonomy of *U. armeniaca* and the extent to which our results agree with the putative differences in shell form described by Lorenz and Beals (2013). Consideration of how a multivariate approach to morphological study of shell form might integrate into cowrie systematics is then treated more broadly.

Infraspecific taxonomy of *Umbilia armeniaca*

Crucial to the validity of taxa differentiated through morphological study of shell form is a replicable and objective approach for comparison. Prior morphological study of shell form in *U. armeniaca* has relied on subjective comparisons of morphometrics and their central tendencies to resolve infraspecific differences, with statistical testing limited to a comparison of relative mass (Bridges and Lorenz 2013; Lorenz and Beals 2013). Given that putative differences were, potentially, an artefact of random chance or subjective inference, the broader application of statistical tests with a clearly defined threshold ($P < 0.01$) for resolving infraspecific differences permits objective validation of the original descriptions of shell form for the subspecies of *U. armeniaca*.

In their original description of *U. armeniaca* subspecies, Lorenz and Beals (2013) qualitatively described the most important infraspecific differences in shell form. The impression that *U. a. clarksoni* is "more elongate and less humped" and has the "lowest dorsal profile" was confirmed in our study by significantly lower H/L, W/L and H/W. Likewise, the impression that *U. a. andreyi* is "slightly more inflated and stunted" and the "most globular and humped" was confirmed by significantly greater H/L and H/W ratios. Significantly lower W/L and H/W of *U. a. diprotodon* relative to *U. a. armeniaca* confirmed the supposition that the former tends to be "less humped" than the latter. The suggestion that *U. a. andreyi* has "fewer teeth on both sides", however, proved true only if considering raw tooth counts. Once normalised (sensu Schilder 1937), we found the slight difference in nLT between *U. a. andreyi* (21.6 ± 1.0) and *U. a. diprotodon* (21.8 ± 0.9) to be non-significant. Results for our univariate analysis of mR were synonymous with those of Lorenz and Beals (2013), with significant differences between all subspecies. Consideration of these and other morphometric-specific differences, collectively, within our multivariate approach to morphological study of shell form, leads us to conclude that *U. a. armeniaca*, *U. a. diprotodon*, *U. a. clarksoni*, and *U. a. andreyi* are morphologically distinct in central tendencies of shell form. This, however, does not necessarily imply that all specimens of a particular subspecies could be reliably identified based on shell form alone.

Certainly, multivariate distributions (Fig. 4) indicate that while central tendencies of shell form differed significantly, some specimens of a particular subspecies were more representative (i.e., closer to the centroid) of another subspecies. For example, while all specimens of *U. a. diprotodon* were unequivocally distinct from *U. a. andreyi* or *U. a. clarksoni*, some *U. a. diprotodon* paratypes were more representative of *U. a. armeniaca* (paratypes 4, 5, and 11) than *U. a. diprotodon*. Thus, we can conclude that all specimens of *U. a. diprotodon* can be reliably differentiated from *U. a. andreyi* and *U. a. clarksoni*, but not necessarily from *U. a. armeniaca* based on shell form. By the same rationale all specimens of *U. a. clarksoni* could be reliably differentiated from *U a. andreyi*, but not necessarily from

U. a. diprotodon or *U. a. armeniaca*, and all specimens of *U. a. andreyi* could be reliably differentiated from *U. a. diprotodon* and *U. a. clarksoni*, but not from *U. a. armeniaca*. None of the subspecies could, therefore, be reliably differentiated from *U. a. armeniaca*, just as *U. a. armeniaca* could not be reliably differentiated from any of the other subspecies. For taxa which cannot be reliably identified from one another based on shell form alone, there is a need to consider additional conchological attributes, beyond the scope of shell form, when assigning specimens of unknown provenance to a particular subspecies.

When comparing taxa, it is important to recognise that not all diagnostic factors can be reliably incorporated into multivariate analysis. Shell pattern, for example, is important in cowrie characterisation (Lorenz 2017a, 2018) and, although quantifiable aspects of shell pattern (e.g., width of dorsal spots) have been included in multivariate analysis of cowries (e.g., Tissot 1984), this is only feasible for taxa with clearly defined patterning. For *U. armeniaca* there exists no common pattern with clearly demarcated boundaries to serve as a basis for replicable and objective quantification (Fig. 2). Rather, Lorenz and Beals (2013) highlighted qualitative differences between the two deep-water subspecies (*U. a. andreyi* and *U. a. armeniaca*), which generally have mottled shells with paler colouration, and the two shallow-water subspecies (*U. a. clarksoni* and *U. a. diprotodon*), which are generally much darker, but with bluish marginal colouration. Other physical features of the shell that may contribute to differentiation between taxa, but are not captured in formulaic or multivariate analyses, include size of the protoconch and prominence of the spire, form of the anterior flange and posterior labral flange, the form of the columellar teeth, dorsal profile, and shape and form of the base, all of which vary among the four subspecies of *U. armeniaca* (Lorenz and Beals 2013). Notwithstanding the inability of multivariate analysis to accommodate all potential conchological attributes of infraspecific variation, the original descriptions of shell form for the *U. armeniaca* subspecies were generally valid when re-evaluated using an objective approach that incorporated statistical tests for resolving infraspecific differences. Considering almost a quarter (24.8%) of the data in our study originated from previously unstudied specimens (n = 28) of *U. armeniaca*, the infraspecific differences in shell form outlined by Lorenz and Beals (2013) were found to appropriately generalise the populations of these subspecies.

Of the four *U. armeniaca* subspecies, the nMDS ordination revealed that shells of the previously unstudied Lancelin population were most similar to the neighbouring population of *U. a. andreyi*. Although Lancelin shells had a significantly reduced relative mass, compared to *U. a. andreyi*, this difference was insufficient to differentiate the Lancelin population from *U. a. andreyi* when accounting for the overall variability in shell form. Differences in relative mass are closely associated with differences in shell callosity (Bridges and Lorenz 2013) which is known to correlate with seawater temperature (Tissot 1984; Irie 2006). Other species of cowries (e.g., *Lyncina vitellus*, *Melicerona felina*, *Monetaria annulus*, *M. caputserpentis*, *Naria erosa*, *N. helvola*, *N. marginalis*, and *Purpuradusta gracilis*) demonstrate latitudinal clines in shell callosity (Schilder and Schilder 1938–1939, 1967; Liversridge 1968; Schilder 1969; Tissot 1984; Irie 2006) and a latitudinal difference in relative mass could therefore be anticipated within the Australian west coast range of *U. armeniaca*. Given a presumed environmental influence on the only morphometric differentiating the Lancelin popu-

lation from *U. a. andreyi*, and overall similarities in shell form, we conclude that the Lancelin population of *U. armeniaca* is best considered a northern extension of the distribution of *U. a. andreyi*.

Considerations for a multivariate approach to cowrie systematics

Most datasets used in the study of shell form are multidimensional and, consequently, a large component of any systematic study will involve consideration of how to extract a meaningful summary of differences in shell form among specimens and/or groups. The multivariate approach taken in this study, couples easy-to-interpret graphics produced via ordination with an objective appraisal of inter-group differences via statistical testing. When combined with a univariate approach, as done here, a broad range of questions of relevance to systematics can be addressed objectively. For example, if the goal is to characterise differences in shell form between groups, multivariate tests comparing differences in central tendencies (such as group centroids) or variability (such as group dispersion) in multidimensional space are most appropriate. Furthermore, if the goal is to characterise how a particular morphometric differs between groups, univariate tests comparing differences in central tendencies (such as group means) for that morphometric will be of value. Regardless of the tests used, statistical testing should only be employed to address questions framed within an appropriate statistical context if sample sizes are large enough to permit detection of statistically significant differences (Cohen 1988; Anderson 2001).

It is also important to consider which morphometrics are most appropriate for statistical testing. Studies comparing shell form among cowries have, over time, varied greatly in the morphometrics selected to represent shell form (Bridges and Lorenz 2013). While theoretically there is no limit to the number of morphometrics which can be incorporated into multivariate analyses, the "curse of dimensionality" (Bellman 1966) favours minimising the number selected from a theoretical perspective. Additionally, for each unique measurement there exists potential for observational error and, where morphometrics make assumptions concerning growth (e.g., Irie 2006), modelling error. Furthermore, some morphometrics (e.g., whorl widths or callus thickness) require cross-sectioning of shells (Tissot 1988; Irie 2006) which is not feasible in situations where destructive sampling is not possible, such as when working with type specimens or those held in public collections. Other morphometrics are inherently taxon-specific (e.g., colouration and/or patterning) which complicates comparisons with taxa lacking the associated trait (Guillerme et al. 2020). Finally, many morphometrics have isometric or allometric relationships and are positively correlated with one another, such that they represent similar sources of variability in shell form (Tissot 1984, 1988). Taken together, these factors incentivise limiting selection to shared morphometrics that are sampled non-destructively and represent unique sources of variation in shell form among cowries. From past studies most of the meaningful variation in shell form among cowries is known to come from shell size, shape, callosity, and the number of basal teeth (Tissot 1984; 1988). For example, when considering 18 morphometrics as part of a multivariate approach to study shell form in *Monetaria caputserpentis*, Tissot (1984) found that three components of variation (shell size, shape and callosity, and number of basal teeth) accounted for almost 70% of the total variation

in shell form among populations sampled across the geographical range of this species. On this basis, care was taken to ensure that the seven morphometrics selected to represent shell form in the present study uniquely represented variation in shell size (i.e., length), shape (i.e., height:length, width:length, and height:width ratios), callosity (i.e., relative mass), and number of basal teeth (i.e., normalised columellar and labral tooth counts).

Aside from representing the primary sources of infra- and interspecific variation in shell form of cowries (Tissot 1984, 1988), a further advantage of these seven morphometrics is that they require only four shell measurements taken with a vernier calliper (e.g., length, width, height) or balance (e.g., mass) and counts of basal teeth, all of which are sampled non-destructively. For similar reasons, the morphometrics considered in our study were also proposed by Bridges and Lorenz (2013), and are commonly adopted (e.g., Lorenz 2017b) for description of Cypraeidae. While acknowledging that morphological studies with other gastropod families have developed methods for quantifying the variation in shell shape from a set of homologous points, or landmarks, positioned on images using the Procrustes method (e.g., Rohlf and Marcus 1993), such methods have not been developed for the Cypraeidae. Gastropods such as Muricidae, for which such methods have been developed, have an exposed shell spire and numerous ribs and spines which provides a broad range of appropriate landmarks for such methods (Doyle et al. 2018; Bocxlaer et al. 2020; Larsson et al. 2020). This is not the case for cowries, however, which demonstrate determinate growth (Vermeij and Signor 1992), generally have a concealed spire, and lack meristic shell ornamentations, such as spines and varices. Furthermore, such methods were developed with the primary intention of detecting minute variation within populations related to ontogenetic development patterns (Larsson et al. 2020) or environmental selective pressures (Doyle et al. 2018; Bocxlaer et al. 2020) rather than establishing novel taxonomic characters. Given the intent of infraspecific taxonomy of cowries to distinguish between populations that are visibly distinct (Lorenz 2017a), an approach that considers morphometrics which are easy to comprehend, such as those used in this study, would seem most appropriate.

Conclusions

Multivariate approaches to the morphological study of shell form of cowries have been utilised primarily to develop hypotheses related to ecological and functional diversity within the target species (Tissot 1984, 1988). Although used more recently in recognition and description of a new species of cowrie from the fossil record (Southgate et al. 2021), integration of a multivariate approach into cowrie systematics has received surprisingly little attention, with univariate comparison of central tendencies, using shell formulae, predominant in recent comparative studies (Bridges and Lorenz 2013; Lorenz 2017a) and in recognising new taxa (e.g., Lorenz 2017b). While useful in describing key morphometric characters and allowing subjective comparisons between taxa (Bridges and Lorenz 2013), including fossils (Landau and Groves 2011; Southgate and Roberts 2022), the shell formula, as applied to cowries, does not convey variability of key morphometric characters, nor does it support the testing of statistical differences between populations or taxa.

This study has demonstrated the utility of a multivariate approach that couples easy-to-interpret graphics produced via ordination with an objective appraisal of inter-group differences via statistical testing with clearly defined thresholds for both outlier detection (i.e., $|Z\text{-score}| > 3$) and resolving infraspecific differences ($P < 0.01$). Using *Umbilia armeniaca* as a case study, we showed how primary data from unstudied specimens might supplement secondary data from prior studies to validate existing infraspecific taxonomy and characterise a previously unstudied (Lancelin) population of this species. The multivariate approach showed the four recognised *U. armeniaca* subspecies to be similarly variable, but confirmed differences in central tendency of shell form. Our analysis did not justify differentiation of the Lancelin population of *U. armeniaca* which is best considered a northward extension of *U. a. andreyi*. Results of this study provide improved understanding of intraspecific differences in shell form of *U. armeniaca* across its broad distribution, and demonstrate how multivariate morphometric methods for statistical comparison of shell form between taxa might benefit cowrie systematics. This approach is complimentary to existing research practices and has broad potential application in future morphometric based studies of cowries.

Acknowledgements

We thank Mr Ray Walker of Busselton, Western Australia for providing the Lancelin specimens used in this study and Nittya S.M. Simard for assistance with figure compilation. This study was supported by University of the Sunshine Coast Research Initiative funding to the first author.

References

Anderson MJ (2001) A new method for non-parametric multivariate analysis of variance. Austral Ecology 26: 32–46. https://doi.org/10.1046/j.1442-9993.2001.01070.x

Bellman R (1966) Dynamic programming. Science 153(3731): 34–37. https://doi.org/10.1126/science.153.3731.34

Bocxlaer BV, Ortiz-Sepulveda CM, Gurdebeke PR, Vekemans X (2020) Adaptive divergence in shell morphology in an ongoing gastropod radiation from Lake Malawi. BMC Evolutionary Biology 20(1): 5. https://doi.org/10.1186/s12862-019-1570-5

Bridges RJ, Lorenz F (2013) A revised morphometric formula for the characterization of cowries (Gastropoda: Cypraeidae). Conchylia 43: 27–40. www.club-conchylia.de/ccinfo/sampleconchylia43_4.pdf

Burgess CM (1970) The living cowries. AS Barnes and Company Inc., New York, 389 pp.

Cohen J (1988) Statistical Power Analysis for the Behavioral Sciences, 2nd edn. Routledge, New York, 567 pp.

Cruz RAL, Pante JR, Rohlf FJ (2012) Geometric morphometric analysis of shell shape variation in *Conus* (Gastropoda: Conidae). Zoological Journal of the Linnean Society 165(2): 296–310. https://doi.org/10.1111/j.1096-3642.2011.00806.x

Doyle D, Gammell MP, Nash R (2018) Morphometric methods for the analysis and classification of gastropods: A comparison using *Littorina littorea*. The Journal of Molluscan Studies 84(2): 190–197. https://doi.org/10.1093/mollus/eyy010

Griffiths RJ (1959) Subspeciation in two species of Cypraeidae. Proceedings of the Malacological Society of London 33: 176–185. https://doi.org/10.1093/oxfordjournals.mollus.a064820

Guillerme T, Cooper N, Brusatte SL, Davis KE, Jackson AL, Gerber S, Goswami A, Healy K, Hopkins MJ, Jones MEH, Lloyd GT, O'Reilly JE, Pate A, Puttick MN, Rayfield EJ, Saupe EE, Sherratt E, Slater GJ, Weisbecker V, Thomas GH, Donoghue PCJ (2020) Disparities in the analysis of morphological disparity. Biology Letters 16(7): 20200199. https://doi.org/10.1098/rsbl.2020.0199

Holm S (1979) A simple sequentially rejective multiple test procedure. Scandinavian Journal of Statistics 6: 65–70. https://www.jstor.org/stable/4615733

Irie T (2006) Geographical variation of shell morphology in *Cypraea annulus* (Gastropoda: Cypraeidae). The Journal of Molluscan Studies 72(1): 31–38. https://doi.org/10.1093/mollus/eyi043

Irie T, Iwasa Y (2005) Optimal growth pattern of defensive organs: The diversity of shell growth among molluscs. American Naturalist 165(2): 238–249. https://doi.org/10.1086/427157

Kay A (1961) On *Cypraea tigris schilderiana* Cate. The Veliger 4: 36–40.

Landau BM, Groves LT (2011) Cypraeidae (Mollusca: Gastropods) from early Miocene Cantuare Formation of northern Venezuela. Novapex 12: 1–38.

Larsson J, Westram AM, Bengmark S, Lundh T, Butlin RK (2020) A developmentally descriptive method for quantifying shape in gastropod shells. Journal of the Royal Society, Interface 17(163): 20190721. https://doi.org/10.1098/rsif.2019.0721

Length R (2022) emmeans: Estimated Marginal Means, aka Least-Squares Means. R package version 1.8.1-1.

Liversridge MJH (1968) On the distribution of *Cypraea* (*Erosaria*) *marginalis* along the east coast of Africa. Journal of Conchology 26: 229–236.

Lorenz F (2001) Monograph of the living *Zoila*. ConchBooks, Hackenheim, 187 pp.

Lorenz F (2002) New worldwide cowries. Descriptions of new taxa and revisions of selected groups of living Cypraeidae (Mollusca: Gastropoda). ConchBooks, Hackenheim, 292 pp.

Lorenz F (2017a) Cowries: A guide to the gastropod family Cypraeidae. Volume 1: Biology and systematics. ConchBooks, Harxheim, 644 pp.

Lorenz F (2017b) A new subspecies of *Bistolida stolida* (Linnaeus, 1758) from Queensland (Gastropoda: Cypraeidae). Acta Conchyliorum 16: 47–57.

Lorenz F (2018) Cowries: A guide to the gastropod family Cypraeidae. Volume 2: Shells and animals. ConchBooks, Harxheim, 715 pp.

Lorenz F, Beals M (2013) The subspecies of *Umbilia armeniaca* (Verco, 1912) (Gastropoda: Cypraeidae). Conchylia 43: 91–100.

Lorenz F, Hubert A (2000) A Guide to Worldwide Cowries, 2nd edn. ConchBooks, Hackenheim, 584 pp.

Meyer CP (2003) Molecular systematics of cowries (Gastropoda: Cypraeidae) and diversification patterns in the tropics. Biological Journal of the Linnean Society. Linnean Society of London 79(3): 401–459. https://doi.org/10.1046/j.1095-8312.2003.00197.x

Meyer CP (2004) Towards comprehensiveness: Increased molecular sampling within Cypraeidae and its phylogenetic implications. Malacologia 46: 127–156.

Meyer CP, Paulay G (2005) DNA barcoding: Error rates based on comprehensive sampling. PLoS Biology 4(12): e422. https://doi.org/10.1371/journal.pbio.0030422

Mitteroecker P, Huttegger SM (2009) The concept of morphospaces in evolutionary and developmental biology: Mathematics and metaphors. Biological Theory 4(1): 54–67. https://doi.org/10.1162/biot.2009.4.1.54

Oksanen J, Simpson G, Blanchet F, Kindt R, Legendre P, Minchin P, O'Hara R, Solymos P, Stevens M, Szoecs E, Wagner H, Barbour M, Bedward M, Bolker B, Borcard D, Carvalho G, Chirico M, De Caceres M, Durand S, Evangelista H, Fitzjohn R, Friendly M, Furneaux B, Hannigan G, Hill M, Lahti L, McGlinn D, Ouellette M, Ribeiro Cunha E, Smith T, Stier A, Ter Braak C, Weedon J (2022) vegan: Community Ecology Package. R package version 2.6-4. https://cran.r-project.org/web/packages/vegan/vegan.pdf

Orr V (1959) A bionomic shell study of *Monetaria annulus* (Gastropods: Cypraeidae) from Zanzibar. Notulae Naturae of the Academy of Natural Sciences of Philadelphia 313: 1–11.

R Core Team (2022) R: A language and environment for statistical computing. R Foundation for Statistical Computing, Vienna.

Renaud ML (1976) Observation on the behaviour and shell types of *Cypraea moneta* (Mollusca, Gastropoda) at Enewetak, Marshall Islands. Pacific Science 30: 147–158.

Rohlf FJ, Marcus LF (1993) A revolution in morphometrics. Trends in Ecology & Evolution 8(4): 129–132. https://doi.org/10.1016/0169-5347(93)90024-J

Schilder FA (1937) Neogene Cypraeacea aus Ost-Java. De Ingenieur in Nederlandsch-Indie 4: 195–210.

Schilder FA (1969) Zoogeographical studies on living cowries. The Veliger 11: 367–377.

Schilder FA, Schilder M (1938–1939) Prodrome of a monograph on living Cypraeidae. Proceedings of the Malacological Society of London 23(3): 119–231. https://doi.org/10.1093/oxfordjournals.mollus.a064354

Schilder FA, Schilder M (1952) Ph. Dautzenbergs collection of Cypraeidae. Institut Royal des Sciences Naturelles de Belgique, Mémoires, Deuxième Series 45: 1–243.

Schilder M, Schilder FA (1967) Studies on east Australian cowries. The Veliger 10: 103–110.

Schilder M, Schilder FA (1968) Studies on populations of the cowrie *Erronea errones* (Linnaeus). The Veliger 11: 109–116.

Southgate PC, Roberts M (2022) A new species of *Austrocypraea* (Mollusca: Gastropoda: Cypraeidae) from the Pliocene of Flinders Island, Tasmania. ZooKeys 1123: 173–185. https://doi.org/10.3897/zookeys.1123.90917

Southgate PC, Militz TA, Roberts M (2021) A new species of *Umbilia* Jousseaume, 1884 (Mollusca: Cypraeidae) from the Australian Pliocene. Molluscan Research 41(3): 214–221. https://doi.org/10.1080/13235818.2021.1962588

Tissot BN (1984) Multivariate analysis of geographic variation in *Cypraea caputserpentis* (Gastropoda: Cypraeidae). The Veliger 27: 106–119.

Tissot BN (1988) Geographic variation and heterochrony in two species of cowries (genus *Cypraea*). Evolution; International Journal of Organic Evolution 42: 103–117. https://doi.org/10.1111/j.1558-5646.1988.tb04111.x

Vayssière A (1910) Nouvelle etude sur les Coquilles de quelques *Cypraea*. Journal de Conchyliologie 58: 301–311.

Vermeij GJ, Signor PW (1992) The geographic, taxonomic and temporal distribution of determinate growth in marine gastropods. Biological Journal of the Linnean Society. Linnean Society of London 47(3): 233–247. https://doi.org/10.1111/j.1095-8312.1992.tb00668.x

Wilson BR (1985) Direct development in southern Australian cowries (Gastropoda: Cypraeidae). Australian Journal of Marine and Freshwater Research 36(2): 267–280. https://doi.org/10.1071/MF9850267

Wilson BR, Clarkson P (2004) Australia's spectacular cowries: A review and field study of two endemic genera, *Zoila* and *Umbilia*. Odyssey Publishing, El Cajon, 396 pp.

Appendix 1

Table A1. Measures of central tendency (i.e., mean and median) and variation (i.e., standard deviation and range) among the studied *Umbilia armeniaca* groups (subspecies or population) for each morphometric considered representative of shell form. Shared alphabetic supercrips identify group means that are not statistically different (Holm-adjusted $P \geq 0.01$) for a morphometric.

Morphometric	*Umbilia armeniaca* groups				
	andreyi	***armeniaca***	***clarksoni***	***diprotodon***	**Lancelin**
length (mm)					
$\bar{x} \pm SD$	73.3 ± 5.8^{c}	94.9 ± 11.1^{b}	92.9 ± 5.4^{b}	107.5 ± 4.5^{a}	70.2 ± 2.5^{c}
median	71.3	94.2	93.9	107.0	69.5
range	65.5–84.0	73.9–118.1	79.8–98.8	100.7–117.5	66.3–75.0
height:length ratio					
$\bar{x} \pm SD$	0.563 ± 0.016^{a}	0.547 ± 0.018^{b}	0.504 ± 0.020^{d}	0.533 ± 0.017^{c}	0.569 ± 0.013^{a}
median	0.566	0.545	0.502	0.531	0.570
range	0.530–0.584	0.505–0.592	0.472–0.553	0.500–0.569	0.541–0.588
width:length ratio					
$\bar{x} \pm SD$	0.633 ± 0.017^{ab}	0.628 ± 0.023^{ab}	0.602 ± 0.019^{c}	0.623 ± 0.019^{b}	0.642 ± 0.017^{a}
median	0.632	0.622	0.596	0.619	0.646
range	0.604–0.668	0.590–0.687	0.579–0.649	0.589–0.664	0.606–0.666
height:width ratio					
$\bar{x} \pm SD$	0.889 ± 0.017^{a}	0.872 ± 0.020^{b}	0.837 ± 0.012^{d}	0.854 ± 0.017^{c}	0.885 ± 0.014^{a}
median	0.889	0.874	0.838	0.857	0.884
range	0.850–0.921	0.805–0.853	0.815–0.853	0.826–0.901	0.869–0.911
normalised columellar teeth					
$\bar{x} \pm SD$	16.7 ± 1.2^{b}	18.4 ± 1.1^{a}	18.6 ± 1.0^{a}	18.3 ± 1.0^{a}	16.3 ± 0.5^{b}
median	16.7	18.4	18.4	18.5	16.2
range	14.2–19.4	15.1–20.3	17.3–20.2	16.2–20.5	15.4–17.1
normalised labral teeth					
$\bar{x} \pm SD$	21.6 ± 1.0^{b}	23.2 ± 1.2^{a}	23.3 ± 1.3^{a}	21.8 ± 0.9^{b}	21.4 ± 0.9^{b}
median	21.8	23.4	23.0	21.9	21.6
range	19.7–23.4	20.8–25.4	21.5–26.3	19.5–23.4	19.6–23.9
relative mass					
$\bar{x} \pm SD$	13.7 ± 1.7^{a}	10.7 ± 1.2^{c}	8.5 ± 0.7^{d}	11.8 ± 0.9^{b}	12.2 ± 1.1^{b}
median	14.0	10.6	8.3	11.8	12.2
range	10.6–16.6	8.6–13.9	7.2–9.6	10.3–13.6	10.5–14.3

Supplementary material 1

Annotated code pertaining to the multivariate approach

Authors: Paul C. Southgate, Thane A. Militz

Data type: docx file

Link: https://doi.org/10.3897/zookeys.1158.98868.suppl1

ZooKeys 1158: 91–120 (2023)
doi: 10.3897/zookeys.1158.94152
https://zookeys.pensoft.net

RESEARCH ARTICLE

A peer-reviewed open-access journal
ZooKeys
Launched to accelerate biodiversity research

Using genomics, morphometrics, and environmental niche modeling to test the validity of a narrow-range endemic snail, *Patera nantahala* (Gastropoda, Polygyridae)

Nathan V. Whelan[1,2], Ellen E. Strong[3], Nicholas S. Gladstone[2], Jason W. Mays[4]

1 *Southeast Conservation Genetics Lab, Warm Springs Fish Technology Center, US Fish and Wildlife Service, 203 Swingle Hall, Auburn, Alabama, 36849, USA* **2** *School of Fisheries, Aquaculture, and Aquatic Sciences, College of Agriculture, Auburn University, 203 Swingle Hall, Auburn, Alabama, 36849, USA* **3** *Department of Invertebrate Zoology, National Museum of Natural History, Smithsonian Institution, PO Box 37012, MRC 163, Washington, DC 20013, USA* **4** *Asheville Ecological Services Field Office, United States Fish and Wildlife Service, 160 Zillicoa ST, Asheville, NC 28801, USA*

Corresponding author: Nathan V. Whelan (nathan_whelan@fws.gov)

Academic editor: Martin Haase | Received 27 August 2022 | Accepted 13 March 2023 | Published 20 April 2023

https://zoobank.org/6D1EA64A-63CB-4C77-82DB-F64FC2352291

Citation: Whelan NV, Strong EE, Gladstone NS, Mays JW (2023) Using genomics, morphometrics, and environmental niche modeling to test the validity of a narrow-range endemic snail, *Patera nantahala* (Gastropoda, Polygyridae). ZooKeys 1158: 91–120. https://doi.org/10.3897/zookeys.1158.94152

Abstract

Terrestrial gastropods are among the most imperiled groups of organisms on Earth. Many species have a complex taxonomic history, often including poorly defined subspecies, most of which have not been the focus of modern systematics research. Genomic tools, geometric morphometrics, and environmental niche modeling were used to assess the taxonomic status of *Patera clarkii nantahala* (Clench & Banks, 1932), a subspecies of high conservation concern with a restricted range of approximately 3.3 km^2 in North Carolina, USA. A genome-scale dataset was generated that included individuals with morphologies matching *P. c. nantahala*, *P. c. clarkii*, and one individual with an intermediate form between *P. c. nantahala* and *P. c. clarkii* that was initially hypothesized as a potential hybrid. Mitochondrial phylogenetics, nuclear species tree inference, and phylogenetic networks were used to assess relationships and gene flow. Differences in shell shape via geometric morphometrics and whether the environmental niches of the two subspecies were significantly different were also examined. Molecular analyses indicated an absence of gene flow among lineages of *P. clarkii* sensu lato. Analyses rejected our hypothesis that the intermediate

shelled form represented a hybrid, but instead indicated that it was a distinct lineage. Environmental niche models indicated significant differences in environmental niche between *P. c. clarkii* and *P. c. nantahala*, and geometric morphometrics indicated that *P. c. nantahala* had a significantly different shell shape. Given multiple lines of evidence, species-level recognition of *P. nantahala* is warranted.

Keywords
3RAD, generalized linear model, Maxent, morphology, Noonday Globe Snail, phylogenetic network, species tree, taxonomy

Introduction

Many conservation and environmental policies rely on functional units like species or subspecies (Primack 2014; Coates et al. 2018). For example, the U.S. Endangered Species Act defines species and subspecies as entities that can be listed as threatened or endangered. Therefore, applied conservation requires an informed taxonomy that accurately reflects diversity so conservation targets are not overlooked or overemphasized. In other words, modern systematics is essential for positive conservation outcomes.

Even though systematists debate the best approach for delineating species (Stankowski and Ravinet 2021), the definition of a species as a distinct evolutionary lineage is implicit in most species concepts (Mayden 1997; De Queiroz 2007). The taxonomic rank of subspecies, however, has been controversial. Unambiguous criteria for recognizing subspecies do not exist. Nevertheless, many systematists consider subspecies to be geographically distinct populations, often with distinct morphologies, that interbreed with other populations of the same species at contact zones (Patten 2015; Taylor et al. 2017). Under this definition, the defining characteristic of subspecies versus species is the ability of subspecies to routinely interbreed with other members of its species. Therefore, one would expect signatures of recent, or ongoing, gene flow between subspecies of the same species. If no such signature exists, then the two subspecies would be better considered as two distinct species.

The number of subspecies per species varies considerably among taxonomic groups. Generally, terrestrial snail groups exhibiting greater conchological complexity and larger ranges contain more subspecies (Páll-Gergely et al. 2019). This bias in use of subspecies implies that the number of subspecies may not always reflect actual terrestrial snail diversity. In the case of morphologically variable species with large ranges and discontinuous habitats, recognized subspecies may warrant species-level recognition. Given that few genome-scale studies have focused on terrestrial snails (but see Razkin et al. 2016; Phillips et al. 2020; Bober et al. 2021; Bamberger et al. 2022), the implicit hypothesis that gene flow occurs among subspecies has not been adequately tested in most cases.

One terrestrial snail species that warrants closer scrutiny to assess the validity of subspecies and inform conservation is *Patera clarkii* (I Lea, 1858). Currently, two subspecies are recognized: *Patera c. clarkii* and *Patera c. nantahala* (Clench & Banks,

1932), the latter of which is a federally listed subspecies under the U.S. Endangered Species Act (Greenwalt 1978). *Patera c. clarkii* is distributed in the southern Appalachian Mountains in northwestern Georgia, western North Carolina, and eastern Tennessee, USA (Fig. 1; Pilsbry 1940). *Patera c. nantahala*, the Noonday Globe Snail, inhabits a much smaller range, occupying approximately 3.3 km^2 on the southeast slope, facing northwest, of the Nantahala Gorge in North Carolina (Fig. 1; Clench and Banks 1932; Van Devender 1984). Clench and Banks (1932) originally described *P. c. nantahala* as a distinct species in the genus *Polygyra* Say, 1818, but Pilsbry (1940) recognized *nantahala* at the rank of subspecies, within *Mesodon clarkii*, based on shell morphology. Emberton (1991) elevated *Patera* Albers, 1850 from *Mesodon* Férussac, 1821 and included *P. clarkii* in *Patera*. Emberton (1995) appeared to consider *P. c. nantahala* a valid subspecies when briefly discussing the listing status of polygyrids under the U.S. Endangered Species Act, but subspecies were not included in his list of species. Perez et al. (2014) was the first molecular phylogenetic study to infer that *Patera* species in the subgenus *Patera*, which includes *Patera clarkii* (Emberton 1995), are monophyletic. However, no molecular study has assessed the status of *P. c. nantahala*.

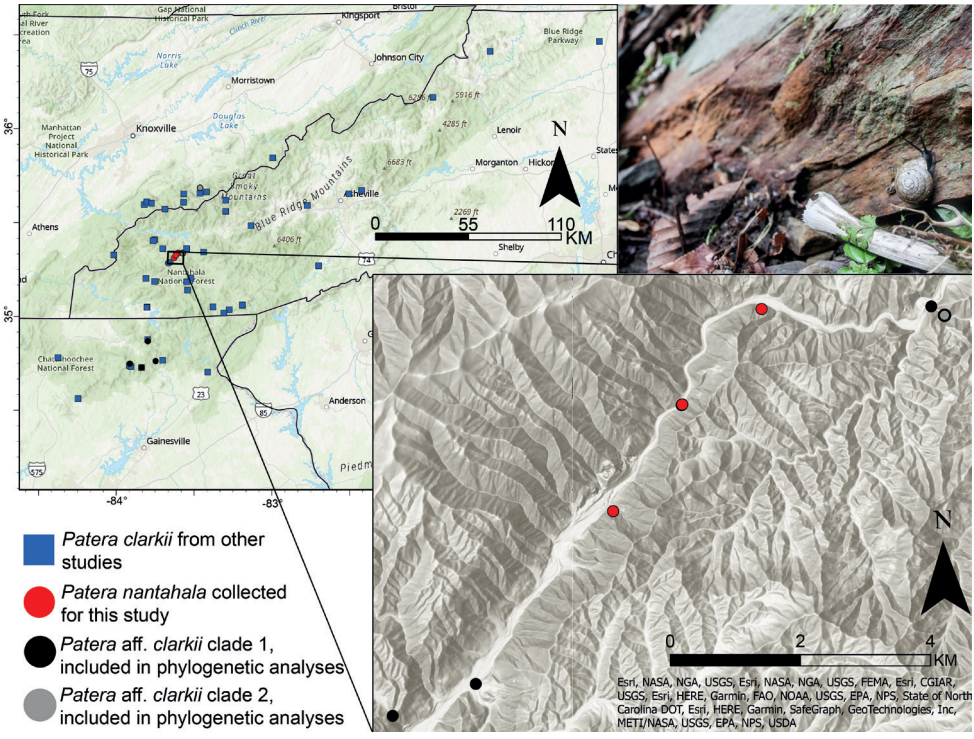

Figure 1. Map of records used for environmental niche modeling and phylogenetic analyses. Inset: Records collected here and included in molecular analyses. Only samples collected from locations in the inset were used for 3RAD analyses. Top right: photograph of *P. nantahala* in its natural habitat. Photograph by Gary Peeples (USFWS).

Aside from morphological and range information from the original species description and museum records, little is known about *P. c. nantahala*. Based on the type specimens, *P. c. nantahala* has a larger shell diameter and a more depressed spire in relation to overall shell size (Fig. 2) than *P. c. clarkii*. *Patera c. nantahala* also has a smaller parietal tooth and a less pronounced denticle on the baso-palatal wall of the aperture. *Patera c. nantahala* inhabits heavily forested calcareous rocks that receive little daylight because of the Nantahala Gorge's slope and position (Fig. 1), making its habitat unique from that of geographically proximate locations where *P. c. clarkii* is found. *Patera c. nantahala* was listed as threatened under the U.S. Endangered Species Act because of its extremely restricted range and concerns about potential habitat destruction from a proposed highway project (Greenwalt 1978). Currently, there are no plans to move forward with the highway project (Mays 2021), but *P. c. nantahala* relies on moist, shaded habitats that could be damaged by impacts to forest canopy such as wildfire, invasive species, and drought. For example, *P.c. nantahala* appeared to decrease in abundance after a prolonged drought in 2007–2009 (Mays 2021).

Objective morphological and phylogenetic analyses are needed to evaluate taxonomic hypotheses (Nekola and Horsák 2022). However, with so few data available, the taxonomic status of *P. c. nantahala* remains untested and its phylogenetic placement uncertain. Here, we generated mitochondrial and nuclear genomic datasets for *P. c. clarkii*, *P. c. nantahala*, an intermediate form, and the outgroup *P. perigrapta* (Pilsbry, 1894) to assess relationships among lineages and to test for evidence of gene flow. We also investigated morphological and environmental niche overlap between putative *P. clarkii* subspecies. Molecular results, in combination with habitat and morphological information, form the basis for proposed taxonomic revisions that better reflect diversity in *Patera* and will result in improved conservation focus.

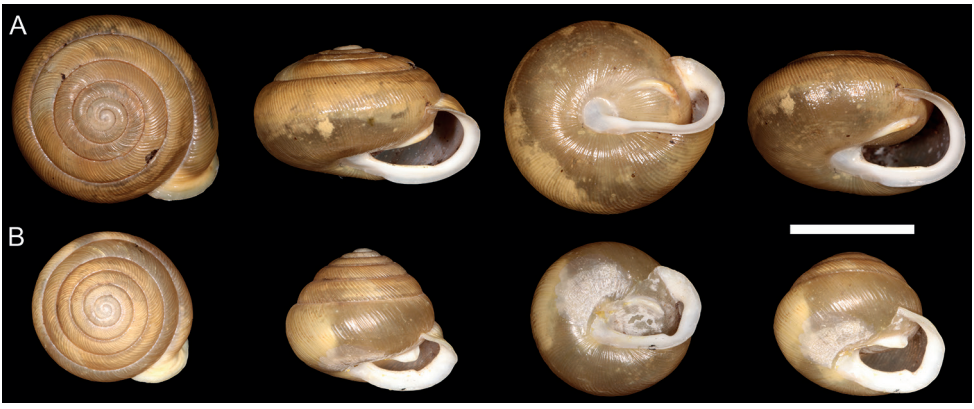

Figure 2. Photographs of type specimens **A** holotype of *Patera nantahala*, MCZ 86429 **B** syntype of *Patera clarkii*, MCZ 93923. Scale bar: 1 cm.

Materials and methods

Taxon sampling and morphological documentation

Patera c. clarkii, *P. c. nantahala*, and *P. perigrapta* were collected from eastern North Carolina in the Nantahala National Forest (Table 1; Figs 1, 3, 4). Collections included one individual with a morphology intermediate between the type specimens of *P. c. clarkii* and *P. c. nantahala* that we initially hypothesized was a hybrid between the two putative subspecies (Fig. 4D; individual "*P.* aff. *clarkii* 008"). Sampling locations were chosen strategically as likely contact zones, making the taxon sampling of this study well-suited to test the taxonomic status of the two subspecies. Individuals were placed in 95% ethanol in the field. A ~ 3 mm^3 tissue clip was taken from each individual for DNA extraction, and some shells had to be cracked to access the tissue. All shells were photographed. The shell vouchers for all sequenced individuals have been deposited at the National Museum of Natural History (Table 1).

Table 1. Collection localities, molecular data accession numbers, and museum catalog numbers of individuals collected in this study.

Individual	Collection Location	GPS Coordinates	USNM ###	GenBank ## (COI, H3, 28S)	SRA ##
Patera aff. *clarkii* 001	Winding Stairs next to Queens Creek	35.285, -83.668	1522402	OQ617117, OQ628057, OQ628452	SRX19664328
Patera aff. *clarkii* 002	Winding Stairs next to Queens Creek	35.285, -83.668	1522403	OQ617115, OQ628064, OQ628453	SRX19664327
Patera aff. *clarkii* 003	Winding Stairs next to Queens Creek	35.285, -83.668	1522404	OQ617116, OQ628063, OQ628454	SRX19664326
Patera aff. *clarkii* 004	Adjacent to Wesser Creek and Nantahala River	35.334, -83.654	1522405	OQ617118, OQ628065, OQ628455	SRX19664325
Patera aff. *clarkii* 005	Adjacent to Handpole Branch	35.281, -83.682	1522406	OQ617119, OQ628058, OQ628456	SRX19664324
Patera aff. *clarkii* 006	Adjacent to Handpole Branch	35.281, -83.682	1522407	————, OQ628059, OQ628457	SRX19664323
Patera aff. *clarkii* 007	Adjacent to Handpole Branch	35.281, -83.682	1522408	OQ617120, OQ628060, OQ628458	SRX19664322
Patera nantahala 001	Southeast Cliff of Nantahala Gorge	35.308, -83.644	1522409	OQ617122, OQ628062, OQ628460	SRX19664333
Patera nantahala 002	Southeast Cliff of Nantahala Gorge	35.308, -83.644	1522410	OQ617123, OQ628056, OQ628461	SRX19664332
Patera nantahala 003	Northeast corner of Nantahala Gorge	35.336, -83.620	1522411	OQ617124, OQ628055, OQ628462	SRX19664329
Patera perigrapta 001	Winding Stairs next to Queens Creek	35.285, -83.668	1522398	OQ617112, OQ628052, OQ628463	SRX19664334
Patera perigrapta 002	Adjacent to Wesser Creek	35.333, -83.587	1522399	OQ617114, OQ628053, OQ628464	SRX19664330
Patera perigrapta 003	Wayah Road, Nantahala	35.257, -83.656	1522400	OQ617113, OQ628054, OQ628465	————
Patera aff. *clarkii* 008	Adjacent to Wesser Creek	35.333, -83.587	1522401	OQ617121, OQ628061, OQ628459	SRX19664331

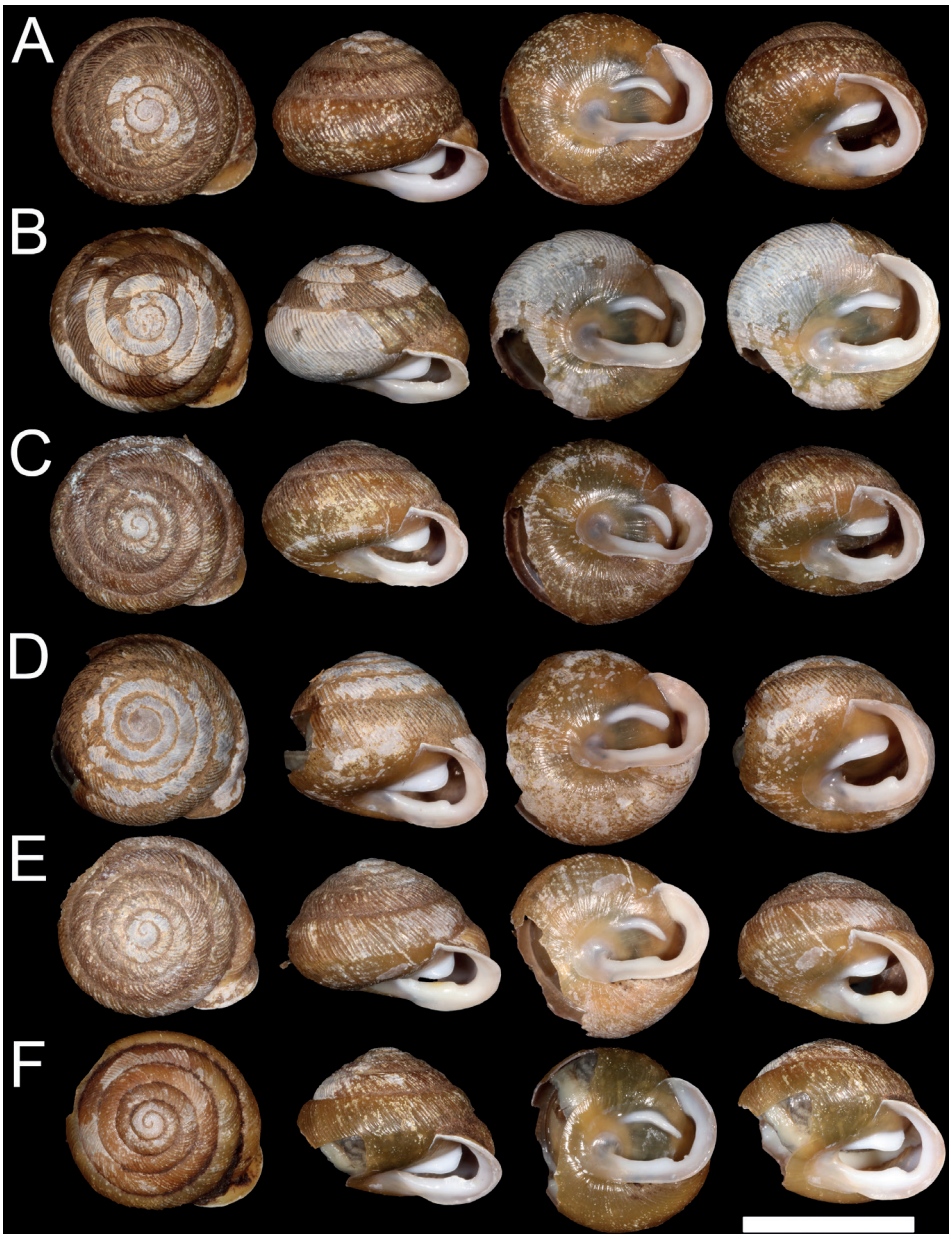

Figure 3. Shell morphology of *Patera* aff. *clarkii* from Clade 1 **A** *P.* aff. *clarkii* 001, USNM 1522402 **B** *P.* aff. *clarkii* 002, USNM 1522403 **C** *P.* aff. *clarkii* 003, USNM 1522404 **D** *P.* aff. *clarkii* 005, USNM 1522406 **E** *P.* aff. *clarkii* 006, USNM 1522407 **F** *P.* aff. *clarkii* 007, USNM 1522408.

We also obtained loans of type material and other *Patera clarkii* ssp. lots from three major natural history collections: Harvard Museum of Comparative Zoology, the Academy of Natural Sciences Philadelphia, and the National Museum of Natural History (Suppl. material 1). Subspecies identification was based on collector identification,

Figure 4. Shell morphology of *P. nantahala* and *P.* aff. *clarkii* from Clade 2 **A** *P. nantahala* 001, USNM 1522409 **B** *P. nantahala* 002, USNM 1522410 **C** *P. nantahala* 003, USNM 1522411 **D** *P.* aff. *clarkii* 008, USNM 1522401.

location of collection, and comparisons to type material. Institutional abbreviations used in the text are:

MCZ Harvard Museum of Comparative Zoology;
ANSP Academy of Natural Sciences Philadelphia;
USNM National Museum of Natural History.

For mitochondrial analyses (see below), we obtained sequences of *Patera* and other Polygyridae from Perez et al. (2014: fig. 1). Sequences were obtained directly from the authors as the data were not available on GenBank. No other sequences for *Patera* were publicly available at the time of this study.

Genetic data generation

DNA was extracted from tissue clips with the Qiagen DNeasy Plant Mini Kit using a slight modification to incorporate a proteinase K tissue digestion step. A plant kit

was used because it handles mucopolysaccharides in snail tissue better than standard animal kits (Whelan et al. 2019). DNA was quantified on a Qubit fluorometer. An aliquot was taken from each DNA extraction and diluted to 20 ng/μL.

Three genes were targeted for Sanger sequencing: 1) mitochondrial cytochrome *c* oxidase I, 2) nuclear 28S rRNA, and 3) nuclear Histone H3. PCR amplification for COI used primers dgLCO-1490 (5' GGTCAACAAATCATAAAGAYATYGG 3') and dgHCO-2198 (5'TAAACTTCAGGGTGACCAAARAAYCA 3') (Meyer 2003). Reactions occurred in 25 μL volumes consisting of 5 μL 5× GoTaq Flexi Buffer (Promega), 2.5 μL $MgCl_2$ (25 mM), 1 μL of each primer (10 μM), 1 μL dNTP solution (10 mM), 0.1 U GoTaq DNA polymerase (Promega), and 20 ng whole genomic DNA. PCR cycling used an initial denaturation at 94 °C for 2 min; 35 cycles of 94 °C for 30 s, 45 °C for 30 s, 72 °C for 1 min; and a final extension at 72 °C for 5 mins. PCR amplification for 28S used primers 28S-VI (5' AAGGTAGCCAAATGCCTCATC-3') and 28S-X (5'-GTGAATTCTGCTTCATCAATGTAGGAAGAGCC-3') (Hillis and Dixon 1991). Reactions occurred in 25 μL volumes consisting of 5 μL GoTaq Flexi Buffer, 2.5 μL $MgCl_2$ (25 mM), 1 μL each primer (10 μM), 1 μL dNTPs (10 μM), 0.1 U GoTaq DNA polymerase, and 10 ng genomic DNA. PCR for 28S cycling used an initial denaturation at 94 °C for 2 min; 30 cycles of 94 °C for 30 s, 50 °C for 30 s, 72 °C for 30 s; and a final extension at 72 °C for 5 mins. PCR for H3 used primers H3F (5'-ATGGCTCGTACCAAGCAGACVGC-3') and H3R (5'-ATATCCTTRGGCATR ATRGTGAC-3') (Colgan et al. 1999), and the same reaction chemistry as 28S. H3 PCR cycling used initial denaturation at 94 °C for 2 min; 30 cycles of 94 °C for 30 s, 55 °C for 30 s, 72 °C for 30 s; and a final extension at 72 °C for 5 mins. Raw PCR products were purified using the New England Biolabs Monarch PCR & DNA cleanup kit following manufacturer's protocol. Cleaned PCR products were sent to GeneWiz for Sanger sequencing in both directions using the same primers as used in PCR reactions.

After finding a lack of variation in nuclear genes (see results), we generated a genome-scale dataset for two individuals of *P. perigrapta* and all *P. clarkii* sensu lato (s.l.) that we successfully Sanger sequenced. To do this, we used the "3RAD" restriction site associated DNA sequencing reduced representation sequencing approach (RAD-seq; Bayona-Vásquez et al. 2019). 3RAD has advantages over other RAD-seq approaches by reducing adapter-dimer formation, allowing incorporation of a random 8 bp Illumina i5 index for removing PCR duplicates during assembly, and using a sequencing strategy (2 × 150 paired-end) that results in 200 bp, or greater, contigs. The long contigs generated with 3RAD, compared to some other RADseq approaches (e.g., 2bRAD; Wang et al. 2012), are particularly useful for phylogenetics. We followed the original 3RAD protocol with slight modification (full protocol available from https://github.com/NathanWhelan/3RAD_protocols/). The digestion step used restriction enzymes NheI, EcoRI, and XbaI. *Patera* libraries were combined with samples from other studies that had unique barcodes, resulting in 192 libraries that were sequenced at the University of Oregon Genomics and Cell Characterization Core facility on an Illumina NovaSeq 6000 using an SP flow cell with 2 × 150 paired-end sequencing chemistry.

Molecular data analyses

Raw Sanger sequencing chromatograms were visualized in Geneious Prime and checked for sequencing errors. For the two nuclear genes, sites with two chromatogram peaks of equal intensity on both the forward and reverse sequences were coded as heterozygous using standard IUPAC codes. Each gene was aligned with Clustal Omega 1.2.2 (Sievers et al. 2011). All 28S sequences were identical, so 28S was not used in phylogenetic analyses. We inferred a COI mitochondrial gene tree and an H3 nuclear gene tree separately. First, the best-fit substitution models and partitions were identified with ModelFinder using the Bayesian information criterion (BIC) (Kalyaanamoorthy et al. 2017) as implemented in IQTREE 1.6.12 (Nguyen et al. 2015); codon positions were used as starting blocks. Maximum likelihood tree inference was then done in IQTREE using best-fit models and partitions. Tree search used default parameters, except perturbation strength was set to 0.2 and number of unsuccessful steps to stop tree inference was set to 500. Support was measured with 1,000 ultrafast bootstrap replicates (Hoang et al. 2018). Average pairwise distances among *P. clarkii* s.l. clades were calculated in MEGAX 10.2.6 (Kumar et al. 2019).

An automatic species delimitation approach was used to generate species-level taxonomic hypotheses. For this, we used COI data with Assemble Species by Automatic Partitioning (ASAP; Puillandre et al. 2021). ASAP has improved performance and less subjectivity in choosing delimitation schemes than its predecessor, the widely used Automatic Barcode Gap Discovery method (ABGD; Puillandre et al. 2012). ASAP was chosen over other methods because ABGD was previously shown to work well compared to other methods on gastropods with low dispersal ability (Strong and Whelan 2019). We also chose to use ASAP because it is not based on the coalescent model, and methods that use the coalescent tend to over split species (Sukumaran and Knowles 2017; Strong and Whelan 2019). For ASAP, the COI dataset was trimmed of outgroups to only include *P. c. clarkii* and *P. c. nantahala*. First, the best fit model for the trimmed dataset was inferred with ModelFinder in IQ-TREE. Second, we calculated best-fit model maximum likelihood distances among individuals with PAUP* 4.0a build 169 (https://paup.phylosolutions.com) using model parameters inferred by ModelFinder. Finally, ASAP analyses were performed with the ASAP web server (https://bioinfo.mnhn.fr/abi/public/asap/) using maximum likelihood distances.

Raw 3RAD sequence data were demultiplexed into individual libraries with the STACKS 2.53 script process_radtags (Rochette et al. 2019). One mismatch per barcode was allowed. Reads that lacked restriction enzyme sites were discarded. After demultiplexing, PCR clones in each library were removed using the STACKS script clone_filter. PCR clones were identified with the random sequence i5 index used during library preparation.

After demultiplexing and clone filtering, data were assembled using the STACKS denovo_map.pl pipeline. We first used the method described by Paris et al. (2017) to identify appropriate assembly parameters. The best parameters for our data were determined to be a minimum stack depth of three (-m 3), five mismatches allowed between

stacks within individuals (-M 5), and five mismatches allowed between stacks among individuals (-n 5). Contigs were assembled by denovo_map using paired-end information. All other assembly parameters were set to default. After assembly, the STACKS program populations was used for final data filtering. To pass filters, loci had to be present in 100% of individuals, have a minimum minor allele frequency of 0.025, and have an observed heterozygosity frequency of no more than 0.5. These parameters were chosen to eliminate missing data and filter potential paralogs or sequencing errors. All SNPs per locus were retained. Processed data were output into various file formats by STACKS for downstream analyses.

Some contigs, or RAD loci, did not have overlapping reads because the locus was longer than 300 bp, which STACKS represented as a string of Ns. These were removed prior to phylogenetic analyses with the custom script noGaps-nucleotides.sh. Maximum likelihood gene trees were inferred for each RAD locus with IQTREE. ModelFinder, as implemented in IQTREE, was used for substitution testing using the BIC; partition finding was not done because RAD loci are unlikely to be found only in exons. Tree inference and bootstrapping for RAD loci were the same as for Sanger sequenced genes.

ASTRAL III (Zhang et al. 2018) and the RAD-loci nuclear gene trees were used to infer a species tree. This method uses the multispecies coalescent to resolve gene tree conflict and assumes that all gene tree discordance is a result of incomplete lineage sorting (Rannala and Yang 2003). Prior to using the inferred maximum likelihood trees of each gene for species tree inference, all branches with 10% ultrafast bootstrap support or less were collapsed with Newick Utilities (Junier and Zdobnov 2010). Collapsed maximum likelihood trees for each gene and default parameters were used as ASTRAL input. Individuals were not assigned a priori taxon designations. Support was measured with local posterior probability (Sayyari and Mirarab 2016).

Given that focal taxa were putative subspecies where some gene flow is expected, introgression is a potential cause of gene tree discordance (Maddison 1997). To test for a signal of introgression, we used the phylogenetic network method SNAQ (Solís-Lemus and Ané 2016) implemented in PhyloNetworks (Solís-Lemus et al. 2017). Unlike implicit network approaches that visualize discordance (e.g., SplitsTree; Huson and Bryant 2006), networks inferred with SNAQ can represent explicit reticulation events and all nodes represent ancestors (Solís-Lemus and Ané 2016). SNAQ is also an appropriate method for the current taxon sampling as genome-wide markers, combined with a network approach, allows estimating gene flow across the evolutionary history of a lineage. Maximum likelihood trees used for ASTRAL input were used in SNAQ to calculate concordance factors, and the ASTRAL species tree was used as the starting tree. Five separate networks that allowed for 0–4 reticulations (h), respectively, were inferred with ten replicates each. The best-fitting number of reticulations was assessed by examining the log pseudolikelihood profile of h, following Solís-Lemus and Ané (2016). Inferred networks that conflicted with the outgroup position of *P. perigrapta* were discarded, and we instead retained the network for each h with the highest log pseudolikelihood value that did not conflict with root position. Goodness-of-fit of

each network was also examined by plotting observed concordance factors versus expected concordance factors for each network. The R package ggplot2 (Wickham 2009) was used for plotting.

Morphological analyses

All shell vouchers for molecular samples and most shells obtained from museum collections were used to assess morphological similarity between *P. c. nantahala* and *P. c. clarkii* via geometric morphometrics (Suppl. material 1). We used a maximum of four shells per museum lot; shells with damage in areas important for assigning landmarks were also excluded. Shells were photographed in apertural view with the axis of coiling parallel to the camera sensor (Fig. 5). Photographs were taken on a Canon E0S 80D with a 100 mm f/2.8 macro lens. Photographs of a ruler at the same scale as the shell photographs were also taken so we could test differences in shell size in addition to shape.

We used tpsUtil version 1.82 (Rohlf 2021a) to convert photographs to tps file format. Photographs were reordered randomly to limit landmark placement biases systematically affecting samples from the same lot. tpsDig2 version 2.32 (Rohlf 2021b) was used to place 12 landmarks on each shell (Fig. 5). Landmarks were chosen based on inferred ability to consistently place them in homologous positions.

Geometric morphometric analyses were conducted in MorphoJ (Klingenberg 2011). First, a Procrustes fit was applied to the dataset to account for differences in shell size,

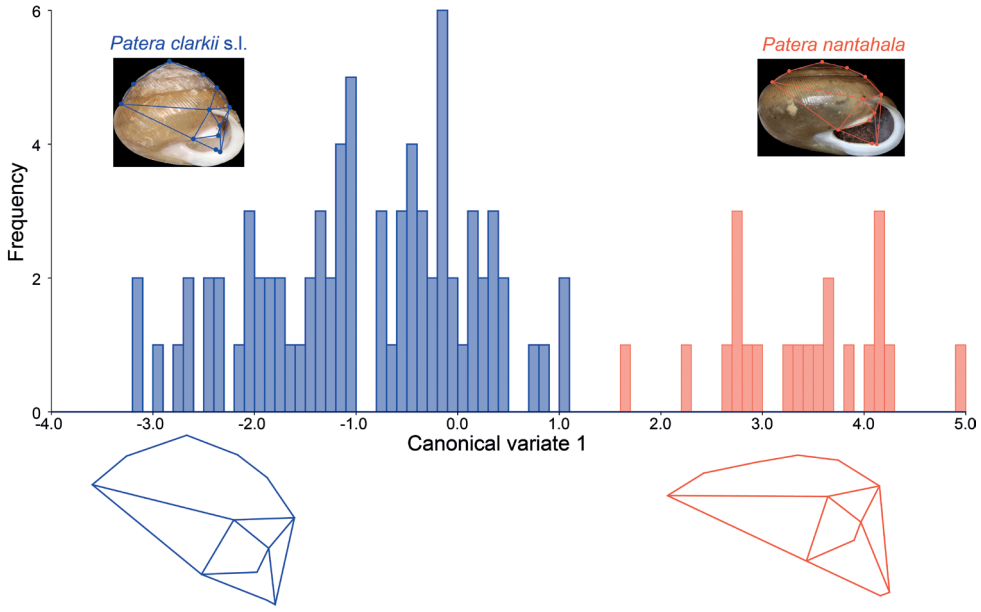

Figure 5. Landmarks used for geometric morphometrics and history of canonical variate scores. Shells are type specimens and points represent landmarks connected by wireframe that shows shape variation. Wireframe graphs under CVA plots represent extremes and show shape changes associated with canonical variates.

position, and image rotation. Correct landmark digitization and the presence of outliers were checked by eye for all samples using Mahalanobis distance (Klingenberg and Monteiro 2005), which was inferred by MorphoJ to be more appropriate than Squared Procrustes distance for our dataset. Incorrect digitization of landmarks was corrected via the "Swap Landmark" command when the deviation from the average of any two landmarks on the same shell clearly pointed at each other (see MorphoJ manual for more details).

Differences in shape were measured using two statistical tests. First, a Procrustes ANOVA was performed to test for significant differences in shape between the two putative subspecies. Then, a canonical variate analysis (CVA) was performed in MorphoJ to visualize shape differences and further assess evidence for shape differences between *P. c. clarkii* and *P. c. nantahala*. For the CVA, a permutation test of pairwise distances between putative subspecies was performed to test for significance using 1,000 iterations per comparison. Wireframe graphs were plotted to visualize morphological variation along the CVA axis. A Procrustes ANOVA was also performed to test for significant differences in centroid size, which is a measure of shell size.

Environmental niche modeling

Patera c. nantahala is an ideal taxon for examining the utility and accuracy of environmental niche models because its range is extremely restricted and well defined. We also wanted to quantify potential environmental niche overlap between *P. c. clarkii* and *P. c. nantahala*. First, we downloaded collection records of *P. clarkii* from the Global Biodiversity Information Facility (GBIF) that had latitude and longitude information (GBIF.org 2022). One record of *P. c. clarkii* from New Jersey was removed from the downloaded dataset (GBIF.org 2022) as *P. clarkii* is not known to occur north of North Carolina (Hubricht 1985). A GBIF record of *P. c. nantahala* from iNaturalist was also removed because the precise location was obscured reflecting the species' threatened status. Records from Perez et al. (2014) and our own collections were added to those downloaded from GBIF (Fig. 1). Perez et al. (2014) did not provide latitude and longitude, so we determined reported locations based on their descriptions and coordinates determined from Google Earth. To reduce potential biases associated with spatial autocorrelation of species records, we spatially rarefied locality records at a distance of 1 km with SDMtoolbox 2.0 (Brown et al. 2017) in ESRI ArcGIS Pro; 1 km was chosen given the small distance between *P. c. nantahala* records.

Continuous environmental variables that covered the spatial extent of collection records (Fig. 1) were downloaded from publicly available sources as raster files. Bioclimatic data from WorldClim (Fick and Hijmans 2017) were downloaded at 30 second resolution with the R package raster (Hijmans 2022). Erodibility and albedo raster files were downloaded from the USA Soils dataset (SSURGO; Soil Survey Staff 2022) via ESRI ArcGIS Living Atlas of the World at 30-meter resolution. Categorical soil map unit data were also downloaded from SSURGO to examine differences in habitat, but categorical data were not included in environmental niche models. Forest canopy cover (i.e., proportion of floor covered by vertical projection of tree crowns), forest canopy

base height (i.e., average height to the top of tree canopy), vegetation height (i.e., vertically projected cover of live plants), and vegetation cover (i.e., average height of dominant vegetation) were downloaded at 30-meter resolution from LANDFIRE version LF 2016 Remap (LANDFIRE 2020). Elevation data were downloaded from The National Map at 1/3 arc-second resolution (U.S. Geological Survey 2020); elevation data at 1/3 arc-second resolution were only available as multiple raster files across the study extent, so raster files were combined in ESRI ArcGIS Pro using the "Mosaic to Layer" tool. Slope and aspect data were created from the elevation data in ArcGIS Pro using the "Slope" and "Aspect" tools, respectively. Environmental data used in niche modeling were chosen to represent potentially unique features of the Nantahala Gorge and its habitat (e.g., steep slope, soil type, vegetation, and limited sunlight).

Environmental data raster files were trimmed to cover the area where samples were collected (Fig. 1) in ArcGIS Pro and bicubic resampling was used to ensure each raster had the same cell size of 0.0005. Data were resampled to a cell size of 0.0005 to balance processing speed and resolution of taxa whose records were sometimes barely more than 1 km apart. For data with the USGS version of USA Contiguous Albers Equal Area Conic as their native projection, we used ArcGIS pro to reproject to the World Geodetic System 1984 projection. After data transformation, all data raster files were exported from ArcGIS Pro as .tif files for use in R. Data points of "NA" were changed to "0" because some datasets (e.g., LANDFIRE) coded water bodies as NA, rather than 0.

Raster files were loaded into R with the "raster" command of the package raster and stacked into a single variable. Correlation of the different environmental data layers was assessed on *P. c. clarkii* collection records with "raster.cor.matrix" and "raster.cor.plot" commands of the R package ENMTools (Warren et al. 2021). Correlated variables were determined with only the *P. c. clarkii* dataset because there were considerably more records for *P. c. clarkii* than *P. c. nantahala*. We removed all but one of any given environmental layer that had high correlation with other layers (Pearson correlation coefficient > 0.70; see Table 2 for variables used in final datasets). To examine effects of performing niche modeling using bioclimatic data such as temperature and precipitation versus geographical and biotic data such as elevation and vegetation cover, we created three datasets: 1) all variables; 2) only bioclimatic data; 3) biotic, geological, and geographic (Table 2).

Environmental niche models, sometimes referred to as species distribution models, of *P. c. clarkii* and *P. c. nantahala* were generated with the R package ENMTools 1.0 (Warren et al. 2021). For each taxon, niche models were generated with all three datasets using Maxent and the generalized linear model (GLM) method in ENMTools. Relative contribution of variables to each model was determined by model-specific variable importance analysis with the command "enmtools.vip" and the "permute" method in ENMTools. Niche models and variable importance plots were plotted in R. We used the "identity.test" function of ENMTools to test whether the niche of each putative subspecies was significantly different. Tests were done with 100 replicates and 10,000 background points. The niche overlap metrics D (Schoener 1968) and I (Warren et al. 2018) were used in significance tests with a critical value of 0.05.

Table 2. Data used for environmental niche modeling.

Data Source	Environmental Layer	Data type	Characteristics
WorldClim	BIO1	Bioclimatic	Annual mean temperature
WorldClim	BIO2	Bioclimatic	Mean diurnal range
WorldClim	BIO3	Bioclimatic	Isothermality
WorldClim	BIO4	Bioclimatic	Temperature seasonality
WorldClim	BIO7	Bioclimatic	Temperature annual range
WorldClim	BIO8	Bioclimatic	Mean temperature of wettest quarter
WorldClim	BIO9	Bioclimatic	Mean temperature of driest quarter
WorldClim	BIO12	Bioclimatic	Annual precipitation
WorldClim	BIO15	Bioclimatic	Precipitation seasonality
SSURGO	erodibility	Geological	Susceptibility of soils to erosion
SSURGO	albedo	Geological	Reflective property of surface
LANDFIRE	LC20_CC_200	Biotic	Forest canopy cover
LANDFIRE	LC20_CBH_200	Biotic	Forest canopy base height
LANDFIRE	LC16_EVH_200	Biotic	Existing vegetation height
LANDFIRE	LC16_EVC_200	Biotic	Existing vegetation cover
The National Map	Elevation	Geographical	Elevation from sea level
Calculated from Elevation Layer	Slope	Geographical	Slope of surface
Calculated from Elevation Layer	Aspect	Geographical	Direction land faces

Data and code availability

All scripts are available from https://github.com/nathanwhelan/Patera. STACKS output, alignments, COI distance matrix, tree files, SNAQ input and output, shell photographs, and environmental data raster files are available on FigShare https://doi.org/10.6084/m9.figshare.19638642. Demultiplexed and decloned 3RAD data are available from NCBI SRA BioProject PRJNA944142.

Results

Molecular analyses

Sanger sequencing for all three genes was successful for three *P. perigrapta* individuals, six *P. c. clarkii*, three *P. c. nantahala*, and one potential hybrid individual with an intermediate morphology (i.e., *P.* aff. *clarkii* 008; Fig. 4D; Table 1). We were able to successfully sequence nuclear genes, but not COI, for one additional *P. c. clarkii* individual. For 3RAD sequencing, after demultiplexing and clone filtering, the number of raw paired-end reads per individual ranged from 256,990 to 1,899,741 (average = 1,018,463). After filtering, 2,905 loci were retained. Loci had an average length of 273 bp, and 74.8% of loci had overlapping read pairs. The number of SNPs per locus ranged from 1–41, with an average of 14 SNPs per locus.

The COI tree had greater taxon sampling than other analyses because only COI data were available for *Patera* and related Polygyridae from previous studies. Generally, deep divergences were inferred within putative species and multiple species were not monophyletic (Fig. 6). This could be the result of misidentifications, taxonomy in need

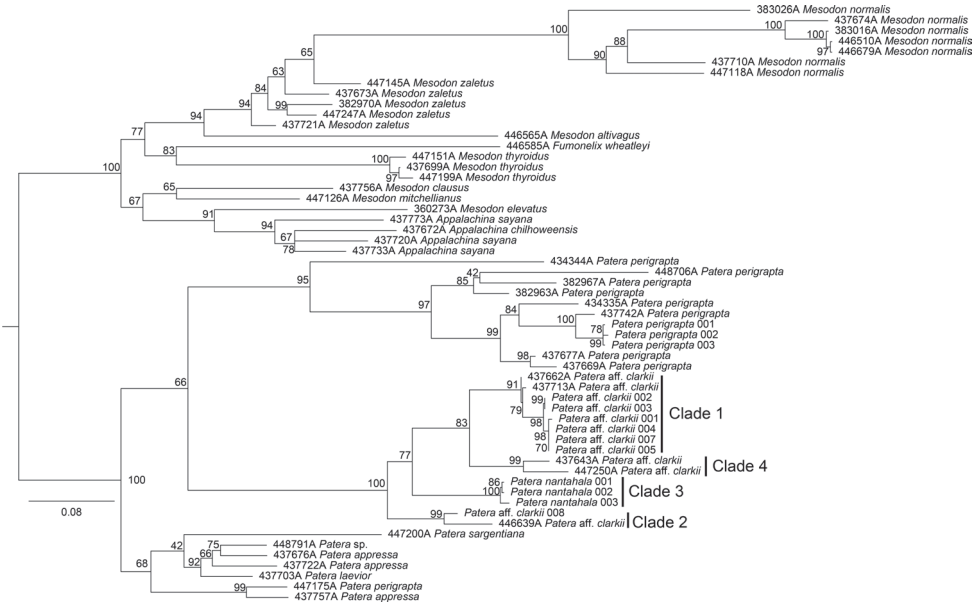

Figure 6. COI maximum likelihood tree. Branches are labelled with ultrafast bootstrap support. Clades within *P. clarkii* s.l. are labelled with numbers referred to in the main text. Scale is in substitutions per site.

of revision, or more likely both. One individual of "*P. perigrapta*", (447175A) that was sequenced by Perez et al. (2014), was placed sister to an individual of *Patera appressa* (Say, 1821), indicating that 447175A was most likely misidentified.

Patera clarkii s.l. was recovered in four main clades on the COI tree, all of which had ultrafast bootstrap support greater than 90 (see labels on Fig. 6). All sequenced individuals that we initially identified as *P. c. clarkii* (i.e., excluding the possible hybrid), were in a clade with two individuals sequenced by Perez et al. (2014) that were collected from northern Georgia (Clade 1, Fig. 6). This clade was sister to two additional *P. c. clarkii* individuals from Perez et al. (2014) that were also collected in northern Georgia (Clade 4, Fig. 6). Clade 3 contained three *P. c. nantahala* individuals and was sister to Clades 1 and 4 (Fig. 6). The sister clade to all other *P. clarkii* s.l. contained the individual that we initially hypothesized to be a hybrid (individual *P.* aff. *clarkii* 008) and an individual from eastern Tennessee that was identified as *P. clarkii* by Perez et al. (2014; Clade 2, Fig. 6). The "aff." epithet is used hereafter because both "*P. c. clarkii*" lineages resemble the type, but we are unable to determine which lineage, if either, is true *P. c. clarkii* (see below). Relationships among the four clades within *P. clarkii* s.l. had limited support on the COI gene tree. However, pairwise distances among *P. clarkii* s.l. clades were high, ranging from 9.3%–12.5%. Automatic species delimitation analysis with ASAP indicated the presence of four putative species, corresponding to the four main clades of *P. clarkii* s.l. on the COI tree (Fig. 6).

In contrast to the COI tree, there was virtually no resolution on the H3 gene tree as no node had greater than 89% ultrafast bootstrap support (Fig. 7). Two *P. c. nantahala* individuals had a private H3 allele and were sister to each other on a long branch

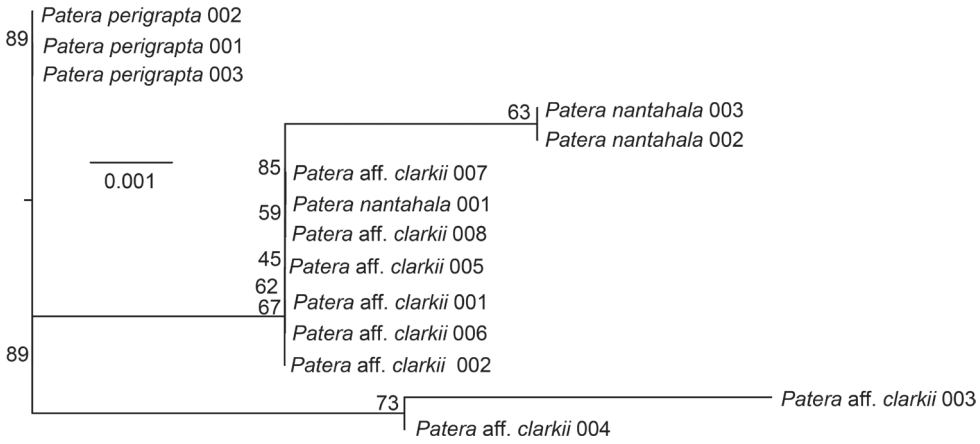

Figure 7. H3 maximum likelihood tree. Branches are labelled with ultrafast bootstrap support. Scale is in substitutions per site.

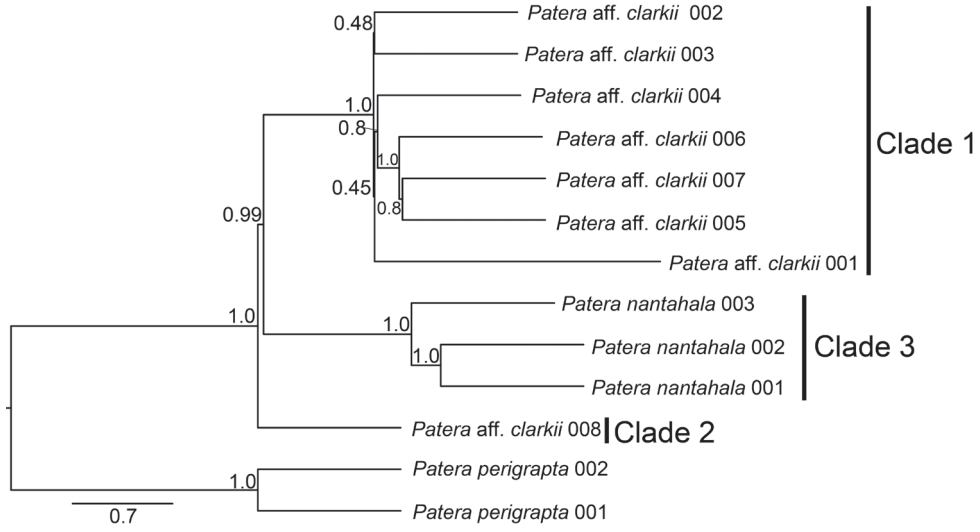

Figure 8. ASTRAL species tree. Branches are labelled with local posterior probability. Clades are labelled with numbers referred to in the main text. Scale is in coalescent units.

within a clade consisting of most *P. clarkii* s.l. individuals. Two *P. c. clarkii* individuals were sister to all other *P. clarkii* s.l. All individuals that we sequenced had the same 28S sequence, including the three *P. perigrapta* individuals that served as outgroups.

Three *P. clarkii* s.l. clades were resolved on the ASTRAL species tree, each having 100% local posterior probability (Fig. 8). The absence of a clade on the ASTRAL tree corresponding to Clade 4 on the COI tree was likely a result of the two Clade-4 individuals from Perez at al. (2014) not being available for genome-based ASTRAL analysis. ASTRAL clades were given designations 1, 2, and 3 to match those on the

COI tree and distinguish between the two *P.* aff. *c. clarkii* lineages and *P. c. nantahala*. The clade with the individual initially identified as a possible hybrid between *P. c. clarkii* and *P. c. nantahala* (i.e., individual *P.* aff. *clarkii* 008) was placed in "Clade 2", whereas other *P. c. clarkii* were placed in "Clade 1". Relationships among clades on the ASTRAL species tree were congruent with the COI mitochondrial gene tree (Figs 5, 8), albeit without individuals from Perez et al. (2014) on the ASTRAL tree. Analyses with SNAQ indicated that the data were tree-like as the zero-reticulation model and one-reticulation model had similar pseudo log-likelihood values (Suppl. material 2: fig. S1). Expected versus observed concordance factor plots were also similar between models with no obvious outliers on the zero-reticulation model compared to the one-reticulation model (Suppl. material 2: fig. S2). The reticulation event on the one-reticulation network had a gamma value of less than 3.5 (Suppl. material 2: fig. S3). Thus, SNAQ analyses rejected our hypothesis that individual *P.* aff. *clarkii* 008 was a hybrid. SNAQ analyses also rejected recent or ongoing gene flow among *P. clarkii* s.l. clades, including among *P. c. nantahala* and the *P.* aff. *c. clarkii* clades.

Shell shape and size variation

The final morphometric dataset had 21 individuals of *P. c. nantahala* and 77 *P. c. clarkii* (Suppl. material 1). We were unable to separate the *P.* aff. *c. clarkii* lineages for geometric morphometrics because we only had sequence data for one individual from Clade 2 and geographic and morphological characters to distinguish the *P.* aff. *c. clarkii* lineages have not been documented and may not exist. This likely resulted in a greater breadth of shape for *P. c. clarkii*, thereby increasing the chance of shape overlap between *P. c. clarkii* and *P. c. nantahala*.

Geometric morphometrics confirmed what was mostly evident by eye. Procrustes ANOVA indicated a significant size and shape difference between *P. c. nantahala* and *P. c. clarkii* ($p < 0.0001$; Table 3). Canonical variate analysis indicated that 100% of shell shape variation was explained by a single axis and there was no overlap between the two subspecies (Fig. 5; Table 3). Permutation tests indicated significant differences in shell shape between *P. c. clarkii* and *P. c. nantahala* ($p < 0.0001$). *Patera c. nantahala* had a wider shell and a more compressed spire height compared to overall width (Fig. 5). The parietal tooth in *P. c. nantahala* did not protrude as far as in *P. c. clarkii* (Fig. 5).

Several qualitative morphological differences distinguish *P. c. nantahala* from *P. c. clarkii*. The denticle on the baso-palatal wall is much more prominent in *P.* aff. *c. clarkii* Clade 1 individuals (Fig. 3) and slightly more prominent in the *P.* aff. *c. clarkii* individual from Clade 2 (Fig. 4D) than in *P. c. nantahala* (Figs 2, 4A–C). Furthermore, the parietal tooth covers a larger part of the aperture in both *P.* aff. *clarkii* Clades 1 and 2 (Figs 3, 4D) compared to *P. c. nantahala* (Figs 2A, 4A–C). In two of the three sampled *P. c. nantahala* individuals, mantle pigmentation displayed a branching pattern (Fig. 4A, B), versus a horizontal band in *P. c. clarkii* clades when present (Figs 3A–D, F, 4D). However, the branching pattern does not appear to be diagnostic as it is not visible on the types (Fig. 2), nor on one individual we collected (Fig. 4C).

Table 3. Results of geometric morphometric statistical tests.

Procrustes ANOVA for Shape							
Effect	Procrustes Sum of Squares	Procrustes mean squares	degrees of freedom	Goodall's *F*	*p* (F)	Pillai's trace	*p* (Pillai's trace)
Species	0.080648	0.004032	20	11.98	< 0.0001	0.76	< 0.0001
Residual	0.646333	0.000337	1920				
Procrustes ANOVA for Centroid Size							
Effect	Procrustes Sum of Squares	Procrustes mean squares	degrees of freedom	Goodall's *F*	*p* (F)		
Species	6.258875	6.258875	1	73.29	< 0.0001		
Residual	8.19893	0.085398	96				
Canonical Variate Analysis							
Eigenvalues	% Variance	Mahalanobis distance between species	*p* (Mahalanobis distance)	Procrustes distance between species	*p* (Procrustes distance)		
3.180948	100	4.302	<0.0001	0.0699	< 0.0001		

Environmental niche models and niche overlap

After removal of several suspect records, occurrence data consisted of nine records for *P. c. nantahala* and 79 for *P. c. clarkii*. Spatial rarification of the data resulted in a reduced dataset with three records for *P. c. nantahala* records and 46 for *P. c. clarkii* (Suppl. material 1).

Environmental niche models inferred with Maxent resulted in much greater predicted suitable habitat for *P. c. nantahala* compared to GLMs, whereas models for *P. c. clarkii* were similar regardless of modeling method (Fig. 9). The relative importance of any given variable was highly dependent on the modeling approach (i.e., Maxent vs. GLM), the variables included, and whether *P. c. nantahala* or *P. c. clarkii* was being modeled (Suppl. material 2: figs S4–S15). Models inferred with only BioClim variables resulted in considerably greater predicted suitable habitat for *P. c. nantahala* than models that used all environmental variables. Similarly, models that used all variables appeared to be least likely to overpredict suitable habitat of *P. c. clarkii* based on its known range (Fig. 9). *Patera c. nantahala* only occupied locations that were classified on the SSURGO soil map units as "Inceptisols: Sylco-Cataska complex, 50 to 95 percent slopes, very rocky". Inceptisols are characterized as being from humid and subhumid regions with subsurface soil layers lacking illuviated material and without an ochric epipedon (Soil Survey Staff 1999). Some records of *P. c. clarkii* were also from locations classified as "Inceptisols: Sylco-Cataska complex, 50 to 95 percent slopes, very rocky". However, these records were separated from *P. c. nantahala* by at least one different soil type, and *P. c. clarkii* also occupied other soil types, including ultisols (i.e., soils with low base saturation and kandic or argillic horizons, generally with a vegetation of coniferous or hardwood forests) and entisols (i.e., soils with little or no evidence of layers). For more details on soil types see Soil Survey Staff (1999).

Overlap comparisons indicated significant differences in niches of *P. c. clarkii* and *P. c. nantahala* when using GLMs and datasets with non-bioclimatic variables ($p < 0.05$; Table 4). Although not statistically significant, D and I values were also low for GLMs

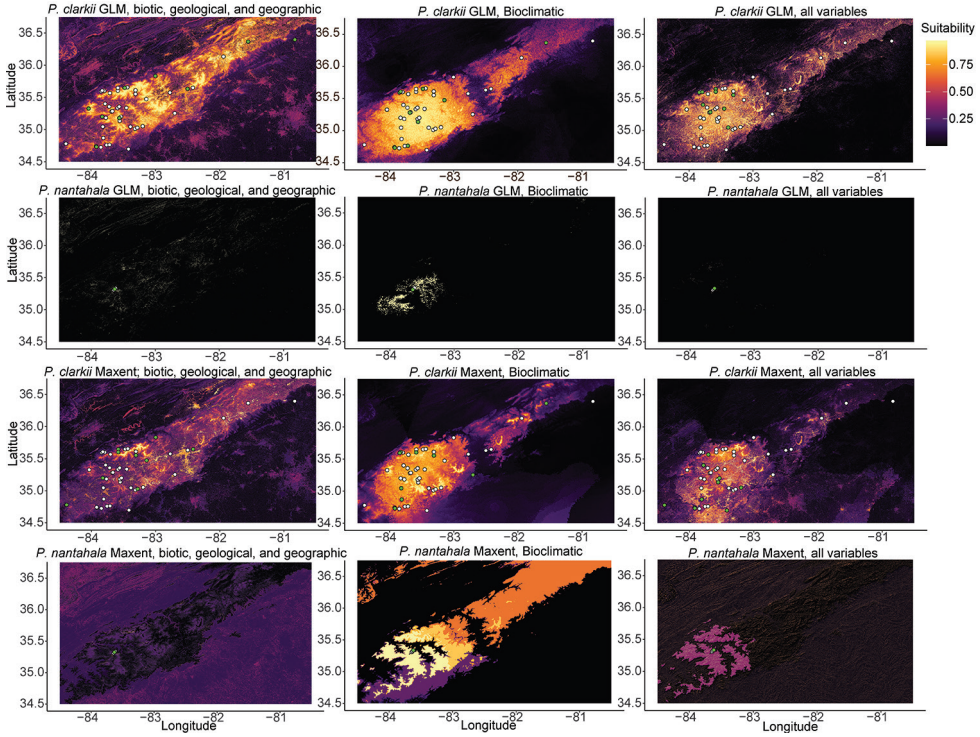

Figure 9. Environmental niche models for *P. clarkii* and *P. nantahala*. Brighter colors indicate locations with greater niche suitability.

Table 4. D and I environmental niche overlap metrics for GLM and Maxent based niche overlap tests. Bold values indicate models with significant niche differences between *P. clarkii* and *P. nantahala* at $\alpha = 0.05$.

	Non-bioclimatic variables	Bioclimatic variables	All environmental variables
GLM: D	**0.013**	0.033	**0.001**
GLM: I	**0.089**	0.166	**0.026**
Maxent: D	0.334	0.361	**0.163**
Maxent: I	0.627	0.659	0.371

with only bioclimatic variables (Table 4). Maxent models did not indicate significant differences ($p > 0.05$), except with the D statistic on the model that was generated with all environmental variables (Table 4). However, the GLM with only bioclimatic variables and all Maxent models clearly overpredicted suitable habitat for *P. c. nantahala* (Fig. 6), which is why we emphasize the significant results. The *P. c. clarkii* records included in environmental niche modeling potentially include more than one species (i.e., the multiple molecular *P. c.* aff. *clarkii* lineages from Clade 1, Clade 2, and Clade 4; Figs 3, 4D, 6), but inferred niche differences should be robust as inclusion of the multiple lineages from GBIF records of "*P. c. clarkii*" is likely to increase and homogenize predicted habitat of *P. c. clarkii*, which would have resulted in overestimating niche overlap.

Systematics

Family Polygyridae Pilsbry, 1895
Subfamily Triodopsinae Pilsbry, 1940
Tribe Mesodontini Tryon, 1866

Genus *Patera* Albers, 1850

Helix (*Patera*) Albers, 1850: 96. Type species: *Helix appressa* Say, 1821, by subsequent designation (Pilsbry 1930: 326) [non *Patera* Lesson, 1839 (Cnidaria)].

Remarks. *Patera* is a junior homonym of *Patera* Lesson, 1839 (Cnidaria). However, *Patera* Lesson, 1839 has only been used in a few treatises during the 19th century and at the beginning of the 20th century, whereas *Patera* Albers, 1850 is in widespread use. As such, continued usage of the junior homonym is in the best interest of stability and the case should be referred to the International Commission on Zoological Nomenclature for a ruling under Art. 23.9.3 of the Code (ICZN 1999).

Patera nantahala (Clench & Banks, 1932)

Polygyra (*Triodopsis*) *nantahala* Clench & Banks, 1932: 17, pl. 2, figs 1–3, 5.
Mesodon clarki nantahala–Pilsbry 1940: 731, fig. 440g; Chambers 1981: 55–59; Hubricht 1983: 13; Hubricht 1985: 44; Richardson 1986: 45.
Patera clarki nantahalae [sic]–Emberton 1995: 72.

Type material. ***Holotype*:** MCZ 86429. GS Banks leg., 27 August 1930.

***Paratypes*:** ANSP 153664 (4 spms), GS Banks leg., 25 August 1930; MCZ 82533 (1 spm), Clench, Archer & Rehder leg., 7 August 1931; MCZ 185877 (3 spms), Clench, Rehder & Archer leg., July 1931, ex. A Archer collection; USNM 408310 (3 spms), Clench, Rehder & Archer leg., 1931.

Type locality. Blowing Springs, cliff ridges, Nantahala Gorge, Swain County, North Carolina.

Other material examined. USNM 1522409, USNM 1522410: Adjacent to unnamed tributary of Nantahala River, southeast cliff of Nantahala Gorge, Swain County, North Carolina, 35.308, -83.644, GenBank: OQ617122, OQ628062, OQ628460, OQ617123, OQ628056, OQ628461, SRA: SRX19664333, SRX19664332; **USNM 1522411:** Adjacent to Pizza by the River, northeast corner of Nantahala Gorge, Swain County, North Carolina, 35.336, -83.620, GenBank: OQ617124, OQ628055, OQ628462, SRA: SRX19664329 **ANSP 171736:** Blowing Springs, Swain County, North Carolina; **ANSP 348077:** Nantahala Gorge, Swain County, North Carolina, 35.40, 83.25; **MCZ 94130:** Blowing Springs, Nantahala Gorge, Swain County, North Carolina.

Diagnosis. Shell imperforate, subglobose, weakly translucent, with 5.5–5.75 whorls. Teleoconch sculpture of coarse, prosocline, axial striae. Spire low, dome-shaped, sutures weakly impressed. Aperture lunate, peristome white, with small basal notch. Slightly curved parietal tooth, moderate in size for the genus. Mantle pigmentation of branching lines in at least some individuals.

Distribution. Restricted to the eastern slope of the Nantahala Gorge in North Carolina, USA.

Ecology. Little is known about the ecology of *P. nantahala*. The species appears to prefer the moist, highly vegetated habitats that receive little sunlight, which are typical of the eastern slope of the Nantahala Gorge. Found only in habitats with soil characterized by the SSURGO soil map as "Inceptisols: Sylco-Cataska complex, 50 to 95 percent slopes, very rocky".

Conservation status. Federally threatened under the U.S. Endangered Species Act. Listed as threatened by the state of North Carolina. Available data indicate that *P. nantahala* is in one of the three "threatened" IUCN ranking categories, likely falling under "endangered".

Remarks. All sampled *P. nantahala* individuals are more similar to the holotype and paratypes of *P. nantahala* than to the types of *P. clarkii*. Shell shape of *P. nantahala* differs significantly from closely related lineages (Figs 2–5; Table 3). We are unable to comment on internal anatomical variation among *P.* aff. *clarkii* lineages and *P. nantahala* because we did not preserve specimens in a manner suitable for anatomical work. Emberton (1995) examined internal anatomy of *Patera* and found no differences among *P. clarkii*, *P. perigrapta*, and other species in the subgenus *Patera* (*Patera*), making it unlikely that anatomical investigations would yield diagnosable features among the lineages examined here.

Discussion

Our results demonstrate that *P. nantahala* is a distinct species based on molecular, morphological, and ecological data. Recognition of *P. nantahala* renders *P. clarkii* polyphyletic, and our phylogenetic analyses indicate that unrecognized species diversity still exists within *P. clarkii* s.l. Recognition of *P. nantahala* at the rank of species is also consistent with the framework developed by Horsáková et al. (2019) for recognizing "cryptic" species in terrestrial snails, who argued that multiple lines of evidence including mitochondrial and nuclear concordance, quantitative morphological differences, and ecology should support a taxonomic hypothesis before recognizing entities at the species level. In contrast, a better understanding of the geographic ranges of the *P.* aff. *clarkii* lineages and establishing which lineage should be ascribed to *P. clarkii* s.s. is needed before a new species can be described. Our results emphasize the need for genome-based analyses to understand diversity and conservation of North American terrestrial snails. From a conservation standpoint, the original listing decision under the Endangered Species Act treated *P. nantahala* as a distinct entity. Thus, our results support continued protection.

Species, morphological, and genetic diversity

Both mitochondrial and 3RAD data are congruent and demonstrate that *P. nantahala* is reciprocally monophyletic with respect to *P.* aff. *clarkii* lineages. Mitochondrial divergence among *P. nantahala* and *P.* aff. *clarkii* lineages exceeds 9%, and both SNAQ and mitochondrial analyses indicate a lack of recent nuclear introgression. Thus, *P. nantahala* is a distinct evolutionary lineage.

The observed absence of recent gene flow is unlikely to be a result of sampling error as sampling locations for *P. clarkii* and *P. nantahala* were in close proximity and within likely contact zones. Furthermore, if gene flow was currently occurring, we would not expect divergence patterns on the mitochondrial tree and ASTRAL species tree to be congruent and to match morphological differences. Although some may argue that additional sampling of *P. nantahala* would be desirable prior to revising its status, this is not preferable given its conservation status. Destructive sampling of museum specimens is not a suitable alternative given the paucity of preserved specimens and because techniques for 3RAD with dry shell material are unproven. Furthermore, network-based approaches with genomic data are sufficiently sensitive to assess gene flow, even with one or two individuals per species (Solís-Lemus and Ané 2016; Mao et al. 2018; Watson et al. 2020).

The branching pattern inferred in phylogenetic analyses supports the presence of several unrecognized species. Analysis with ASAP indicated that Clades 1–4 on the COI tree were each a distinct species (Fig. 6). As noted above, ASAP is not based on the multispecies coalescent, but rather barcode gaps, which has been shown to be more conservative in splitting entities into hypothesized species than other automatic delimitation methods (Strong and Whelan 2019). Nevertheless, automatic species delimitation methods can give incongruent results, and the best automatic approach for land snails, if there is one, is unclear (Sauer and Hausdorf 2011; Greve et al. 2012; Prévot et al. 2013; Bamberger et al. 2022).

The absence of gene flow among *Patera clarkii* s.l. lineages inferred with SNAQ also corroborates ASAP results. Notably, SNAQ found no gene flow between individual "*P.* aff. *clarkii* 008" (i.e., Clade 2; Figs 6, 8) with other clades, therefore rejecting our initial hypothesis that individual "*P.* aff. *clarkii* 008" was a hybrid between *P. clarkii* and *P. nantahala*. However, we refrain from describing a new species pending additional work to determine its geographic range. Furthermore, we are unsure whether Clade 1, 2, 4, or an unsampled lineage, represents true *P. clarkii* because phylogenetic analyses did not include individuals from the type locality Tuskee [sic, Tuskeegee] Cove, Cherokee County [now Graham County], North Carolina. However, individuals sampled closest to the type locality were in Clade 1. Topotypic material of the other available species-group name currently in the synonymy of *P. clarkii* is also needed (i.e., *Polygyra clarkii* var. *bradleyi* Vanatta 1912) prior to species descriptions. We note that *P. clarkii* is the correct original spelling and should be preserved under Article 31.1.3 of the Code (ICZN, 1999) even though "*P. clarki*" is more commonly used in the recent literature.

Geometric morphometrics showed that *P. nantahala* has a significantly different shell shape compared to closely related congeners. We were unable to unambiguously

assign museum records to one of the three *Patera* aff. *clarkii* lineages because distinguishing shell features or geographic ranges have not been established. Future studies with more *P. clarkii* s.l. sampling for molecular phylogenetics will be necessary to allow confident clade assignments that can be used in geometric morphometrics. However, truly cryptic species may exist within *Patera*.

Hubricht (1983) claimed that *P. clarkii* exists in the Nantahala Gorge and *P. nantahala* exists outside the Nantahala Gorge. These conclusions were based on comparisons of shell morphology, but the exact shell features, aside from shell size, used to support these conclusions were not reported. Phylogenetic analyses, geometric morphometrics, and environmental modeling results reject Hubricht's (1983, 1985) hypothesis that *P. nantahala* is not a valid subspecies. Although we cannot completely rule out that future survey work will find overlap in the range of *P. clarkii* and *P. nantahala*, the absence of gene flow and high genetic divergence indicate that the two species are reproductively isolated.

Our results add to a growing body of research that used genomic tools to better understand terrestrial snail evolution (e.g., Razkin et al. 2016; Phillips et al. 2020; Bober et al. 2021; Bamberger et al. 2022). When used in conjunction with distributional, ecological, and morphological data, as done here, genomic data appear especially well-suited for resolving polygyrid relationships. Our conclusions about species diversity likely would have been different, and incorrect, if we had relied only on 28S and H3 for nuclear genetic data. For instance, the H3 tree indicated little genetic differentiation among *P. clarkii* s.l. lineages (Fig. 7), and 28S was invariant across *P. perigrapta*, *P. nantahala* and *P. clarkii* s.l. Prior to generating nuclear data via 3RAD sequencing, we thought gene flow among sampled *P. clarkii* s.l. was possible, if not probable, based on the 28S and H3 data. In contrast, 3RAD data indicate that incomplete lineage sorting, rather than gene flow, is responsible for a lack of resolution in the 28S and H3 genes. This finding is essential for future research on polygyrids, and we encourage future studies to employ genomic data for population- and species-level research.

Environmental niche models

The environmental niches of *P. nantahala* and *P. clarkii* are significantly different according to GLM analyses with non-bioclimatic data included, which appear to be the most accurate given environmental niche model plots and known ranges (Fig. 9). For example, predicted suitable habitat using GLMs appears reasonable and not overpredicted, particularly when all environmental variables were used. We hypothesize that niche models with non-bioclimatic variables are more accurate because of unique abiotic features of the southeastern slope of the Nantahala Gorge. Maxent models for *P. nantahala* predicted suitable habitat far outside the known species range and in locations where only shells that match the morphology of *P. clarkii* have been recorded. Thus, disagreement in the significance of environmental niche differences between GLM and Maxent analyses appears to be a result of Maxent making overpredictions in the suitable habitat of *P. nantahala* (Fig. 9).

Our results indicate the need to be cautious when using environmental niche modeling approaches for understudied, narrow-range endemics. Most analyses overestimated the distribution of *P. nantahala* (Fig. 9), and we do not think that suitable habitat inferred with Maxent represents true suitable habitat or an unrecognized, potential niche for *P. nantahala*. Furthermore, models that used only bioclimatic data performed worse, especially with *P. nantahala* (Fig. 9). We argue that overestimation of environmental niche is at least possible, if not likely, for any narrow range endemic, especially when relying entirely on bioclimatic data. Most environmental data used in niche modeling, particularly BioClim data, are likely not of adequate resolution for distinguishing the environmental niches of extreme narrow-range endemics. Our results indicate that if environmental niche models are to be generated for narrow-range endemics, environmental data other than bioclimatic variables are essential.

Environmental niche models that include data other than bioclimatic information can be useful for assessing the potential for narrow-range endemics to occupy other habitats, but they may not always be necessary to make inferences about terrestrial snail distributions and environmental niches. For example, even before running environmental niche models, SSURGO soil classifications of collection sites made clear that *P. nantahala* only inhabits a single, uncommon soil type, whereas *P. clarkii* s.l. inhabits many different soil types. More broadly, our results indicate that Maxent models will tend to overpredict ranges for narrow-range endemics. These findings should be applicable to other terrestrial snails.

Conclusions

Morphological, ecological, and phylogenetic data support *Patera nantahala* as a valid species. We hypothesize that the ancestor of *P. nantahala* invaded the Nantahala Gorge, or became isolated in the gorge, and subsequently underwent allopatric speciation, with the Nantahala Gorge and Nantahala River serving as dispersal barriers. Although the recognition of *P. nantahala* is a step in the right direction, the systematics of Polygyridae requires comprehensive revision. Despite calls for increased study (Perez 2011; Perez et al. 2014), little progress has been made. Our results suggest that phylogenetically distinct lineages of polygyrids remain unrecognized. As such, species that may require conservation attention are being overlooked. This could lead to a loss of diversity and evolutionary potential before we know how many species of polygyrids exist. To improve polygyrid systematics, both increased sampling and genome-wide markers will be needed.

Acknowledgements

This work would not have been possible without the resources provided by Biodiversity Heritage Library. Frank Köhler and Philippe Bouchet answered questions we had about MolluscaBase records, which improved the manuscript. Thanks to Paul Callo-

mon (ANSP), Amanda Robinson (NMNH), and Jennifer Trimble (MCZ) for facilitating museum loans. Two anonymous reviewers and M. Haase provided feedback that improved an earlier version of this work. This work was made possible in part by a grant of high-performance computing resources and technical support from the Alabama Supercomputer Authority. The findings and conclusions in this article are those of the authors and do not necessarily represent the views of the U.S. Fish and Wildlife Service.

References

Bamberger S, Xu J, Hausdorf B (2022) Evaluating species delimitation methods in radiations: The land snail *Albinaria cretensis* complex on Crete. Systematic Biology 71(2): 439–460. https://doi.org/10.1093/sysbio/syab050

Bayona-Vásquez NJ, Glenn TC, Kieran TJ, Pierson TW, Hoffberg SL, Scott PA, Bentley K, Finger JW, Louha S, Troendle N, Diaz-Jaimes P, Mauricio R, Faircloth BC (2019) Adapterama III: Quadruple-indexed double/triple-enzyme RADseq libraries (2RAD/3RAD). PeerJ 7: e7724. https://doi.org/10.7717/peerj.7724

Bober S, Glaubrecht M, Hausdorf B, Neiber MT (2021) One, two or three? Integrative species delimitation of short-range endemic *Hemicycla* species (Gastropoda: Helicidae) from the Canary Islands based on morphology, barcoding, AFLP and ddRADseq data. Molecular Phylogenetics and Evolution 161: e107153. https://doi.org/10.1016/j.ympev.2021.107153

Brown JL, Bennet JR, French CM (2017) SDMtoolbox 2.0: The next generation Python-based GIS toolkit for landscape genetics, biogeographic and species distribution model analyses. PeerJ 5: e4095. https://doi.org/10.7717/peerj.4095

Chambers SM (1981) Protection of mollusks under the Endangered Species Act of 1973. The Bulletin of the American Malacological Union. Inc 1981: 55–59.

Clench WJ, Banks GS (1932) Descriptions of some land snails of southwestern North Carolina. The Nautilus 46: 14–18. https://doi.org/10.5962/bhl.part.28159

Coates DJ, Byrne M, Moritz C (2018) Genetic diversity and conservation units: Dealing with species-population continuum in the age of genomics. Frontiers in Ecology and Evolution 6: e165. https://doi.org/10.3389/fevo.2018.00165

Colgan DJ, Ponder WF, Eggler PE (1999) Gastropod evolutionary rates and phylogenetic relationships assessed using partial 28S rDNA and histone H3 sequences. Zoologica Scripta 29(1): 29–63. https://doi.org/10.1046/j.1463-6409.2000.00021.x

De Queiroz K (2007) Species concepts and species delimitation. Systematic Biology 56(6): 849–886. https://doi.org/10.1080/10635150701701083

Emberton KC (1991) The genitalic, allozymic and conchological evolution of the tribe Mesodontini (Pulmonata, Stylommatophora: Polygyridae). Malacologia 33: 71–178.

Emberton KC (1995) When shells do not tell: 145 million years of evolution in North America's polygyrid land snails, with a revision and conservation priorities. Malacologia 37: 68–110.

Fick SE, Hijmans RJ (2017) Worldclim 2: New 1-km spatial resolution climate surfaces for global land areas. International Journal of Climatology 37(12): 4302–4315. https://doi.org/10.1002/joc.5086

GBIF.org (2022) Occurrence Download. The Global Biodiversity Information Facility. https://doi.org/10.15468/dl.xmeqxt

Greenwalt LA (1978) Determination that seven eastern U.S. land snails are endagered or threatened species. Federal Register 43: 28932–28935.

Greve C, Gimnich F, Hutterer R, Misof B, Hasse M (2012) Radiating on oceanic islands: Patterns and processes of speciation in the land snail genus *Theba* (Risso 1826). PLoS ONE 7(4): e34339. https://doi.org/10.1371/journal.pone.0034339

Hijmans RJ (2022) raster: Geographic Data Analysis and Modeling. R package version 3.5-15.

Hillis DM, Dixon MT (1991) Ribosomal DNA: Molecular evolution and phylogenetic inference. The Quarterly Review of Biology 66(4): 411–453. https://doi.org/10.1086/417338

Hoang DT, Chernomor O, Von Haeseler A, Minh BQ, Vinh LS (2018) UFBoot2: Improving the ultrafast bootstrap approximation. Molecular Biology and Evolution 35(2): 518–522. https://doi.org/10.1093/molbev/msx281

Horsákava V, Nekola JC, Horsák M (2019) When is a "cryptic" speices not a cryptic species: a consideration from the Holarctic micro-landsnail genus *Euconulus* (Gastropoda: Stylommatophora). Molecular Phylogenetics and Evolution 132: 307–320. https://doi.org/10.1016/j.ympev.2018.12.004

Hubircht L (1983) Five new species of land-snails from the southeastern United States with notes on other species. Gastropodia 2: 13–19.

Hubricht L (1985) The distributions of native land mollusks of the eastern United States. Fieldiana Zoology 24: 1–191. https://doi.org/10.5962/bhl.title.3329

Huson DH, Bryant D (2006) Application of phylogenetic networks in evolutionary studies. Molecular Biology and Evolution 23(2): 254–267. https://doi.org/10.1093/molbev/msj030

ICZN (1999) International code of zoological nomenclature. Fourth Edition. International Trust For Zoological Nomenclature, London.

Junier T, Zdobnov EM (2010) The newick utilities: High-throughput phylogenetic tree processing in the UNIX shell. Bioinformatics 26(13): 1669–1670. https://doi.org/10.1093/bioinformatics/btq243

Kalyaanamoorthy S, Minh BQ, Wong TKF, von Haeseler A, Jermiin LS (2017) ModelFinder: Fast model selection for accurate phylogenetic estimates. Nature Methods 14(6): 587–589. https://doi.org/10.1038/nmeth.4285

Klingenberg CP (2011) MorphoJ: An integrated software package for geometric morphometrics. Molecular Ecology Resources 11(2): 353–357. https://doi.org/10.1111/j.1755-0998.2010.02924.x

Klingenberg CP, Monteiro LR (2005) Distances and directions in multidimensional shape spaces: Implications for morphometric applications. Systematic Biology 54(4): 678–688. https://doi.org/10.1080/10635150590947258

Kumar S, Stecher G, Li M, Knyaz C, Tamura K (2019) MEGA X: Molecular evolutionary genetics analysis across computing platforms. Molecular Biology and Evolution 35(6): 1547–1549. https://doi.org/10.1093/molbev/msy096

LANDFIRE (2020) Landfire. https://landfire.gov/version_download.php# [Accessed January 2022].

Maddison WP (1997) Gene trees in species trees. Systematic Biology 46: 523–536. https://doi.org/10.1093/sysbio/46.3.523

Mao Y, Economo EP, Satoh N (2018) The roles of introgression and climate change in the rise to dominance of Acropora corals. Current Biology 28(21): 3373–3382. https://doi.org/10.1016/j.cub.2018.08.061

Mayden RL (1997) A hierarchy of species concepts: the denouement in the saga of the species problem. In: Claridge MF, Dawah HA, Wilson MR (Eds) Species: the Units of Diversity. Chapman & Hall, 381–423.

Mays JW (2021) Noonday Globe (*Patera clarki nantahala*) 5-year review. Asheville, North Carolina, 24 pp.

Meyer CP (2003) Molecular systematics of cowries (Gastropoda: Cypraeidae) and diversification patterns in the tropics. Biological Journal of the Linnean Society 79(3): 401–459. https://doi.org/10.1046/j.1095-8312.2003.00197.x

Nekola JC, Horsák M (2022) The impact of empirically unverified taxonomic concepts on ecological assemblage patterns across multiple spatial scales. Ecography 2022(5): e06063. https://doi.org/10.1111/ecog.06063

Nguyen L-T, Schmidt HA, von Haeseler A, Minh BQ (2015) IQ-TREE: A fast and effective stochastic algorithm for estimating maximum-likelihood phylogenies. Molecular Biology and Evolution 32(1): 268–274. https://doi.org/10.1093/molbev/msu300

Páll-Gergely B, Asami T, Sólymos P (2019) Subspecies description rates are higher in morphologically complex land snails. Zoologica Scripta 48(2): 185–193. https://doi.org/10.1111/zsc.12319

Paris JR, Stevens JR, Catchen JM (2017) Lost in parameter space: A road map for Stacks. Methods in Ecology and Evolution 8(10): 1360–1373. https://doi.org/10.1111/2041-210X.12775

Patten MA (2015) Subspecies and the philosophy of science. The Auk 132(2): 481–485. https://doi.org/10.1642/AUK-15-1.1

Perez KE (2011) A new species of *Praticolella* (Gastropoda: Polygyridae) from northeastern Mexico and revision of several species of this genus. The Nautilus 125(3): 113–126.

Perez KE, Defreitas N, Slapcinsky J, Minton RL, Anderson FE, Pearce TA (2014) Molecular phylogeny, evolution of shell shape, and DNA barcoding in Polygyridae (Gastropoda: Pulmonata), an endemic North American clade of land snails. American Malacological Bulletin 32(1): 1–31. https://doi.org/10.4003/006.032.0103

Phillips JG, Linscott TM, Rankin AM, Kraemer AC, Shoobs NF, Parent CE (2020) Archipelago-wide patterns of colonization and speciation among an endemic radiation of Galápagos land snails. The Journal of Heredity 111(1): 92–102. https://doi.org/10.1093/jhered/esz068

Pilsbry HA (1894) Manual of Conchology, Structural and Systematic, with Illustrations of the Species (Vol. 9). Conchology Section, Academy of Natural Sciences, Philadelphia, Pennsylvania, 366 pp.

Pilsbry HA (1930) Anatomy and relationships of some American Helicidae and Polygyridae. Proceedings of the Academy of Natural Sciences of Philadelphia 82: 303–337.

Pilsbry HA (1940) Land Mollusca of North America (North of Mexico) (Vol. 1, Part 2). Academy of Natural Sciences, Philadelphia, 542 pp.

Prévot V, Jordaens K, Sonet G, Backeljau T (2013) Exploring species level taxonomy and species delimitation methods in the facultatively self-fertilizing land snail Genus *Rumina* (Gastropoda: Pulmonata). PLoS ONE 8(4): e60736. https://doi.org/10.1371/journal.pone.0060736

Primack RB (2014) Essentials of Conservation Biology. Sinauer Associates, United Kingdom, 603 pp.

Puillandre N, Lambert A, Brouillet S, Achaz G (2012) ABGD, automatic barcode gap discovery for primary species delimitation. Molecular Ecology 21(8): 1864–1877. https://doi.org/10.1111/j.1365-294X.2011.05239.x

Puillandre N, Brouillet S, Achaz G (2021) ASAP: Assemble species by automatic partitioning. Molecular Ecology Resources 21(2): 609–620. https://doi.org/10.1111/1755-0998.13281

Rannala B, Yang Z (2003) Bayes estimation of species divergence times and ancestral population sizes using DNA sequences from multiple loci. Genetics 164(4): 1645–1656. https://doi.org/10.1093/genetics/164.4.1645

Razkin O, Sonet G, Breugelmans K, Madeira MJ, Gómez-Moliner BJ, Backeljau T (2016) Species limits, interspecific hybridization and phylogeny in the cryptic land snail complex *Pyramidula*: The power of RADseq data. Molecular Phylogenetics and Evolution 101: 267–278. https://doi.org/10.1016/j.ympev.2016.05.002

Richardson L (1986) Polygyracea: Catalog of species (Parts 1, Polygyridae; 2, Corillidae; 3, Sagdidae). Tryonia 13(Part 1): 1–139.

Rochette N, Rivera-Colón A, Catchen J (2019) Stacks 2: Analytical methods for paired-end sequencing improve RADseq-based population genomics. Molecular Ecology 28(21): 4737–4754. https://doi.org/10.1111/mec.15253

Rohlf FJ (2021a) tpsDig version 2.32. https://www.sbmorphometrics.org/soft-dataacq.html [Accessed December 2022]

Rohlf FJ (2021b) tpsUtil version 1.82. https://www.sbmorphometrics.org/soft-utility.html [Accessed December 2022]

Sauer J, Hausdorf B (2011) A comparison of DNA-based methods for delimiting species in a Cretan land snail radiation reveals shortcomings of exclusively molecular taxonomy. Cladistics 28(3): 300–316. https://doi.org/10.1111/j.1096-0031.2011.00382.x

Sayyari E, Mirarab S (2016) Fast coalescent-based computation of local branch length support from quartet frequencies. Molecular Biology and Evolution 33(7): 1654–1668. https://doi.org/10.1093/molbev/msw079

Schoener TW (1968) The *Anolis* lizards of Bimini: Resource partitioning in a complex fauna. Ecology 49(4): 704–726. https://doi.org/10.2307/1935534

Sievers F, Wilm A, Dineen D, Gibson TJ, Kevin K, Li W, Lopez R, McWilliam H, Remmert M, Söding J, Thompson JD, Higgins DG (2011) Fast, scalable generation of high-quality protein multiple sequence alignments using Clustal Omega. Molecular Systems Biology 7(1): e539. https://doi.org/10.1038/msb.2011.75

Soil Survey Staff (2022) Soil Survey Geographic (SSURGO) Database for the United States. http://websoilsurvey.sc.egov.usda.gov/ [Accessed January 2022]

Solís-Lemus C, Ané C (2016) Inferring phylogenetic networks with maximum pseudolikelihood under incomplete lineage sorting. PLoS Genetics 12: e1005896. https://doi.org/10.1371/journal.pgen.1005896

Soil Survey Staff (1999) Soil Taxonomy. A basic system fo soil classification for making and interpreting soil surveys. United States Department of Agriculture Natural Resources Conservation Service, 886 pp.

Solís-Lemus C, Bastide P, Ané C (2017) PhyloNetworks: A package for phylogenetic networks. Molecular Biology and Evolution 34(12): 3292–3298. https://doi.org/10.1093/molbev/msx235

Stankowski S, Ravinet M (2021) Quantifying the use of species concepts. Current Biology 31(9): R428–R429. https://doi.org/10.1016/j.cub.2021.03.060

Strong EE, Whelan NV (2019) Assessing the diversity of Western North American *Juga* (Semisulcospiridae, Gastropoda). Molecular Phylogenetics and Evolution 136: 87–103. https://doi.org/10.1016/j.ympev.2019.04.009

Sukumaran J, Knowles LL (2017) Multispecies coalescent delimits structure, not species. Proceedings of the National Academy of Sciences of the United States of America 114(7): 1607–1612. https://doi.org/10.1073/pnas.1607921114

Taylor BL, Perrin WF, Reeves RR, Rosel PE, Wang JY, Cipriano F, Baker CS, Bronwell Jr RL (2017) Why we should develop guidelines and quantitative standards for using genetic data to delimit subspecies for data-poor organisms like cetaceans. Marine Mammal Science 33(S1): 12–26. https://doi.org/10.1111/mms.12413

Tryon GW (1866) Monograph of the terrestrial Mollusca of the United States. American Journal of Conchology 2: 218–279. [pls 211–214; 306–327, pls 215–216.]

US Geological Survery (2022) 3D Elevation Program 1/3-arc second Resolution Digital Elevation Model. https://www.usgs.gov/3d-elevation-program [Accessed January 2022]

Van Devender AS (1984) Recovery Plan for the Noonday Snail *Mesodon clarki nantahala*. 30 pp.

Wang S, Meyer E, McKay JK, Matz MV (2012) 2b-RAD: A simple and flexible method for genome-wide genotyping. Nature Methods 9(8): 808–810. https://doi.org/10.1038/nmeth.2023

Warren DL, Beaumont LJ, Dinnage R, Baumgartner JB (2018) New methods for measuring ENM breadth and overlap in environmental space. Ecography 42(3): 444–446. https://doi.org/10.1111/ecog.03900

Warren DL, Matzke NJ, Cardillo M, Baumgartner JB, Beaumont LJ, Turelli M, Glor RE, Huron NA, Simões M, Iglesias TL, Piquet JC, Dinnage R (2021) ENMTools 1.0: An R package for comparative ecological biogeography. Ecography 44(4): 504–511. https://doi.org/10.1111/ecog.05485

Watson LE, Siniscalchi CM, Mandel J (2020) Phylogenomics of the hyperdiverse daisy tribes: Anthemideae, Astereae, Calenduleae, Gnaphalieae, and Senecioneae. Journal of Systematics and Evolution 58(6): 841–852. https://doi.org/10.1111/jse.12698

Whelan NV, Galaska MP, Sipley BN, Weber JM, Johnson PD, Halanych KM, Helms BS (2019) Riverscape genetic variation, migration patterns, and morphological variation of the threatened Round Rocksnail, *Leptoxis ampla*. Molecular Ecology 28(7): 1593–1610. https://doi.org/10.1111/mec.15032

Wickham H (2009) ggplot2: elegant graphics for data analysis. Springer-Verlag, New York, 212 pp. https://doi.org/10.1007/978-0-387-98141-3

Zhang C, Rabiee M, Sayyari E, Mirarab S (2018) ASTRAL-III: Polynomial time species tree reconstruction from partially resolved gene trees. BMC Bioinformatics 19(S6): 153. https://doi.org/10.1186/s12859-018-2129-y

Supplementary material 1

Species information

Authors: Nathan V. Whelan, Ellen E. Strong, Nicholas S. Gladstone, Jason W. Mays

Data type: table (excel document)

Link: https://doi.org/10.3897/zookeys.1158.94152.suppl1

Supplementary material 2

Additional images

Authors: Nathan V. Whelan, Ellen E. Strong, Nicholas S. Gladstone, Jason W. Mays

Data type: figures (PDF file)

Link: https://doi.org/10.3897/zookeys.1158.94152.suppl2

ZooKeys 1158: 121–131 (2023)
doi: 10.3897/zookeys.1158.101347
https://zookeys.pensoft.net

RESEARCH ARTICLE

A peer-reviewed open-access journal
ZooKeys
Launched to accelerate biodiversity research

Genetic diversity among sea snakes of the genus *Hydrophis* (Elapidae, Reptilia) in the Persian Gulf and Gulf of Oman

Seyyed Saeed Hosseinian Yousefkhani[1], Amaal Yasser[2,3], Murtada Naser[2,4], Mohsen Rezaie-Atagholipour[5], Majid Askari Hesni[6], Fariba Yousefabadi[7], Eskandar Rastegar Pouyani[8]

1 *Department of Animal Science, School of Biology, Damghan University, Damghan, Iran* **2** *Marine Science Centre, University of Basrah, Basra, Iraq* **3** *Australian Rivers Institute, Griffith University, 170 Kessels Road, Nathan, Queensland 4111, Australia* **4** *School of Environment and Science, Griffith University, 170 Kessels Road, Nathan, Queensland, 4111, Australia* **5** *Qeshm Environmental Conservation Institute (QECI), Qeshm Island, Hormozgan Province, Iran* **6** *Department of Biology, Faculty of Sciences, Shahid Bahonar University of Kerman, Kerman Province, Iran* **7** *Department of Biology, Faculty of Science, Ferdowsi University of Mashhad, Mashhad, Iran* **8** *Department of Biology, Hakim Sabzevari University, Sabzevar, Iran*

Corresponding author: Eskandar Rastegar Pouyani (rastegarpouyani45@gmail.com)

Academic editor: Robert Jadin | Received 1 February 2023 | Accepted 1 April 2023 | Published 20 April 2023

https://zoobank.org/6E071A9E-7978-4690-B8AE-75C58F44B1D1

Citation: Hosseinian Yousefkhani SS, Yasser A, Naser M, Rezaie-Atagholipour M, Askari Hesni M, Yousefabadi F, Rastegar Pouyani E (2023) Genetic diversity among sea snakes of the genus *Hydrophis* (Elapidae, Reptilia) in the Persian Gulf and Gulf of Oman. ZooKeys 1158: 121–131. https://doi.org/10.3897/zookeys.1158.101347

Abstract

Sea snakes of the genus *Hydrophis* are important components of animal diversity in Iranian waters of the Persian Gulf and Gulf of Oman. Ten species of *Hydrophis* have been identified from the these waters and, in this study, genetic structure of seven species was compared with other populations in the eastern Indian Ocean and the West Pacific. We found that six species (*H. platurus*, *H. cyanocinctus*, *H. spiralis*, *H. schistosus*, *H. gracilis*, and *H. lapemiodes*) show high genetic similarity with conspecific populations in the Indian Ocean and Australia. However, *H. curtus* from southern Iran shows a high level of genetic differentiation from conspecific populations in Sri Lanka and Indonesia (0.6% and 6% genetic distance from Sri Lankan samples for *16S* and *COI* gene fragments, respectively). Variation between Iranian and Southeast Asian populations may reflect new genetic lineages and suggest the need of further morphological evaluations to re-evaluate their taxonomic position.

Keywords

Dispersal, Indian Ocean, microhabitat adaptation, true sea snakes, variation

Introduction

Sea snakes are a well-known part of marine ecosystems and play an irreplaceable role in the food chain as both predators of small marine fauna and prey for larger predators within their geographical distribution range, which comprises the tropical Indo-Pacific (Voris 1972; Udyawer et al. 2018). True sea snakes of the tribe Hydrophiini share a common ancestor approximately six million years ago, but the major speciation events and radiation within the group and the genus *Hydrophis* have taken place over the last 3.5 million years (Sanders et al. 2013). While studies on different subjects (e.g., Ukuwela et al. 2012, 2016) have been conducted on sea snakes on the eastern half of their geographic range (i.e., Southeast Asia, India, Indonesia, and northern Australia), their populations remain relatively understudied in the western Indian Ocean (Rezaie-Atagholipour et al. 2016).

Iranian coastal waters of the Persian Gulf and Gulf of Oman are known for their high biological diversity (Owfi et al. 2016) and share a marine herpetofauna with the Indian Ocean (Gasperetti 1988; Heatwole 1999). Ten species of *Hydrophis* have been recorded in these gulfs: *H. platurus*, *H. schistosus*, *H. curtus*, *H. viperinus*, *H. spiralis*, *H. cyanocinctus*, *H. ornatus*, *H. lapemiodes*, *H. gracilis*, and *H. cantoris* (Rezaie-Atagholipour et al. 2016; Rajabizadeh 2019). Among these, *H. platurus* has a wider geographic range toward eastern Africa (Heatwole 1999), but the westernmost ranges of the other species extend to the Persian Gulf (Rezaie-Atagholipour et al. 2016). The semi-enclosed basin of the Persian Gulf (i.e., connected to the Gulf of Oman and western Indian Ocean via the narrow Strait of Hormuz) and its unique extreme environment with high salinity and temperatures (i.e., sea surface temperatures can exceed 34 °C and salinity more than 39 ppt in most areas; Sheppard et al. 2010) may pose ecological and geographical barriers and limit gene flow between the Gulf and Indian Ocean marine communities (e.g., Natoli et al. 2017). Therefore, it seems important to compare the genetic structure of sea snakes, which are known to have undergone rapid speciation (see Sanders et al. 2013), between the Persian Gulf and the rest of the Indo-Pacific.

In this study, available genetic markers (16S rRNA, *COI*, and *G1888*) of species of sea snakes of the genus *Hydrophis* from the Persian Gulf and the Gulf of Oman were compared to populations in other areas of the Indian Ocean, Southeast Asia, and Indonesia. Examining the genetic structure of the species in the Persian Gulf and comparing them with other populations can illustrate the degree of genetic connection between these populations.

Materials and methods

Tissue sampling and DNA extraction

Tissue samples were obtained from the specimens collected in the southern coastal regions of Iran (Persian Gulf and Gulf of Oman) during fieldwork in 2013 (Rezaie-Atagholipour et al. 2016) and were preserved in 96% ethanol. A total of 31 samples used in this study belong to seven species from four localities in southern Iran (Fig. 1,

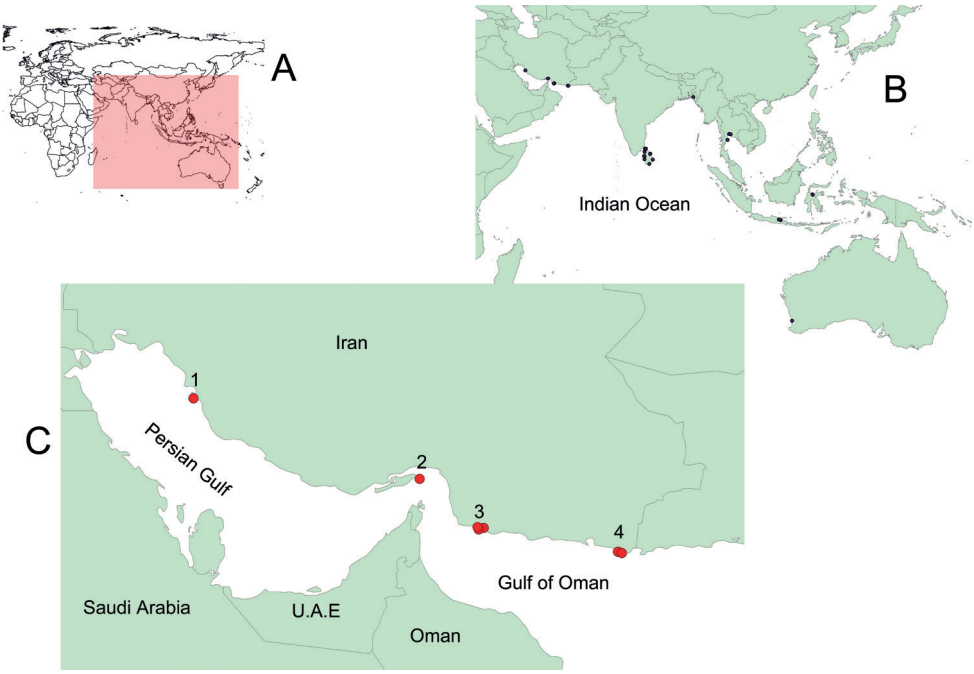

Figure 1. A map of the world and the selected region as study area **B** localities in South and Southeast Asia from which samples were used in this study **C** localities in southern Iran where samples were collected: 1 = Bushehr; 2 = Larak Island; 3 = Jask; 4 = Beris and Pasabandar.

Suppl. material 1) and 27 comparative sequences were downloaded from GenBank. Sequences of *Ephalophis greyae*, used as the outgroup, were also downloaded from GenBank (Suppl. material 1). Total genomic DNA was extracted from muscle tissue using the standard proteinase K – salt method (Kabir et al. 2006), and the quality and concentration of extracted DNA were measured using Nanodrop 1000.

Mitochondrial and nuclear fragment sequences

Two mitochondrial sequences, 16S rRNA (*16S*) (Kocher et al. 1989) and cytochrome oxidase subunit 1 (*COI*), and one anonymous nuclear marker (*G1888*) (Bertozzi et al. 2012) were used to reconstruct the molecular phylogenetic relationships between Iranian and Southeast Asian species of sea snakes. Two of these markers were obtained from previous successful studies (Lukoschek and Keogh 2006; Sanders et al. 2013), but *COI* is a new marker generated for sea snakes in the present study. The following primers were used for each gene fragment: *16S*: 16SL 5'-CGCCTGTTT ATCAAAAACAT-3'/ 16SH 5'-CCGGTCTGAACTCAGATCACG-3'; *COI*: RepCOIF 5'-TNTTMTCAACNAACCACAAAGA-3'/ RepCOIR 5'-ACTTCTGGRTGKCCAAARAATCA-3'; G1888: G1888F 5'- CAGGGCCTTGCCTTGTGCCA-3'/ G1888R 5'-ACCTCTGCGCACTATGACTCTTGA-3' (Bertozzi et al. 2012). All DNA sequences were amplified using a standard PCR protocol with denaturation at

94 °C for 5 min, annealing temperatures of 49 °C for mitochondrial fragments and 52 °C for anonymous nuclear marker for 45 s, and extension at 72 °C for 70 s (36 cycles), and the final extension for 8 min. Sequencing of the PCR products was performed by the Kodon Genetic Group in Tehran, Iran. Sequences of the same species and the same genetic fragments from Southeast Asia and the outgroup were downloaded from GenBank and added to the dataset (Suppl. material 1). All sequences were aligned using the ClustalW algorithm implemented within Bioedit v. 7.0.9.0 (Hall 1999), and the protein coding genes were translated to amino acid sequences using MEGA v. 6.0 (Tamura et al. 2013) to check for internal stop codons and to determine the correct reading frame. The sequences generated in this study were deposited in GenBank and will be added into Suppl. material 1. Uncorrected genetic distances (*p*-distances) were calculated (for *16S* and *COI*) and number of variable sites (*V*) and parsimony informative sites (*Pi*) were obtained using MEGA v. 6.0 for all markers. The sequences of the *COI* gene fragment were few and we only calculate genetic distance among some clades that revealed relatively high values.

Molecular phylogenetic analyses and haplotype network

The one mitochondrial and the nuclear fragment were concatenated (total length: 1015 bp; *16S*: 523 bp; *G1888*: 492 bp) and *COI* gene fragment (708 bp) separately were considered to reconstruction phylogenetic trees using Bayesian inference (BI) and maximum-likelihood (ML) methods. The best substitution models for each alignment were: TrNef+I, F81+I, TIM+G, GTR+I+G and TVM+I+G for the first, second, and third codon positions of *COI* and *16S* and *G1888*, respectively. RaxML v. 7.4.2 (Stamatakis 2006) as implemented in RaxmlGUI v. 1.3 (Silvestro and Michalak 2012) was employed for the ML analyses. The substitution model was set to GTR+G+I in RaxMl software for the molecular phylogenetic reconstruction. Bootstrapping was set to 1000 replicates to estimate nodal support, and the analysis was run as a heuristic search (Felsenstein 1985). MrBayes v. 3.2.1 (Ronquist et al. 2012) was used to run the BI analysis and the number of generations were set as 10^7 with a sample frequency of every 1000 generations, four Markov chains, and a burn-in with each 1000 samples.

The relationships among lineages and subclades of *Hydrophis* were assessed with the mitochondrial *16S rRNA* gene, because the number of sequences of *16S* covered all species. Aligned sequences were entered in DNAsp v. 5.0. (Librado and Rozas 2009) and a *.rdf extension file was created. The haplotype network was then constructed using the median-joining method in Network 1.2.1.

Results

Our dataset includes 59 samples containing two mitochondrial gene fragments *16S* (495 bp; 77 *V*; 40 *Pi*) and *COI* (661 bp; 158 *V*; 112 *Pi*) and one nuclear anonymous fragment G1888 (375 bp; 265 *V*; 250 *Pi*) totaling 1531 bp. Both the ML and BI

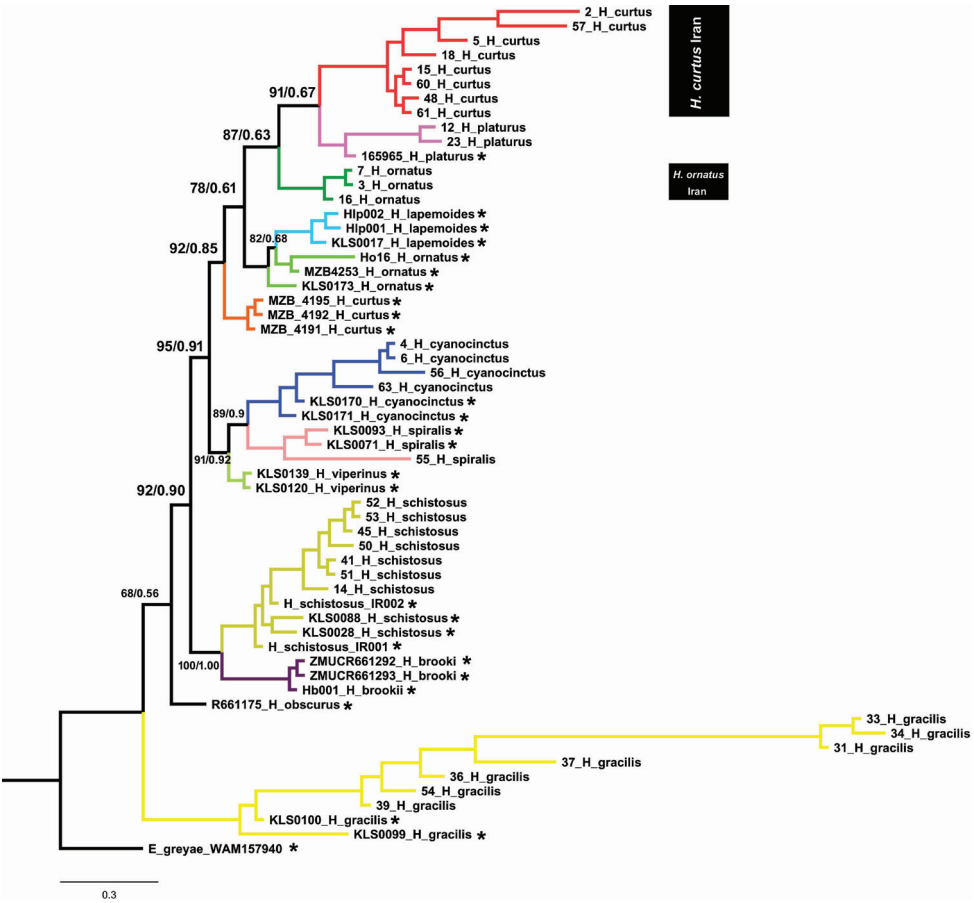

Figure 2. Molecular phylogenetic tree of the genus *Hydrophis*. Red and green clades indicate distinct populations of *H. curtus* and *H. ornatus* from the Persian Gulf relative to other populations in the Indian Ocean. Data from samples with an asterisk (*) were downloaded from GenBank.

trees show similar topology and therefore we present only the BI tree (Fig. 2). Our results show that all species of *Hydrophis* in the Persian Gulf and Gulf of Oman similar with their corresponding species in Southeast Asia except *H. curtus* and *H. lapemiodes*. *Hydrophis curtus* in the western part of its geographic range (Persian Gulf and Gulf of Oman) shows clear divergence from Indian Ocean (Sri Lanka) and Indonesian samples (Ukuwela et al. 2014). *Hydrophis ornatus* also shows minor variation between Iranian and Indian Ocean populations, but not as extensive.

Tree topology was used to group the sequences and calculate the uncorrected genetic distance (*p*-distance) among the lineages (Table 1). Mean genetic distance in *16S rRNA* is relatively low (average 3.25% among all lineages) in *Hydrophis*. Iranian lineages of *H. curtus* are differentiated from those in Southeast Asia by 0.6% and 6% in *16S* and *COI* gene fragments, respectively (Tables 1, 2). Two other distinct species,

Table 1. *P*-distances among lineages of sea snakes in *16S* gene fragment: 1 = *H. spiralis*; 2 = *H. curtus* Iran; 3 = *H. cyanocinctus*; 4 = *H. gracilis*; 5 = *H. ornatus*_Iran; 6 = *H. platurus*; 7 = *H. schistosus*; 8 = *H. curtus*; 9 = *H. ornatus*; 10 = *H. viperinus*; 11 = *H. obscurus*; 12 = *H. lapemiodes*; 13 = *H. brooki*.

	1	2	3	4	5	6	7	8	9	10	11	12	13
1													
2	1.8												
3	1.8	1.9											
4	3.6	2.5	3.7										
5	1.7	1.6	1.6	3.4									
6	1.4	1.3	1.3	3.1	0.9								
7	2.3	1.6	2.2	3.4	1.9	1.6							
8	1.2	0.6	1.3	2.5	0.9	0.6	1.6						
9	1.9	1.8	1.8	3.6	0.6	1.2	1.9	1.2					
10	1.4	1.3	1.3	3.1	0.9	0.6	1.6	0.6	1.2				
11	2.6	1.9	2.5	3.1	2.2	1.9	2.2	1.9	2.4	1.9			
12	1.7	1.6	1.6	3.4	0.6	0.9	1.9	0.9	0.8	0.9	2.2		
13	3.6	2.8	3.5	4.6	3.1	2.8	1.9	2.8	3.4	2.8	3.5	3.1	

Table 2. *P*-distances among lineages of sea snakes in *COI* gene fragment: 1 = *H. curtus* Iran; 2 = *H. yanocinctus* Iran; 3 = *H. gracilis* Iran; 4 = *H. lapemiodes* Iran; 5 = *H. ornatus* Iran; 6 = *H. platurus* Iran; 7 = *H. schistosus* Iran; 8 = *H. viperinus* Iran; 9 = *H. brooki*; 10 = *H. lapemiodes*; 11 = *H. schistosus*; 12 = *H. cyanocinctus*; 13 = *H. obscurus*; 14 = *H. curtus*; 15 = *H. ornatus*.

	1	2	3	4	5	6	7	8	9	10	11	12	13	14	15
1															
2	6.7														
3	11.2	9.1													
4	7.2	4.7	9.4												
5	5	4.9	10.1	4.7											
6	5.3	6.3	9.8	6	4.3										
7	5.5	5.4	10.4	5.6	4.9	5.8									
8	6.2	5.4	10.4	5.4	3.7	5.5	5.1								
9	8.4	8.3	11.3	7.6	6.9	6.7	8.3	6.9							
10	7	2	9.4	4.9	5.1	6.5	5.6	5.6	8.1						
11	6.1	5.8	11	6.5	5.8	6.1	1.6	5.8	9.2	6					
12	6.2	1.4	9.5	5.1	4.3	5.7	5.8	5.1	8.3	1.6	6.1				
13	5.5	5.4	9.1	5.6	5.1	5.5	5.4	5.4	7.1	5.6	6.3	5.1			
14	6	5.9	10.9	6.4	4.9	5.3	5.4	6.1	7.4	6.1	6.3	5.8	5.6		
15	4.8	4.7	9.9	4.4	0.7	4	4.7	3.4	6.6	4.9	5.5	4.1	4.9	4.7	

H. platurus and *H. viperinus*, show the genetic differentiation of 0.6% in *16S* and 5.1% in *COI* (Tables 1, 2). The haplotype network calculated for the *16S rRNA* fragment confirmed the relationship among lineages in the concatenated phylogenetic tree (Fig. 3). The Iranian clade of *H. curtus* had a separate haplotype (haplotype number 2), but the other conspecific samples (Pacific Ocean) had a different distinct haplotype (haplotype number 16).

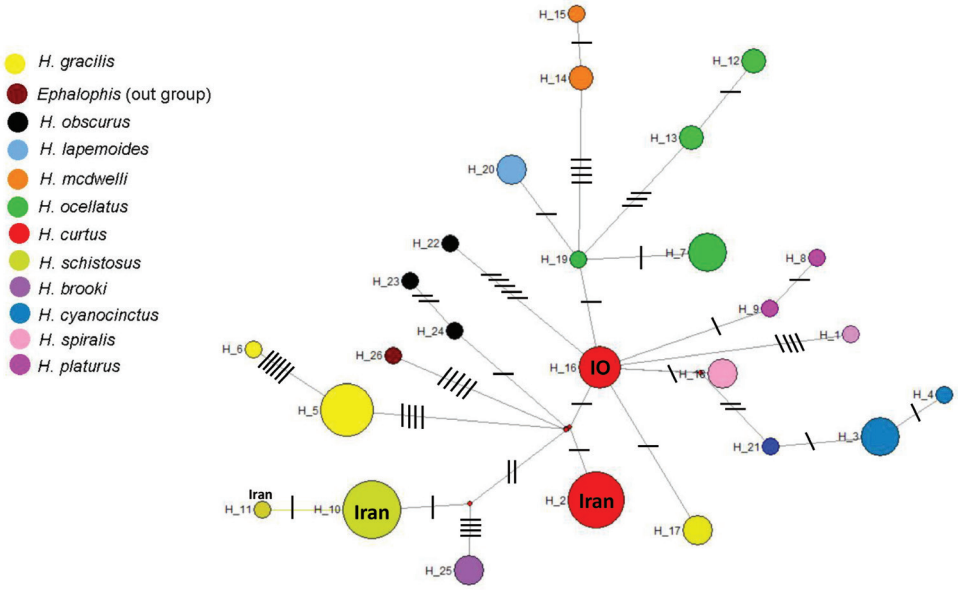

Figure 3. Haplotype network of the genus *Hydrophis* for the *16S* gene fragment. The haplotype colors correspond with the those in the molecular phylogenetic tree in Fig. 2.

Discussion

Sea snakes are one of the most interesting reptiles in biogeographic and phylogeographic studies (Ukuwela et al. 2022). A biogeographical study of the genus *Hydrophis* indicated that the diversification of true sea snakes has been the result of sea level changes during the last 2.5 million years (Ukuwela et al. 2016). Our molecular results indicate that the sea snakes in the Persian Gulf and Gulf of Oman share a genetic structure with Indian Ocean and Southeast Asian taxa (Fig. 2). Among them, *H. curtus* has differentiated relatively more than others, so that it may represent a genetically distinct species. Ukuwela et al. (2014) had the same findings for *H. curtus*. Genetic variation among Persian Gulf populations of *H. curtus* and other populations in southeast Asia (0.6% for *16S* and 6% for *COI*) indicate that the former may representative a new genetic lineage in Southwest Asia (Tables 1, 2). This variation among this taxon indicates that the threshold of genetic variation may reveal distinct populations at the species level, although this variation has not yet been established on the basis of morphology (Rezaie-Atagholipour et al. 2016).

A recent study on the genetic structure of *H. curtus* in the Indo-West Pacific revealed the presence of high variation among its populations. The phylogeny indicated that this species was affected by climatic fluctuations in late Pliocene and early Pleistocene (Ukuwela et al. 2014, 2022). Adding the Iranian dataset confirms that *H. curtus* populations in the Persian Gulf in the western part of its range have a close relationship with those in Sri Lanka and exhibit genetic variability greater than those populations in

Southeast Asia (Fig. 2). Other species of *Hydrophis* have not yet been studied, but our study indicates that their differentiation requires conducting a comprehensive study. However, the variation among populations of these species implies a pattern of variation in the Indian Ocean and West Pacific regions that may occur either in Sri Lanka or in the Persian Gulf as well (Lambeck 1996; Voris 2000; Lambeck et al. 2002).

Other species of the genus, *H. platurus*, *H. cyanocinctus*, *H. spiralis*, *H. ornatus*, *H. schistosus* and *H. gracilis*, included in the analyses, clearly placed within their conspecific Southeast Asian clades, and this may indicate high gene flow and recent (i.e. 10,000 years) dispersal from their source populations (Fig. 2). We assume that different local adaptations among *H. curtus* and the other six other taxa make them more variable.

The total diversity of the true sea snakes of the genus *Hydrophis* in the Persian Gulf and Gulf of Oman is 10 species (Rezaie-Atagholipour et al. 2016). According to the literature (Ukuwela et al. 2014; Rezaie-Atagholipour et al. 2016; Rajabizadeh 2019), *H. schistosus*, *H. viperinus*, *H. lapemiodes*, *H. cantoris*, *H. gracilis*, *H. spiralis*, and *H. platurus* are abundant in Gulf of Oman as opposed to the Persian Gulf, which means the species prefer to not inhabit the Gulf. But *H. curtus* and *H. ornatus* are mostly distributed in the Persian Gulf and in the Gulf of Oman. Our results revealed the variation between Persian Gulf and Southeast Asia population of *H. curtus* (6% genetic distance in the *COI* gene fragment) and reveals a new distinct genetic lineage. The genetic difference between DNA sequences of *H. curtus* populations in the Persian Gulf and Pacific Ocean is very likely due to genetic drift. In general, biodiversity conservation requires information (demographic and microhabitat information) from local populations. Only then we can encourage conservationists to reassess the status of the species in the Persian Gulf and the Gulf of Oman, because the latest International Union for the Conservation of Nature (IUCN) status of most species is Least Concern and one is Data Deficient (IUCN 2022).

Acknowledgements

We thank L. Lee Grismer, Ann Paterson, Aaron Bauer, and Kamelia Algiers who edited the early draft of the manuscript. This study was partially supported by Iran National Science Foundation (INSF) with project number of 99025967. Tissue samples were collected during field surveys financially supported by the Iranian UNDP/GEF/SGP (grant number: IRA/SGP/OP5/Y3/STAR/BD/13/12-188).

References

Bertozzi T, Sanders KL, Sistrom MJ, Gardner MG (2012) Anonymous nuclear loci in non-model organisms: Making the most of high-throughput genome surveys. Bioinformatics 28(14): 1807–1810. https://doi.org/10.1093/bioinformatics/bts284

Felsenstein J (1985) Confidence limits on phylogenies: An approach using the bootstrap. Evolution; International Journal of Organic Evolution 39(4): 783–791. https://doi.org/10.2307/2408678

Gasperetti J (1988) The snakes of Saudi Arabia. In: Büttiker W, Krupp F (Eds) Fauna of Saudi Arabia (Vol. 9). National Commission for Wildlife Conservation and Development (NCWCD), Riyadh, 169–450.

Hall TA (1999) BioEdit: A user-friendly biological sequence alignment editor and analysis program for Windows 95/98/NT. Nucleic Acids Symposium Series 41: 95–98.

Heatwole H (1999) Sea Snakes. University of New South Wales Press, Sydney.

IUCN (2022) The IUCN Red List of Threatened Species. Version 2022-2. [Accessed on 2023-01-10]

Kabir S, Shahriar M, Kabir AH, Uddin MG (2006) High salt SDS-based method for the direct extraction of genomic DNA from three different gram-negative organisms. CDR 1: 57–64.

Kocher TD, Thomas WK, Meyer A, Edwards SV, Pääbo S, Villablanca FX, Wilson AC (1989) Dynamics of mitochondrial DNA evolution in animals: Amplification and sequencing with conserved primers. Proceedings of the National Academy of Sciences of the United States of America 86(16): 6196–6200. https://doi.org/10.1073/pnas.86.16.6196

Lambeck K (1996) Shoreline reconstructions for the Persian Gulf since the last glacial maximum. Earth and Planetary Science Letters 142(1–2): 43–57. https://doi.org/10.1016/0012-821X(96)00069-6

Lambeck K, Esat TM, Potter EK (2002) Links between climate and sea levels for the past three million years. Nature 419(6903): 199–206. https://doi.org/10.1038/nature01089

Librado P, Rozas J (2009) DnaSP v5: A software for comprehensive analysis of DNA polymorphism data. Bioinformatics 25(11): 1451–1452. https://doi.org/10.1093/bioinformatics/btp187

Lukoschek V, Keogh JS (2006) Molecular phylogeny of sea snakes reveals a rapidly diverged adaptive radiation. Biological Journal of the Linnean Society. Linnean Society of London 89(3): 523–539. https://doi.org/10.1111/j.1095-8312.2006.00691.x

Natoli A, Phillips KP, Richardson DS, Jabado RW (2017) Low genetic diversity after a bottleneck in a population of a critically endangered migratory marine turtle species. Journal of Experimental Marine Biology and Ecology 491: 9–18. https://doi.org/10.1016/j.jembe.2017.01.009

Owfi F, Braulik GT, Rabbaniha M (2016) Species diversity and distribution pattern of marine mammals of the Persian Gulf and Gulf of Oman-Iranian waters. Iranian Journal of Fisheries Science 15: 927–944.

Rajabizadeh M (2019) The Snakes of Iran. Iranshenasi Press, Tehran.

Rezaie-Atagholipour M, Ghezellou P, Hesni MA, Dakhteh SMH, Ahmadian H, Vidal N (2016) Sea snakes (Elapidae, Hydrophiinae) in their westernmost extent: An updated and illustrated checklist and key to the species in the Persian Gulf and Gulf of Oman. ZooKeys 622: 129–164. https://doi.org/10.3897/zookeys.622.9939

Ronquist F, Teslenko M, Van Der Mark P, Ayres DL, Darling A, Höhna S, Huelsenbeck JP (2012) MrBayes 3.2: Efficient Bayesian phylogenetic inference and model choice across

a large model space. Systematic Biology 61(3): 539–542. https://doi.org/10.1093/sysbio/sys029

Sanders KL, Lee MS, Bertozzi T, Rasmussen AR (2013) Multilocus phylogeny and recent rapid radiation of the viviparous sea snakes (Elapidae: Hydrophiinae). Molecular Phylogenetics and Evolution 66(3): 575–591. https://doi.org/10.1016/j.ympev.2012.09.021

Sheppard CRC, Al-Husiani M, Al-Jamali F, Al-Yamani F, Baldwin R, Bishop J, Benzoni F, Dutrieux E, Dulvy NK, Durvasula SRV, Jones DA, Loughland R, Medio D, Nithyanandan M, Pilling GM, Polikarpov I, Price ARG, Purkis S, Riegl B, Saburova M, Namin KS, Taylor O, Wilson S, Zainal K (2010) The Gulf: A young sea in decline. Marine Pollution Bulletin 60(1): 13–38. https://doi.org/10.1016/j.marpolbul.2009.10.017

Silvestro D, Michalak I (2012) raxmlGUI: A graphical front-end for RAxML. Organisms, Diversity & Evolution 12(4): 335–337. https://doi.org/10.1007/s13127-011-0056-0

Stamatakis A (2006) RAxML-VI-HPC: Maximum likelihood-based phylogenetic analyses with thousands of taxa and mixed models. Bioinformatics 22(21): 2688–2690. https://doi.org/10.1093/bioinformatics/btl446

Tamura K, Stecher G, Peterson D, Filipski A, Kumar S (2013) MEGA6: Molecular evolutionary genetics analysis version 6.0. Molecular Biology and Evolution 30(12): 2725–2729. https://doi.org/10.1093/molbev/mst197

Udyawer V, Barnes P, Bonnet X, Brischoux F, Crowe-Riddell JM, D'anastasi B, Fry BG, Gillett A, Goiran C, Guinea ML, Heatwole H, Heupel MR, Hourston M, Kangas M, Kendrick A, Koefoed I, Lillywhite HB, Lobo AS, Lukoschek W, McAuley R, Nitschke C, Rasmussen AR, Sanders KL, Sheehy C III, Shine R, Somaweera R, Sweet SS, Voris HK (2018) Future directions in the research and management of marine snakes. Frontiers in Marine Science 5: e00399. https://doi.org/10.3389/fmars.2018.00399

Ukuwela KD, Sanders KL, Fry BG (2012) *Hydrophis donaldi* (Elapidae, Hydrophiinae), a highly distinctive new species of sea snake from northern Australia. Zootaxa 3201(1): 45–57. https://doi.org/10.11646/zootaxa.3201.1.3

Ukuwela KD, de Silva A, Fry BG, Sanders KL (2014) Multilocus phylogeography of the sea snake *Hydrophis curtus* reveals historical vicariance and cryptic lineage diversity. Zoologica Scripta 43(5): 472–484. https://doi.org/10.1111/zsc.12070

Ukuwela KD, Lee MS, Rasmussen AR, De Silva A, Fry BG, Ghezellou P, Sanders KL (2016) Evaluating the drivers of Indo-Pacific biodiversity: speciation and dispersal of sea snakes (Elapidae: Hydrophiinae). Journal of Biogeography 43(2): 243–255. https://doi.org/10.1111/jbi.12636

Ukuwela KDB, de Silva A, Sivaruban A, Sanders KL (2022) Diversity, distribution, and natural history of the marine snakes of Sri Lanka. Marine Biodiversity 52(2): 1–24. https://doi.org/10.1007/s12526-022-01259-3

Voris HK (1972) The role of sea snakes (Hydrophiidae) in the trophic structure of coastal ocean communities. Journal of the Marine Biological Association of India 14: 429–442.

Voris HK (2000) Maps of Pleistocene sea levels in Southeast Asia: Shorelines, river systems and time durations. Journal of Biogeography 27(5): 1153–1167. https://doi.org/10.1046/j.1365-2699.2000.00489.x

Supplementary material 1

Information of sequences used in this study and those obtained from GenBank

Authors: Seyyed Saeed Hosseinian Yousefkhani, Amaal Yasser, Murtada Naser, Mohsen Rezaie-Atagholipour, Majid Askari Hesni, Fariba Yousefabadi, Eskandar Rastegar Pouyani

Data type: occurences, accession numbers

Explanation note: Information of sequences used in this study and those obtained from GenBank (sequences with an asterisk, *). Accession numbers for the sequences added to the table. Accession numbers in red related to the new sequences of this study.

Link: https://doi.org/10.3897/zookeys.1158.101347.suppl1

Supplementary material 2

Bayesian tree of COI gene fragment that clearly shows variation in *Hydrophis curtus* clade

Authors: Seyyed Saeed Hosseinian Yousefkhani, Amaal Yasser, Murtada Naser, Mohsen Rezaie-Atagholipour, Majid Askari Hesni, Fariba Yousefabadi, Eskandar Rastegar Pouyani

Data type: figure

Link: https://doi.org/10.3897/zookeys.1158.101347.suppl2

ZooKeys 1158: 133–146 (2023)
doi: 10.3897/zookeys.1158.100396
https://zookeys.pensoft.net

RESEARCH ARTICLE

A peer-reviewed open-access journal
ZooKeys
Launched to accelerate biodiversity research

Opacoptera Gozmány (Lepidoptera, Lecithoceridae) from China, with descriptions of four new species

Shuai Yu[1,2], Shuxia Wang[2]

1 *School of Life Sciences, Liaocheng University, Liaocheng 252000, China* **2** *College of Life Sciences, Nankai University, Tianjin 300071, China*

Corresponding author: Shuxia Wang (shxwang@nankai.edu.cn)

Academic editor: Mark Metz | Received 11 January 2023 | Accepted 24 March 2023 | Published 21 April 2023

https://zoobank.org/649720BF-A67C-4633-B29C-9594C807B3E3

Citation: Yu S, Wang S (2023) *Opacoptera* Gozmány (Lepidoptera, Lecithoceridae) from China, with descriptions of four new species. ZooKeys 1158: 133–146. https://doi.org/10.3897/zookeys.1158.100396

Abstract

The genus *Opacoptera* Gozmány, 1978 is reviewed. Four species are described as new: *O. condensata* **sp. nov.**, *O. hybocentra* **sp. nov.**, *O. introflexa* **sp. nov.** and *O. longissima* **sp. nov.** *Opacoptera kerastiodes* Park, 2021 is newly recorded for China. Images of adults are provided, along with a key to the males of all the known species.

Keywords

Gelechioidea, identification key, Lecithocerinae, new record, taxonomy

Introduction

Opacoptera is a small genus classified in the subfamily Lecithocerinae. Gozmány (1978) established the genus for the single species *Lecithocera callirrhabda* Meyrick, 1936 from China, the type species. Species of *Opacoptera* are known only from the Oriental Region. Wu and Liu (1992) and Wu (1996) described two Chinese species in the genus, *O. flavicana* Wu & Liu, 1992 and *O. ecblasta* Wu, 1996. Park and Kim (2021) described an additional species, *O. kerastiodes* Park, 2021, from Thailand. *Opacoptera* currently comprises four described species.

The aim of this paper is to review the genus *Opacoptera* and to describe four new species.

Materials and methods

Specimens were collected in China since 1998 using light traps. Wingspan was measured from the tip of the left forewing to the tip of the right forewing. Genitalia slides were prepared following the methods introduced by Li (2002). All images were captured with digital microscopes (Leica M205A and Leica DM750), coupled with the Leica Application Suite 4.2 software. Terminology follows Gozmány (1978). The male and female genitalia are described from the ventral view.

All the specimens examined, including the type series of the new species, are deposited in the Insect Collection of Nankai University, Tianjin, China (NKU).

Abbreviations

NHMUK	Natural History Museum, London, United Kingdom
IZCAS	Institute of Zoology, Chinese Academy of Science, Beijing, China
NKU	Insect Collection of Nankai University, Tianjin, China
TD	Type depository
TL	Type locality
ZMUC	Zoological Museum, Natural History Museum of Denmark, Copenhagen, Denmark

Taxonomic accounts

Opacoptera Gozmány, 1978

Opacoptera Gozmány, 1978. Type species: *Lecithocera callirrhabda* Meyrick, 1936, by monotypy.

Generic characters. Antenna as long as or slightly longer than forewing. Labial palpus with second palpomere thickened, third palpomere slender. Forewing narrowly elongate, usually dark brown with black patches; R_1, R_2 and R_3 free, R_4 and R_5 stalked, M_1, M_2 and M_3 separate, CuA_1 and CuA_2 short-stalked (Fig. 1) or separate (Fig. 2). Hindwing trapezoidal; M_2 present, M_3 and CuA_1 coincident. All abdominal tergites with zones of spiniform setae.

Male genitalia. Cucullus narrowed, usually with a ventrobasal process. Juxta with horn-shaped or needle-like posterior lobes extending dorsad and smaller posterolateral lobes extending laterally. Aedeagus with two dorsal denticles; cornuti spiniform or needle-like.

Female genitalia. Antrum sclerotized along posterior margin forming a band. Signa of corpus bursae usually consisting of several teeth and a denticulate plate.

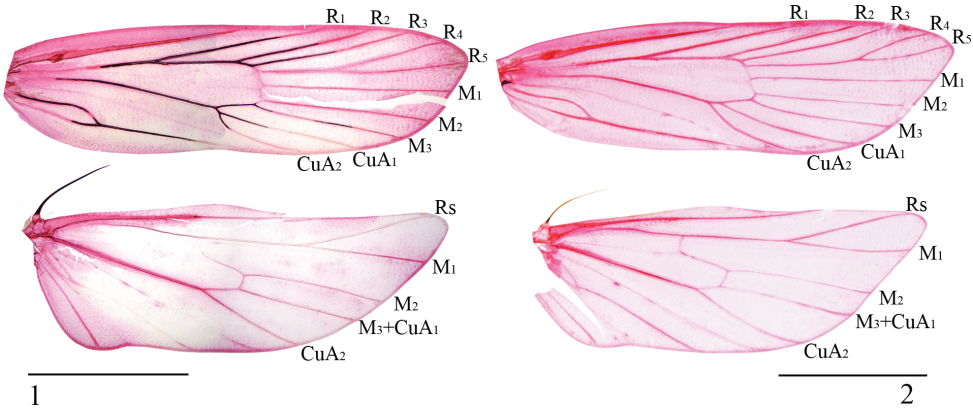

Figures 1, 2. Wing venation of *Opacoptera* spp. **1** *O. condensata* sp. nov., holotype, male, slide No. LSR12090 **2** *O. hybocentra* sp. nov., paratype, male, slide No. YS19431. Scale bars: 2.0 mm.

Diagnosis. The genus is close to the monotypic genus, *Monerista* Meyrick, 1925. It can be distinguished by the trapezoidal hindwing without streak; whereas in *Monerista*, the lanceolate hindwing has a thinly scaled submedian streak (Clarke 1965: 183, fig. 1)

Distribution. China (Gozmány 1978; Wu and Liu 1992; Wu 1996), Thailand (Park and Kim 2021).

Remarks. The generic characters of *Opacoptera* were originally defined by Gozmány (1978) based on the type species, *Opacoptera callirrhabda* (Meyrick, 1936). Wu (1996) gave the female characters of the genus. In this paper, we revised the generic characters including the forewing venation, male and female genitalia after examining all species of the genus.

Key to the males of *Opacoptera*

1 Forewing pale, yellowish brown; juxta without posterior lobes (Fig. 6) ..... ***O. flavicana***

– Forewing dark; juxta with posterior lobes..... **2**

2 Apices of posterior lobes of juxta extending posteriorly well beyond middle of tegumen (Fig. 17) ..... ***O. longissima* sp. nov.**

– Apices of posterior lobes of juxta extending posteriorly to anterior margin of tegumen or only slightly beyond..... **3**

3 Inner margin of base of posterior lobes of juxta with medial, triangular projection (Fig. 15) ..... ***O. introflexa* sp. nov.**

– Posterior lobes of juxta smooth on inner margin..... **4**

4 Posterior lobes of juxta needle-like; uncus longer than width (Fig. 13)..... ***O. ecblasta***

– Posterior lobes of juxta horn-shaped; uncus wider than length..... **5**

5 Length of ventrobasal process on cucullus greater than basal width of cucullus (Fig. 14)..... ***O. hybocentra* sp. nov.**
– Length of ventrobasal process on cucullus less than basal width of cucullus.....**6**
6 Cucullus widened or dilated apically (Fig. 16) ..... ***O. kerastiodes***
– Cucullus slightly narrowed apically.....**7**
7 Juxta incised in triangle at middle on posterior margin; posterior lobes straight (Fig. 11).....***O. callirrhabda***
– Juxta broadly concave on posterior margin; posterior lobes curved laterally at middle (Fig. 12).....***O. condensata* sp. nov.**

Opacoptera callirrhabda (Meyrick, 1936)

Figs 3, 11, 18

Lecithocera callirrhabda Meyrick, 1936: 158. TL: China (Yunnan). TD: NHMUK.
Opacoptera callirrhabda (Meyrick): Gozmány, 1978: 179.

Material examined. China: 1♀, 30.vii.2014, 3♂, 2–3.viii.2014, Yunnan, Dali, Mt. Weibao, 2205 m, KJ Teng et al. leg., slide nos. YS19428♂, YS19435♀.

Diagnosis. This species is diagnostic in the male genitalia by the juxta incised at middle in a triangle on the posterior margin (Fig. 11). It is similar to *O. condensata* sp. nov., and the differences between them are stated in the diagnosis of the latter species.

Description. Wingspan 13.5–15.0 mm (Fig. 3).

Female genitalia (Fig. 18). Eighth abdominal sternite obtuse on posterior margin. Apophyses posteriores twice length of apophyses anteriores. Antrum cup-shaped, wrinkled, membranous except sclerotized along posterior margin forming a band. Ductus bursae subelliptical, slightly wider than corpus bursae, partly wrinkled anteriorly; ductus seminalis broad basally, slender distally. Corpus bursae elliptical; signa placed medially, consisting of five teeth in a longitudinal row and a small rounded, denticulate plate.

Distribution. China (Sichuan, Yunnan) (Gozmány 1978; Wu 1996).

Remarks. Meyrick (1936) described this species based on five male specimens (one from Shandong, two from Shaanxi and Yunnan, respectively) and placed it in the genus *Lecithocera*. Clarke (1965) assigned one of the specimens from Yunnan as the lectotype according to the original description. Gozmány (1978) noted that only the two specimens from Yunnan were conspecific. He also hypothesized that they were distinct from *Lecithocera*, so diagnosed the genus *Opacoptera* and placed the species therein. Wu (1996) was first to described the female of *O. callirrhabda* based on specimens with associated males collected at different times and from different localities of Sichuan. According to the description and the drawing given by Wu (1996), the female genitalia of *O. callirrhabda* has a narrowed ductus bursae and a single signum. However, the female of the species examined in this study from Yunnan is quite different, and we describe it herein.

Figures 3–10. Dorsal habitus of *Opacoptera* spp. **3** *O. callirrhabda* (Meyrick, 1936), female, YS19435 **4** *O. condensata* sp. nov., paratype, female, LSR13198 **5** *O. ecblasta* Wu, 1996, male, LSR11240 **6** *O. flavicana* Wu & Liu, 1992, female, LSR11247 **7** *O. hybocentra* sp. nov., holotype, male, YS19424 **8** *O. introflexa* sp. nov., paratype, male **9** *O. kerastiodes* Park, 2021, male, YS19048 **10** *O. longissima* sp. nov., paratype, male. Scale bars: 2.0 mm.

Opacoptera condensata **Yu & Wang, sp. nov.**
https://zoobank.org/BC7D6FE9-EABC-4BE8-B186-0A95C9CA359B
Figs 4, 12, 19

Type material. ***Holotype*****: China:** ♂, Chongqing, Mt. Simian (29°19'N, 106°22'E), 1280 m, 14.vii.2012, YH Sun & AH Yin leg., slide No. LSR12090♂. ***Paratypes*****: China:** 9♂1♀, 1280 m, 12–14.vii.2012, 9♂2♀, 900 m, 18–19.vii.2012, same locality and collector as holotype, slide No. YS19556♂; 12♂3♀, Zhejiang, Mt. Tianmu, 555 m, 3–6.vii.2014, AH Yin, XM Hu & QY Wang leg., slide No. YS19427♂; 1♂, Jiangxi, Xiaoxidong, 8.vii.1978, slide No. ZYM06008; 25♂, Henan, Neixiang, Xiaguan, 650 m, 10–12.vii.1998, HH Li et al. leg., slide Nos. LSR11295, ZYM05011, ZYM05052, ZYM0505, ZYM05054, ZYM06202, ZMR09020; 2♂2♀, Hubei, Zhuxi County, Quanxi Town, 868 m, 10–11.vii.2017, WD Qi et al. leg., slide Nos. YS17039♀, YS17040♀, YS17041♂, YS17042♂; 3♀, Hubei, Zhuxi County, Mt. Bagua, 790 m, 12–13.vii. 2017, WD Qi et al. leg., slide Nos. YS17055, YS17056, YS17057; 4♂4♀, Yunnan, Weishan County, Mt. Weibao, 2200 m, 20.vii.2001, HH Li & XP Wang leg., slide Nos. ZMR09017♂, ZYM06092♂, ZYM06198♂, ZYM06199♀; 5♂2♀, Yunnan, Weishan County, Mt. Weibao, 2244 m, 22–24.vii.2013, SR Liu, YQ Wang & KJ Teng leg., slide Nos. LSR13197♂, LSR13198♀; 12♂4♀, Shaanxi, Houzhenzi, 1330 m, 23–24.vii.2018, YY Li & JL Zhuang leg., slide No. YS19433♂, YS19434♀.

Diagnosis. The male genitalia of the new species is similar to that of the type species, *O. callirrhabda* (Meyrick, 1936). It can be distinguished by the forewing having two black patches, CuA_1 stalked with CuA_2, and ductus seminalis having dense granules; in *O. callirrhabda*, the forewing has no black patches, CuA_1 and CuA_2 are separate, and the ductus seminalis has no granules.

Description. Wingspan 13.0–15.0 mm (Fig. 4). Head dark brown. Antenna yellowish brown in basal 1/4, pale yellow in distal 3/4. Labial palpus yellowish brown, paler on inner surface; third palpomere as long as second palpomere. Thorax and tegula dark brown. Forewing dark brown, with two large, elliptical, black patches anteriorly reaching anterior margin of discal cell: first at basal 1/4, posteriorly reaching fold; second at middle, posteriorly reaching above dorsum; fringe dark brown; CuA_1 and CuA_2 short-stalked. Hindwing and fringe greyish brown; fringe with an orange white basal line.

Male genitalia (Fig. 12). Uncus subcrescent. Gnathos with basal plate bell-shaped, bearing a papillary process at middle on posterior margin; median process wide in basal 1/3, narrowed to distal 2/5, thereafter slender to pointed apex, curved ventrad at distal 1/4 by a right angle. Valva wide in basal 1/4, narrowed slightly to cucullus; cucullus about half length of valva, narrowed slightly to obtusely oblique apex, costal margin shallowly concave except convex at base, ventrobasal process subtriangular, with a rounded apex; costal bar narrow, slightly expanded dorsad medially; sacculus a broad band, about 1/4 length of ventral margin of valva. Saccus rounded on anterior margin.

Juxta broadly concave on posterior margin, denticulate along lateral sides of concavity; with a trapezoidal process at middle on anterior margin; posterior lobe strongly horn-shaped, curved outward at middle; posterolateral lobe short, narrow, extending laterally. Aedeagus nearly as long as valva, slightly widened medially, dorsal denticles larger than cornuti; cornuti consisting of 1–3 conic spines.

Female genitalia (Fig. 19). Eighth abdominal sternite convex on posterior margin. Apophyses posteriores twice the length of apophyses anteriores. Antrum subrectangular, wrinkled, membranous except sclerotized along posterior margin forming a band. Ductus bursae narrowed posteriorly, widened distinctly toward corpus bursae, with diffused granules near base of ductus seminalis; ductus seminalis broad, with dense granules on inner wall. Corpus bursae large, elliptical; with two signa: one elliptical, with dense denticles, the other plate-shaped, bearing 3–6 teeth (Fig. 19a, b).

Distribution. China (Chongqing, Henan, Hubei, Jiangxi, Shaanxi, Yunnan, Zhejiang).

Etymology. The specific epithet is derived from the Latin *condensatus*, referring to the dense granules in the ductus seminalis.

Opacoptera ecblasta Wu, 1996

Figs 5, 13

Opacoptera ecblasta Wu, 1996: 12. TL: China (Sichuan). TD: IZCAS.

Material examined. China: 1♂, Hubei, Xianfeng, Mahexiang, 400 m, 24.vii.1999, HH Li et al. leg., slide No. LSR11174; 3♂, Chongqing, Mt. Jinfo, 1100 m, 6–7. viii.2012, XF Yang & TT Liu leg.; 2♂, Chongqing, Mt. simian, 1280 m, 11–12. viii.2012, XF Yang & TT Liu leg.; 9♂, Guizhou, Mayanghe, 430 m, 5–10.vi.2007, XC Du leg., slide Nos. LSR11239, LSR11240, LSR14013; 1♂, 28.ix.2007, 1♂, 1.x.2007, Guizhou, Mayanghe, 700 m, H Zhen leg.; 3♂, Guizhou, Xishui County, 500 m, 24, 26.ix.2000, HL Yu leg.; 2♂, Guizhou, Xishui County, 500 m, 31.v.2000, YL Du leg., slide No. ZMR09041; 1♂, Guizhou, Chishui, Suoluo, 240 m, 23.ix.2000, HL Yu leg.; 1♂, Guizhou, Chishui, Suoluo, 390 m, 27.v.2000, YL Du leg.; 3♂, Yunnan, Malipo County, Xiajinchang, 1470 m, 26, 29.vii.2016, KJ Teng, GE Lee & T Wang leg., slide No. YS19423; 11♂, Yunnan, Daozhen County, Xiannvdong, 600 m, 17–18.viii.2004, YL Xiao leg., slide No. LSR13339.

Diagnosis. This species is similar to *O. kerastiodes* Park, 2021 both in appearance and male genitalia. It can be distinguished by the third palpomere of the labial palpus with hair-pencils, the heart-shaped uncus and the needle-like posterior lobes of the juxta (Fig. 13); in *O. kerastiodes*, the third palpomere of the labial palpus is smooth, the uncus is subrectangular, and the posterior lobes of the juxta are horn-shaped.

Description. Wingspan 11.0–13.5 mm (Fig. 5).

Distribution. China (Chongqing, Guizhou, Hubei, Sichuan, Yunnan).

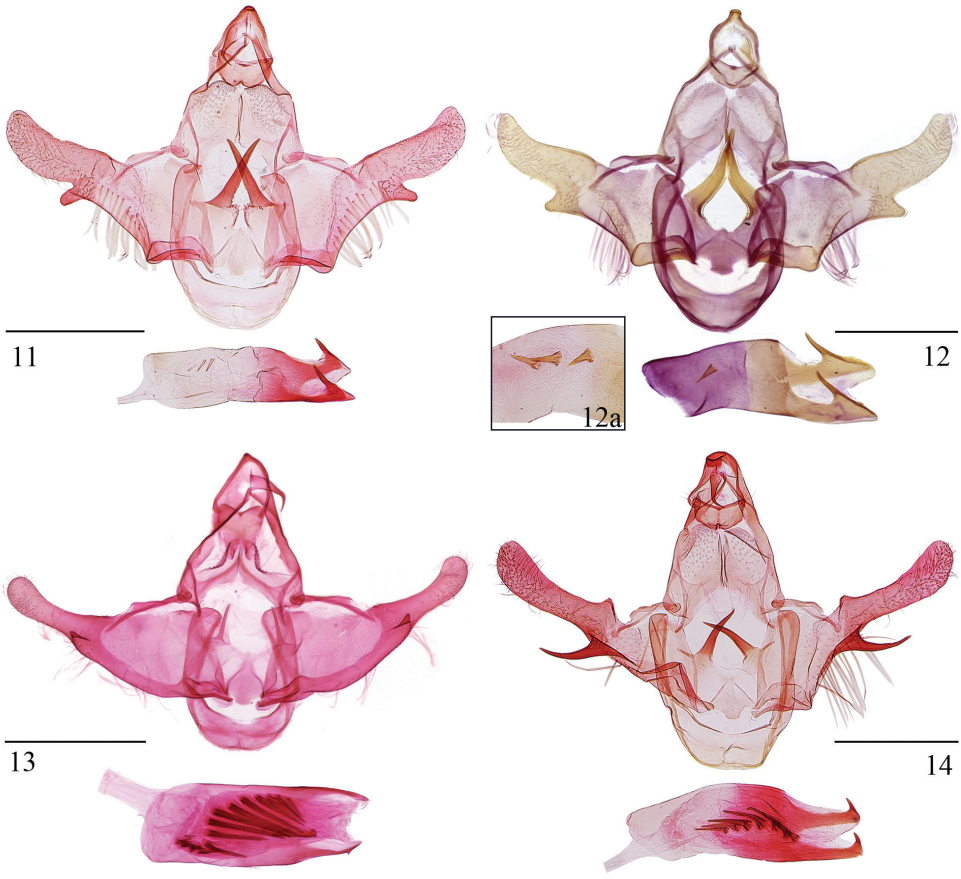

Figures 11–14. Male genitalia of *Opacoptera* spp. **11** *O. callirrhabda* (Meyrick, 1936), slide No. YS19428 **12** *O. condensata* sp. nov., holotype, slide No. LSR12090 **12a** cornuti of *O. condensata* sp. nov., paratype, slide No. YS17042 **13** *O. ecblasta* Wu, 1996, slide No. LSR14013 **14** *O. hybocentra* sp. nov., holotype, slide No. YS19424. Scale bars: 0.5 mm.

Opacoptera flavicana Wu & Liu, 1992

Figs 6, 20

Opacoptera flavicana Wu & Liu, 1992 in Peng and Liu 1992: 618. TL: China (Hunan). TD: IZCAS.

Material examined. China: 1♀, Guizhou, Mt. Fanjing, 1700 m, 1.vi.2002, XP Wang leg., slide No. LSR11247.

Diagnosis. This species can be distinguished from its congeners by the pale yellowish brown forewing, the juxta without posterior lobes in the male genitalia (Wu and Liu 1992: 681, fig. 2148), and the corpus bursae with a single signum in the female genitalia (Fig. 20).

Description. Wingspan 16.0 mm (Fig. 6).

Distribution. China (Guizhou, Hunan).

Remarks. Wu and Liu (1992) described the species from Hunan, China on a male and four females, and placed it in the genus *Opacoptera* based mainly on the wing venation. But the species seems distinctive in the genus *Opacoptera* both in appearance and genitalia as stated in the diagnosis. It probably does not belong to the present genus and the taxonomic status needs further study.

***Opacoptera hybocentra* Yu & Wang, sp. nov.**

https://zoobank.org/B6432DFD-7F96-4055-BFC4-505F86CAD05C

Figs 7, 14, 21

Type material. ***Holotype*: China:** ♂, Yunnan, Baoshan, Nankang (24°49'N, 98°47'E), 2009 m, 20.vii.2015, KJ Teng & X Bai leg., slide No. YS19424. ***Paratypes*: China, Yunnan:** 39♂27♀, same data as holotype except dated 16–20.vii.2015, slide Nos. YS19431♂, YS19432♀; 1♂3♀, 10, 17.viii.2014, KJ Teng et al. leg., other same data as holotype; 2♂1♀, Longling County, Mt. Xiaohei, 1974 m, 18–19.vii.2013, SR Liu et al. leg., slide Nos. LSR13199♂, LSR13208♂, LSR13214♀; 1♂, Longling County, Mt. Xiaohei, 1974 m, 30.vii.2015, KJ Teng & X Bai leg.

Diagnosis. The male genitalia of the new species is similar to that of *O. introflexa* sp. nov. It can be distinguished by the forewing having CuA_1 and CuA_2 separate and the horn-shaped ventrobasal process of the cucullus; in *O. introflexa* sp. nov., the forewing has veins CuA_1 and CuA_2 stalked and the ventrobasal process of the cucullus is broadly rounded, thumb shaped.

Description. Wingspan 12.0–13.5 mm (Fig. 7). Head dark brown. Antenna with scape yellowish brown, flagellum pale brownish yellow. Labial palpus pale brownish yellow, third palpomere as long as second palpomere. Thorax and tegula dark brown. Forewing dark brown, with two black patches: one at basal 1/4, elliptical, the other at middle, shape ill-defined; fringe yellowish brown; CuA_1 and CuA_2 separate. Hindwing and fringe pale brownish yellow except yellowish brown around apical area.

Male genitalia (Fig. 14). Uncus wide, shallowly concave on posterior margin, obtuse on anterior margin; caudal lobe papillary. Gnathos with basal plate obtuse on posterior margin; median process wide at base, narrowed to distal 1/3 where it curves, distal 1/3 spine-shaped. Valva wide basally, narrowed distinctly to cucullus; cucullus about half length of valva, parallel-sided in basal half, widened slightly to obtuse apex, costal margin shallowly concave except gently produced at base; ventrobasal process horn-shaped, curved, longer than basal width of cucullus; costal bar narrow, slightly expanded dorsad medially; sacculus wide, about 1/4 length of ventral margin of valva. Saccus obtuse on anterior margin. Juxta subquadrate, broadly concave on posterior margin, obtusely produced at middle on anterior margin; posterior lobe large, horn-shaped, nearly as long as juxta; posterolateral lobe short, spiniform, extending posterolaterally. Aedeagus slightly shorter than valva, slightly widened medially, with two

dorsal denticles; cornuti consisting of six large, needle-like spines running from basal 1/3 to 2/3.

Female genitalia (Fig. 21). Eighth abdominal sternite obtusely rounded on posterior margin. Apophyses posteriores about 1.5 times length of apophyses anteriores. Antrum funnel-shaped, wrinkled, membranous except sclerotized along posterior margin forming a band. Ductus bursae narrowed posteriorly, widened toward corpus bursae; ductus seminalis broad, roundly sac-like and bearing dense spinules basally. Corpus bursae ovate; signa consisting of six small teeth in a longitudinal row and a rounded, densely denticulate plate.

Distribution. China (Yunnan).

Etymology. The specific name is derived from the Latin *hybocentrus*, referring to the curved ventrobasal process of the cucullus.

***Opacoptera introflexa* Yu & Wang, sp. nov.**

https://zoobank.org/2B567F45-C597-4898-BEF4-F4A8682A337E

Figs 8, 15, 22

Type material. ***Holotype*: China:** ♂, Baoshan, Baihualing, Hanlongzhai (25°18'N, 98°49'E), 1577 m, 2.viii.2015, KL Liu & JX Zhao leg., slide No. YS19429. ***Paratypes*: China:** 1♂11♀, same data as holotype, slide No. YS19430♀; 9♂1♀, Yunnan, Gongshan County, Naqiutong Village, 1767 m, 16–18.vi.2017, KJ Teng et al. leg., slide No. YS19426♂.

Diagnosis. The new species is unique among other species in the genus by having a triangular process at the base of the posterior lobe of the juxta at the inner margin. It is similar to *O. hybocentra* sp. nov., and the differences between them are stated in the diagnosis of the latter species.

Description. Wingspan 13.0–13.5 mm (Fig. 8). Head dark brown. Antenna with scape brownish yellow; flagellum orange yellow. Labial palpus orange yellow except dark brown ventrally on third palpomere; third palpomere as long as second palpomere. Thorax and tegula dark brown. Forewing dark brown, with two, narrow black patches, one at the basal 1/4 and one in the middle, distal 1/3 with diffused black scales; fringe dark brown; CuA_1 and CuA_2 short-stalked. Hindwing and fringe brown.

Male genitalia (Fig. 15). Uncus subcrescent, broad V-shaped on posterior margin. Gnathos with median process slightly broad in basal 1/3, thereafter slendered to pointed apex, curved ventrad at distal 1/3 by a right angle. Valva wide in basal 1/4, narrowed distinctly to cucullus; cucullus about half length of valva, almost tubular, apex obtuse, costal margin shallowly concave, ventrobasal process thumbed; costal bar narrow, expanded dorsad medially; sacculus wide in basal half, slender in distal half, reaching cucullus. Saccus obtuse on anterior margin. Juxta subquadrate, broadly concave on posterior margin, densely denticulate along lateral sides of concavity; anterior margin obtusely produced at middle; posterior lobe large horn-shaped, longer than juxta, curved inward, triangularly produced at base on inner margin; posterolateral

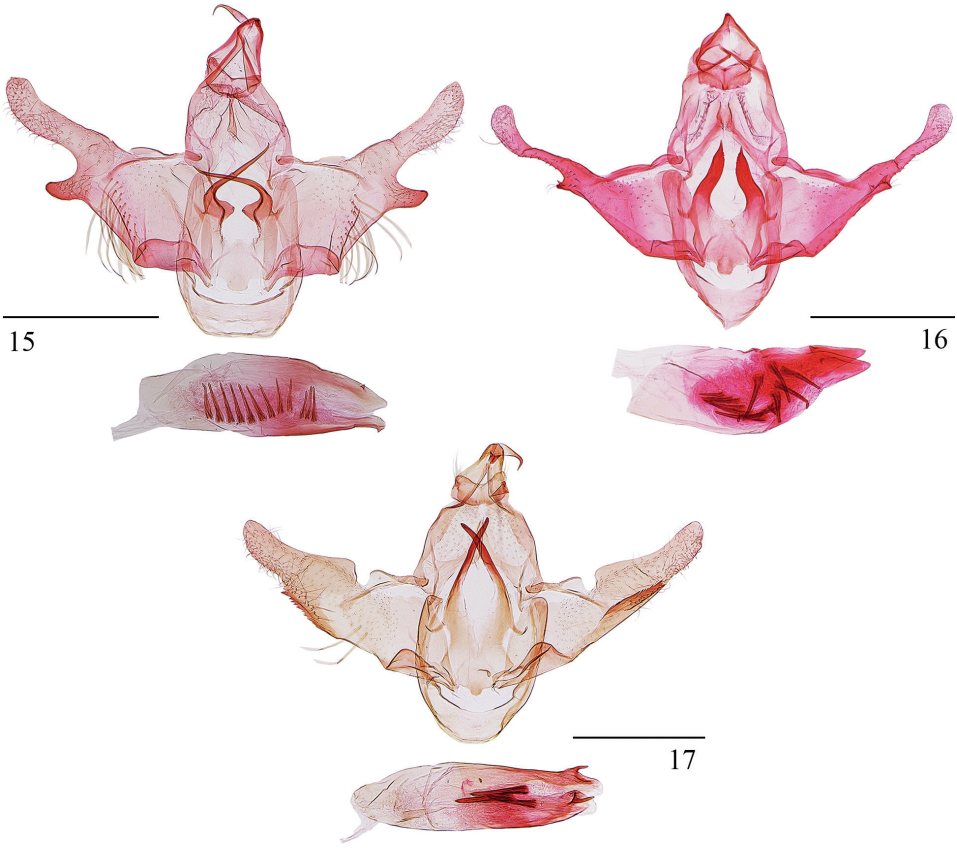

Figures 15–17. Male genitalia of *Opacoptera* spp. **15** *O. introflexa* sp. nov., holotype, slide No. YS19429 **16** *O. kerastiodes* Park, 2021, slide No. YS19048 **17** *O. longissima* sp. nov., holotype, slide No. YS19422. Scale bars: 0.5 mm.

lobe small, spiniform. Aedeagus shorter than valva, slightly widened medially, with two tiny dorsal denticles; cornuti consisting of more than ten large, needle-like spines running from basal 1/4 to 3/4.

Female genitalia (Fig. 22). Eighth abdominal sternite obtuse on posterior margin, with a sclerotized sac at anterolateral corner. Apophyses posteriores about twice length of apophyses anteriores. Antrum membranous except sclerotized along posterior margin forming a band, with two symmetrically sclerotized, leaf-like sclerites medially. Ductus bursae wrinkled, narrowed posteriorly, widened toward corpus bursae, with numerous conic spinules in anterior 3/5; ductus seminalis broad, arising from ductus bursae anteriorly, with sparse thorns on inner wall. Corpus bursae elliptical; signa consisting of several teeth of varied size in a longitudinal row placed posteriorly and a densely denticulate plate placed at middle.

Distribution. China (Yunnan).

Etymology. The specific epithet is derived from the Latin *introflexus*, referring to the medially curving posterior lobes of the juxta.

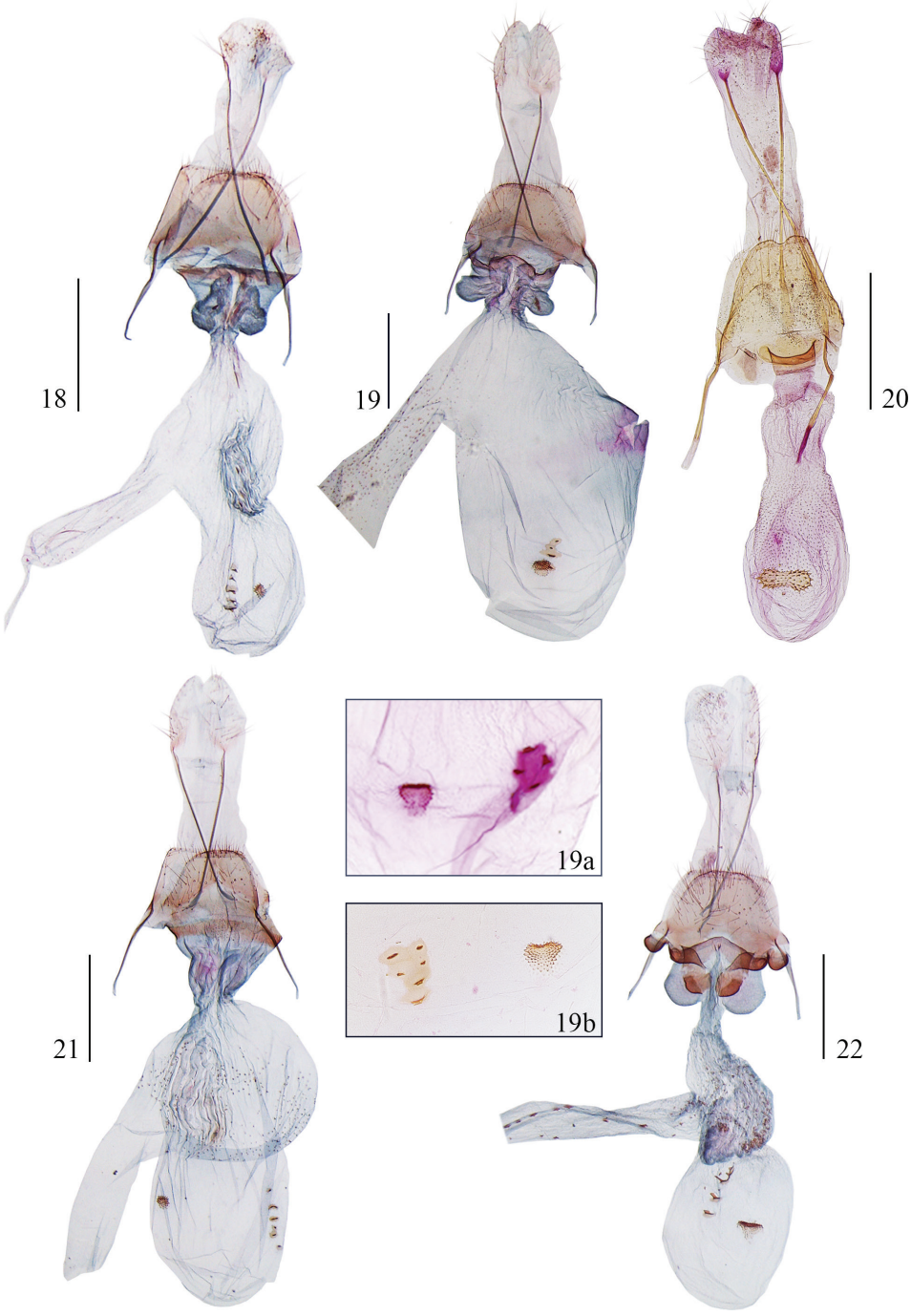

Figures 18–22. Female genitalia of *Opacoptera* spp. **18** *O. callirrhabda* (Meyrick, 1936), slide No. YS19435 **19** *O. condensata* sp. nov., paratype, slide No. YS19434 **19a** signa of *O. condensata* sp. nov., slide No. LSR11297 **19b** signa of *O. condensata* sp. nov., slide No. YS17057 **20** *O. flavicana* Wu & Liu, 1992, slide No. LSR11247 **21** *O. hybocentra* sp. nov., paratype, slide No. YS19432 **22** *O. introflexa* sp. nov., paratype, slide No. YS19430. Scale bars: 0.5 mm.

***Opacoptera kerastiodes* Park, 2021**
Figs 9, 16

Opacoptera kerastiodes Park, 2021 in Park and Kim 2021: 175. TL: Thailand (Chiang Mai). TD: ZMUC.

Material examined. China: 1♂, 31.vii.2019, 2♂, 2.viii.2019, Yunnan, Menghai County, Damanlu Village, 1128 m, KJ Teng et al. leg., slide No. YS19048.

Description. Wingspan 12.5–13.0 mm (Fig. 9).

Diagnosis. This species is distinct among other species by having a clavate valva (Fig. 16). It is similar to *O. ecblasta* Wu, 1996, and the differences between them are stated in the diagnosis of the latter species.

Distribution. China (Yunnan, new record), Thailand (Park and Kim 2021).

Remarks. This species was originally described from Thailand based on a single male. It is recorded from China for the first time in this paper.

***Opacoptera longissima* Yu & Wang, sp. nov.**
https://zoobank.org/D99A862A-F378-4A30-A9EE-FA2A109FDAC8
Figs 10, 17

Type material. *Holotype*: China: ♂, Yunnan, Tengchong, Cuanlong Village (25°19'N, 98°42'E), 1329 m, 10.viii.2015, KL Liu & JX Zhao leg., slide No. YS19422. ***Paratypes*: China:** 2♂, same data as holotype.

Diagnosis. The new species can be distinguished from its congeners by the ventrobasally serrate cucullus and the apices of the posterior lobes of the juxta extending beyond the middle of the tegumen.

Description. Wingspan 13.0–14.0 mm (Fig. 10). Head dark brown. Antenna orange yellow, paler distally. Labial palpus orange yellow except third palpomere dark brown ventrally; third palpomere as long as second palpomere. Thorax and tegula dark brown. Forewing dark brown, with diffused black scales distally; with two ill-defined black patches at basal 1/4 and middle respectively; fringe dark brown; CuA_1 and CuA_2 short-stalked. Hindwing and fringe brown; fringe with an orange white basal line.

Male genitalia (Fig. 17). Uncus subrectangular, semicircularly concave on posterior margin; caudal lobe seimiovate. Gnathos with median process wide at base, narrowed to middle, slendered from middle to pointed apex, curved ventrad at distal 1/4 by a right angle. Valva wide at base, narrowed slightly to cucullus; cucullus about half length of valva, narrowed to obtusely rounded apex, costal margin expanded dorsad basally, ventral margin serrate ventrobasally and gently concave at middle; costal bar narrow, slightly arched, triangularly produced at middle on dorsal margin; sacculus narrow basally, widened distally, about 1/4 length of ventral margin of valva. Saccus rounded on anterior margin. Juxta deeply concave in V-shape on posterior margin, with a papillary process at middle on anterior margin; posterior lobe large horn-shaped, extending beyond middle of tegumen apically; posterolateral lobe small,

narrowly banded, extending posterolaterally. Aedeagus nearly as long as valva, slightly widened medially, with two dorsal denticles; cornuti consisting of three large needle-like spines.

Female unknown.

Distribution. China (Yunnan).

Etymology. The specific name is derived from the Latin *longissimus*, referring to the long posterior lobe of the juxta.

Acknowledgements

We would like to express our cordial thanks to all the team members for their participating in the field collection. This study is supported by the National Key Research and Development Program "Intergovernmental Cooperation on International Science and Technology Innovation" Special Project of the Ministry of Science and Technology of China (No. 2022YFE0115200).

References

Clarke JFG (1965) Catalogue of the Type Specimens of Microlepidoptera in the British Museum (Natural History) Described by Edward Meyrick. Vol. 5. Trustees of the British Museum Natural History, London, 581 pp.

Gozmány L (1978) Lecithoceridae. In: Amsel HG, Reisser H, Gregor F (Eds) Microlepidoptera Palaearctica. Georg Fromme & Co., Wien, 5, 306 pp.

Li HH (2002) The Gelechiidae of China (I) (Lepidoptera: Gelechioidea). Nankai University Press, Tianjin, 504 pp.

Meyrick E (1936) Materialien zu einer lepidopterenfauna des Taisanmassivs, Provinz Shantung. Supplement. Species from other places. Deutsche Entomologische Zeutscgruft Iris 50: 135–159.

Park KT, Kim HU (2021) Descriptions of five new species of the family Lecithoceridae from Thailand (Lepidoptera: Gelechioidea). SHILAP Revista de Lepidopterologia 49(193): 171–182. https://doi.org/10.57065/shilap.333

Wu CS (1996) Revision of the genus *Opacoptera* Gozmány (Lepidoptera: Lecithoceridae). Entomologia Sinica 3(1): 9–13. https://doi.org/10.1111/j.1744-7917.1996.tb00395.x

Wu CS, Liu YQ (1992) Lecithoceridae. In: Peng JW, Liu YQ (Eds) Iconography of forest insects in Hunan, China. Hunan Technology and Science House, 1473 pp.

ZooKeys 1158: 147–162 (2023)
doi: 10.3897/zookeys.1158.101936
https://zookeys.pensoft.net

RESEARCH ARTICLE

A peer-reviewed open-access journal
ZooKeys
Launched to accelerate biodiversity research

Molecular characterisation of three *Ixodes* (*Pholeoixodes*) species (Ixodida, Ixodidae) and the first record of *Ixodes* (*Pholeoixodes*) *kaiseri* from Slovakia

Zuzana Krumpálová[1], Barbara Mangová[2], Slávka Purgatová[1], Yuliya M. Didyk[2,3], Mária Kazimírová[2]

1 *Constantine the Philosopher University, Faculty of Natural Sciences and Informatics, Tr. A. Hlinku 1, Nitra, Slovakia* **2** *Institute of Zoology, Slovak Academy of Sciences, Dúbravská cesta 9, Bratislava, Slovakia* **3** *I.I. Schmalhausen Institute of Zoology, National Academy of Sciences of Ukraine, Vul. B. Khmelnytskogo 15, Kyiv, Ukraine*

Corresponding author: Mária Kazimírová (maria.kazimirova@savba.sk)

Academic editor: D. Apanaskevich | Received 14 February 2023 | Accepted 29 March 2023 | Published 21 April 2023

https://zoobank.org/7253655E-1864-4B23-A5C5-BC0B900CE6B8

Citation: Krumpálová Z, Mangová B, Purgatová S, Didyk YuM, Kazimírová M (2023) Molecular characterisation of three *Ixodes* (*Pholeoixodes*) species (Ixodida, Ixodidae) and the first record of *Ixodes* (*Pholeoixodes*) *kaiseri* from Slovakia. ZooKeys 1158: 147–162. https://doi.org/10.3897/zookeys.1158.101936

Abstract

A study of ticks on wildlife was carried out in the area of Levice, Bratislava, Stupava, and Vrbovce (southwestern Slovakia) during 2021 and 2022. Overall, 512 ticks were collected from 51 individuals of six wild mammalian species. Eight tick species were identified, namely *Dermacentor reticulatus*, *D. marginatus*, *Haemaphysalis inermis*, *H. concinna*, *Ixodes ricinus*, *I. hexagonus*, and two *Ixodes* spp. *Ixodes hexagonus* were collected from northern white-breasted hedgehogs (*Erinaceus roumanicus*), females belonging to *Ixodes* spp. were collected from red fox (*Vulpes vulpes*) and nymphs from European badger (*Meles meles*). *Ixodes hexagonus* and the *Ixodes* spp. were identified morphologically and molecularly based on sequences of fragments of two mitochondrial genes, *COI* and 16S rRNA. Molecular analysis of *Ixodes* spp. confirmed the identity of *Ixodes kaiseri* Arthur, 1957 and *I. canisuga* (Johnston, 1849). Sequence analyses show that the *I. kaiseri* isolate from Slovakia is identical to *I. kaiseri* isolates from Romania, Poland, Germany, Turkey, and Croatia. We demonstrate for the first time the presence of *I. kaiseri* in Slovakia using both morphological and molecular methods.

Keywords

European badger, hedgehog, *Ixodes canisuga*, *Ixodes kaiseri*, red fox, ticks

Introduction

Ticks (Ixodida) belong to the most important ectoparasites of terrestrial vertebrate species. Hard ticks of the subgenus *Pholeoixodes* Schulze, 1942 (*Ixodes*, Ixodidae) are usually associated with burrow-dwelling mammals and terrestrial birds that nest in cavities (tree holes or burrows). All representatives of the subgenus *Pholeoixodes* are endophilic three-host ticks with a rather uniform circle of hosts for all active ontogenetic stages. For a long time, the taxonomy of the subgenus *Pholeoixodes* was rather confused (Estrada-Peña et al. 2017a; Tsapko 2018). This can be explained by the large intraspecific morphological variability of the species, when morphologically differing specimens of the same species were described under different names or were misdiagnosed. At the same time, as mentioned by Filippova (1977) and Emelyanova (1979), new findings from previously unknown hosts were described as new species. In the Western Palaearctic the *Ixodes* (*Pholeoixodes*) group currently includes *I.* (*P.*) *kaiseri* Arthur, 1957, *I.* (*P.*) *crenulatus* Koch, 1844, *I.* (*P.*) *canisuga* Johnston, 1849, *I.* (*P.*) *hexagonus* Leach, 1815, and *I.* (*P.*) *rugicollis* Schulze & Schlottke, 1929, which usually feed on mammals, particularly carnivores (mainly Canidae and Mustelidae) and hedgehogs (Erinaceidae), and *I.* (*P.*) *arboricola* Schulze & Schlottke, 1929 and *I.* (*P.*) *lividus* Koch, 1844, which parasitize birds (Karbowiak et al. 2017; Estrada-Peña et al. 2017a; Guglielmone et al. 2020). However, the taxonomic status of *I. crenulatus* and *I. canisuga* needs further clarification (Estrada-Peña et al. 2017b; Guglielmone et al. 2020; Karbowiak et al. 2020).

Ixodes kaiseri was for the first time described from Common Egyptian fox from Burg EJ Arab, Mariut, Western Desert Governorate, Egypt (Arthur 1957). It is a Palaearctic species and all its parasitic stages have been found on Carnivora (Canidae, Felidae, and Mustelidae) and Erinaceomorpha (Erinaceidae). Adults were also recovered from Rodentia (Sciuridae), adults and nymphs were collected from Carnivora (Hyaenidae) and Rodentia (Hystricidae), and larvae and nymphs from Rodentia (Cricetidae) (Guglielmone et al. 2020). There are no records of *I. kaiseri* parasitizing humans. The presence of *I. kaiseri* has been reported in several European countries including Poland, Germany, Hungary, Serbia, Croatia, Romania, Ukraine, Malta (Akimov and Nebogatkin 2002; Hornok et al. 2017, 2020a, 2021; Dwużnik et al. 2020; Krčmar et al. 2022), and Turkey (Orkun and Karaer 2018). Hornok et al. (2017), while reporting presence of *I. kaiseri* specimens on red foxes and dogs in Romania, also noted that the species is more widespread in Europe than previously thought. The species was also recorded in Moldova, southern Ukraine, Georgia, Azerbaijan, Iran, Syria, Lebanon, and Israel (Filippova 1977; Tsapko 2018). In addition, it is known from Kazakhstan (Dzungarian Alatau) and from the North Caucasus (Tsapko 2018). In most parts of the established range, *I. kaiseri* co-occurs with the closely related *I. crenulatus* (*I. canisuga*?) and can also simultaneously parasitize the same host individuals (Tsapko 2018). Predatory mammals play the primary role as hosts of this tick species. According to Filippova (1977), *I. kaiseri* was found on the following hosts: European badger *Meles meles*, red fox *Vulpes vulpes*, raccoon dog *Nyctereutes procyonoides*, domestic dog *Canis lupus familiaris*, steppe polecat *Mustela eversmanii*, striped hyena *Hyaena hyaena*, wildcat *Felis silvestris*, and jungle cat *F. chaus*. In addition to carnivores, *I. kaiseri* were

collected from the Indian crested porcupine *Hystrix indica* and from the northern (*Erinaceus roumanicus*) and southern (*E. concolor*) white-breasted hedgehogs. Hornok et al. (2017) analysed the phylogenetic relationships by using two mitochondrial genes and morphological differences in females of three *Ixodes* species of the subgenus *Pholeoixodes* including *I. kaiseri*. Furthermore, Hornok et al. (2021) published pictorial keys for identification of *I. kaiseri*, *I. canisuga*, and *I. hexagonus* males, nymphs, and larvae. *Ixodes kaiseri* was found to harbour several tick-borne pathogens of veterinary and medical importance (Hornok et al. 2020b; Wodecka et al. 2022); however, it is not clear if and to what extent this species contributes to pathogen circulation in nature.

Ixodes canisuga, considered by some authors as a synonym of *I. crenulatus* (e.g. Filippova and Uspenskaya 1973; Filippova 1977; Siuda 1993), is associated with mammals which inhabit burrows. The most infested species are medium-sized mustelids and canids such as the red fox and European badger, among others (Cornely and Schultz 1992; Santos-Silva et al. 2011). This tick species is also a common parasite of domestic dogs and has also been found on cats (Liebisch and Walter 1986; Földvári and Farkas 2005; Hornok et al. 2017). Overall, *I. canisuga* is distributed from the Spanish Pyrenees through Russia, Iran, Afghanistan, India (Kashmir), to eastern China (Estrada-Peña et al. 2017a). In Europe, this species has been recorded in almost all countries, from United Kingdom, Ireland, France, Austria, and Germany in the west (Walter et al. 1986; Cornely and Schultz 1992; Ogden et al. 2000), Portugal in the south (Santos-Silva et al. 2011), and in countries of central and south-eastern Europe, i.e., Hungary, Poland, Romania, Croatia, Serbia, and Bosnia and Herzegovina (Hornok et al. 2017; Krčmar et al. 2022). It was possibly recorded also in the former Czechoslovakia, but under different names (Černý 1972).

Ixodes hexagonus is a common species in the Western Palaearctic. However, the species was sometimes mistakenly identified as *I. canisuga* (Hornok et al. 2017). *Ixodes hexagonus* is associated with hedgehogs, *Erinaceus europaeus* and *E. roumanicus*, which are the main hosts among the broad spectrum of medium-sized burrow-inhabiting mammals. The species was also found on wild carnivores such as red foxes, mustelids, and the European badger (Estrada-Peña et al. 2017a; Karbowiak et al. 2020). In addition, *I. hexagonus* can frequently be encountered on domestic pets (cats and dogs) and harbours various tick-borne pathogens (Walker 2018). The distribution of *I. hexagonus* covers almost the whole of Europe, ranging from the British Islands in the west, across all the countries in central and eastern Europe, including Slovakia (Černý 1972; Estrada-Peña et al. 2017a; Karbowiak et al. 2020). The species was also found outside this range, e.g. in north-western Iran (Tavassoli and Mohamadi 2015).

Materials and methods

Ethics statement

The study complies with current laws of the Slovak Republic and with species conservation guidelines. The animals were killed for hunting reasons during the legal hunting

season and not specifically for this study. Collections of ticks from hedgehogs were in accordance with Decision No. 8711/2022-6.3 – Exemption from Act No. 543/2022 on Nature and Landscape Protection.

Study area

Hunted animals originated from the area of Žemberovce (south-western Slovakia). The village of Žemberovce (48°15'30"N, 18°44'30"E) borders with the town of Levice. There are extensive thermophilous forest communities, mainly oak–hornbeam Carpathian forests with *Carpinus betulus* and *Quercus petraea*. Mixed oak forests (*Quercus cerris*, *Acer campestre*, *Cerasus avium*, and *Tilia cordata*) are also found in suitable habitats. Hedgehogs were captured in parks within residential zones of Bratislava (48°14'85"N, 17°10'77"E), Stupava (48°27'89"N, 16°99'55"E), and in the village of Vrbovce (48°79'98"N, 17°46'89"E) (western Slovakia).

Tick collection and identification

We collected ticks individually with tweezers directly from the skin of hunted mammals. The searches for hedgehogs were performed at night (10 p.m. to 3 a.m.) by two persons. The equipment consisted of headlamps and thick welding gloves for hedgehog handling. After removing the ticks, all the hedgehogs were released back in their original capture location without significant manipulation.

Ticks were stored in 80% ethanol at 4 °C. They were examined morphologically; adult ixodid ticks are usually easier to identify to species than immature stages, and therefore morphological comparisons followed Siuda (1993), Slovák (2010, 2014), and Bristol University Tick ID (http://www.bristoluniversitytickid.uk). Species of the subgenus *Pholeoixodes* are the most problematic group in the genus *Ixodes*. Reports of *Pholeoixodes* spp. from carnivores are frequently contradictory, and their identification is not based on key diagnostic characters. Moreover, identification of engorged ticks is even more difficult. Nymphs of *Ixodes* spp. were morphologically identified according to Hornok et al. (2017, 2021) using a stereomicroscope (Olympus SZ61). Photographs were taken using a Leica M205C stereo microscope and a Leica Flexacam C1 camera, including LAS X software with a Z-stack projection tool. The photographed specimens were immersed in 80% ethanol, because they were stored for further molecular detections of microorganisms.

Molecular analysis

Genomic DNA was isolated individually from legs of females and nymphs of *I. hexagonus* and *Ixodes* spp. by the method of alkaline hydrolysis with modifications (Guy and Stanek 1991) and from whole engorged ticks with the DNeasy Blood & Tissue Kit (Qiagen, Hilden, Germany) following the manufacturer's instructions. DNA samples were stored at –20 °C until further analyses. Fragments of the mitochondrial

16S rRNA and the *COI* genes were chosen for molecular analyses and tick species identification (Black and Piesman 1994; Hornok et al. 2017). PCR amplified approximately 710 bp of the *COI* gene using the primers LCO1490 and HCO2198 (Hornok et al. 2017) and approximately 460 bp of the 16S rRNA gene of Ixodidae, using the primers 16S+1 and 16S-1 (Black and Piesman 1994). PCR products were analysed by electrophoresis in 1.5% agarose gel stained with GoodView Nucleic Acid Stain (SBS Genetech, Beijing, China) and visualized under UV light. Amplicons were purified using a QIAquick Spin PCR Purification Kit (Qiagen, Hilden, Germany) as described by the manufacturer. The sequencings were performed by Eurofins Genomics Europe (https://www.eurofinsgenomics.eu). DNA sequences were compared with available databases in GenBank using the Basic Local Alignment Search Tool (BLAST) NCBI. The MEGA model selection method was applied to choose the appropriate model for phylogenetic analyses. Phylogenetic analyses were conducted using the maximum likelihood method based on the Tamura-Nei model (Tamura and Nei 1993) using MEGA v. 7.0 (Kumar et al. 2016). Nucleotide sequences of *COI* genes obtained in this study were submitted to BOLD: The Barcode of Life Data System (http://www.barcodinglife.org) under the accession numbers UZINS193 23 SK, UZINS194 23 SK, UZINS195 23 SK, UZINS197 23 SK, UZINS198 23 SK, UZINS199 23 SK, UZINS204 23 SK, UZINS205 23 SK, UZINS206 23 SK, and UZINS182 23 SK.

Data availability statement

The data presented in this study are available upon request from the corresponding author. Nucleotide sequences of *COI* genes derived from the study are available in BOLD: The Barcode of Life Data System (http://www.barcodinglife.org).

Results

During 2021 and 2022, we obtained ticks from hunted wild mammals belonging to five species in the Levice region of south-western Slovakia. The wildlife consisted of red fox *Vulpes vulpes*, European badger *Meles meles*, wild boar *Sus scrofa*, red deer *Cervus elaphus*, and European roe deer *Capreolus capreolus*. At the same time, we collected ticks from hedgehogs (*Erinaceus roumanicus*) in green areas of Bratislava, Stupava, and Vrbovce.

In total, 335 ticks (54 nymphs, 191 females, and 90 males) were collected from 35 hunted wild mammalian individuals and 178 ticks (48 larvae, 77 nymphs, 44 females, and 9 males) from hedgehogs. We identified the presence of eight tick species, namely *Dermacentor reticulatus*, *D. marginatus*, *Haemaphysalis inermis*, *H. concinna*, *Ixodes ricinus*, *I. canisuga*, *I. hexagonus*, and *I. kaiseri*.

In terms of species (Table 1), *I. ricinus* was the most frequent and abundant species, accounting for 71.1% of all specimens collected, and it was found on five hosts (wild boar, red deer, roe deer, red fox, and hedgehog). *Dermacentor reticulatus* accounted for 7% of all specimens and *D. marginatus* for 5.1%; both were confirmed on one

Table 1. Total number of ticks collected from wildlife (all life stages combined, identification comprises also results of molecular analyses).

Host/tick species	*I. ricinus*	*I. canisuga*	*I. kaiseri*	*I. hexagonus*	*D. reticulatus*	*D. marginatus*	*H. inermis*	*H. concinna*
Vulpes vulpes	2		2					
Meles meles		5	4					
Capreolus capreolus	19							
Cervus elaphus	146						3	7
Sus scrofa	43				36	26	27	15
Erinaceus roumanicus	155			23				
Total	365	5	6	23	36	26	30	22

host, wild boar. Fewer *H. concinna* (4.3%) and *H. inermis* (5.9%) were found on two hosts (wild boar and red deer), and *I. hexagonus* (4.5%) was found on hedgehogs only. The remaining specimens (2.2%) belonged to *Ixodes* spp. and were collected from red fox and European badger.

Morphological diagnosis

In total, three female ticks and one male were collected from red fox and nine nymphs from European badger. Initially, based on the existence of an anal groove and the typical structure of the mouthparts, they were morphologically identified as *Ixodes* spp. One of the females and the male from red fox were further identified as *I. ricinus* and the other two females from the red fox and all nymphs from the European badger as *Ixodes* spp. Because mouthparts of the females and part of the nymphs were damaged during their removal from the host skin, morphological identification was only possible in six undamaged nymphs. Two of them were identified as *I. canisuga* and four as *I. kaiseri* (Figs 1, 2) according to detailed morphological examinations showing that the nymphs have the characters described by Hornok et al. (2021).

Molecular identification

By amplification of the *COI* gene, two *Ixodes* spp. females from the red fox and four nymphs from the European badger were identified as *I. kaiseri* and four nymphs as *I. canisuga*. Amplification was not successful for one nymph morphologically identified as *I. canisuga*. By amplification of fragments of the 16S rRNA gene in DNA samples from one female and two nymphs of *I. kaiseri* and three nymphs of *I. canisuga* the identification of the species was confirmed. Molecular analyses of amplified fragments of the *COI* and 16S rRNA genes in DNA samples derived from two females and one nymph of *I. hexagonus* from hedgehogs confirmed the correct identification of the species based on morphology.

The isolates UZINS204 23 SK, UZINS205 23 SK, and UZINS206 23 SK were uniform based on the *COI* sequences. BLAST search showed 100% identity of the Slovak isolates with *COI* gene sequences of *I. kaiseri* isolates from Turkey (ON527576),

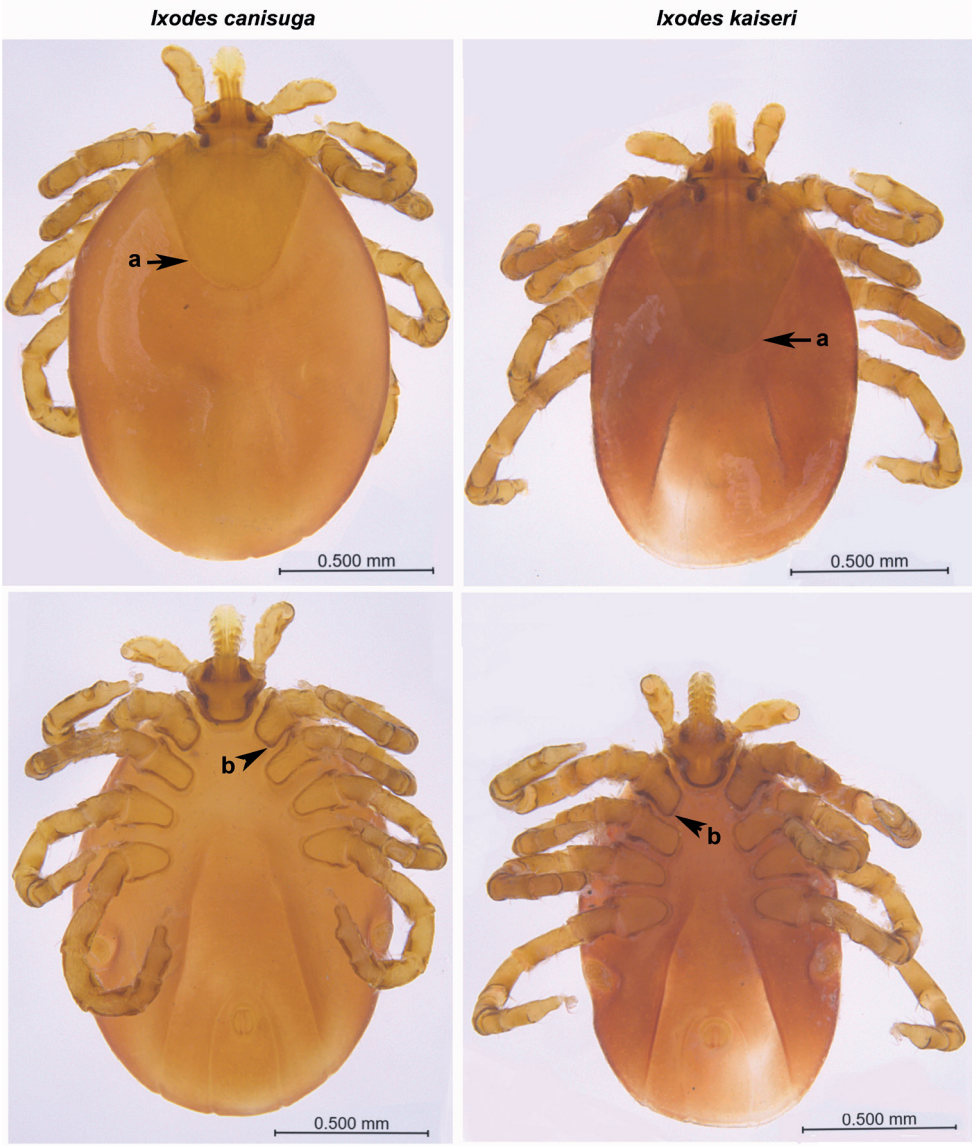

Figure 1. Partially engorged *Ixodes canisuga* and *I. kaiseri* nymphs (dorsal views – upper panels, ventral views – lower panels) collected from *Meles meles* in Slovakia. Differences are seen in the shape of scutum (**a**) which is shorter in *I. canisuga* than in *I. kaiseri.* There is a broad internal spur on coxa I (**b**) in both species. Photo: Ľ. Vidlička

Croatia (MZ305531), and Romania (KY962020), 99.84% identity with isolate from Hungary (KY962015), and 99.52% with isolate from Serbia (KY962033). Isolates UZINS193 23 SK, UZINS194 23 SK, and UZINS195 were uniform and showed 100% identity with the *COI* gene sequences in isolates of *I. hexagonus* from Hungary

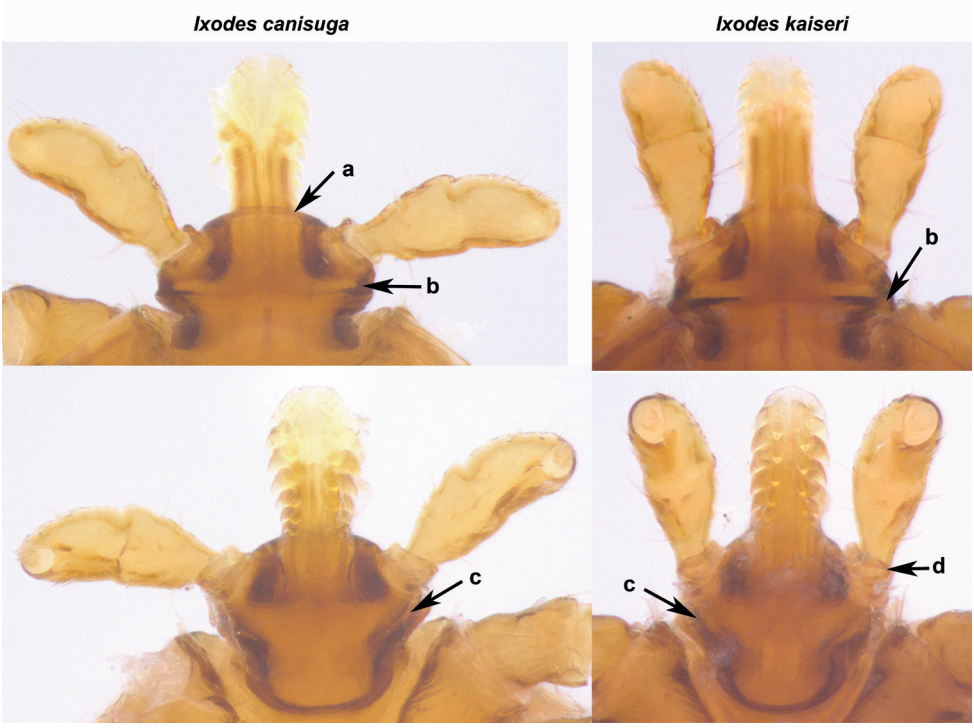

Figure 2. Gnathosoma of *Ixodes canisuga* and *I. kaiseri* nymphs (dorsal views – upper panels, ventral views – lower panels) collected from *Meles meles* in Slovakia. *Ixodes canisuga* – anteriorly flattened basis capituli (**a**); dorsally absence of cornua (**b**); long, moderately thick auricular ridge (**c**). *Ixodes kaiseri:* cornua well developed (**b**); short, thin auricular ridge (**c**); anteriorly rounded, sclerotized protuberance on palpal segment I (**d**).

(OM200350), Croatia (MZ305530), and Germany (KY962046), and 99.54% identity with isolates from Italy (MG432679) and Portugal (LC508366). Isolate UZINS197 23 SK showed 100% identity with the *COI* gene sequence of *I. canisuga* isolate from Romania (KY962023), and 99.84% identity with isolates from France (KY962049), United Kingdom (KY962048), Germany (KY962045), and 99.53% with isolate from Hungary (KX218106). Samples UZINS198 23 SK and UZINS199 23 SK showed 100% identity with the *COI* gene sequences of *I. canisuga* isolate from Hungary (KX218106) and 99.68% with isolates from France (KY962049), United Kingdom (KY962048), and Germany (KY962045) (Fig. 3).

Sequence of the 16S rRNA gene in our samples UZINS205 23 SK and UZINS206 23 SK showed 100% identity with the 16S rRNA gene sequences in *I. kaiseri* isolates from Poland (MK613135), Romania (MT658766), and Germany (MT658770), 99.76% identity with isolate from Turkey (ON540356), and 99.51% identity with isolate from China (MG763864). Sequence in our sample UZINS204 23 SK showed 100% identity with the 16S rRNA gene sequences in *I. kaiseri* isolate from Turkey

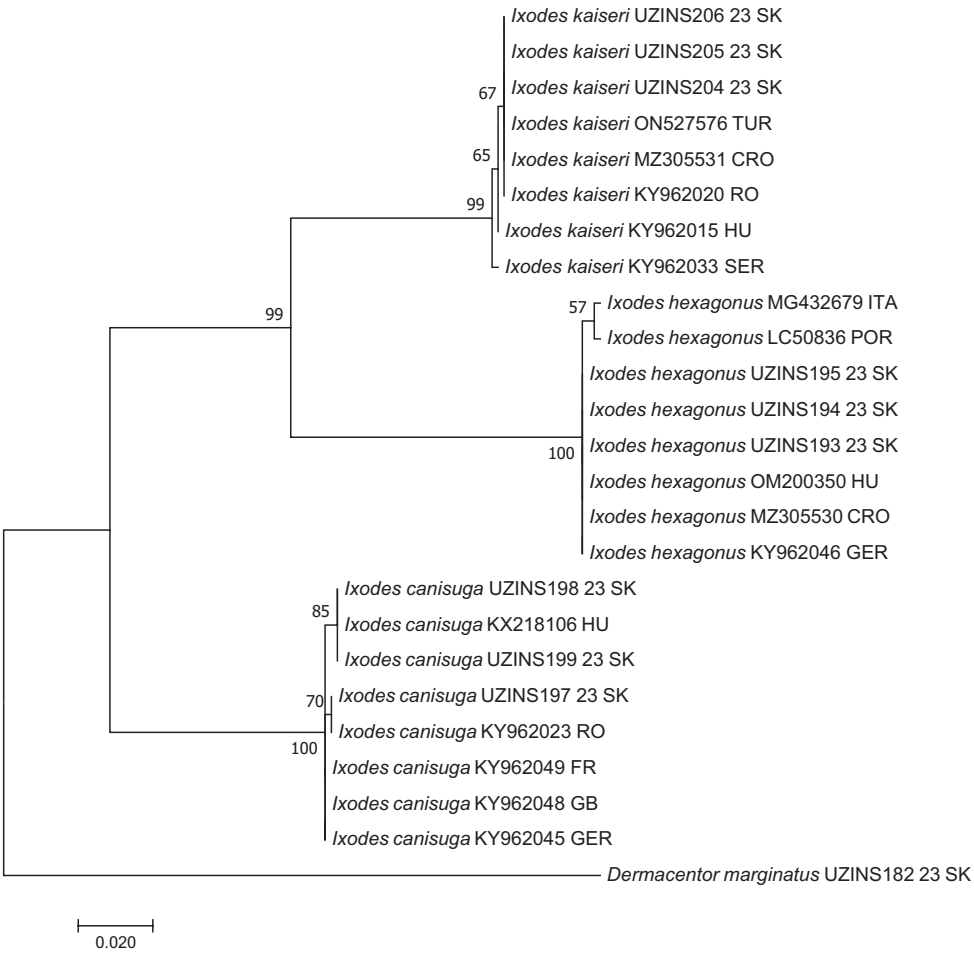

Figure 3. Phylogenetic tree of *Ixodes* spp. constructed by using a maximum-likelihood analysis of the *COI* gene. Bootstrap 1000 bp. Branch lengths represent the number of substitutions per site inferred according to the scale shown. *COI* gene of *D. marginatus* (iBOL source) was used as the outgroup.

(ON540356), 99.76% identity with isolates from Poland (MK613135) and China (MG763864), and 99.75% identity with isolates from Germany (MT658770) and Romania (MT658766). Sequences in samples UZINS193 23 SK, UZINS194 23 SK and UZINS195 23 SK were uniform and showed 100% identity with the 16S rRNA gene sequences in *I. hexagonus* isolates from Croatia (KY962077), Austria (KY962058), Germany (JF928502), and Poland (AF001400) and 99.76% identity with isolate from Italy (KY319189). Sequence of the 16S rRNA gene in our sample UZINS197 23 SK was 100% identical with the 16S rRNA gene sequences of *I. canisuga* isolate from Poland (MK613137), France (KY962074), and United Kingdom (KY962071), and 99.75% identical with isolates from Germany (KY962068) and Croatia (KY962072). Sequences in samples UZINS198 23 SK and UZINS199 23SK

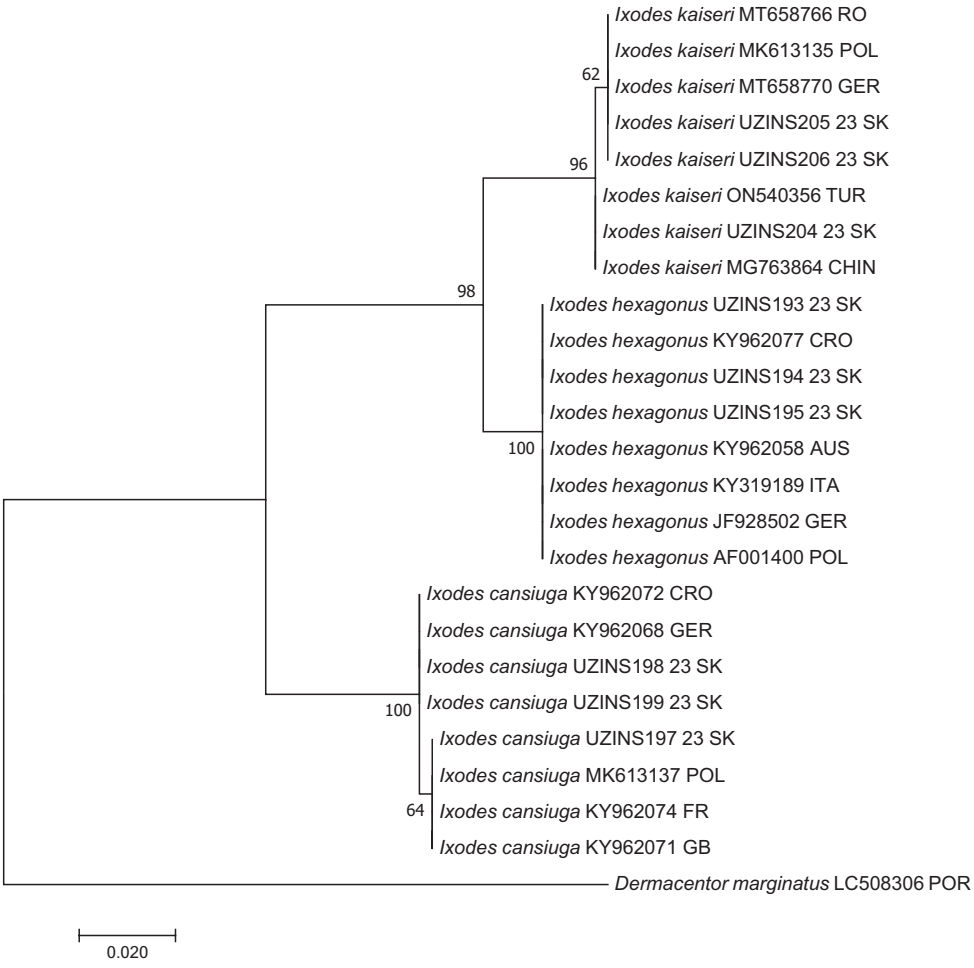

Figure 4. Phylogenetic tree of *Ixodes* spp. constructed by using a maximum-likelihood analysis of 16S rRNA gene. Bootstrap 1000 bp. Branch lengths represent the number of substitutions per site inferred according to the scale shown. 16S rRNA gene of *D. marginatus* (NCBI source) was used as outgroup.

showed 100% identity with the 16S rRNA gene sequences in *I. canisuga* isolates from Croatia (KY962072) and Germany (KY962068), 99.76% identity with isolate from Poland (MK613137), and 99.75% with isolates from France (KY962074) and United Kingdom (KY962071) (Fig. 4).

Molecular identification with markers *COI* and 16S rRNA confirmed the morphological identification of *I. kaiseri*, *I. canisuga*, and *I. hexagonus* from Slovakia (Figs 3, 4). We demonstrated the presence of *I. kaiseri* for the first time in Slovakia using both morphological and molecular methods. Consequently, Slovakia was added to the list of countries where *I. kaiseri* was reported from red fox and European badger.

Discussion

We recorded the co-occurrence of two endophilic *Ixodes* spp. of the subgenus *Pholeoixodes*, *I. kaiseri* and *I. canisuga* on European badger, and of *I. kaiseri* and *I. ricinus* on red fox. For the first time, the occurrence of *I. kaiseri* is confirmed in Slovakia. The presence of *I. kaiseri* in this country was predictable (Karbowiak et al. 2020), as it was found to parasitize wild carnivores and dogs in neighbouring countries of Hungary, Poland, and Ukraine, but also in Germany and south-eastern Europe (Romania, Croatia, Serbia) (Akimov and Nebogatkin 2002; Hornok et al. 2017, 2021; Dwużnik et al. 2020; Krčmar et al. 2022).

Meyer-Kayser et al. (2012) found on foxes in Germany predominance of tick larvae (48%), followed by adults (34%), and nymphs (18%). *Ixodes ricinus* was the most frequent tick species, followed by *I. canisuga* and *I. hexagonus*. In previous studies from Slovakia, *D. reticulatus*, *H. concinna*, *I. ricinus*, and two *Pholeoixodes* species, *I. hexagonus* and *I. crenulatus* identified based on morphology, had been found to parasitize red foxes (Kočišová et al. 2006; Karbowiak et al. 2020). Dwużnik et al. (2020) investigated ectoparasites of red foxes in three regions of Poland. *Ixodes ricinus* and *D. reticulatus* were the dominant tick species on adult foxes, but *I. kaiseri* was also recorded. We found *I. canisuga* on European badger, but not on red fox, and *I. kaiseri* on red fox and European badger. However, we examined only one individual of each host species for ticks, which is not enough to draw conclusions on their parasitofauna in Slovakia.

Ixodes ricinus and *I. hexagonus* are common ectoparasites of hedgehogs in urban and suburban areas of Europe. For example, by examining hedgehogs in a city park in Budapest (Hungary), the high prevalence (93.7%) of *I. ricinus* and presence of *I. hexagonus* were recorded. Nymphs prevailed in both species (Földvári et al. 2011). In four urban habitats in Cluj-Napoca city, Romania, in addition to birds and small mammals, ticks were collected from northern white-breasted hedgehogs. *Ixodes ricinus* prevailed (89.7%), followed by *I. hexagonus* (7.7%) and *Haemaphysalis punctata* (2.6%). With regards to life stages, larvae dominated in *I. ricinus* (67%) and *H. punctata* (71.4%) and females (75.9%) in *I. hexagonus* (Borşan et al. 2020). We identified *I. ricinus* and *I. hexagonus* on hedgehogs from three urbanized areas of Slovakia. Immature stages (nymphs and larvae) prevailed in both species. Thus, the ratios of adult ticks and immature stages differ between sites and are probably affected by microclimate and the presence of other hosts for ticks.

In general, changes in land usage patterns and climate, i.e., milder winters and earlier onset of spring in the northern hemisphere, can significantly affect the geographic distribution, phenology, and population density of some tick species and the occurrence of tick-borne zoonoses (Gray et al. 2009; Gilbert 2021). In addition, ticks can easily spread and colonize new regions via international pet trade, domestic animal transport, or bird migration (Földvári et al. 2016). Given the vector role of ticks, accurate species identification is very important, but it requires time and considerable experience. Among hard ticks (Ixodidae), the genus *Ixodes* contains the

most species, which are grouped into subgenera. Species of the subgenus *Phloeixodes* belong to a problematic group, as they share morphologic and ecologic characters (Estrada-Peña et al. 2017a, b). In a recent review of available taxonomic literature, Guglielmone et al. (2020) pointed to the problems and importance of correct tick identification, mainly for species of medical, veterinary, and evolutionary importance. For example, a comparative test of tick species identification conducted by a network of European researchers in 14 laboratories specialising in ticks provided an overall misidentification rate of almost 29.6% (Estrada-Peña et al. 2017c), which highlighted the need for molecular methods to identify ticks. DNA barcoding methods serve for accurate and rapid identification of tick species and provide the basis for a molecular data platform for the family Ixodidae (Krčmar et al. 2022). Recently, molecular methods have increasingly been used for accurate tick identification, especially in groups of morphologically very similar species (Hornok et al. 2017, 2021; Krčmar et al. 2022). Thanks to the DNA barcoding method, the occurrence of *I. kaiseri* was recorded in Croatia, Germany, Serbia, Hungary, and Romania (Hornok et al. 2017, 2021; Krčmar et al. 2022), Turkey (Orkun and Karaer 2018), and now Slovakia (this study). Subsequently, Slovakia was added to the list of countries where *I. kaiseri* has been recorded. Moreover, by using DNA barcoding, the identity of *I. canisuga* and *I. hexagonus* was also confirmed.

We hypothesize that *I. kaiseri* has been present in Slovakia but was misidentified because of the variability of morphological characters in species of the subgenus *Pholeoixodes*. Moreover, due to the endophilic mode of life, only engorged individuals can be collected from hosts and their identification is generally more difficult than unfed ticks. Therefore, further studies of species of the subgenus *Pholeoixodes* are needed, and morphological identifications in previous studies should be confirmed by molecular methods.

Acknowledgements

This study was carried out with the financial support of various institutions. As representative for all those who contributed in one way or another, we would like to express our gratitude to the Slovak Grant Agencies VEGA No. 1/0604/20 (Environmental assessment of specific habitats of the Danubian Lowland), KEGA No. 019UKF-4/2021 (Creation and innovation of education – Zoology for Ecologists, part – Invertebrates) and VEGA No. 2/0004/22, as well as the European Fund for Regional Development (EFRD) ITMS2014 + 313021W683-DNA barcoding of Slovakia (SK-BOL), as a part of international initiative International Barcode of Life (iBOL). The study was funded by the statutory activities of Faculty of Natural Sciences, Constantine the Philosopher University, Nitra (Slovakia) and the Slovak Academy of Sciences Institute of Zoology (Slovakia). We thank Assoc. prof. Ľubomír Vidlička for taking photographs.

The authors declare no conflict of interest. The funders had no role in the design of the study; in the collection, analyses, or interpretation of data; in the writing of the manuscript; or in the decision to publish the results.

References

Akimov IA, Nebogatkin IV (2002) Ticks of Kyiv–Urbozoological and epyzootological aspects. Vestnik Zoologii 36(1): 91–95.

Arthur DR (1957) Two north African *Ixodes* ticks. *I. kaiseri* sp. nov. from Egyptian desert fox cubs. A redescription of the female and a description of the male of *I. festai*, Rondelli, 1926 (Ixodoidea, Ixodidae). The Journal of Parasitology 43(5): 578–585. https://doi.org/10.2307/3274481

Black 4th WC, Piesman J (1994) Phylogeny of hard and soft-tick taxa (Acari: Ixodida) based on mitochondrial 16S rDNA sequences. Proceedings of the National Academy of Sciences of the United States of America 91(21): 10034–10038. https://doi.org/10.1073/pnas.91.21.10034

Borşan SD, Toma-Naic A, Péter Á, Sándor AD, Peştean C, Mihalca AD (2020) Impact of abiotic factors, habitat type and urban wildlife on the ecology of hard ticks (Acari: Ixodidae) in urban and peri-urban habitats. Parasites & Vectors 13(1): e476. https://doi.org/10.1186/s13071-020-04352-3

Černý V (1972) The tick fauna of Czechoslovakia. Folia Parasitologica 19(1): 87–92.

Cornely M, Schultz U (1992) Zur Zeckenfauna Ostdeutschlands. Angewandte Parasitologie 33: 173–183.

Dwużnik D, Mierzejewska E, Kowalec M, Alsarraf M, Stańczak Ł, Opalińska P, Krokowska-Paluszak M, Górecki G, Bajer A (2020) Ectoparasites of red foxes (*Vulpes vulpes*) with a particular focus on ticks in subcutaneous tissues. Parasitology 147(12): 1359–1368. https://doi.org/10.1017/S003118202000116X

Emelyanova ND (1979) The taxonomic position of ixodid ticks of the genus *Pholeoixodes* in the subfamily Ixodinae and its subdivision into subgenera. Zooparasitology of the Lake Baikal Basin: 5–27.

Estrada-Peña A, Mihalca AD, Petney TN (2017a) Ticks of Europe and North Africa: a Guide to Species Identification. Springer International, Cham, 425 pp. https://doi.org/10.1007/978-3-319-63760-0

Estrada-Peña A, Pfäffle M, Baneth G, Kleinerman G, Petney TN (2017b) Ixodoidea of the Western Palaearctic: A review of available literature for identification of species. Ticks and Tick-Borne Diseases 8(4): 512–525. https://doi.org/10.1016/j.ttbdis.2017.02.013

Estrada-Peña A, D'Amico G, Palomar AM, Dupraz M, Fonville M, Heylen D, Habela MA, Hornok S, Lempereur L, Madder M, Núncio MS, Otranto D, Pfaffle M, Plantard O, Santos-Silva MM, Sprong H, Vatansever Z, Vial L, Mihalca AD (2017c) A comparative test of ixodid tick identification by a network of European researchers. Ticks and Tick-Borne Diseases 8(4): 540–546. https://doi.org/10.1016/j.ttbdis.2017.03.001

Filippova NA (1977) Fauna of the USSR: Arachnida, Subfamily Ixodinae 4(4). Nauka, Leningrad, 396 pp.

Filippova NA, Uspenskaya IG (1973) *Ixodes kaiseri* Arthur, 1957 (Ixodidae) species taxonomic status. Parazitologiia 7: 297–306.

Földvári G, Farkas R (2005) Ixodid tick species attaching to dogs in Hungary. Veterinary Parasitology 129(1–2): 125–131. https://doi.org/10.1016/j.vetpar.2004.11.032

Földvári G, Rigó K, Jablonszky M, Biró N, Majoros G, Molnár V, Tóth M (2011) Ticks and the city: Ectoparasites of the northern white-breasted hedgehog (*Erinaceus roumanicus*) in an urban park. Ticks and Tick-Borne Diseases 2(4): 231–234. https://doi.org/10.1016/j.ttbdis.2011.09.001

Földvári G, Široký P, Szekeres S, Majoros G, Sprong H (2016) *Dermacentor reticulatus*: A vector on the rise. Parasites & Vectors 9(1): e314. https://doi.org/10.1186/s13071-016-1599-x

Gilbert L (2021) The impacts of climate change on ticks and tick-borne disease risk. Annual Review of Entomology 66(1): 373–388. https://doi.org/10.1146/annurev-ento-052720-094533

Gray JS, Dautel H, Estrada-Peña A, Kahl O, Lindgren E (2009) Effects of climate change on ticks and tick-borne diseases in Europe. Climate Change and Infectious Disease 593232: 1–12. https://doi.org/10.1155/2009/593232

Guglielmone AA, Petney TN, Robbins RG (2020) Ixodidae (Acari: Ixodoidea): descriptions and redescriptions of all known species from 1758 to December 31, 2019. Zootaxa 4871(1): 1–322. https://doi.org/10.11646/zootaxa.4871.1.1

Guy EC, Stanek G (1991) Detection of *Borrelia burgdorferi* in patients with Lyme disease by the polymerase chain reaction. Journal of Clinical Pathology 44(7): 610–611. https://doi.org/10.1136/jcp.44.7.610

Hornok S, Sándor AD, Beck R, Farkas R, Beati L, Kontschán J, Takács N, Földvári G, Silaghi C, Meyer-Kayser E, Hodžić A, Tomanović S, Abdullah S, Wall R, Estrada-Peña A, Duscher GG, Plantard O (2017) Contributions to the phylogeny of *Ixodes* (*Pholeoixodes*) *canisuga*, *I.* (*Ph.*) *kaiseri*, *I.* (*Ph.*) *hexagonus* and a simple pictorial key for the identification of their females. Parasites & Vectors 10(1): e545. https://doi.org/10.1186/s13071-017-2424-x

Hornok S, Grima A, Takács N, Szekeres S, Kontschán J (2020a) First records and molecular-phylogenetic analyses of three tick species (*Ixodes kaiseri*, *Hyalomma lusitanicum* and *Ornithodoros coniceps*) from Malta. Ticks and Tick-Borne Diseases 11(3): e101379. https://doi.org/10.1016/j.ttbdis.2020.101379

Hornok S, Sándor AD, Földvári G, Ionică AM, Silaghi C, Takács N, Schötta AM, Wijnveld M (2020b) First broad-range molecular screening of tick-borne pathogens in *Ixodes* (*Pholeoixodes*) *kaiseri*, with special emphasis on piroplasms. Acta Veterinaria Hungarica 68(1): 30–33. https://doi.org/10.1556/004.2020.00003

Hornok S, Meyer-Kayser E, Kontschán J, Takács N, Plantard O, Cullen S, Gaughran A, Szekeres S, Majoros G, Beck R, Boldogh SA, Horváth G, Kutasi C, Sándor AD (2021) Morphology of *Pholeoixodes* species associated with carnivores in the Western Palearctic: Pictorial key based on molecularly identified *Ixodes* (*Ph.*) *canisuga*, *I.* (*Ph.*) *hexagonus* and *I.* (*Ph.*) *kaiseri* males, nymphs and larvae. Ticks and Tick-Borne Diseases 12(4): e101715. https://doi.org/10.1016/j.ttbdis.2021.101715

Karbowiak G, Nowak-Chmura M, Szewczyk T, Siuda K (2017) Występowanie kleszczy z podrodzaju *Pholeoixodes* w Polsce w pierwszej dekadzie XXI wieku (The occurrence of *Pholeoixodes* ticks in Poland in the beginning of the XXI century). In: Buczek A, Błaszak C (Eds) Stawonogi w Środowisku Miejskim i Podmiejskim. Koliber, Lublin, 69–81.

Karbowiak G, Stanko M, Miterpaková M, Hurníková Z, Víchová B (2020) Ticks (Acari: Ixodidae) parasitizing red foxes (*Vulpes vulpes*) in Slovakia and new data about subgenus

Pholeoixodes occurrence. Acta Parasitologica 65(3): 636–643. https://doi.org/10.2478/s11686-020-00184-4

Kočišová A, Lazar P, Letková V, Čurlík J, Goldová M (2006) Ectoparasitic species from red foxes (*Vulpes vulpes*) in East Slovakia. Veterinarski Arhiv 76(Supplement): S59–S63.

Krčmar S, Klobučar A, Vucelja M, Boljfetić M, Kučinić M, Madić J, Cvek M, Mađarić BB (2022) DNA barcoding of hard ticks (Ixodidae), notes on distribution of vector species and new faunal record for Croatia. Ticks and Tick-Borne Diseases 13(3): e101920. https://doi.org/10.1016/j.ttbdis.2022.101920

Kumar S, Stecher G, Tamura K (2016) MEGA7: Molecular Evolutionary Genetics Analysis version 7.0 for bigger datasets. Molecular Biology and Evolution 33(7): 1870–1874. https://doi.org/10.1093/molbev/msw054

Liebisch A, Walter G (1986) Untersuchungen von Zecken bei Haus- und Wildtieren in Deutschland: Zum Vorkommen und zur Biologie der Igelzecke (*Ixodes hexagonus*) und der Fuchszecke (*Ixodes canisuga*). Deutsche Tierarztliche Wochenschrift 9: 377–464.

Meyer-Kayser E, Hoffmann L, Silaghi C, Pfister K, Mahling M, Passos LMF (2012) Dynamics of tick infestations in foxes in Thuringia, Germany. Ticks and Tick-Borne Diseases 3(4): 232–239. https://doi.org/10.1016/j.ttbdis.2012.05.004

Ogden NH, Cripps P, Davison CC, Owen G, Parry JM, Timms BJ, Forbes AB (2000) The ixodid tick species attaching to domestic dogs and cats in Great Britain and Ireland. Veterinary and Medical Entomology 14(3): 332–338. https://doi.org/10.1046/j.1365-2915.2000.00244.x

Orkun Ö, Karaer Z (2018) First record of the tick *Ixodes* (*Pholeoixodes*) *kaiseri* in Turkey. Experimental & Applied Acarology 74(2): 201–205. https://doi.org/10.1007/s10493-018-0219-1

Santos-Silva MM, Beati L, Santos AS, De Sousa R, Núncio MS, Melo P, Santos-Reis M, Fonseca C, Formosinho P, Vilela C, Bacellar F (2011) The hard-tick fauna of mainland Portugal (Acari: Ixodidae): an update on geographical distribution and known associations with hosts and pathogens. Experimental & Applied Acarology 55(1): 85–121. https://doi.org/10.1007/s10493-011-9440-x

Siuda K (1993) Kleszcze Polski (Acari: Ixodida): Systematyka i Rozmieszczenie. Monografie Parazytologiczne, Polskie Towarzystwo Parazytologiczne, Warsaw, 375 pp.

Slovák M (2010) Obrázkový kľúč dospelých kliešťov (Acari: Ixodida) fauny Slovenska. Entomofauna Carpathica 22(1–2): 8–13.

Slovák M (2014) Obrázkový kľúč lariev a nýmf kliešťov (Acari: Ixodida) fauny Slovenska. Entomofauna Carpathica 26(1): 12–18.

Tamura K, Nei M (1993) Estimation of the number of nucleotide substitutions in the control region of mitochondrial DNA in humans and chimpanzees. Molecular Biology and Evolution 10(3): 512–526.

Tavassoli M, Mohamadi E (2015) First report of *Ixodes* (*Pholeoixodes*) *hexagonus* on chukar (*Alectores chukar*) in northwest of Iran and it's public health importance. Persian Journal of Acarology 4(2): 205–211. https://doi.org/10.22073/pja.v4i2.11441

Tsapko NVT (2018) The tick *Ixodes kaiseri* (Acari, Ixodidae) in the North Caucasus and Transcaucasia according to the material from the collection of Stavropol Anti-Plague Institute. Entomological Review 98(1): 125–128. https://doi.org/10.1134/S0013873818010116

Walker MD (2018) The hedgehog tick, *Ixodes hexagonus* (Leach, 1815) (Acari: Ixodidae); the natural history and ecology of a nest ectoparasite. Systematic and Applied Acarology 23(4): 680–714. https://doi.org/10.11158/saa.23.4.9

Walter G, Kock D, Liebisch A (1986) Beitrag zur Zecken-Fauna der Bundesrepublik Deutschland (Arachnida: Acarina: Ixodidae). Senckenbergiana Biologica 67: 199–206.

Wodecka B, Michalik J, Grochowalska R (2022) Red foxes (*Vulpes vulpes*) are exposed to high diversity of *Borrelia burgdorferi* sensu lato species infecting fox-derived *Ixodes* ticks in west-central Poland. Pathogens (Basel, Switzerland) 11(6): e696. https://doi.org/10.3390/pathogens11060696

ZooKeys 1158: 163–177 (2023)
doi: 10.3897/zookeys.1158.96886
https://zookeys.pensoft.net

RESEARCH ARTICLE

A peer-reviewed open-access journal
ZooKeys
Launched to accelerate biodiversity research

Food preference strategy of four sympatric rodents in a temperate forest in northeast China

Dianwei Li[1,2,3], Chengzhi Zhang[2], Yuwei Cao[2], Ming Gao[2], Shiqi Chang[2], Menghao Xu[2], Zhimin Jin[2], Hongwei Ni[1]

1 *Heilongjiang Academy of Forestry, No. 134 Haping Road, Harbin, Heilongjiang 150081, China* **2** *College of Life Sciences and Technology, Mudanjiang Normal University, No. 191 Wenhua Road, Mudanjiang, Heilongjiang 157011, China* **3** *College of Wildlife and Protected Area, Northeast Forestry University, No. 26 Hexing Road, Harbin 150040, China*

Corresponding authors: Dianwei Li (lidianwei@mdjnu.edu.cn); Zhimin Jin (swxjzm@126.com); Hongwei Ni (nihongwei2000@163.com)

Academic editor: R. López-Antoñanzas | Received 2 November 2022 | Accepted 13 March 2023 | Published 21 April 2023

https://zoobank.org/BEAEE250-EC38-4384-A0F2-2C313A758B1F

Citation: Li D, Zhang C, Cao Y, Gao M, Chang S, Xu M, Jin Z, Ni H (2023) Food preference strategy of four sympatric rodents in a temperate forest in northeast China. ZooKeys 1158: 163–177. https://doi.org/10.3897/zookeys.1158.96886

Abstract

Rodents are well known as both seed predators and dispersers of various plant species in forest ecosystems, and they play an important role in the regeneration of vegetation. Thus, the research on seed selection and vegetation regeneration by sympatric rodents is an interesting topic. To understand the characteristics of preferences of rodents for different seeds, a semi-natural enclosure experiment was performed with four rodent species (*Apodemus peninsulae*, *Apodemus agrarius*, *Tscherskia triton*, and *Clethrionomys rufocanus*) and the seeds of seven plant species (*Pinus koraiensis*, *Corylus mandshurica*, *Quercus mongolica*, *Juglans mandshurica*, *Armeniaca sibirica*, *Prunus salicina*, and *Cerasus tomentosa*) to investigate the differentiation in niches and patterns of resource utilization of sympatric rodents. The results showed that all the rodents had consumed many seeds of *Pi. koraiensis*, *Co. mandshurica*, and *Q. mongolica* but differed significantly in how they selected the different seeds. The rate of utilization (R_i) of *Pi. koraiensis*, *Co. mandshurica*, and *Q. mongolica* exhibited the highest values. The E_i values indicated that the rodents tested exhibited differences in their priorities used to select the seeds from different plant species. All four species of rodents exhibited obvious preferences for certain seeds. Korean field mice preferentially consumed the seeds of *Q. mongolica*, *Co. mandshurica*, and *Pi. koraiensis*. Striped field mice favor the seeds of *Co. mandshurica*, *Q. mongolica*, *P. ikoraiensis*, and Nanking cherry. Greater long-tailed hamsters prefer to consume the seeds of *Pi. koraiensis*, *Co. mandshurica*, *Q. mongolica*, *Pr. salicina*, and *Ce. tomentosa*. *Clethrionomys rufocanus*

likes to eat the seeds of *Pi. koraiensis*, *Q. mongolica*, *Co. mandshurica*, and *Ce. tomentosa*. The results supported our hypothesis that sympatric rodents overlap in food selection. However, each rodent species has a marked preference for food selection, and different rodent species differ in their food preferences. This reflects the role of distinct food niche differentiation in their coexistence.

Keywords
Coexistence, competition, fitness, food selection, niche, niche differentiation

Introduction

The coexistence of species and the maintenance of biodiversity are important topics of ecological study. Food is an essential resource for survival, so there are obvious effects of differences in food selection and feeding behavior among animal species on their coexistence. Furthermore, the food choices of animals directly affect their survival and reproduction. However, the factors that affect the selection of food by animals in forest ecosystems are very complicated, and the choices of different rodent species of the seeds from different plant species depend on many factors. The characteristics of the seeds of different plant species vary by size (Vander Wall 2001; Xiao et al. 2005; Chang and Zhang 2014; Luna et al. 2016); the contents of nutrients, tannins, and other secondary metabolites (Steele et al. 1993; Wang and Chen 2012; Chang and Zhang 2014); and the hardness and thickness of the seed coat (Li et al. 2018). All these factors affect the food choices of rodent species and further influence their behavior (Li et al. 2018).

The selective foraging of all animals is a key factor that affects their survival and reproduction. Animals in nature generally exhibit food preference or selective foraging (Hughes and Croy 1993), and no animal uses all the food types that occur in the environment equally, particularly when there are other competing species. In general, animals only prefer a small fraction of the available foods. They rarely feed on most foods and even completely reject some. Effective food preference ensures that animals efficiently intake energy and nutrients and maximize their food selection fitness (Moss 1991; Rogers and Blundell 1991).

Large seeds produced by many plant species are a valuable food source for rodents, which often prefer certain seeds from various plant species within their habitats and are capable of accurately distinguishing the seeds with different characteristics (Vander Wall 2001; Chang and Zhang 2014; Luna et al. 2016; Li et al. 2018). Their identification and choice of food affects the fate of seeds, while the rodents must weigh the input costs (time and energy) when foraging to utilize different eating and dispersal strategies to ensure supplies of optimal food and energy (Vander Wall 1990; Lima 1998; Li et al. 2021).

Seed characteristics, including size and weight (Vander Wall 2001; Luna et al. 2016); seed coat characteristics, such as thickness and hardness (Vander Wall 1990; Luna et al. 2016; Li et al. 2018); seed quality, such as seeds damaged by pests, mildewed, or empty-shelled (Vander Wall 1990; Chang et al. 2010; Vander Wall 2010; Wang et al. 2012); moisture content; nutrients, such as starch, fat, and protein (Vander

Wall 1990; Vander Wall 2001); and secondary metabolic compounds, such as tannins and other polyphenolics (Steele et al. 1993; Wang and Chen 2012; Chang and Zhang 2014) affect the decision making of rodents during food selection. Most studies have shown that seed size and nutrients are key factors that determine the foraging strategies of animals, and rodents usually prefer large seeds that are rich in nutrients (Smith and Reichman 1984; Xiao et al. 2006). Harper et al. (1970) strongly suggested that large seeds are favored because they provide a greater return to the seed predators. The optimal foraging theory (OFT; Charnov 1976) suggests that animals favor seeds that generate the largest net return. In general, the total return in foraging increases as the seed size increases, and during the same duration of foraging, the probability that large seeds with higher nutritional content and benefit will be eaten is higher because such foods can better compensate the energy expenditure by the animal during foraging and thus, are more attractive (Xiao et al. 2005; Luna et al. 2016).

The time that seeds are handled is another important factor that influences animal behavior and decision making, and it significantly affects the foraging strategy of rodents (Jacobs 1992; Chang et al. 2010; Li et al. 2020). Because the time of seed handling is associated with the weighing of predation risk against foraging efficiency (Chang et al. 2010; Wang et al. 2012; Li et al. 2020), it tends to be minimized by rodents to enhance survival. The choice of food by rodents is also affected by the size and ability of the individual. A rodent will set an upper threshold for the preferred seed size based on its own size, so seeds from the same plant species may provide very different net returns to varying predators (Jacobs 1992; Luna et al. 2016). Because of differences in body size, strength and mouth type, predators differ in their ability to handle different seeds.

Studies of animal food choice are significant to understand the co-evolution of animal and plant systems, as well as niche differentiation among sympatric animals (Vander Wall 2001; Li and Zhang 2003; Vander Wall and Beck 2011; Li et al. 2018). Since rodents are the primary predators and dispersers of seeds in forest ecosystems (Vander Wall 1990), they form a system of foraging and reciprocity with seeds. The degree of preference of rodents for a certain type of seed and the differential selection of different seeds can lead to changes in predation pressure and the rate of dispersion among plant species (Pons and Pausas 2006), and it may have important impacts on seed dispersal and the natural regeneration of forest communities through the heavy consumption of seeds by animals (Vander Wall 1990; Perea et al. 2011; Li et al. 2021). Their consumption can distribute seeds and lead to seedling establishment as a result of hoarding behavior (Janzen 1971; Grubb 1977; Clark and Clark 1984; Willson and Whelan 1990; Vander Wall 2001; Briggs et al. 2009). The seed mortality owing to the foraging of animals affects the fitness, population structure, and composition of species of the plant community (Willson and Whelan 1990). The competition for resources among sympatric animals has been an important topic in community ecology, and numerous studies have shown that competition is the primary factor that causes variation in the use of resources by animals, thus, leading to differences in morphology and behavioral strategies among species.

Currently, the differential selection of seeds of a given plant species by sympatric rodent species has not been well researched. In this study, we used four sympatric rodent species and the seeds of seven plant species distributed in northern temperate forests to investigate the differences in seed choice related to the species under semi-natural enclosure conditions, as well as the effect of seed characteristics on the strategic differentiation in food choice by rodents to gain insight into the niche partitioning of sympatric rodents and its effect on the fate of the seeds of specific plants and vegetation renewal. We hypothesized that sympatric rodents feed on largely similar food items but differ significantly in their preferred choices.

Materials and methods

Study site and species

This study was conducted from April to June in 2019 in the Zhang Guangcai Mountains in Mudanjiang (elevation 400 to 900 m; 44°47'N, 129°07'E) located in Heilongjiang Province, northeast China. The research area is located north of the Changbai Mountain. The climate at the site is dominated by the northern temperate zonal continental monsoon climate, with four distinct seasons and a short frost-free period of approximately 90–115 days. The annual average air temperature is 4.3 °C, with a maximum of 34.4 °C and a minimum of -39 °C. The average annual precipitation is approximately 670 mm. The representative vegetation in the study area primarily includes secondary broad-leaf forest and coniferous broad-leaf forest. At the study site, four rodent species, *Apodemus peninsulae* (Thomas, 1907), *Apodemus agrarius* (Pallas, 1771), *Tscherskia triton* (De Winton, 1899), and *Clethrionomys rufocanus* (Sundevall, 1846), rely on seeds as important food sources. Seven sympatric seeds, including *Pinus koraiensis* (Siebold & Zuccarini, 1861), *Corylus mandshurica* (Maximowic, 1856), *Quercus mongolica* (Fischer & Ledebour, 1850), *Juglans mandshurica* (Maximowic, 1856), *Armeniaca sibirica* (Lamarck, 1783), *Prunus salicina* (Lindley, 1830), and *Cerasus tomentosa* (Thunberg) Masamune and S. Suzuki 1936), were used in the experiment. Fresh seeds were collected during the fruiting season and then dried naturally at field temperatures until use.

Capture of live animals by cage trapping

Live rodent samples were caught through cage trapping. In each trap (30 cm × 25 cm × 20 cm), fried pumpkin (*Cucurbita* spp.) seeds (for food) and carrots (*Daucus carota* var. *sativa* Hoffmann, 1791) (for water) were placed as bait, and cotton rolls were provided as denning material. The cages were placed along two transects in the sample plot at 20 m spaces with one cage per 20 m × 5 m. On the second day after the cages were placed, the captures were examined, and pregnant females and juveniles were immediately released. Captured adult rodents were transferred to terraria (65 cm × 35 cm × 25 cm) covered with wire mesh and supplied with drinking water and a suitable amount of litter, and the terraria were placed in the natural environment.

Seed preference sequence experiment

The captured rodents were allowed one day of acclimation to the new environment and the seeds. Plump seeds were randomly selected from each of seven plant species, and one seed from each species was placed on the feeding plate in a terrarium occupied by one rodent. The order in which the rodent took the seeds was monitored using a video camera. Each rodent was tested for more than three hours, during which all the seeds were consumed, or the rodent no longer selected the seeds. The seeds for experiments were replaced, and the experimental process was repeated. After the experiment had been repeated three times for each rodent, the terrarium was cleaned, and the experimental animal was replaced with another individual. Four sympatric rodent species, i.e., *A. peninsulae* (n = 16), *A. agrarius* (n = 10), *T. triton* (n = 10), and *Cl. rufocanus* (n = 9), and a total of 135 seeds from seven plant species was used in the experiment.

Seed preference experiment

Four semi-natural enclosures (1 m × 1 m × 1 m) were constructed on relatively flat terrain in the study area. At one corner of each enclosure, a den was made that contained some cotton rolls to keep the rodent warm, and a small water container was set up and replenished regularly to allow the rodent to drink freely. A feeding plate was placed in the center of the enclosure, which was where the seeds were supplied for the experimental rodent.

Based on the body size of the rodents and their food consumption observed in the previous experiment, one *J. mandshurica* seed and two seeds of the remaining plant species were supplied in tests that involved *A. peninsulae*, *A. agrarius*, and *Cl. rufocanus*, and those that involved *T. triton*. Three seeds from each plant species were supplied to eliminate the effect of consumption capacity and body size of the species of rodent. The rationale was to supply an appropriate amount of food to avoid the situation in which the rodent took all the seeds owing to insufficient food supply or the situation in which it only consumed its most favorite seeds from one or two plant species but not the seeds from other plants. The data from the individuals that died during the experiment were excluded, so 26 *A. peninsulae*, 17 *A. agrarius*, 10 *T. triton*, and 14 *Cl. rufocanus* were tested using 432 seeds from each of six plant species, i.e., *Pi. koraiensis*, *Co. mandshurica*, *Q. mongolica*, *A. sibirica*, *Pr. salicina*, *Ce. tomentosa*, and 261 seeds from *J. mandshurica*.

Electivity index

The Ivlev electivity index (E_i) (Scarlett and Smith 1991) was used to describe the food preference. Its formula is as follows: $E_i = (R_i - P_i) / (R_i + P_i)$ in which the seed utilization rate R_i = (the total number of seeds from the i^{th} species that have been consumed/ the total number of seeds from all species that have been consumed) × 100%; and the rate of seed availability P_i = (the total number of seeds from the i^{th} species that have been supplied/ the total number of seeds from all species supplied) × 100%. The E_i ranges

from -1 to 1> if $E_i > 0$, the rodent positively selects for the seeds from the species. If $E_i < 0$, the rodent negatively selects. If $E_i = 0$, the rodent exhibits no preference for the seeds, and if $E_i = -1$, the rodent makes no choice at all. Based on the E_i value, the preference of rodents for the seeds was categorized into four levels: strongly preferred ($E_i \geq 0.5$), preferred ($E_i > 0$), barely ate ($E_i > -0.5$), and avoided ($E_i \geq -1$).

Statistical analysis

Data processing and statistical analyses were performed with Microsoft Excel 2007 (Redmond, WA, USA) and SPSS 21.0 (IBM, Inc., Armonk, NY, USA). The data were subjected to the Kolmogorov-Smirnov normality and Homogeneity-of-variance tests before processing, and in the case that the data did not comply with parametric assumptions, nonparametric tests were conducted. The Kruskal-Wallis H test was used to compare the differences in the choice of seeds from different plant species by the same species of rodent, and the Mann-Whitney U test was used to perform pair-wise comparisons of the differences in food choice between different species of rodents. Descriptive statistics were expressed as the mean ± SD. The level of statistical significance was set to $\alpha = 0.05$, and high statistical significance was set to $\alpha = 0.01$.

Results

Feeding and utilization of the seeds

The consumption of food differed significantly among the four species of rodents. The amount of all the seeds taken each time by *T. triton* was 16.57 ± 2.47 ($n = 30$), which was significantly higher than those of *A. peninsulae* (5.65 ± 2.43, $n = 78$), *Cl. rufocanus* (4.88 ± 2.05, $n = 42$), and *A. agrarius* (4.65 ± 2.44, $n = 51$). *Apodemus peninsulae* consumed significantly more seeds than *A. agrarius*. The species also showed differences in the amounts of each type of seed consumed at each feeding.

The four species of rodent exhibited varying total rates of consumption (r_i) on different seeds, but they all had a higher total rate of consumption on the seeds of *Pi. koraiensis*, *Co. mandshurica*, and *Q. mongolica*. Among them, *A. peninsulae* consumed 85.90% of the *Q. mongolica* seeds, 67.95% of the *Co. mandshurica* seeds, and 64.10% of the *Pi. koraiensis* seeds. *Apodemus agrarius* consumed 61.76% of the *Co. mandshurica* seeds, 57.84% of the *Q. mongolica* seeds, and 54.90% of the *Pi. koraiensis* seeds. *Tscherskia triton* consumed 100% of the seeds of *Pi. koraiensis*, *Co. mandshurica*, and *Q. mongolica*, and in addition to the *J. mandshurica* seeds, *T. triton* consumed more of the seeds of other plant species than the other species of rodents (*Pr. salicina*: 88.89%; *Ce. tomentosa*: 84.44%; *A. sibirica*: 77.78%). *Cl. rufocanus* consumed 65.31% of the *Pi. koraiensis* seeds, 54.08% of the *Q. mongolica* seeds, and 47.96% of the *Co. mandshurica* seeds (Table 1).

Table 1. Statistical data and analysis of the feeding and utilization of seven species of seeds by four rodents.

Rodent species	Index	*Pinus koraiensis*	*Corylus mandshurica*	*Quercus mongolica*	*Juglans mandshurica*	*Armeniaca sibirica*	*Prunus salicina*	*Cerasus tomentosa*	Kruskal-Wallis H test
Apodemus peninsulae (n = 26)	*SN*	2	2	2	1	2	2	2	
	CN	1.28±0.91	1.36±0.82	1.72±0.64	0.23±0.42	0.78±0.82	0.28±0.58	0±0	χ^2=247.897, df=6, P<0.001
	TS	156	156	156	78	156	156	156	
	TC	100	106	134	18	61	22	0	
	r_i(%)	64.10	67.95	85.90	23.08	39.10	14.10	0	χ^2=219.514, df=6, P<0.001
	R_i(%)	22.68	24.04	30.39	4.08	13.83	4.99	0	χ^2=247.897, df=6, P<0.001
	E_i	0.192	0.219	0.328	-0.307	-0.053	-0.510	-1.000	χ^2=219.514, df=6, P<0.001
Apodemus agrarius (n = 17)	*SN*	2	2	2	1	2	2	2	
	EN	1.10±0.92	1.24±0.86	1.16±0.70	0±0	0.08±0.34	0.29±0.61	0.78±0.88	χ^2=129.378, df=6, P<0.001
	TS	102	102	102	51	102	102	102	
	TC	56	63	59	0	4	15	40	
	r_i(%)	54.90	61.76	57.84	0	3.92	14.71	39.21	χ^2=129.378, df=6, P<0.001
	R_i(%)	23.63	26.58	24.89	0	1.69	6.33	16.88	χ^2=129.636, df=6, P<0.001
	E_i	0.211	0.267	0.236	-1.000	-0.802	-0.417	0.046	χ^2=126.897, df=6, P<0.001
Tscherskia triton (n = 10)	*SN*	3	3	3	3	3	3	3	
	CN	3.00±0.00	3.00±0.0	3.00±0.0	0.03±0.18	2.33±1.09	2.67±0.88	2.53±1.04	χ^2=136.548, df=6, P<0.001
	TS	90	90	90	90	90	90	90	
	TC	90	90	90	1	70	80	76	
	r_i(%)	100	100	100	1.11	77.78	88.89	84.44	χ^2=136.548, df=6, P<0.001
	R_i(%)	18.11	18.11	18.11	0.2	14.08	16.10	15.29	χ^2=136.548, df=6, P<0.001
	E_i	0.118	0.118	0.118	-0.972	-0.007	0.060	0.034	χ^2=136.548, df=6, P<0.001
Clethrionomys rufocanus (n = 14)	*SN*	2	2	2	1	2	2	2	
	CN	1.48±0.55	1.07±0.89	1.19±0.74	0.00±0.00	0.07±0.26	0.31±0.60	0.76±0.88	χ^2=132.491, df=6, P<0.001
	TS	84	84	84	42	84	84	84	
	TC	62	45	50	0	4	15	34	
	r_i(%)	73.81	53.57	59.52	0	3.57	15.48	38.10	χ^2=132.491, df=6, P<0.001
	R_i(%)	30.24	21.95	24.39	0	1.46	6.34	15.61	χ^2=132.491, df=6, P<0.001
	E_i	0.326	0.176	0.226	-1.000	-0.826	-0.416	0.007	χ^2=132.491, df=6, P<0.001
Kruskal-Wallis H test	R_i, df=3	χ^2=85.670 P<0.001	χ^2=40.321 P<0.001	χ^2=57.718 P<0.001	χ^2=28.199 P<0.001	χ^2=84.937 P<0.001	χ^2=74.190 P<0.001	χ^2=74.744 P<0.001	
	E_i, df=3	χ^2=24.924 P<0.001	χ^2=15.581 P=0.001	χ^2=34.367 P<0.001	χ^2=28.199 P<0.001	χ^2=65.362 P<0.001	χ^2=43.913 P<0.001	χ^2=67.271 P<0.001	

* *SN* (Supply number): the number of s eeds supplied each time. *CN* (Consumption number): the average number of seeds consumed. *TS* (Total supply number): the total number of seeds from the i^{th} species that had been supplied, $TS = \sum SN$. *TC* (Total consumption number): the total number of seeds from the i^{th} species that had been selected. $TC = \sum CN$. r_i (the rate of consumption of seeds from the i^{th} species), $r_i = (TC_i / TS_i) \times 100\%$. R_i (the rate of utilization of seeds from the i^{th} species), $R_i = (TC_i / \sum TC) \times 100\%$. P_i (the rate of availability of seeds from the i^{th} species), $P_i = (TS_i / \sum TS) \times 100\%$. E_i (the Ivlev electivity index), $E_i = (R_i - P_i) / (R_i + P_i)$.

In terms of R_i, *Pi. koraiensis*, *Co. mandshurica*, and *Q. mongolica* exhibited the highest values (*A. peninsulae*: 77.11%; *A. agrarius*: 75.10%; *T. triton*: 54.33%; *Cl. rufocanus*: 76.58%). The seeds of *A. sibirica*, *Pr. salicina*, and *Ce. tomentosa* accounted for 45.47% of the food spectrum of *T. triton* (Fig. 1).

Priority of seed selection

The rodents tested exhibited differences in the priority by which they selected the seeds from different plant species. For *A. peninsulae*, the order was *Q. mongolica* > *Co. mandshurica* > *Pi. koraiensis* > *A. sibirica* > *Pr. salicina* > *J. mandshurica* > *Ce. tomentosa*. For *A. agrarius*, the order was *Pi. koraiensis* > *Q. mongolica* > *Co. mandshurica* > *Ce. tomentosa* > *Pr. salicina* > *A. sibirica* > *J. mandshurica*. For *T. triton*, the order was *Q. mongolica* > *Co. mandshurica* > *Pi. koraiensis* > *Pr. salicina* > *Ce. tomentosa* > *A. sibirica* > *J. mandshurica*. Finally, for *Cl. rufocanus*, the order was *Pi. koraiensis* > *Q. mongolica* > *Co. mandshurica* > *Ce. tomentosa* > *Pr. salicina* > *A. sibirica* > *J. mandshurica* (Fig. 2).

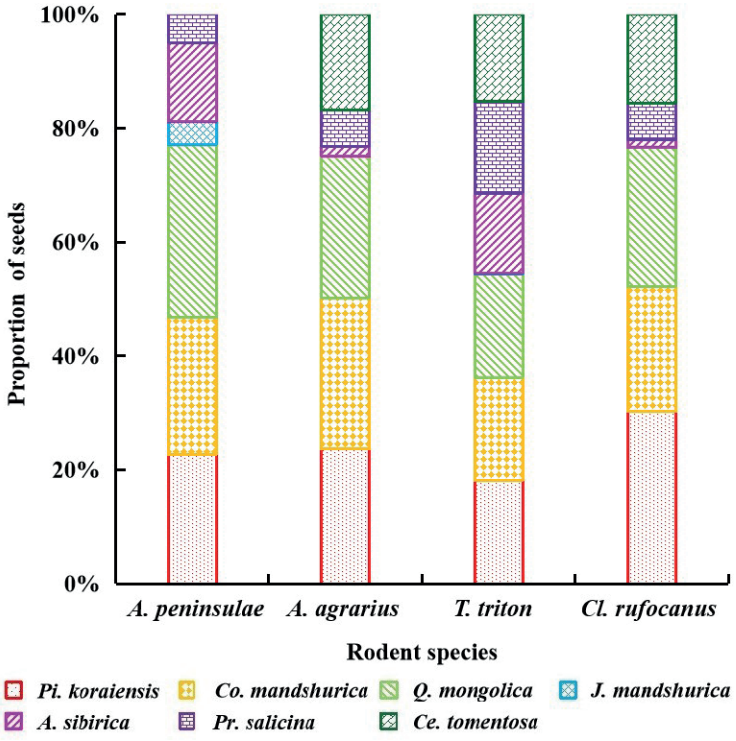

Figure 1. The food spectrum of four rodents. In each bar chart, different types of shading represent the proportion of different seeds.

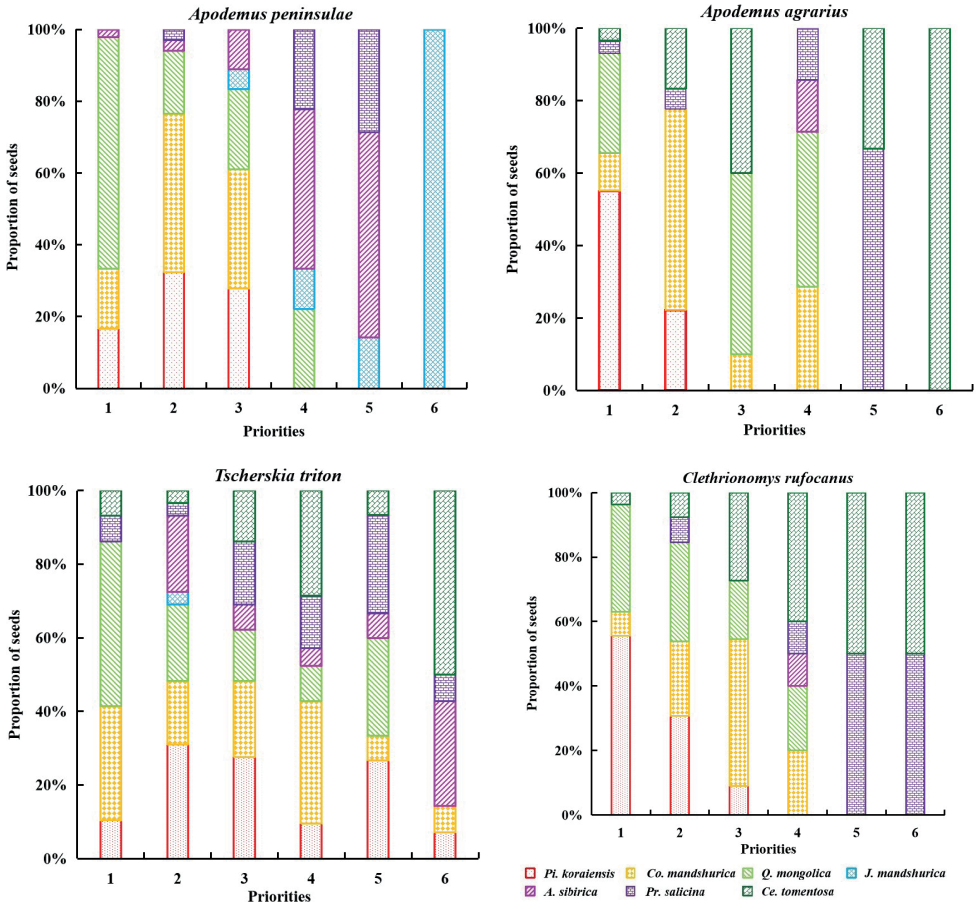

Figure 2. The priorities of seven seeds were selected by four rodents *Apodemus peninsulae*, *A. agrarius*, *Tscherskia triton*, *Clethrionomys rufocanus*. 1–6: The order of seeds that were selected. In each bar chart of 1–6, different types of shading represent the proportion of different seeds as in the color key.

Rodent choices of different seeds

The E_i values indicate that the four rodent species differed in their choices of seeds.

Apodemus peninsulae obviously preferred certain seeds (E_i : χ^2 = 219.514, df = 6, P < 0.001) of *Q. mongolica*, *Co. mandshurica*, and *Pi. koraiensis* (E_i : 0.328, 0.219, 0.192). It rarely ate the seeds of *A. sibirica* or *J. mandshurica* (E_i: -0.053, -0.307) and avoided those of *Pr. salicina* and *Ce. tomentosa* (E_i : -0.510, -1.000). The favored seeds were consumed at significantly higher levels than the others (P < 0.001). The species consumed more seeds of *Q. mongolica* than those of *Pi. koraiensis* or *Co. mandshurica* (U = 2300.000, P = 0.001; U = 2314.000, P = 0.001), and it favored the seeds of *A. sibirica* over those of *J. mandshurica* or *Pr. salicina* (U = 2010.500, P < 0.001;

U = 2313.000, P = 0.003). It did not show a preference between the seeds of *J. mandshurica* and *Pr. salicina* (U = 2895.000, P = 0.474).

Apodemus agrarius noticeably preferred certain seeds (E_i : χ^2 = 126.897, df = 6, P < 0.001), those of *Co. mandshurica*, *Q. mongolica*, *Pi. koraiensis*, and *Ce. tomentosa* (E_i: 0.267, 0.236, 0.211, 0.046). It rarely ate the seeds of *Pr. salicina* (E_i : -0.417), and it avoided those of *A. sibirica* and *J. mandshurica* with a significantly higher consumption of the favored seeds over the others (P < 0.05). The species consumed more seeds of *Co. mandshurica* or *Q. mongolica* than those of *Ce. tomentosa* (U = 928.500, P = 0.008 < 0.05; U = 948.500, P = 0.013 < 0.05), and it favored the seeds of *Pr. salicina* over those of *A. sibirica* (U = 1105.00, P = 0.029).

Tscherskia triton exhibited obvious preferences for certain seeds (E_i : χ^2 = 136.548, df = 6, P < 0.001), consuming the seeds of *Pi. koraiensis*, *Co. mandshurica*, *Q. mongolica*, *P. salicina*, and *Ce. tomentosa* (E_i: 0.118, 0.118, 0.118, 0.060, 0.034) and rarely ate those of *A. sibirica* (E_i:-0.007). This rodent entirely avoided those of *J. mandshurica* (E_i: -0.972). The species consumed more seeds of *Pi. koraiensis*, *Co. mandshurica*, and *Q. mongolica* than those of *Pr. salicina* (U = 390.000, P = 0.040) or *Ce. tomentosa* (U = 360.000, P = 0.011), but it showed no preference among the seeds of *Pi. koraiensis*, *Co. mandshurica*, and *Q. mongolica* or among those of *P. salicina*, *Ce. tomentosa*, and *A. sibirica* (U = 366.000, P = 0.93; U = 420.000, P = 0.494; U = 396.000, P = 0.304). However, the seeds of *J. mandshurica* (P < 0.001) were the least preferred.

Clethrionomys rufocanus exhibited obvious preferences for certain seeds (E_i: χ^2 = 132.491, df = 6, P < 0.001) and preferentially consumed the seeds of *Pi. koraiensis*, *Q. mongolica*, *Co. mandshurica*, and *Ce. tomentosa* (E_i: 0.326, 0.226, 0.176, 0.007), while it rarely ate those of *Pr. salicina* (E_i: -0.416). It avoided those of *A. sibirica* and *J. mandshurica* (E_i: -0.826, -1.000). Among its favored seeds, the species consumed more seeds of *Pi. koraiensis* than of *Co. mandshurica* (U = 673.500, P = 0.043 < 0.05) and more seeds of *Pi. koraiensis* and *Q. mongolica* than those of *Ce. tomentosa* (U = 477.000, P < 0.001; U = 632.000, P = 0.018 < 0.05). It exhibited no significant difference in selecting the seeds of *Q. mongolica*, *Pi. koraiensis*, and *Co. mandshurica* (U = 706.000, P = 0.082, U = 825.000, P = 0.587) while it showed no preference between the seeds of *Co. mandshurica* and *Ce. tomentosa* (U = 717.000, P = 0.112).

Rodent choices of seeds from the same plant species

The four rodent species exhibited differences in the choice of seeds from the same plant species (Kruskal-Wallis H, E_i: df = 3, P < 0.05; Table 1).

Clethrionomys rufocanus preferred the seeds of *Pi. koraiensis* the most of those studied and had similar preferences to *A. agrarius* (U = 956.500, P = 0.365). They were higher than those of *A. peninsulae* (U = 986.000, P < 0.001) or *T. triton* (U = 30.000, P < 0.001).

For the seeds of *Co. mandshurica*, the preference by *A. agrarius* was the greatest, similar to that of *Cl. rufocanus* (U = 1447.500, P = 0.275) and higher than that of *A. peninsulae* (U = 1468.000, P = 0.009) or *T. triton* (U = 420.000, P < 0.001).

For the seeds of *Q. mongolica*, *A. peninsulae* liked them the most and had levels of preference similar to that of *A. agrarius* (U = 1112.000, P = 0.152) and *Cl. rufocanus* (U = 1532.000, P = 0.525), while that of *T. triton* was significantly lower than that of each of the remaining three species (*A. peninsulae*: U = 420.000, P < 0.001; *A. agrarius*: U = 480.000, P < 0.001; *Cl. rufocanus*: U = 240.000, P < 0.001) .

The preference of *A. peninsulae* for *J. mandshurica* seeds was significantly greater than that of each of the other rodent species (*A. agrarius*: U = 1530.000, P < 0.001; *A. agrarius*: U = 930.000, P = 0.013; *Cl. rufocanus*: = 1260.000, P = 0.001).

For the seeds of *A. sibirica*, *T. triton* most strongly preferred these seeds, and it significantly preferred them than each of the other rodent species (*A. peninsulae*: U = 872.000, P = 0.034 < 0.05; *A. agrarius*: U = 186.000, P < 0.001; *Cl. rufocanus*: U = 168.000, P < 0.001); that of *A. peninsulae* was also higher than that of *A. agrarius* (U = 1060.000, P < 0.001) or *Cl. rufocanus* (U = 879.000, P < 0.001).

For the seeds of *Pr. Salicina*, the preference by *T. triton* was the greatest and significantly higher than that of each of the other rodent species (*A. peninsulae*: U = 259.000, P < 0.001; *A. agrarius*: U = 370.000, P < 0.001; *Cl. rufocanus*: U = 332.000, P < 0.001), among which there was no difference in preference (Mann-Whitney U, E_i: P > 0.05).

For the seeds of *Ce. tomentosa*, three rodent species, *A. agrarius*, *T. triton*, and *Cl. rufocanus* exhibited no differences in preferences; *A. peninsulae* exhibited no choice at all (Mann-Whitney U, E_i: P > 0.05).

Discussion

Analyses of food consumption, the order of seed selection, and E_i demonstrated that the four rodent species in this study all favored or preferred the seeds of *Pi. koraiensis*, *Co. mandshurica*, and *Q. mongolica*. These seeds are large and commonly found in boreal forests that have high numbers of *J. mandshurica* of the appropriate sizes, easily handled, and containing abundant resources. Thus, they have become a favored food for most species of small rodents during the long natural process of evolution. Furthermore, the long history of competition has led to food niche differentiation in sympatric rodents, whose preference for the seeds of certain plant species has largely been demonstrated in this work. Among the three plant species most favored, *A. peninsulae* preferred the seeds of *Q. mongolica*; *A. agrarius* preferred the seeds of *Co. mandshurica*, and *Cl. rufocanus* preferred the seeds of *Pi. koraiensis*. *Tscherskia triton* exhibited no preference. The preferences of the four rodent species for the seeds of different plant species reflect a mutually beneficial symbiotic relationship that has evolved over a long time. As food resources, the seeds of these plants provide the necessary nutrients for the survival and reproduction of these rodents and thus, affect animal behavior and population dynamics (Janzen 1971; Vander Wall 2001; Luna et al. 2016; Li et al. 2018). The foraging, transportation, and hoarding of plant seeds and fruits by these rodent species influences the spread and renewal of vegetation (Janzen 1971;

Grubb 1977; Clark and Clark 1984; Willson and Whelan 1990; Vander Wall 2001; Briggs et al. 2009; Li et al. 2021).

Intrinsic factors of a rodent, such as its body size and ability to process food, also exert important effects on its food selection. Among the four rodent species tested in this study, *T. triton* is the largest in body size followed by *A. peninsulae*, while *A. agrarius* and *Cl. rufocanus* are smaller. The large-sized *T. triton* therefore has a higher capacity for handling food and consumed all the seeds of *Pi. koraiensis*, *Co. mandshurica*, and *Q. mongolica*, as well as most of the seeds of *A. sibirica*, *Pr. salicina*, and *Ce. tomentosa*. Furthermore, its E_i values demonstrated that it favors seeds from additional plant species, indicating that the diet breadth and eating capacity of *T. triton* are higher than those of each of the other three rodent species. The food preference of *T. triton* was not as refined as that of other species, possibly because the supply of its favored seed resources is too small to meet its large demand for food, so it must exploit other seed resources.

According to the Optimal Foraging Theory, natural selection has enabled animals to maximize their net benefits during foraging, and the most efficient foraging strategy ensures survival and reproductive success (Charnov 1976). Many small rodent species have been found to not feed on the seeds of *J. mandshurica*, and *A. peninsulae* only consumed a small percentage (23.08%) of these seeds. This resulted in an R_i that only accounted for 4.08% of its total food consumption. This result is related to the seed-handling ability of the rodents. Although the seeds of *J. mandshurica* are rich in nutrients and can provide more benefit in a single seed, they are large and have a hard seed coat, which pose substantial challenges to small rodents during both transport and consumption, making it difficult for them to substantially benefit from the seeds (Xiao et al. 2005). This is consistent with the result of our field studies (unpublished results) that showed the small rodents rarely chose the seeds of *J. mandshurica*. The preferences of the four rodent species in this study for the seeds of *A. sibirica*, *Pr. salicina*, and *Ce. tomentosa*, three sparsely distributed plant species, varied markedly, and the consumption of *Ce. tomentosa* seeds by *A. agrarius* and *Cl. rufocanus* was greater than that of *A. sibirica* or *Pr. salicina*, likely owing to differences in the seed-handling abilities of the different species. *Apodemus agrarius* and *Cl. rufocanus* are the smallest rodents and therefore, must invest tremendous effort to handle the seeds of *A. sibirica* and *Pr. salicina* with their thick, hard seed coats, whereas it is easier for them to handle the smaller seeds of *Ce. tomentosa*. However, we found that *A. peninsulae* did not feed on the seeds of *Ce. tomentosa*, which could be because these seeds are too small to provide sufficient food resources.

According to the principle of competitive exclusion, competitors for the same limiting resource cannot coexist, but it is very difficult to directly observe competition in nature, particularly in the cases of interspecific and intraspecific competition in rodents. The food selection results of this study indicate that the four sympatric rodent species compete with each other for food and could have a high degree of niche overlap for the same food resources. However, this study did not account for factors such as differences in the levels of resource availability and competition, which are the outcome of long-term adaptation of the animals to their natural environment,

and thus reflect their potential patterns of food resource niche differentiation. Niche differentiation avoids competition and enables sympatric species to coexist despite limited resources, thus enriching biodiversity and being necessary to sustain the coexistence of species (Kartzinel et al. 2015). Such niche differentiation also depends on the different habitats or microhabitats in which the animals live. *Apodemus peninsulae* is the dominant species in the broad-leaved coniferous and broad-leaved mixed forests in the north. *Apodemus agrarius* is primarily distributed in the purlieus of forests. *Tscherskia triton* occupies various habitats but dominates in grassland, farmland, and hilly areas, while *Cl. rufocanus* is primarily distributed in coniferous forest habitats. Moreover, feeding niche differentiation does not necessarily indicate the absence of competition, which is related to the amount of food resources. Abundant food resources enable greater interspecies niche overlap, whereas scarce food resources lead to competition (Lawlor 1980).

Conclusions

The characteristics of seeds and the intrinsic factors of the rodents exert important effects on the food selection. Rodents can identify different seed properties of the sympatric distribution and form specific feeding preferences. The four rodents all favored the seeds of *Pi. koraiensis*, *Co. mandshurica*, and *Q. mongolica* in a temperate forest in northeast China. Therefore, there are different degrees of overlap in food selection among the sympatric species of rodents because of different degrees of shared food preferences. In order to avoid excessive sympatric competition, rodents adjust their food preference strategies to differentiate feeding niches and thus achieve coexistence.

Acknowledgements

This research was funded by the Natural Science Foundation of Heilongjiang Province of China (SS2021C006), the Science Research Project of Mudanjiang Normal University (GP2021006), the Science Research Project of the Education Department of Heilongjiang Province (1451PT007). We are grateful to the people who helped collect behavioral data in Sandao forest farm. We thank the anonymous reviewers for their constructive comments on the manuscript. We thank Zhulin Han, Man Jiang, and LEXIS (Scientific editorial experts, United States, LEXIS Academic Service, LLC) for their linguistic assistance during the preparation of this manuscript.

References

Briggs JS, Vander Wall SB, Jenkins SH (2009) Forest rodents provide directed dispersal of Jeffrey pine seeds. Ecology 90(3): 675–687. https://doi.org/10.1890/07-0542.1

Chang G, Zhang Z (2014) Functional traits determine formation of mutualism and predation interactions in seed-rodent dispersal system of a subtropical forest. Acta Oecologica 55(1): 43–50. https://doi.org/10.1016/j.actao.2013.11.004

Chang G, Xiao Z, Zhang Z (2010) Effects of burrow condition and seed handling time on hoarding strategies of Edward's long-tailed rat (*Leopoldamys edwardsi*). Behavioural Processes 85(2): 163–166. https://doi.org/10.1016/j.beproc.2010.07.004

Charnov EL (1976) Optimal foraging, the marginal value theorem. Theoretical Population Biology 9(2): 129–136. https://doi.org/10.1016/0040-5809(76)90040-X

Clark DA, Clark DB (1984) Spacing dynamics of a tropical rain forest tree: Evaluation of the Janzen-Connell model. American Naturalist 124(6): 769–788. https://doi.org/10.1086/284316

Grubb PJ (1977) The maintenance of species-richness in plant communities: The importance of the regeneration niche. Biological Reviews of the Cambridge Philosophical Society 52(1): 107–145. https://doi.org/10.1111/j.1469-185X.1977.tb01347.x

Harper JL, Lovell PH, Moore KG (1970) The shapes and sizes of seeds. Annual Review of Ecology and Systematics 1(1): 327–356. https://doi.org/10.1146/annurev.es.01.110170.001551

Hughes RN, Croy MI (1993) An experimental analysis of frequency-dependent predation (switching) in the 15-spined stickleback, *Spinachia spinachia*. Journal of Animal Ecology 62(2): e341. https://doi.org/10.2307/5365

Jacobs LF (1992) The effect of handling time on the decision to cache by grey squirrels. Animal Behaviour 43(1): 522–524. https://doi.org/10.1016/S0003-3472(05)80111-3

Janzen DH (1971) Seed predation by animals. Annual Review of Ecology and Systematics 2(1): 465–492. hhttps://doi.org/10.1146/annurev.es.02.110171.002341

Kartzinel TR, Chen PA, Coverdale TC, Erickson DL, Kress WJ, Kuzmina ML (2015) DNA metabarcoding illuminates dietary niche partitioning by African large herbivores. Proceedings of the National Academy of Sciences of the United States of America 112(26): 8019–8024. https://doi.org/10.1073/pnas.1503283112

Lawlor LR (1980) Overlap, similarity, and competition coefficients. Ecology 61(1): 245–251. https://doi.org/10.2307/1935181

Li HJ, Zhang ZB (2003) Effect of rodents on acorn dispersal and survival of the Liaodong oak (*Quercus liaotungensis* Koidz.). Forest Ecology and Management 176(1–3): 387–396. https://doi.org/10.1016/S0378-1127(02)00286-4

Li DW, Jin ZM, Yang CY, Yang CW, Zhang MH (2018) Scatter-hoarding the seeds of sympatric forest trees by *Apodemus peninsulae* in a temperate forest in northeast China. Polish Journal of Ecology 66(4): 382–394. https://doi.org/10.3161/15052249PJE2018.66.4.006

Li DW, Hao JW, Yao X, Liu Y, Peng T, Jin ZM, Meng FX (2020) Observations of the foraging behavior and activity patterns of the Korean wood mouse, *Apodemus peninsulae*, in China, using infra-red cameras. ZooKeys 992: 139–155. https://doi.org/10.3897/zookeys.992.57028

Li DW, Liu Y, Shan HJ, Li N, Hao JW, Yang BB, Peng T, Jin ZM (2021) Effects of season and food on the scatter-hoarding behavior of rodents in temperate forests of Northeast China. ZooKeys 1025: 73–89. https://doi.org/10.3897/zookeys.1025.60972

Lima SL (1998) Stress and decision making under the risk of predation: Recent developments from behavioral, reproductive, and ecological perspectives. Advances in the Study of Behavior 27(08): 215–290. https://doi.org/10.1016/S0065-3454(08)60366-6

Luna CA, Loayza AP, Squeo FA (2016) Fruit size determines the role of three scatter-hoarding rodents as dispersers or seed predators of a fleshy-fruited atacama desert shrub. PLoS ONE 11(11): e0166824. https://doi.org/10.1371/journal.pone.0166824

Moss R (1991) Diet selection-an ecological perspective. The Proceedings of the Nutrition Society 50(01): 71–75. https://doi.org/10.1079/PNS19910012

Perea R, Miguel AS, Gil L (2011) Flying vs. climbing: Factors controlling arboreal seed removal in oak-beech forests. Forest Ecology and Management 262(7): 1251–1257. https://doi.org/10.1016/j.foreco.2011.06.022

Pons J, Pausas JG (2006) Rodent acorn selection in a Mediterranean oak landscape. Ecological Research 22(4): 535–541. https://doi.org/10.1007/s11284-006-0053-5

Rogers PJ, Blundell JE (1991) Mechanisms of diet selection: The translation of needs into behaviour. The Proceedings of the Nutrition Society 50(1): 65–70. https://doi.org/10.1079/PNS19910011

Scarlett TL, Smith KG (1991) Acorn preference of urban blue jays (*Cyanocitta cristata*) during fall and spring in Northwestern Arkansas. The Condor 93(1): 438–442. https://doi.org/10.2307/1368961

Smith CC, Reichman OJ (1984) The evolution of food caching by birds and mammals. Annual Review of Ecology and Systematics 15(1): 329–351. https://doi.org/10.1146/annurev.es.15.110184.001553

Steele MA, Knowles T, Bridle K, Simms EL (1993) Tannins and partial consumption of acorns: Implications for dispersal of oaks by seed predators. American Midland Naturalist 130(2): 229–238. https://doi.org/10.2307/2426123

Vander Wall SB (1990) Food Hoarding in Animals. University of Chicago Press, Chicago, 445 pp.

Vander Wall SB (2001) The evolutionary ecology of nut dispersal. Botanical Review 67(1): 74–117. https://doi.org/10.1007/BF02857850

Vander Wall SB (2010) How plants manipulate the scatter-hoarding behaviour of seed-dispersing animals. Philosophical Transactions of the Royal Society of London 365(1542): 989–997. https://doi.org/10.1098/rstb.2009.0205

Vander Wall SB, Beck MJ (2011) A comparison of frugivory and scatter–hoarding seed–dispersal syndromes. Botanical Review 78(1): 10–31. https://doi.org/10.1007/s12229-011-9093-9

Wang B, Chen J (2012) Effects of fat and protein levels on foraging preferences of tannin in scatter-hoarding rodents. PLoS ONE 7(7): e40640. https://doi.org/10.1371/journal.pone.0040640

Wang B, Ye CX, Cannon CH, Chen J (2012) Dissecting the decision-making process of scatter-hoarding rodents. Oikos 122(7): 1027–1034. https://doi.org/10.1111/j.1600-0706.2012.20823.x

Willson MF, Whelan CJ (1990) Variation in postdispersal survival of vertebrate-dispersed seeds: Effects of density, habitat, location, season, and species. Oikos 57(2): 191–198. https://doi.org/10.2307/3565939

Xiao Z, Zhang Z, Wang Y (2005) Effects of seed size on dispersal distance in five rodent-dispersed fagaceous species. Acta Oecologica 28(3): 221–229. https://doi.org/10.1016/j.actao.2005.04.006

Xiao Z, Wang Y, Harris M, Zhang Z (2006) Spatial and temporal variation of seed predation and removal of sympatric large-seeded species in relation to innate seed traits in a subtropical forest, Southwest China. Forest Ecology and Management 222(1–3): 46–54. https://doi.org/10.1016/j.foreco.2005.10.020

ZooKeys 1158: 179–193 (2023)
doi: 10.3897/zookeys.1158.98572
https://zookeys.pensoft.net

RESEARCH ARTICLE

A peer-reviewed open-access journal
ZooKeys
Launched to accelerate biodiversity research

Discovery and redescription of the true *Nuvol umbrosus* Navás and naming of a new *Nuvol* species (Neuroptera, Chrysopidae, Leucochrysini)

Francisco José Sosa-Duque[1], Catherine A. Tauber[2,3]

1 *Universidade Federal Rural da Amazônia (UFRA) Campus de Capitão Poço, Pará, Brazil* **2** *Department of Entomology, Comstock Hall, Cornell University, Ithaca, NY 14853, USA* **3** *Department of Entomology and Nematology, University of California, Davis, CA 95616, USA*

Corresponding author: Catherine A. Tauber (cat6@cornell.edu)

Academic editor: A. Contreras-Ramos | Received 14 December 2022 | Accepted 7 March 2023 | Published 21 April 2023

https://zoobank.org/131896B5-5657-4579-9633-4476D9730A32

Citation: Sosa-Duque FJ, Tauber CA (2023) Discovery and redescription of the true *Nuvol umbrosus* Navás and naming of a new *Nuvol* species (Neuroptera, Chrysopidae, Leucochrysini). ZooKeys 1158: 179–193. https://doi.org/10.3897/zookeys.1158.98572

Abstract

Examination of a newly discovered specimen of *Nuvol* showed that our earlier species determination of *Nuvol umbrosus* Navás had been incorrect and that our "redescription" of the species actually applied to an undescribed species. Here, we redescribe the true *N. umbrosus*, based on a newly discovered male specimen. This specimen closely resembles Navás' description, and it was collected from the Atlantic Forest as was the original type specimen. In addition, we assign the previously misidentified *Nuvol* specimens from the Amazonian region to a separate species, *Nuvol satur* Sosa & Tauber, **sp. nov.** As a result of these actions, the genus *Nuvol* now contains two morphologically and geographically distinct species. In addition, the abdomens and genitalia of both sexes of *Nuvol* are now described (although each from a separate species).

Keywords

Chrysopinae, lacewing, misidentification, new species, taxonomy

Introduction

The Neotropical green lacewing tribe Leucochrysini, a diverse and largely unstudied group in the neuropteran family Chrysopidae, currently contains ~190 described species uncomfortably classified into seven genera (Mantoanelli et al. 2006; Tauber 2007; Tauber et al. 2008; Breitkreuz et al. 2021). One of the small genera in the tribe is the monotypic *Nuvol* Navás (1916) – a genus that has remained largely unstudied because specimens are very few. Navás retained the type specimen of the type species, *Nuvol umbrosus* Navás, in his personal collection; it is missing (Monserrat 1985: 240; Tauber and Sosa 2015: 143). Also missing are two other specimens from Brasil: one from the state of Rio de Janeiro (Navás 1929a: 860, as "*Newol umbrosus*"; Navás 1929b: 319) and another from the state of São Paulo [photographed and studied by P. A. Adams at the Museu de Universidade de Zoologia da São Paulo (MZUSP), as reported by Brooks and Barnard (1990: 251, reference to P. A. Adams' unpublished notes)]; see Tauber and Sosa (2015: 142)].

Approximately one hundred years after the species description, we discovered two female specimens from the Amazonian region that we tentatively identified as *N. umbrosus* Navás (Tauber and Sosa 2015). Based on our comparison of these two specimens with other leucochrysines, we concluded that aspects of the wing venation and a unique pattern of suffused banding on the wings were sufficient to warrant, at least temporarily, the retention of *Nuvol* as a valid genus within Leucochrysini (Tauber and Sosa 2015). However, we were not satisfied with our tentative determination of the two specimens as phenotypic variants of *N. umbrosus*. They exhibited several morphological features not reported for *N. umbrosus*, and they had been collected from sites far from the type locality. Thus, we continued to question if the two specimens actually represented a second species of *Nuvol*.

Recently, we discovered an additional specimen of *Nuvol* – a male in the collection at the Instituto de Ciências Biológicas, Universidade Federal de Minas Gerais, Belo Horizonte, Brazil. This specimen clearly fits Navás' original description and drawing closely – much more closely than the specimens we had studied earlier. Its discovery indicated that Navás' description and drawing were quite accurate, and that our hesitancy to firmly identify the Amazonian specimens as *N. umbrosus* was well founded. The specimen also indicated that our description and images of the Amazonian specimens depict a new, unnamed species in the genus.

Here, based on the newly found specimen, we first redescribe the true *N. umbrosus* Navás and provide information on the terminalia of a *Nuvol* male. Second, we correct the misidentification of our earlier specimens from the Amazonian region and recognize them as representing a new species. Finally, with the addition of male abdominal characteristics, we update the available diagnostic information for the genus *Nuvol* and briefly discuss the relationship of *Nuvol* with other leucochrysine genera.

Materials and methods

The procedures used here were identical to those used in our previously published work, specifically: Tauber and Sosa (2015); Tauber et al. (2017).

Our abbreviations for museums are as follows:

EMUS Entomological Museum, Utah State University, Logan, Utah, USA;
INPA Coleção de Invertebrados do Instituto Nacional de Pesquisas da Amazônia, Manaus, Amazonas, Brazil;
MZUSP Museu de Zoologia da Universidade de São Paulo, São Paulo, Brazil.

Taxonomy

Nuvol umbrosus Navás, 1916

Nuvol umbrosus Brotéria (Zoológica) 14: 25; "Rio de Janeiro, Febrero de 1912" (only one specimen). Navás 1929a: 860 (locality record, as *Newol* [sic] *umbrosus*); Navás 1929b: 319 (locality record); Penny 1977: 28 (species list); Brooks and Barnard 1990: 251 (taxonomy, drawing of wings from Adams' notes on MZUSP specimen); Oswald 2013 (catalog listing); Tauber and Sosa 2015: 141–153 (taxonomic treatment based on incorrect species identification).

Redescription. One male specimen preserved in alcohol, examined by FS: "MG, São Gonzalo Rio Abaixo, EA [Estação Ambiental, 19°53'2.86"S, 43°22'26.14"W, 751m] Peti, 30.iv.2012, A. F. Kumagai" (deposited in the collection of the Instituto de Ciências Biológicas, Universidade Federal de Minas Gerais (ICB – UFMG), Belo Horizonte, Brazil).

Body (Fig. 1): Slender, yellowish to greenish, with elongate, slender antennae (both broken), hyaline wings marked with conspicuous brown to golden bands. ***Head*** (Figs 1A, 2A–C): Vertex raised, yellowish green, with two wide, reddish-brown longitudinal stripes dorsally, two smaller stripes laterally near edge of eyes. Frons, clypeus greenish; genae red. Labial, maxillary palpi yellow, unmarked. Antennae with scapes elongate, relatively large, close to each other mesally, cream colored, with light reddish-brown stripe dorsally (Fig. 2A, B); pedicel apparently unmarked; flagellar segments (basal section of flagellum) elongate, each with four swirls of robust, acute black setae (Fig. 1B). Measurements: head width (dorsal) 1.7 mm, ratio of head width / eye width 1:2.2; scape length 0.46 mm, width 0.35 mm.

Thorax (Fig. 2A, C, D): Prothorax slightly wider than long (length 0.9 mm, width 1.2 mm), notum with five thin, longitudinal, reddish-brown stripes, three dorsal [as illustrated by Navás (1916)], two on lateral margin [absent from Navás' drawing]; surface with elongate, golden setae mesolaterally. Mesothorax, metathorax with dark red marks laterally. Legs pale, without markings, with numerous light-brown to amber setae; tarsal claws with broad, dilated base, deep narrow cleft (Fig. 1C).

Note: Navás' figure illustrated only the dorsal marks on the pronotum, not the lateral stripes; however, he explicitly mentioned the lateral stripes in his description. Thus, the specimen we describe here matches Navás' type specimen in having five distinct dark red longitudinal stripes on the pronotum and two thin, somewhat diffuse, lateral stripes on the mesonotum and metanotum.

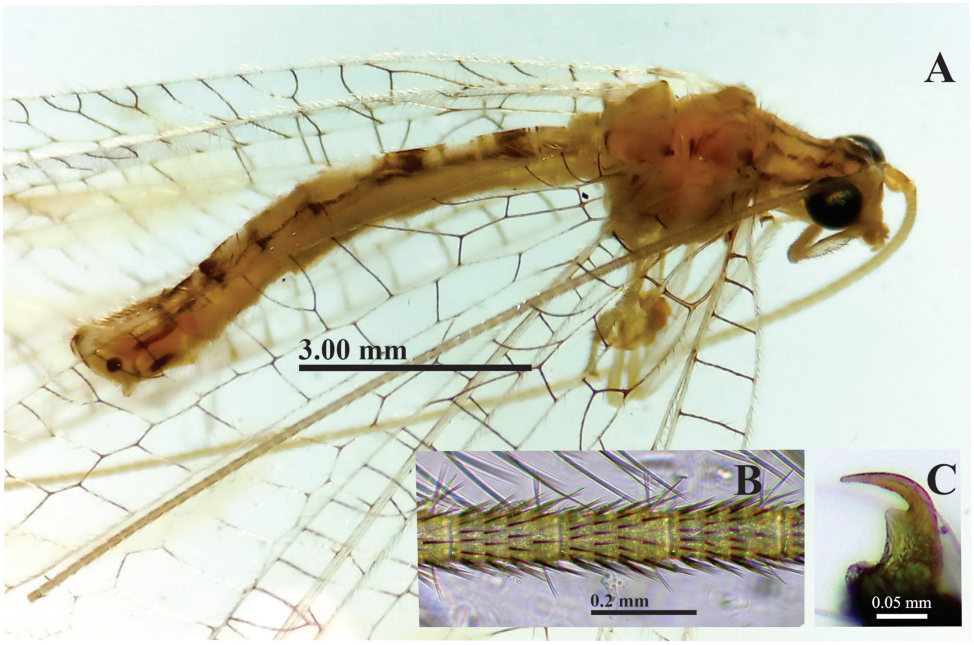

Figure 1. *Nuvol umbrosus* (Brazil, Minas Gerais) **A** habitus, dorsolateral **B** antennomeres ~ 1/3 distance from base of antenna **C** protarsal claw.

Wings (Fig. 3): Forewing 17.0 mm long, 6.1 mm wide (at widest point), with ratio of length / maximum width = 2.8:1; width at midpoint 5.6 mm, width along distal margin of basal quadrant, 4.2 mm; at base of distal quadrant 5.7 mm. Costal area relatively narrow; tallest costal cell (#8) 0.9 mm tall, with height 1.5 times its width, 0.16 times width of wing (midwing). First intramedian cell (*im1*) triangular, height at base (along median arculus, ma) 0.46 mm, width 2.1 times height, 0.57 times width of third median cell (*m3*). First radial crossvein distal to origin of radial sector (Rs); radial area (between R and Rs) with single row of 14 short, closed cells; tallest radial cell (*ra-rp1*) 0.69 mm in height, 0.72 times shorter than its width; two *b* cells (cells beneath Rs, not including an inner gradate vein); eight *b'* cells (cells beneath Psm, after *im2*). Nine discrete inner gradates in regularly ascending, almost linear pattern, basal one not reaching Psm. Nine to eleven outer gradates aligned in relatively straight line adjacent to margin of wing, from tip of Psm to tip of Rs. Height of fourth inner gradate cell 1.1 times width. Four intracubital cells (*icu1-icu3* closed, *icu4* open). Subcosta, radial sector forked apically; thirteen to fourteen posterior terminal veins forked, distal six simple, without forks. Longitudinal veins, crossveins simple, slender, largely without crassate sections. Alar membrane with three large, conspicuous, diffuse, light yellowish-brown marks; stigma brown marked (Fig. 3B). Most veins dark, those beneath diffused alar markings appearing hyaline.

Hindwing 15.8 mm long, 5.1 mm wide. Nine discrete inner gradates, basal one not reaching Psm. Six outer gradates ascending in relatively straight to slightly zigzag trajectory

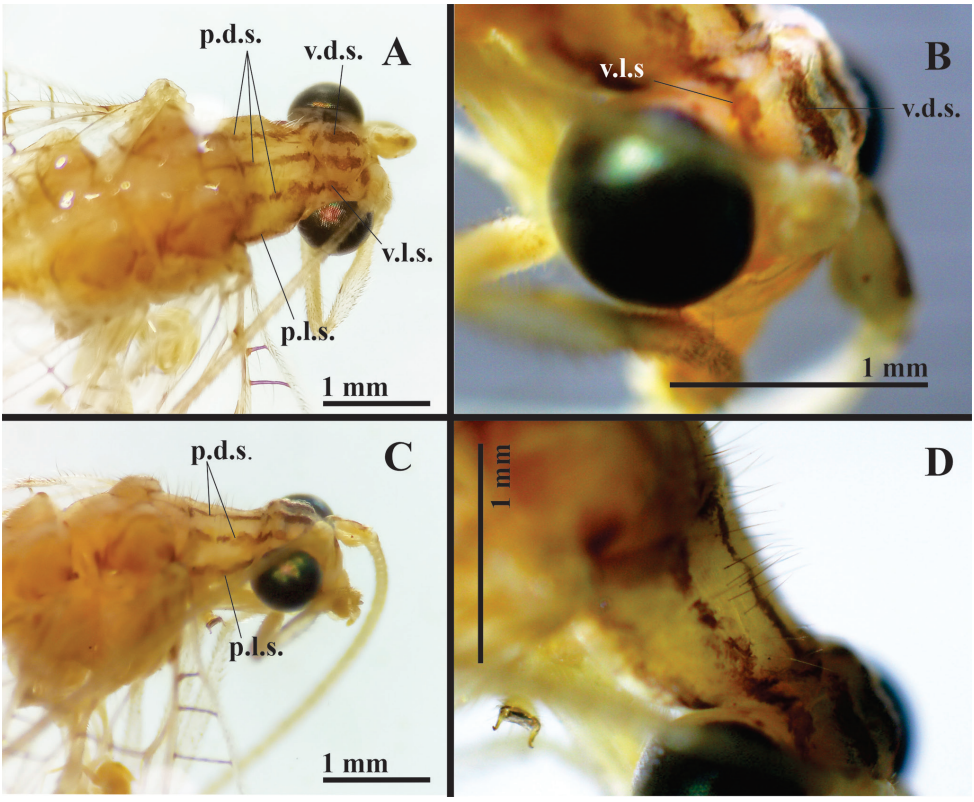

Figure 2. *Nuvol umbrosus* (Brazil, Minas Gerais) **A** head and thorax, dorsal **B** vertex, dorsolateral **C, D** head and thorax, dorsolateral. Abbreviations: **p.d.s.** pronotal dorsal stripe; **p.l.s.** pronotal lateral stripe; **v.d.s.** dorsal stripe on vertex; **v.l.s.** lateral stripe on vertex.

adjacent to wing margin. Thirteen radial cells (counted from origin of radius, not false origin). Two large *b* cells (no small *"t"* cell); seven *b'* cells beyond *im2*. Membrane with yellowish-brown diffused marks, similar to those on forewing; veins generally dark, but light in areas of diffused markings; stigma with single, weak brown spot basally, brown veins.

Abdomen, male (Figs 4–6): Yellowish with dark brown to black spots on tergites, sternites as follows: posterior sections of T1–T3, T6–T7, lateral margins of T1–T7, along dorsal apodeme below T8, tip of T9+ect, dorsal margin of S9 (Fig. 4A–C). Tergites, sternites quadrate, with all margins relatively straight, with long, robust setae, scattered short setae, dense microsetae, except S9 without microsetae (Fig. 5E); pleuron with sparse short setae except P7, P8 with setae large, dense. Microtrichiae covering the pleuron throughout. Spiracles small, round externally, atria not enlarged; rim sclerotized weakly. Callus cerci brown to black, round to slightly oval, located medially on T9+ect, with ~32 densely spaced trichobothria (Figs 4C, 5D). T9+ect fused dorsally, elongate, extending basally beneath T8 to distal margin of T7, with dorsal apodeme extending along full length of ventral margin, articulating basally with proximal

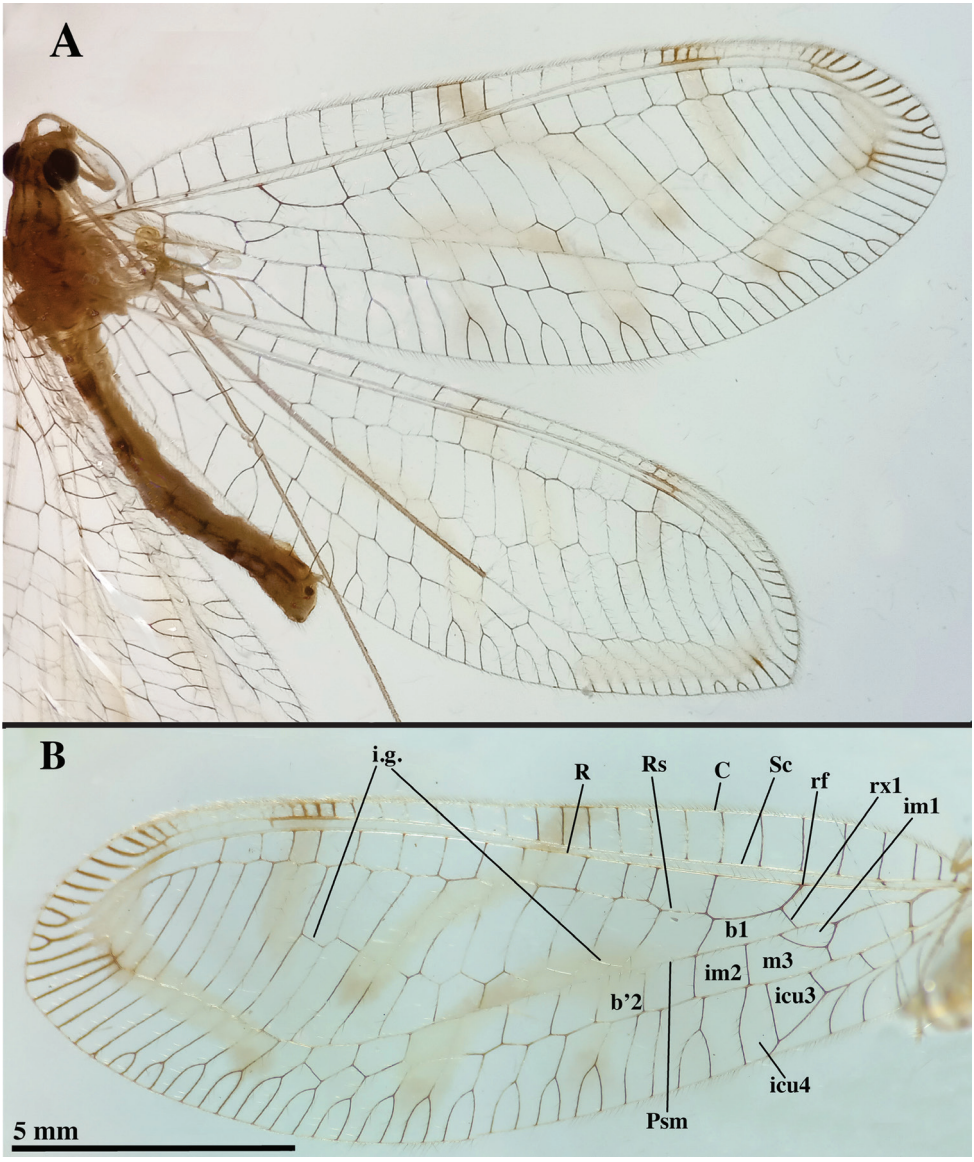

Figure 3. *Nuvol umbrosus* wings (Brazil, Minas Gerais) **A** right forewing and hindwing **B** left forewing with cells and veins identified. Note presence of apical veinlets with and without forks, markings, radius turning downward at tip of wing, forewing with four intracubital cells. Abbreviations: **b1** first upper Banksian cell; **b'2** second lower Banksian cell; **C** costa; **icu3, icu4** third and fourth intracubital cells; **im1, im2** first and second intramedian cells; **i.g.** inner gradate series; **m3** third median cell; **Psm** pseudomedia; **R** radius; **Rs** radial sector; **rf** origin of radial sector; **rx1** first radial crossvein; **Sc** subcosta.

end of ventral apodeme on dorsal margin of S8+9. Dorsal apodeme (Fig. 5A) strongly sclerotized throughout, bifurcated mesally, proximal to callus cerci, with dorsal spur almost reaching the dorsal margin of T9+ect, with lower section extending distally into

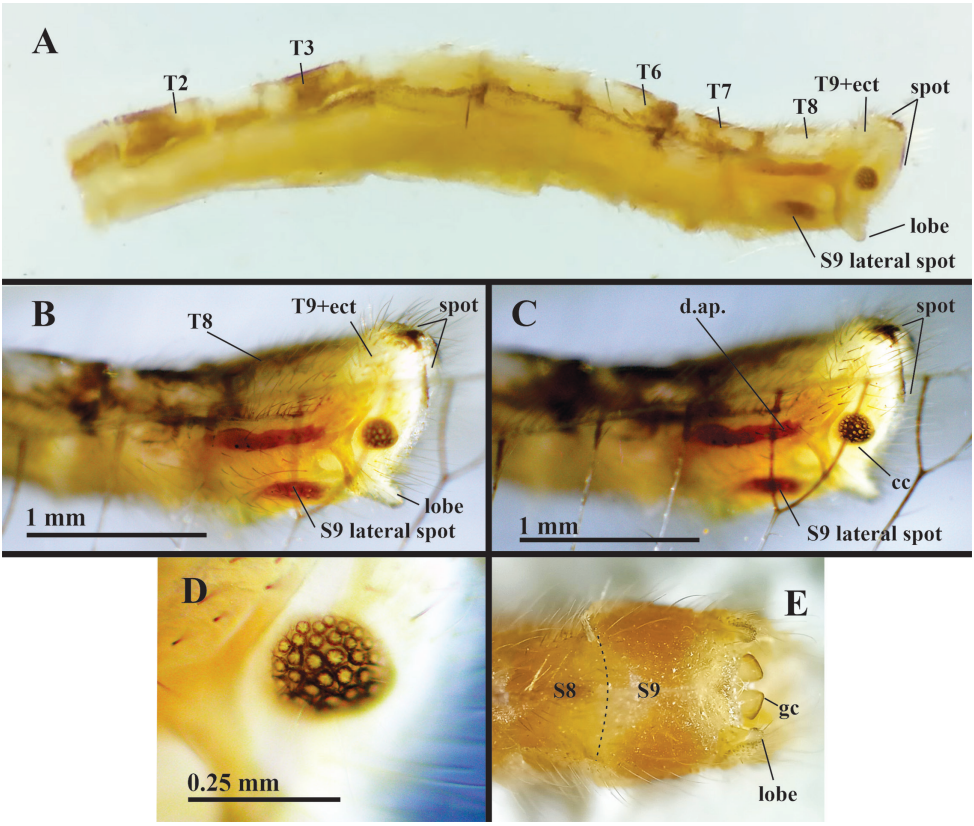

Figure 4. *Nuvol umbrosus* male abdomen (Brazil, Minas Gerais) **A–C** uncleared abdomen, lateral. Note apical lobe on distoventral corner of T9+ect with dense field of long, robust setae. Setae surrounding dorsal apodeme below T8, lateral spot on S9 **D** callus cerci and trichobothria (setae obscured) **E** S8+9, ventral. Note exposed gonocornua at apex of S9; dashed line showing possible suture scar between S8 and S9. Abbreviations: **cc** callus cerci; **d.ap.** dorsal apodeme; **gc** gonocornu; **S8, S9** eighth and ninth sternites; **T2–T8** second to eighth abdominal tergites; **T9+ect** fused ninth tergite and ectoproct.

setose lobe, well beyond distal margin of T9+ect (Fig. 5A–C). Basal section of S8+9 connected to T9+ect via membrane with scattered, long setae (Figs 4B, C, 5A). Dorsal margin of S8+9 (lateral view) with deep mesal cleft (Figs 4C, 5A); ventral surface of S8+9 with small suture-like separation, S8 with microsetae, S9 without microsetae (Fig. 5A). Dorsal margin of S8 with distinct apodeme (ventral apodeme) descending abruptly to base of cleft, covered by dense field of robust setae (Fig. 5A). Dorsal margin of S9 heavily convex, with sclerotized apodeme along upper edge, with round, sclerotized tips extending beyond end of segment (Fig. 5A–C, E). Sternites with ratio of maximum height / maximum length (lateral view): S2 = 0.5:1; S3 = 0.6:1; S4 = 0.8:1; S5 = 1:1; S6 = 1:1; S7 = 1.1:1; S8 = 1.5:1; S9 = 0.6:1; surfaces without microtholi.

Gonarcus well sclerotized, widely arcuate (maximum span 0.31 mm; minimum span between posterior apices of the lateral apodemes 0.28 mm); gonarcal bridge broad,

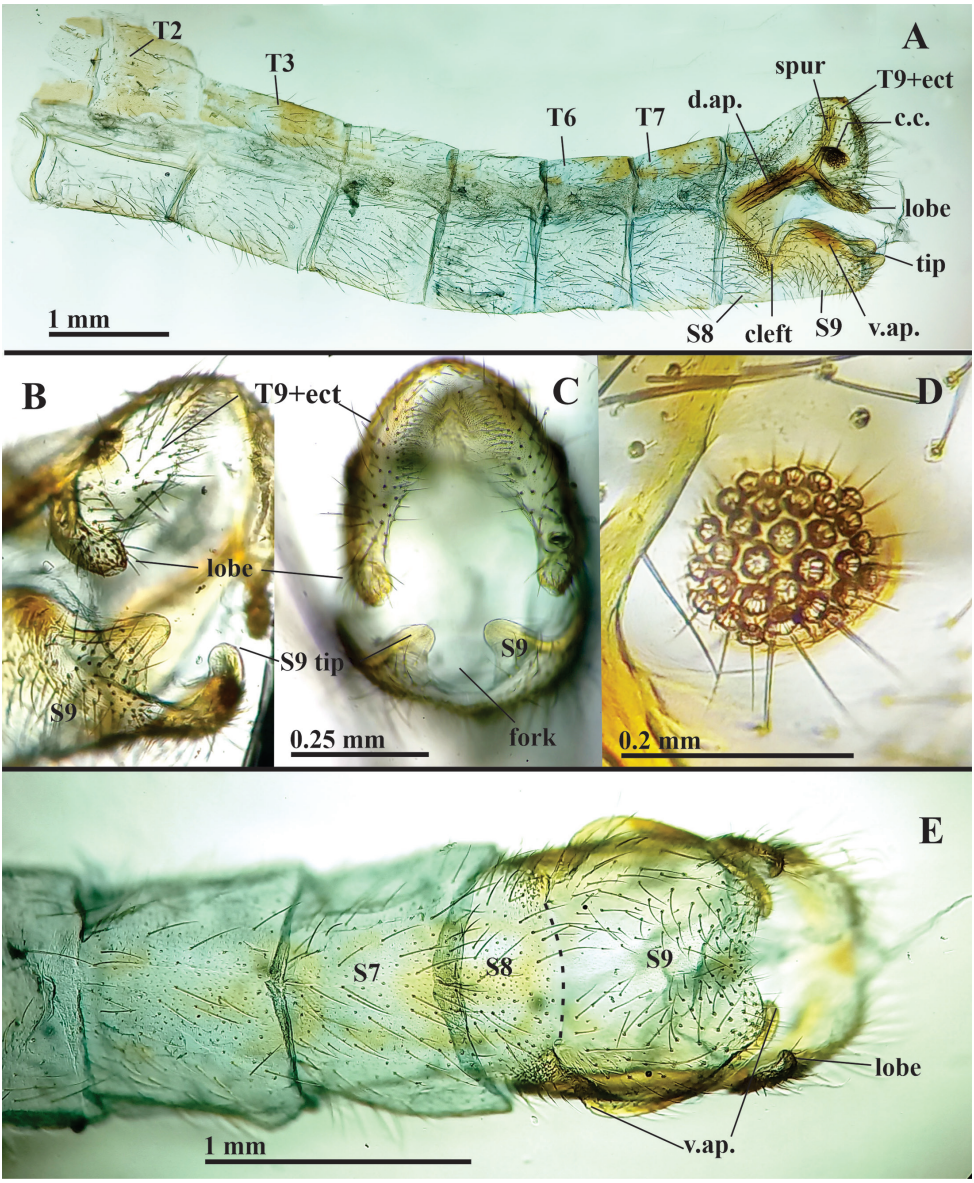

Figure 5. *Nuvol umbrosus* male terminalia cleared, with genitalia removed (Brazil, Minas Gerais) **A** abdomen, lateral **B** abdominal tip, posterolateral **C** abdominal tip, caudal **D** callus cerci **E** terminal segments, ventral [**Note for (E):** S6–S8 densely covered by microtrichiae; dashed line between S8 and S9 indicating a possible suture scar; S9 bearing long, robust setae and lacking microtrichiae.] Abbreviations: **c.c.** callus cerci; **d.ap.** dorsal apodeme; **lobe** setose lobe at distal apex of dorsal apodeme; **S7, S8, S9** seventh, eighth and ninth abdominal sternites; **T2, T3, T6, T7** second, third, sixth, seventh abdominal tergites; **T9+ect** fused ninth abdominal tergite and ectoproct; **v.ap.** ventral apodeme.

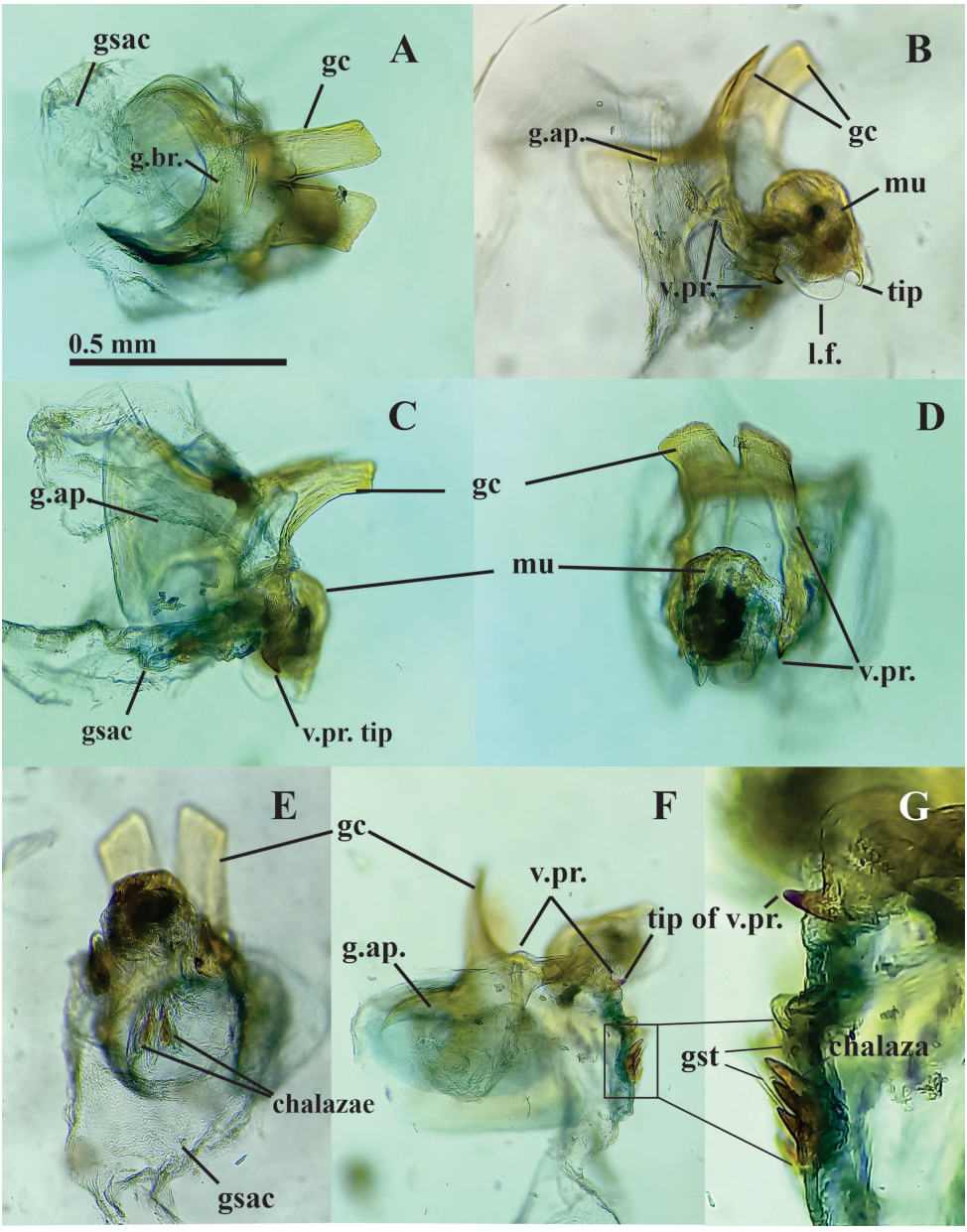

Figure 6. *Nuvol umbrosus* male gonarcal complex **A** dorsal **B** lateral slightly tilted to left **C** lateral slightly tilted to right **D, E** frontal **F** lateral (field of chalazate setae in box] **G** enlarged frontal section of gonosaccus, lateral. **Note: F, G** illustrate the placement and structure of the acute tip of the gonarcal ventral projection and the frontal section of the gonosaccus bearing a group of three heavily sclerotized chalazae with fine setae. Abbreviations: **g.ap.** gonarcal apodeme; **g.br.** gonarcal bridge; **gc** gonocornu; **gsac** gonosaccus; **gst** gonosetae; **l.f.** lateral flank of mediuncus; **mu** mediuncus; **tip of v.pr.** beaklike apex of gonarcal ventral projection; **v.pr.** ventral projection of gonarcus. Scale bar applies to **A–F**.

curved, bearing two long, flat, quadrate gonocornua dorsally (~0.28 mm long, 0.14 mm wide), pair of broad oval-shaped gonarcal apodemes basally (0.46 mm tall, 0.22 wide); gonarcal bridge strongly fused with base of gonocornua (Fig. 6A), pair of ventral projections (~0.24 mm long) extending from the ventral surface of the gonarcal bridge (Fig. 6B–D, F), with distal area swollen, terminating in beak-like apex (Fig. 6B, C). Mediuncus attached to gonarcal bridge and ventral processes via membranes extending from lower surface of gonarcal bridge, from inner margins of ventral processes; dorsal surface of mediuncus apparently smooth (Fig. 6B–D), terminating distally in curved beak, flanked laterally by prominent lateral lobe (Fig. 6B). Gonosaccus with dorsal surface striate (Fig. 6E), with two mesal fields of three large, heavily sclerotized chalazae, each bearing one or two long, thin setae subapically (Fig. 6F, G); area on gonosaccus above heavy chalazae with additional smaller chalazate gonosetae (Fig. 6G). Hypandrium internum not seen.

Note: The hypandrium internum can often be difficult to find. One was not found in this specimen. Either the specimen did not have one, it was not well developed, or it was lost.

Abdomen, female: Undescribed.

Immatures and biology. Unknown.

Known geographic distribution. Brazil: Rio de Janeiro, Minas Gerais (new record).

***Nuvol satur* Sosa & Tauber, sp. nov.**

https://zoobank.org/F4CCB95B-67EA-4A56-B5B5-5E89DE2FD422

Type specimens. ***Holotype:*** Female, INPA; Brazil, Amazonia, Novo Aripuanã, 05°15'53"S, 60°07'08"W. Armadilha Malaise em igarapé; Floresta úmida, ix.2004, Henriques Silva & Pena leg. Specimen pinned. ***Paratype:*** Female, EMUS; Brazil, Rondônia, 62 km SE Ariquemes, 7–18 Nov. 1995, W. J. Hanson.

Etymology. The genus name "*Nuvol*" is a masculine noun meaning "cloud" in Catalan; the species name "*satur*" is a Latin adjective (masculine form) meaning "deep or full", as applied to color (R. A. Pantaleoni, pers. comm.). The species name refers to the more intense coloration of the diffuse markings on the wings of the species, as compared with *N. umbrosus*.

Diagnosis. The most notable features that distinguish *N. satur* from *N. umbrosus* are the head and pronotal markings, markings on the abdomen, wing size, and wing markings, as follows: (1) The head and prothoracic markings of *N. satur* are red and diffuse, whereas those of *N. umbrosus* are brown and longitudinally striped; (2) The wings of *N. satur* are 14.8–15.8 mm long, slightly shorter than those of *N. umbrosus* (17.0 mm); and (3) Although both *Nuvol* species express some degree of suppressed forking in the terminal veinlets of the forewings and hindwings, *N. satur* has a much greater degree of suppression than *N. umbrosus.* Almost none of the terminal veinlets of the *N. satur* wings are forked, whereas only a small proportion of the veinlets on the posterior margin of the *N. umbrosus* wings are unforked. Finally, (4) the wing markings of *N. satur* are considerably more pronounced and in a different pattern than those of *N. umbrosus* (Fig. 7).

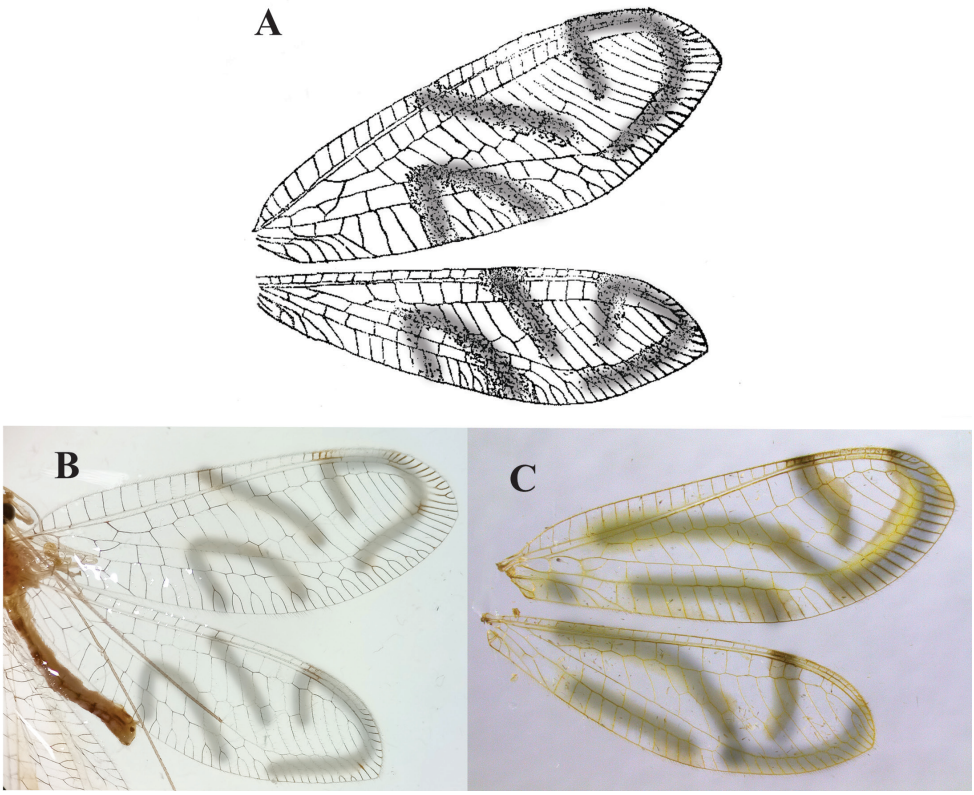

Figure 7. Cartoon showing pattern of wing markings of two *Nuvol* species **A** *N. umbrosus* type specimen (Brazil, Rio de Janeiro), from original drawing by Navás (1916) **B** *N. umbrosus* from current study (Brazil, Minas Gerais) **C** *N. satur*, new species, holotype (Amazonas, Brazil), from Tauber and Sosa 2015 (as *N. umbrosus*).

Description. Provided by Tauber and Sosa 2015: 144–150 (as *Nuvol umbrosus*). Note: In the description, we neglected to mention the length of the antennae; they measured 28.6 and 31.5 mm, over twice as long as the wing length (13.8 mm). The antennal length for *N. umbrosus* is unknown.

Immatures and biology. Unknown.

Known geographic distribution. Brazil: Amazonas, Rondônia.

Genus *Nuvol* Navás, 1916

Type species. *Nuvol umbrosus* Navás, 1916.

Known geographic distribution. South America: Brazil (Amazonas, Rondônia, Minas Gerais, Rio de Janeiro).

Generic diagnosis. Based on a small number of specimens from two species:

N. umbrosus – one specimen of unknown sex described by Navás (1916) and one male described here.

N. satur – two females described by Tauber and Sosa (2015, as *N. umbrosus*).

Medium to large lacewings, forewing length 14.8–17.0 mm. Head, pronotum with longitudinal black stripes or diffuse reddish marks; setae long. Legs unmarked; claws basally dilated. Forewing marked with faint to dark yellowish-brown transverse streaks through center and margins of wing; costal area narrow throughout; costal setae short, inclined; stigma marked with one to two small dark spots; Sc and R well separated throughout; R extended apically, curving posteriorly around wing apex; terminal subcostal and radial veinlets at apex of wing largely unforked, darkly marked; *im* short, broadly ovate; Rs almost straight, parallel to R; radial cells short, height relatively uniform from base to below stigma; gradate veins arranged in two roughly parallel series; outer gradates closely aligned, flowing smoothly from PsM; inner gradates extending basally, not meeting PsM; four intracubital cells, with *icu1*, *icu2*, *icu3* closed, *icu4* (*dcc*) open. Hindwing venation, markings similar to forewing.

Possible additional generic features, with supporting evidence from only one species and/or one specimen: Antennae very long (over twice length of forewing). ***Female*:** T9+ect separated dorsally by longitudinal groove. Spermatheca doughnut shaped, with elongate narrow spermathecal duct, substantial, sail-like velum opening directly to bursa copulatrix via dorsal slit. Bursa copulatrix with delicate membrane, elongate bursal glands. Subgenitale substantial, with bilobed knob protruding from broad triangular base. ***Male*:** T9+ect with prominent, heavily sclerotized, bifurcated dorsal apodeme: with dorsal spur extending upward behind and well above callus cerci, with ventral branch extending distally, protruding as lobe well beyond distal margin of ectoproct. T9+ect fused dorsally; callus cerci round to very slightly oval, dark against pale background. Sternites S8, S9 weakly fused, with conspicuous cleft or suture scars. Gonarcus well sclerotized, widely arcuate; bridge broad, curved, with pair of elongate ventral projections extending ventrally; gonocornua long, broad. Mediuncus bulbous basally, with slender terminus, membranous dorsal attachment to gonarcal bridge, lateral attachments to inner sides of ventral projections of gonarcus.

Generic relationships

The largely Neotropical green lacewing tribe Leucochrysini currently contains ~190 species classified into seven genera. One very large genus (*Leucochrysa*), with its two subgenera, accounts for the vast majority of leucochrysine species. Other species are distributed among a midsized genus of eight described species and five genera with only one or two species each (Brooks and Barnard 1990; Tauber et al. 2008; Oswald 2013). Although the tribe itself appears to be monophyletic, relationships within the group are largely unresolved (e.g., Garzón-Orduña et al. 2019; Winterton et al. 2019; Breitkreuz et al. 2021). In its original description (Navás 1916) and in subsequent discussion (Brooks and Barnard 1990; Tauber and Sosa 2015), *Nuvol* was distinguished from *Leucochrysa* and other leucochrysine genera largely on the basis of forewing fea-

tures, notably: an elongate radius that parallels the subcosta as it extends along the length of the wing and curves upward at the tip of the wing; terminal veins at the apex of the wing largely unforked; outer gradates aligned with neighboring gradates in a smooth trajectory that parallels the wing margin; an elongate, marked stigma; and four intracubital cells, rather than the typical three. Most noticeable are the distinctively diffuse and patterned markings on the forewings and hindwings. Both *Nuvol* species now known express this full suite of character states, but most of the features do not appear to be unique to the genus. For example, although most Leucochrysines that have been studied have three intracubital cells, the pattern of four intracubital cells that typifies *Nuvol* is also present in *Berchmansus* spp. [now assigned to Leucochrysini (Tauber 2007)] and in *Nothancyla verreauxi* Navás [previously assigned to Leucochrysini by Brooks & Barnard (1990), now tentatively assigned to Apochrysini by Winterton & Brooks (2002)]. Similarly, the linear alignment of the outer gradates and their flow into the PsM can be seen in most *Leucochrysa* (*L.*) species [notable examples: *L.* (*L.*) *boxi* Navás, *L.* (*L.*) *nigrilabris* (Banks), *L.* (*L.*) *insularis* (Walker) (Tauber et al. 2011a, b; Tauber et al. 2013)]. However, although diffused markings and streaks on the forewings are also found in other leucochrysine genera such as *Gonzaga*, *Leucochrysa* (*Nodita*), and *Santocellus* (see Brooks and Barnard 1990; Tauber et al. 2008, 2011b; Tauber 2012), they are usually not found on the hindwings and their patterns differ from those of the *Nuvol* species. And finally, unforked terminal veins at the apex of the forewing are unusual among Leucochrysini. So, at this time, we retain *Nuvol* as a distinct genus, while simultaneously acknowledging that the intriguing characters, and the frustrating lack of information associated with leucochrysine lacewings in general, provide stimulus for future investigation.

Acknowledgements

Thanks to Marcio Luiz de Oliveira, Curator of Invertebrates at the Coleção de Invertebrados do Instituto Nacional de Pesquisas da Amazônia, Manaus, Amazonas, Brazil (INPA), and the "Fundação de Amparo à Pesquisa do Estado do Amazonas" (FAPEAM) Edital: N. 011/2013 – COLEÇÕES BIOLÓGICAS, Protocol: 16066. UNI423.6372.29052013 for hosting the visit of FS to INPA. Thanks to Renato Machado, Universidade Federal do Paraná, for alerting FS to the *N. umbrosus* specimen. Special thanks to Lica Haseyama, Universidade Federal de Minas Gerais, for generously providing access to the unique specimen of *Nuvol umbrosus* under her care; to Carol Von-Dohlen, Utah State University, for loan of chrysopid specimens; to Roberto Pantaleoni, Sassari University, for information on the genus and species names; and to A. J. Tauber for editorial comments. The "Lacewing Digital Library" website, developed and maintained by J. D. Oswald (Texas A & M University, College Station), was useful during this study. CAT's work continues to benefit from earlier funding by the National Science Foundation (DEB 0542373, with M. J. Tauber), USDA/NRI Competitive Grants Programs (9802447, with MJT), Cornell University, and the Cornell University Library.

References

Breitkreuz LCV, Garzón-Orduña IJ, Winterton SL, Engel MS (2021) Phylogeny of Chrysopidae (Neuroptera), with emphasis on morphological trait evolution. Zoological Journal of the Linnean Society 20: 1–22. https://doi.org/10.1093/zoolinnean/zlab024

Brooks SJ, Barnard PC (1990) The green lacewings of the world: a generic review (Neuroptera: Chrysopidae). Bulletin of the British Museum of Natural History. Entomology 59: 117–286.

Garzón-Orduña IJ, Winterton SL, Jiang Y, Breitkreuz LCV, Duelli P, Engel MS, Penny ND, Tauber CA, Mochizuki A, Liu X (2019) Evolution of green lacewings (Neuroptera: Chrysopidae): a molecular supermatrix approach. Systematic Entomology 44(3): 499–513. https://doi.org/10.1111/syen.12339

Mantoanelli E, Albuquerque GA, Tauber CA, Tauber MJ (2006) *Leucochrysa* (*Leucochrysa*) *varia* (Schneider) (Neuroptera: Chrysopidae): larval descriptions, developmental rates, and adult color variation. Annals of the Entomological Society of America 99(1): 7–18. https://doi.org/10.1603/0013-8746(2006)099[0007:LLVNCL]2.0.CO;2

Monserrat VJ (1985) Lista de los tipos de Mecoptera y Neuroptera (Insecta) de la colección L. Navás, depositados en el Museo de Zoología de Barcelona. Miscellània Zoològica 9: 233–243.

Navás L (1916) Neurópteros Sudamericanos. Tercera [III] serie. Neurópteros del Brasil recogidos por el R. P. Joaquín da Silva Tavares S. J. Brotéria (Zoológica) 14: 14–35.

Navás L (1929a) Insectos del Brasil. 3.a serie. Revista do Museu Paulista 16: 857–864. [IIIa]

Navás L (1929b) Insectos Neurópteros del Museo de Hamburgo. Memorias de la [Real] Sociedad Española de Historia Natural 15: 315–322.

Oswald JD (2013) Neuropterida Species of the World. Version 3.0. http://lacewing.tamu.edu/species-catalogue/ [Last access: 13 March 2015]

Penny ND (1977) Lista de Megaloptera, Neuroptera e Raphidioptera do México, América Central, ilhas Caraíbas e América do Sul. Acta Amazonica 7(4, Suplemento): 1–61. https://doi.org/10.1590/1809-43921977074s005

Tauber CA (2007) Review of *Berchmansus* and *Vieira* and description of two new species of *Leucochrysa* (Neuroptera: Chrysopidae). Annals of the Entomological Society of America 100(2): 110–138. https://doi.org/10.1603/0013-8746(2007)100[110:ROBAVA]2.0.CO;2

Tauber CA (2012) *Santocellus* (Neuroptera, Chrysopidae, Leucochrysini): Taxonomic changes, new description, and a key to the species. ZooKeys 255: 93–101. https://doi.org/10.3897/zookeys.255.4111

Tauber CA, Sosa F (2015) Rediscovery of *Nuvol umbrosus* Navás (Neuroptera, Chrysopidae, Leucochrysini): A redescription and discussion. ZooKeys 519: 141–153. https://doi.org/10.3897/zookeys.519.5996

Tauber CA, Tauber MJ, Albuquerque GS (2008) *Gonzaga nigriceps* (McLachlan) (Neuroptera: Chrysopidae): descriptions of larvae and adults, biological notes, and generic affiliation. Proceedings of the Entomological Society of Washington 110(2): 417–438. https://doi.org/10.4289/07-045.1

Tauber CA, Albuquerque GS, Tauber MJ (2011a) Nomenclatorial changes and redescriptions of three of Navás' *Leucochrysa* (*Nodita*) species (Neuroptera, Chrysopidae). ZooKeys 92: 9–33. https://doi.org/10.3897/zookeys.92.828

Tauber CA, Mantoanelli E, Albuquerque GS, Reguilón C, González Olazo E, Tauber MJ (2011b) A taxonomically significant polymorphism in *Leucochrysa* (Neuroptera: Chrysopidae): Nomenclature, larval and adult descriptions, and biological notes. Zootaxa 3130(1): 1–29. https://doi.org/10.11646/zootaxa.3130.1.1

Tauber CA, Sosa F, Albuquerque GS, Tauber MJ (2013) Adults and larvae of two *Leucochrysa* (*Leucochrysa*) species (Neuroptera, Chrysopidae): Descriptions, biological notes, and relationships. Zootaxa 3750(2): 101–129. https://doi.org/10.11646/zootaxa.3750.2.1

Tauber CA, Sosa F, Albuquerque GS, Tauber MJ (2017) Revision of the Neotropical green lacewing genus *Ungla* (Neuroptera, Chrysopidae). ZooKeys 674: 1–188. https://doi.org/10.3897/zookeys.674.11435

Winterton, SL, Brooks SJ (2002) Phylogeny of the Apochrysine green lacewings (Neuroptera: Chrysopidae: Apochrysinae). Annals of the Entomological Society of America 95(1): 16–28. https://doi.org/10.1603/0013-8746(2002)095[0016:POTAGL]2.0.CO;2

Winterton SL, Gillung JP, Garzón-Orduña IJ, Badano D, Breitkreuz LCV, Duelli P, Engel MS, Liu X, Machado RJP, Mansell M, Mochizuki A, Penny ND, Tauber CA, Oswald JD (2019) Evolution of green lacewings (Neuroptera: Chrysopidae): an anchored phylogenomics approach. Systematic Entomology 44(3): 514–526. https://doi.org/10.1111/syen.12347

ZooKeys 1158: 195–196 (2023)
doi: 10.3897/zookeys.1158.104708
https://zookeys.pensoft.net

CORRIGENDUM

A peer-reviewed open-access journal
ZooKeys
Launched to accelerate biodiversity research

Corrigendum: Kato M, Kawakita A (2023) Diversity and larval leaf-mining habits of Japanese jewel beetles of the tribe Tracheini (Coleoptera, Buprestidae). ZooKeys 1156: 133–158. doi:10.3897/zookeys.1156.97768

Makoto Kato[1], Atsushi Kawakita[2]

1 *Graduate School of Human and Environmental Studies, Kyoto University, Sakyo 606-8501, Kyoto, Japan*
2 *The Botanical Gardens, Graduate School of Science, The University of Tokyo, Tokyo, 112-0001, Japan*

Corresponding author: Makoto Kato (makotokato1313@gmail.com)

Academic editor: Christopher Majka | Received 8 April 2023 | Accepted 11 April 2023 | Published 21 April 2023

https://zoobank.org/B3BF883C-BFB0-42A2-9051-909FBC80BFDE

Citation: Kato M, Kawakita A (2023) Corrigendum: Kato M, Kawakita A (2023) Diversity and larval leaf-mining habits of Japanese jewel beetles of the tribe Tracheini (Coleoptera, Buprestidae). ZooKeys 1156: 133–158. doi:10.3897/zookeys.1156.97768. ZooKeys 1158: 195–196. https://doi.org/10.3897/zookeys.1158.104708

We recently published the description of two new buprestid beetle species *Habroloma elaeocarpusi* and *Habroloma taxillusi* (Kato & Kawakita, 2023). However, no holotype depository is indicated in the paper. This is mandatory after 1999 according to the International Code of Zoological Nomenclature, and the new species names would be nomina nuda and unavailable (ICZN 1999: Art. 16.4.2). In this corrigendum, we indicate the holotype depository and correct the code numbers of the type specimens, which were incorrect. We thank Dr. Yutaka Tamadera (Hokkaido University) for kindly pointing out this error.

Habroloma elaeocarpusi sp. nov.

Material examined. ***Holotype*:** Japan: ♂ (MK-BP-a327), Mt. Osuzu, Tsuno-cho, Miyazaki Pref. NSMT-I-C-200345.

***Paratypes*:** Japan: 1♂ (MK-BP-a360), same data as holotype, NSMT-I-C-200346; 1♀ (MK-BP-k35), Isso, Yakushima-cho, Yaku Island, NSMT-I-C-200347.

Type depository. The holotype and the paratypes are deposited at the National Museum of Nature and Science, Tokyo (NSMT).

***Habroloma taxillusi* sp. nov.**

Material examined. ***Holotype*:** Japan: ♂ (MK-BP-k40), Yakukachi, Amami-shi, Kagoshima Pref., NSMT-I-C-200348.

***Paratype*:** Japan: 1♀(MK-BP-k39), same data as holotype, NSMT-I-C-200349.

Type depository. The holotype and the paratype are deposited at the National Museum of Nature and Science, Tokyo (NSMT).

References

ICZN [International Commission on Zoological Nomenclature] (1999) International Code of Zoological Nomenclature, Fourth Edition. The International Trust for Zoological Nomenclature, London, 306 pp. https://www.iczn.org/the-code/the-code-online/ [accessed on 2 April 2023]

Kato M, Kawakita A (2023) Diversity and larval leaf-mining habits of Japanese jewel beetles of the tribe Tracheini (Coleoptera, Buprestidae). ZooKeys 1156: 133–158. https://doi.org/10.3897/zookeys.1156.97768